Impact of Oncological Therapies on Genomic Stability and Differentiation Capacity of Human Bone Marrow-derived Mesenchymal Stromal Cells in the Context of Hematopoietic Insufficiency and Therapy-related Myeloid Neoplasms

Inaugural dissertation

for the attainment of the title of doctor
in the Faculty of Mathematics and Natural Sciences
at the Heinrich Heine University Düsseldorf

presented by

Bo Scherer
from Kirchheimbolanden

Düsseldorf, November 2024

from the Department of Hematology, Oncology and Clinical Immunology at the University Hospital Düsseldorf and at the Heinrich Heine University Düsseldorf

Published by permission of the
Faculty of Mathematics and Natural Sciences at
Heinrich Heine University Düsseldorf

Supervisor: Univ.-Prof. Dr. med. Thomas Schroeder
Co-supervisor: Univ.-Prof. Dr. Sebastian Wesselborg

Date of the oral examination: 12.06.2025

Der Einfluss von Onkologischen Therapien auf die Genomische Stabilität und Differenzierungsfähigkeit Humaner Mesenchymaler Stromazellen aus dem Knochenmark im Hinblick auf Hämatopoietische Insuffizienz und Therapie-bedingte Myeloische Neoplasien

Inaugural-Dissertation

zur Erlangung des Doktorgrades
der Mathematisch-Naturwissenschaftlichen Fakultät
der Heinrich-Heine-Universität Düsseldorf

vorgelegt von

Bo Scherer
aus Kirchheimbolanden

Düsseldorf, November 2024

aus der Klinik für Hämatologie, Onkologie und Klinische Immunologie am Universitätsklinikum Düsseldorf
der Heinrich-Heine-Universität Düsseldorf

Gedruckt mit der Genehmigung der
Mathematisch-Naturwissenschaftlichen Fakultät der
Heinrich-Heine-Universität Düsseldorf

Berichterstatter:

1. Univ.-Prof. Dr. med. Thomas Schroeder

2. Univ.-Prof. Dr. Sebastian Wesselborg

Tag der mündlichen Prüfung: 12.06.2025

Statutory Declaration/Eidesstattliche Erklärung

Ich versichere an Eides Statt, dass die Dissertation von mir selbstständig und ohne unzulässige fremde Hilfe unter Beachtung der „Grundsätze zur Sicherung guter wissenschaftlicher Praxis an der Heinrich-Heine-Universität Düsseldorf“ erstellt worden ist.

Düsseldorf, den 12.06.2025

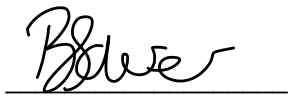

Bo Scherer

Table of Contents

Abbreviations

%	Percent
µm	Micrometer
µM	Micromolar
AML	Acute myeloid leukemia
ANGPT1	Angiopoietin 1
AZA	Azacitidine
B-ALL	B-lymphoblastic leukemia/lymphoma
BCL	B-cell lymphoma
BFU-E	Burst forming unit - Erythroid
BM	Bone marrow
BMP	Bone morphogenetic protein
CD	Cluster of differentiation
CDKN1A	Cyclin Dependent Kinase Inhibitor 1A
CDKN2A	Cyclin Dependent Kinase Inhibitor 2A
CFU	Colony forming unit
CFU-E	CFU - Erythroid
CFU-G	CFU - Granulocyte
CFU-GEMM	CFU - Granulocyte, Erythroid, Macrophage, Megakaryocyte
CFU-GM	CFU - Granulocyte-Macrophage
CFU-M	CFU - Macrophage
CLL	Chronic lymphocytic leukemia
CLP	Common lymphoid progenitor
CML	Chronic myeloid leukemia
CMP	Common myeloid progenitor
CPD	Cumulative population doublings
CXCL12	CXC motif chemokine ligand 1 (or stromal-derived factor 1, SDF1)
DMEM	Dulbecco's Modified Eagle Medium
DMSO	Dimethylsulfoxide
DNA	Desoxyribonucleic acid
DNMT1	DNA methyltransferase 1
ECM	Extracellular matrix
e.g.	*Exempli gratia* (for example)
EPO	Erythropoietin
et. al.	*Et aliae* (and others)
ETO	Etoposide
FDA	Food and Drug Administration
FGF	Fibroblast growth factor
G-CSF	Granulocyte colony-stimulating factor
GMALL	German Multicenter Study Group for ALL
GMP	Granulocyte monocyte progenitor
GSEA	Gene set enrichment analysis
Gy	Gray
HSPC	Hematopoietic stem and progenitor cells

IL	Interleukin
INF	Interferon
IPA	Ingenuity pathway analysis
IR	Ionizing radiation
ISCT	International Society of Cellular Therapy
JAG1	Jagged 1
LTC-IC	Human long-term culture-initiating cell
MDS	Myelodysplastic syndromes/myelodysplastic neoplasms
MEP	Megakaryocyte erythrocyte progenitor
MGMT	O6-methylguanine-DNA methyltransferase
MGUS	Monoclonal gammopathy of undetermined significance
MLL	Mixed lineage leukemia
MM	Multiple myeloma
MN	Myeloid neoplasm
MN-pCT	Myeloid neoplasm post cytotoxic therapy
MPN	Myeloproliferative neoplasms
MRC	Myelodysplasia-related changes
mRNA	Messenger ribonucleic acid
MS	Microsoft
MSC	Mesenchymal stromal cell
MTIC	(5-(3-*N*-methyltriazen-1-yl)-imidazole-4-carboxamide)
NC	Negative control
NHL	Non-Hodgkin lymphoma
O6BG	O6-benzyl guanine
OCN	Osteocalcin
OPG	Osteopontin
qPCR	Quantitative polymerase chain reaction
RJT	Radioactive iodine therapy
RNA	Ribonucleic acid
SASP	Senescence associated secretory phenotype
SCF	Stem cell factor (or kit ligand)
SMM	Smoldering myeloma
T-ALL	T-lymphoblastic leukemia/lymphoma
t-AML	Therapy-related acute myeloid leukemia
TGFB1	Transforming growth factor beta 1
t-MDS	Therapy-related myelodysplastic syndromes
t-MN	Therapy-related myeloid neoplasm
TMZ	Temozolomide
TNF	Tumor necrosis factor
TP53	Tumor protein 53
TPM	Transcripts per million
TPO	Thrombopoietin
VEN	Venetoclax (or ABT-199)
WHO	World Health Organization
WNT	Wingless [*wg*] gene in *Drosophila*; *Int-1* in mice

Abstract

Hematological neoplasms are among the most commonly diagnosed cancers with hematopoietic insufficiency as a common hallmark. Hematotoxicity is also among the most serious dose-limiting side effects of anticancer therapy, contributing to increased patient morbidity and mortality, and the development of therapy-related myeloid neoplasms (t-MN). Despite the increasing recognition of the bone marrow (BM) microenvironment, particularly mesenchymal stromal cells (MSC), in supporting and regulating normal hematopoiesis, the role of MSC hematological neoplasms and in therapy-related adverse side effects is not fully understood so far.

This thesis comprises four manuscripts with results that expand our understanding of MSC in myeloid and lymphoid neoplasms and may provide starting points for the prevention of hematotoxicity as a consequence of anticancer therapies. Manuscripts 2.1, 2.2, and 2.3 demonstrate the functional involvement of MSC in hematopoietic insufficiency in *de novo* cases of MDS, MPN, AML, NHL, ALL, and in the progression of MM, as well as therapy-related MDS and AML. TGFB signaling was identified as a potential central mechanism of stromal alterations, differing between myeloid and lymphoid neoplasms via canonical and non-canonical signaling respectively, and possibly offers a novel therapeutic strategy in the future. The main manuscripts 2.3 and 2.4 focus on the impact of different substances used in anticancer therapy on MSC and their role in hematotoxic effects. While functional and molecular aberrations overlapped with MSC from *de novo* neoplasms, RNA sequencing analysis of t-MN-derived MSC revealed a distinct immunomodulatory signature on the molecular level, which was not found in equivalent *de novo* myeloid neoplasms, suggesting a therapy-related origin of these alterations. Further, substance-specific alterations of healthy MSC were induced by azacitidine and etoposide affecting MSC proliferation and differentiation capacity, thereby contributing to insufficient hematopoietic support.

Overall, the findings in this thesis enhance our understanding of the role of MSC in the pathogenesis of *de novo* and therapy-related hematological neoplasms and highlight MSC as a potential, undesired target tissue of anticancer therapy. These insights could help to improve patient outcomes by targeting and managing of hematotoxicity during anticancer therapy more specifically in the future.

Zusammenfassung

Hämatologische Neoplasien gehören zu den am häufigsten diagnostizierten Krebsarten und zeichnen sich durch insuffiziente Blutbildung aus. Auch ist Hämatotoxizität eine der schwerwiegendsten dosis-limitierenden Nebenwirkungen der Krebstherapie und trägt zu einer erhöhten Morbidität und Mortalität der Patienten bei, sowie zur potenziellen Entwicklung einer therapie-assoziierten myeloischen Neoplasie (t-MN). Trotz der wachsenden Anerkennung des Knochenmarkmikromilieus besonders der mesenchymalen Stromazellen (MSC), die normale Hämatopoiese zu unterstützen und zu regulieren, ist die Rolle der MSC in der Pathogenese von hämatologischen Neoplasien und von therapie-assoziierten Nebenwirkungen bis heute nicht komplett verstanden.

Diese Arbeit umfasst vier Manuskripte mit Resultaten, die das Verständnis der Rolle von MSC bei myeloischen und lymphoiden Neoplasien erweitern, und gegebenfalls Ansatzpunkte zur Vermeidung von Hämatotoxizität infolge von Krebstherapien liefern können. Die Manuskripte 2.1, 2.2 und 2.3 zeigen die funktionelle Beteiligung von MSC an der hämatopoietischen Insuffizienz bei *de novo* Erkrankungen von MDS, MPN, AML, NHL, ALL und im Krankheitsverlauf von MM, sowie bei therapie-assoziierten MDS und AML. Der TGFB Signalweg erwies sich als potenzieller zentraler Mechanismus stromaler Veränderungen, der sich bei myeloischen und lymphoiden Neoplasien durch kanonische bzw. nicht-kanonische Signalübertragung unterscheidet und möglicherweise einen neuen therapeutischen Ansatz in der Zukunft bietet. Die Hauptmanuskripte 2.3 und 2.4 befassen sich mit den Auswirkungen von verschiedenen Substanzen, die als Krebstherapie angewendet werden, auf MSC und ihrer Rolle bei therapie-bedingten Nebenwirkungen. Während funktionelle und molekulare Aberrationen mit den *de novo* Neoplasien überlappen, zeigten die Ergebnisse einer RNA-Sequenzierungsanalyse von t-MN MSC eine ausgeprägte immunmodulatorische Signatur auf molekularer Ebene, die bei äquivalenten *de novo* Neoplasien nicht gefunden wurde, und auf einen therapie-bedingten Ursprung dieser Veränderungen hindeutet. Darüber hinaus wurden durch Azacitidine und Etoposid substanzspezifische Veränderungen gesunder MSC hervorgerufen, die die Proliferations- und Differenzierungsfähigkeit von MSC beeinträchtigen und so zu einer unzureichenden hämatopoietischen Unterstützung beitragen. Diese Resultate hinsichtlich der Rolle der MSC in diesem Kontext könnten die derzeitigen Behandlungsmöglichkeiten zur Milderung von Nebenwirkungen während der Krebstherapie erweitern.

Insgesamt verbessern die Ergebnisse dieser Arbeit unser Verständnis der Rolle von MSC in der Pathogenese von *de novo* und therapie-assoziierten, hämatologischen Neoplasien

und heben MSC als mögliches, unerwünschtes Zielgewebe von Krebstherapie hervor. Diese Erkenntnisse könnten durch eine gezieltere therapeutische Ausrichtung zu einem besseren Nebenwirkungsmanagement hinsichtlich der Hämatotoxizität während der Krebstherapie führen.

1. Introduction

1.1. The Hematopoietic System

The hematopoietic system guarantees a continuous supply of functional and mature blood and immune cells (Aust, 2017). The cells circulate through the bloodstream suspended in protein-rich plasma to all bodily tissues to exert their functions. Erythrocytes, the major cellular component of blood, are essential for gas exchange between lung and tissue and nutrient delivery. Leukocytes represent the cells of the innate and adaptive immune systems, while thrombocytes contribute to blood clotting (Hoffbrand & Moss, 2015). Due to their limited lifespan, over 10^{11} functional cells are replenished daily to maintain blood homeostasis (Ogawa, 1993).

1.1.1. Hematopoietic Stem Cells

Hematopoietic stem and progenitor cells (HSPC) are the origin of mature blood cells. The majority of the tissue-specific stem cells reside quiescently in the bone marrow (BM) (Bradford et. al., 1997; Pietras et. al., 2011) where their self-renewal capacity maintains a constant stem cell pool, and their differentiation capacity ensures a life-long supply of functional blood cells. This process is termed hematopoiesis (Wagers et. al., 2002). Initially, HSPC differentiate into multipotent progenitors with full lineage potential but limited self-renewal capacity (Seita & Weissman, 2010). These early hematopoietic progenitor cells are characterized by their surface marker CD34, which is not found on lineage-committed progenitors (Simmons et. al., 1992). From these early CD34-positive cells, oligopotent common lymphoid progenitors (CLP) and common myeloid progenitors (CMP) emerge, with CLP further differentiating to natural killer cells, and B- and T-cells (Kondo et. al., 1997), and CMP giving rise to granulocyte-macrophage progenitors (GMP) and megakaryocyte-erythroid progenitors (MEP). Finally, these cells differentiate into mature blood cells (Akashi et. al., 2000) that migrate into peripheral blood and tissues to exert their functions (Aust, 2017).

The balance between the proliferation and differentiation of HSPC is tightly regulated to adapt to the variable demands of the organism. This balance is controlled by a complex interplay of mechanisms, including genetically and epigenetically determined intrinsic factors and intercellular, bidirectional interaction between HSPC and the surrounding BM microenvironment. Together, these convoluted mechanisms govern the maintenance, survival, and activation of HSPC (Blank et. al., 2008; Warr et. al., 2011).

1.2. The Bone Marrow Microenvironment

The concept of a so-called hematopoietic niche that regulates harboring stem cells was first suggested by Schofield in 1978. Since then, it has been revealed that the BM microenvironment is a complex and dynamic tissue, consisting of different cell types and non-cellular components interacting to regulate HSPC. The elucidation of these complex relationships and how they influence normal hematopoiesis helps to understand their role in pathological situations and may contribute to the development of novel therapeutic interventions.

The BM microenvironment is functionally divided into two niches integral to HSPC regulation: the endosteal niche, located near the bone surface, and the vascular niche, surrounding the blood vessels. The endosteal niche harbors a dormant stem cell pool in a hypoxic and calcium-rich environment (Calvi et. al., 2003), while the vascular niche is more saturated with oxygen by the proximity of blood vessels and facilitates the mobilization of specialized effector cells into the bloodstream (Itkin et. al., 2016). Cell types within the niches interact with each other and HSPC to maintain this equilibrium of HSPC maintenance and differentiation (Xie et. al., 2009; Méndez-Ferrer et. al., 2010). Intercellular communication is largely governed by the extracellular matrix (ECM), a non-cellular, highly complex network of proteins and other macromolecules. Besides providing structural support, the ECM mediates the signaling for HSPC by functioning in cellular adhesion and building a reservoir for the signaling molecules, which are provided by the surrounding cells of the niches (Klein, 1995; Zanetti & Krause, 2020). For example, bone-lining cells of the endosteal niche provide collagen I and II, or osteocalcin (OCN) and osteopontin (OPN), localizing HSPC by their adhesive properties and contributing to their survival, proliferation, and differentiation (Nilsson et. al., 2005; Celebi et. al., 2012; Zanetti & Krause, 2020). Endothelial and mesenchymal cells of the vascular niche build an ECM rich in collagen IV and laminin, facilitating the migration of HSPC (Gu et. al., 2003). Additionally, signaling molecules from cellular niche components like Fibroblast Growth Factors (FGFs), Interleukins (IL), and members of the WNT (named after Wg [wingless] gene in *Drosophila* and *INT-1* in mice) and Transforming Growth Factor Beta (TGFB) family are embedded in the ECM and influence cell survival, proliferation, and the cell fate of HSPC (Bodo et. al., 2009; Gattazzo et. al., 2014; Domingues et. al., 2017; Zanetti & Krause, 2020).

The cellular components providing signaling molecules to the ECM include non-hematopoietic and hematopoietic cells. Mature immune cells, such as neutrophils (Casanova-Acebes et. al., 2013), macrophages (Winkler et. al., 2010; Chow et. al., 2011),

megakaryocytes, natural killer cells, and B- and T-cells (Slifka et. al., 1998; Geerman et. al., 2018), reside transiently or permanently in the BM and modulate HSPC maintenance and mobilization by cytokine secretion. Residing immune cells also interact with non-hematopoietic stromal cells (Schürch et. al., 2021), e.g. by expressing chemokines and receptors regulating the mobilization of HSPC in concert with endothelial cells that in turn facilitate vascular permeability to release mature blood cells to the periphery (Rafii et. al., 1995; Itkin et. al., 2016; Zhang J et. al., 2019). Additionally, endothelial cells are source for angiogenic Notch ligands, and key regulatory factors such as E-selectin, stem cell factor (SCF, also known as KIT-ligand), CXC motif chemokine ligand 12 (CXCL12), or Jagged 1 (JAG1, also known as CD339), additionally regulating HSPC quiescence and self-renewal (Butler et. al., 2010; Kobayashi et. al., 2010; Ding et. al., 2012; Poulos et. al., 2013).

A further central cellular component of the BM microenvironment is represented by mesenchymal stromal cells (MSC). MSC are a heterogeneous group, consisting of pleiotropic subpopulations with distinct properties and functionalities (Baccin et. al., 2020; Xiao et. al., 2022), that are found in both, the endosteal and vascular niches and provide the main supply of regulatory factors. Subpopulations include MSC with a high expression level of Leptin receptor (LepR+ cells), CXCL12-abundant reticular (CAR) cells, NG2+ pericytes, and Nestin+ cells (Kunisaki et. al., 2013; Anthony & Link, 2014), each contributing to hematopoietic regulation by differential expression and secretion of regulatory factors. The understanding of MSC subpopulations and their functions remains incomplete, and a considerable overlap among the populations can be assumed (Baccin et. al., 2020). Therefore, the International Society for Cellular Therapy (ISCT) formulated minimal characteristics of MSC, including plastic adherence *in vitro*, the expression of specific surface antigens (CD105, CD73, and CD90) but absence of hematopoietic markers (CD45, CD34, CD14 or CD11b, CD79α or CD19, and HLA-DR), and an *in vitro* trilineage potential to differentiate into the adipogenic, chondrogenic and osteogenic lineage (Dominici et. al., 2006). Guided by this principle, coherent and comparable studies consider MSC to be one population despite their heterogeneity.

MSC were originally termed “mesenchymal stem cells” due to their stem cell-like properties (Owen, 1988). However, their proliferative and multipotent capacity is lost after several divisions, distinguishing them from true stem cells (Horwitz EM & Keating, 2000). The heterogeneity within MSC populations further complicates the term "stem cells”. To address this, the ISCT recommended using the term “stromal cells”, reserving the term “stem cells” for cases where stem cell properties are explicitly demonstrated (Horwitz EM et. al., 2005).

Nevertheless, both terms are still used in the literature, but “stromal cell” is increasingly preferred to “stem cell” (Table 1) and is used in this thesis. Given the central role of MSC in the BM and the focus of this thesis, the following chapter provides a detailed introduction to their function in normal hematopoiesis.

Table 1. PubMed search results for MSC terminology. The data is based on a search by Ankrum *et. al.* in 2013 (published 2014) and own search results from August 2024.

PubMed search term	Number of PubMed results	
	2013 (Ankrum et. al., 2014)	2024 (own research)
“mesenchymal stem cell”	18,284	96,327
“mesenchymal stromal cell”	14,586	99,016
“bone marrow stromal cell”	4,254	105,638
“multipotent stromal cell”	183	5,308

1.2.1. Mesenchymal Stromal Cells: Central Regulators of Normal Hematopoiesis

Stromal cells of mesenchymal origin are a supporting cell tissue present throughout the body where they mainly offer structural and functional support, as well as play a crucial role in tissue regeneration. These cells can be isolated from multiple sources, including adipose tissue, placenta, cord blood, liver, kidney, and BM (Campagnoli et. al., 2001; Zuk et. al., 2002; Bieback et. al., 2004; In 't Anker et. al., 2004; da Silva Meirelles et. al., 2006; Plotkin & Goligorsky, 2006). MSC were first identified in the BM by Friedenstein *et. al.* in 1968, and their multilineage differentiation potential was demonstrated two decades later (Caplan, 1991). Since then, MSC have been recognized as key players in hematopoiesis during development and throughout adulthood. MSC were detected in direct proximity to HSPC (Méndez-Ferrer et. al., 2010) and identified as the main source of regulatory factors essential for hematopoietic support and regulation (Nakamura et. al., 2010; Omatsu et. al., 2010; Stik et. al., 2017).

The regulatory factors expressed and secreted by MSC can result in a variety of outcomes for HSPC. Cellular cross-talk, indirect by soluble factors or direct by ligand-receptor interaction, is essential to regulate hematopoiesis and maintain the micro milieu. For example, the glycoprotein Angiopoietin 1 (ANGPT1) is excreted by MSC, interacting with the tyrosine kinase receptor TIE2 on HSPC to regulate angiogenesis, hematopoiesis, adhesion, and self-renewal of HSPC (Arai et. al., 2004; Wu Y et. al., 2007). The chemokine CXCL12 (also stromal-derived factor 1, SDF1) is expressed by MSC and MSC-derived osteoblasts to regulate the chemotaxis, survival, and mobilization of HSPC via its interaction

with CXCR4 on HSPC (Aiuti et. al., 1997; Omatsu et. al., 2010). SCF (or Kit-ligand) is secreted as a cytokine or anchored to the membrane of MSC and interacts with the tyrosine kinase receptor C-Kit on HSPC to regulate the proliferative activity, localization, differentiation, and localization of HSPC (Kapur & Zhang, 2001; Kent et. al., 2008; Kimura et. al., 2011). Further, the Notch1 ligand JAG1 is expressed mainly by MSC and osteoblasts to support the survival and multilineage differentiation of HSPC (Jones P et. al., 1998; Karanu et. al., 2000).

Besides supplying signaling molecules, BM-derived MSC have trilineage differentiation capacity and are the origin of other components that contribute to the regulation of HSPC. Upon distinct stimuli, MSC differentiate into adipogenic progenitors, maturing into adipocytes, or into osteogenic-chondrogenic progenitors, which further differentiate into either chondrocytes or osteoblasts (Muraglia et. al., 2000). In particular, osteoblasts offer a diverse and complex set of properties to build the BM niche and regulate hematopoiesis. Osteoblasts are bone-forming cells that, alongside myeloid-derived osteoclasts, line the surface of the endosteal niche. They supply endosteal-specific ECM components and contribute to the calcium gradient along the BM microenvironment by expressing calcium derivatives (Lerner, 2012). Further, MSC-derived osteoblasts are pivotal in the homing of dormant HSPC through their interaction with N-cadherin at the endosteum (Arai et. al., 2004). The expression and secretion of cytokines such as ANGPT1, SCF, CXCL12, or JAG1 by osteoblasts further support HSPC maintenance and mobilization (Calvi et. al., 2003; Zhang J et. al., 2003). Deriving from the same progenitor, chondrocytes embody the building blocks of cartilage. Chondrocytes offer mechanical support, especially in regions undergoing repair or remodeling, and offer another source for ECM proteins such as collagen and minerals (Michelacci et. al., 2023). Growth factors such as Indian Hedgehog or Bone Morphogenetic Protein (BMP) are secreted by chondrocytes and participate in hematopoiesis, although their direct role is less extensively studied (Muir, 1995; Domingues et. al., 2017). The role of adipocytes in hematopoiesis is still discussed, but they have been shown to exert inhibitory effects on hematopoiesis (Naveiras et. al., 2009). However, following BM injury, large amounts of SCF are secreted by adipocytes, significantly contributing to hematopoietic regeneration (Zhou BO et. al., 2017).

Accumulating *in vitro* and *in vivo* data underscores the central role of MSC in hematopoietic support. Additionally, MSC are recognized for their immunomodulatory functions (Le Blanc & Davies, 2015; Huang et. al., 2022). MSC confer a dual role in tissue homeostasis as they exert immunosuppressive and inflammatory functions by modulating the innate and adaptive

immune response. MSC surveil the local milieu for signals from local immune cells to adequately respond to the dynamic immunological milieu (Le Blanc & Davies, 2015). MSC interact with natural killer cells, regulating their cytotoxicity and cytokine production, or macrophages, modulating their pro- and anti-inflammatory phenotypes. Further, T-cell proliferation and antibody production by B-cell-derived plasma cells are modulated by MSC (Di Nicola et. al., 2002; Glennie et. al., 2005; Rafei et. al., 2008; Luz-Crawford et. al., 2016). Thereby, MSC exert an important function in regulating an adequate immune response as well as regeneration and tissue repair. With a special focus on MSC to protect sensitive HSPC from inflammatory stress, they are primarily acknowledged for their immunosuppressive functions (Huang et. al., 2022). Therefore, MSC are more and more recognized as therapeutic tools for tissue regeneration, autoimmunity diseases, such as diabetes, lupus, rheumatoid arthritis, multiple sclerosis, or other immune-related conditions, e.g. Graft-versus-Host Disease (Horwitz E et. al., 2006; Ankrum et. al., 2014).

While exact mechanisms need to be elucidated further, MSC and its descendants take on a central role in the orchestration of immunomodulation and hematopoietic support (Figure 1). The MSC population comprises distinct and interconnected parts that contribute to generating the balance of the BM microenvironment to regulate HSPC cell fate during ontogeny and adult hematopoiesis. With this growing acknowledgment of their physiological significance, MSC gain more focus as a contributing factor to age-related changes such as osteoporosis (Hu et. al., 2018) or hematological pathologies such as leukemia (Korn & Mendez-Ferrer, 2017; Asada, 2018).

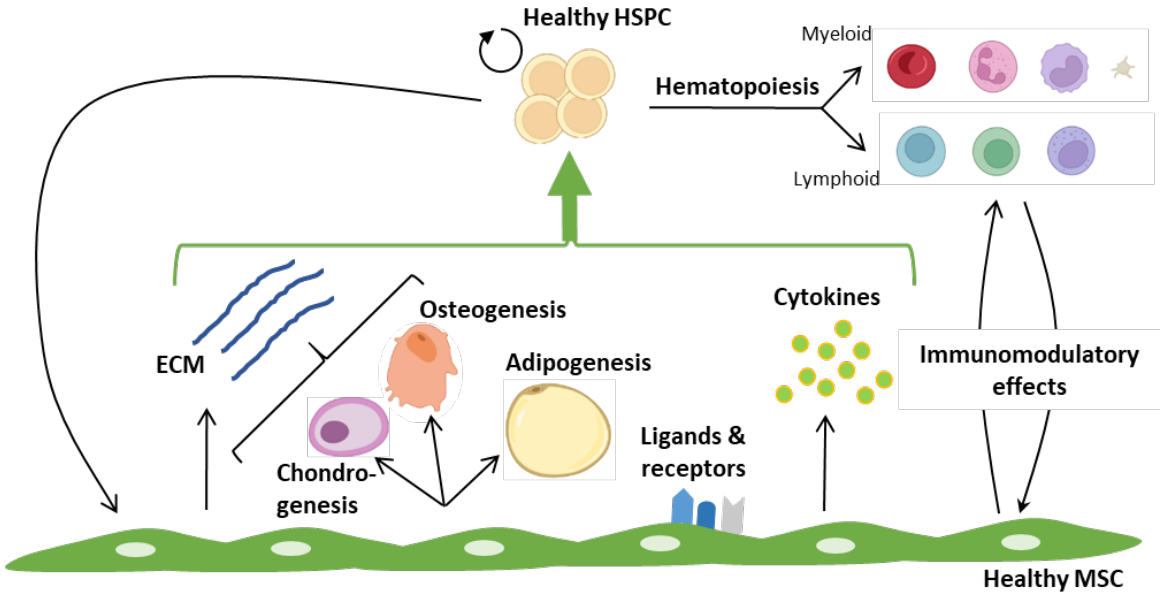

Figure 1. The contribution of MSC in healthy hematopoiesis. Healthy MSC support and regulate healthy HSPC by various characteristics as indicated by the green arrow. MSC are in direct receptor-ligand contact with HSPC and additionally mediate their supportive function indirectly by the expression and secretion of cytokines, chemokines, and growth factors. Further, MSC differentiate into other niche components, contributing to the microenvironments' architecture and integrity, and further supplying non-cellular components to support hematopoiesis. Immunomodulatory functions are exerted by interaction with immune cells (lymphoid cells) within the BM. Graphics were designed using Biorender.com and MS PowerPoint 2013.

1.3. Hematological Neoplasms: A Major Global Burden

Hematological neoplasms are a heterogeneous group of blood and lymph cancers and represent one of the most commonly diagnosed neoplasms. Increasing incidences worldwide are mainly attributed to the increasing life expectancy of humans, while age-standardized death rates are declining as a result of extensive research for a deeper understanding of hematological neoplasms and improved treatment strategies (Zhang N et. al., 2023).

The World Health Organization (WHO) subcategorizes hematological neoplasms according to the affected blood cell and the maturity of the malignant clone (Arber et. al., 2016; Swerdlow et. al., 2016; Alaggio et. al., 2022; Khoury et. al., 2022). Neoplasms affecting the myeloid lineage of the hematopoietic system comprise myelodysplastic syndromes (MDS), which is represented by the dysplasia of one or more myeloid lineages, and myeloproliferative neoplasia (MPN), characterized by the overproduction of mature blood cells. MDS patients confer an increased risk of progressing to the third pillar of myeloid

neoplasms (MN): acute myeloid leukemia (AML). When leukemia is preceded by MDS this disease is referred to as AML with myelodysplasia-related changes (AML MRC). The characterization of AML is based on the excessive BM infiltration of myeloid blasts, where 20 % blasts in the BM represent a threshold for the diagnosis of AML instead of MDS or MPN.

When the lymphoid lineage is affected, neoplasms are referred to as lymphoid neoplasms and comprise a variety of entities. Besides Hodgkin lymphomas, Non-Hodgkin lymphoma (NHL) confers the highest incidences (103.62 cases per 100,000 population) and death rates (62.18 deaths per 100,000 population) among hematological neoplasms (Zhang N et. al., 2023). NHL is diagnosed in the absence of the distinctive morphology and immunophenotypic diagnostics of Hodgkin lymphomas and is further categorized depending on the cellular origin and disease progression. Hence, NHL comprises diseases such as T-lymphoblastic leukemia/lymphoma (T-ALL), B-lymphoblastic leukemia/lymphoma (B-ALL), chronic lymphocytic leukemia (CLL), or multiple myeloma (MM) as plasma cell disease. Each of these hematological neoplasms is highly complex and can be further subcategorized based on recurrent genetic alterations, clinical features, cytology, histopathology, and immunophenotype, which gives clues on the etiology of the disease (Arber et. al., 2016; Swerdlow et. al., 2016).

Hematological neoplasms are usually age-related, although ALL is predominantly diagnosed during childhood and displays a second incidence peak in older adults, most likely caused by individual etiologies (Roberts, 2018). Stochastically, or due to a genetic predisposition of a genetic syndrome, driver mutations occur and accumulate over time and lead to cancerous transformation of a hematological neoplasm (Wlodarski & Niemeyer, 2017). Also, viral infections, e.g. the Epstein-Barr virus, Hepatitis, or Human Immunodeficiency Virus, can contribute to the development of neoplasms of the lymphoid lineage (Franceschi et. al., 2011; Chadburn et. al., 2013; Cesarman, 2014). The extrinsic exposure to environmental toxins, such as benzene, heavy metals, pesticides, or radiation was additionally correlated with an increased relative risk of developing a hematological neoplasm (Pasqualetti et. al., 1991; Rodriguez-Abreu et. al., 2007; Poynter et. al., 2017). As of that, medical exposure to genotoxic agents, e.g. during anticancer therapy, is also associated with an increased risk of secondary cancer, particularly MN. Due to the specific relevance of therapy-related neoplasms in this thesis, their etiology and characterization are specifically addressed in chapter 1.3.2.

The classification of hematological disorders has advanced over the years, with the latest WHO classification update in 2022. The updated version highlights the advancements in molecular and genetic research to understand hematological neoplasms and introduced several changes in terminology and criteria for diagnosis (Alaggio et. al., 2022; Khoury et. al., 2022). For instance, the term “myelodysplastic syndromes” has been updated to “myelodysplastic neoplasms”, although the abbreviation “MDS” remains unchanged and still in practical use. Additionally, a new battery for defining genetic alterations was established, as well as adjusted terminology for AML MRC, now referred to as AML, myelodysplasia-related (AML MR). The term therapy-related myeloid neoplasm (t-MN) has been updated to MN-pCT (post-cytotoxic therapy) (Khoury et. al., 2022). In lymphoid neoplasms, a refined definition for diagnostics was introduced that more specifically incorporate molecular and genetic criteria (Alaggio et. al., 2022). As the majority of samples in this study were collected before 2022 and previously taken parameters are not always available for re-classification, the 2016 WHO classification was applied in this work.

1.3.1. Hematopoietic Insufficiency in Hematological Neoplasms

Hematological neoplasms are characterized by degrees of hematopoietic insufficiency that arise from the BM’s inability to produce sufficient numbers of mature and functional blood cells (Hoffbrand & Moss, 2015). As a result, patients commonly experience a range of symptoms. Fatigue is a frequent consequence of anemia, where low amounts of erythrocytes are available for oxygen transport across the body. Increased susceptibility to infections is due to leukopenia and the lack of functional immune cells. Lack of platelet production (thrombocytopenia), leads to increased bleeding tendencies and bruising (Manitta et. al., 2011). These symptoms vary depending on the specific neoplasm, but the root cause of these symptoms is found in the BM.

Hematopoietic insufficiency in hematological neoplasms primarily results from malignant cell infiltration in the BM and disruption of its normal function to produce blood cells. Depending on the entity, the malignant cells are of distinct origin. MDS results from accumulating genetic alterations in HSPC leading to dysplasia affecting either single- or multi-lineages of myeloid blasts. In the disease progression, the proliferation of immature blasts and arrest in functional differentiation ultimately lead to a displacement of functional progenitors and a deficiency of mature blood cells. An AML is diagnosed, either overt or preceded by MDS when the proportion of blasts in the BM and peripheral blood exceeds 20 %. MPN on the other hand is characterized by an overproduction of mature blood cells due to genetic alterations (Visvader, 2011; Hoffbrand & Moss, 2015). NHL encompasses a diverse group

of lymphoid neoplasms where the malignant cells derive from lymphocytes (Jones RJ & Armstrong, 2008). In MM, malignant cells are aberrant plasma cells producing abnormal antibodies, additionally harming the body (Barwick et. al., 2019). The commonly resulting hematopoietic insufficiency is primarily attributed to the increasing infiltration of malignant cells in the BM, which physically replace normal hematopoietic progenitors and disrupt the BM microenvironment, leading to impaired differentiation and hematopoiesis (Greaves & Maley, 2012; van Nieuwenhuijzen et. al., 2018). Additionally, malignant cells inhibit remaining healthy HSPC and their potency by aberrant signaling of members of the TGFB signaling family (Jäger et. al., 2021) or mediating the intrinsic induction of transcriptional regulators (Cheng et. al., 2015). Moreover, there is growing evidence that malignant cell signaling further exerts altering effects on the BM microenvironment, impairing the functionality of stromal cells to support normal hematopoiesis and reprogramming them to enhance malignant cell growth (Colmone et. al., 2008; Raaijmakers et. al., 2010; Geyh et. al., 2013; Boyd et. al., 2014; Kode et. al., 2014; Pievani et. al., 2021).

Together, the clonal expansion of malignant cells and their signaling towards HSPC and the BM stroma disrupt normal hematopoiesis, eventually leading to hematopoietic insufficiency (Warr et. al., 2011). Whether the BM microenvironment plays an initiating, contributing, or subordinate role in this process and whether this can be therapeutically modulated to counteract leukemia-induced alterations is subject to current research and this thesis.

1.3.2. Therapy-Related Myeloid Neoplasms: Severe Late Complications of Anticancer Treatment

Therapy-related neoplasms present a critical challenge in oncology as they emerge as a severe late-onset complication following the administration of genotoxic anticancer therapies (Travis, 2006). While the goal of anticancer treatment is the elimination of cancer cells, classical therapies induce unselective damage to all exposed proliferating cells, including healthy tissues (Sinkule, 1984; Friedmann et. al., 2000). The BM has a fast turn-over rate and is particularly vulnerable to therapy-induced damage. The multicellular composition of the BM is crucial for the effective regulation of hematopoiesis and the immune response but consequently consists of cell types with varying proliferative capacities that are potentially damaged by unselective chemotherapy (McNerney et. al., 2017). Therefore, the BM is a primary site of adverse side effects from anticancer therapy, actually used to treat cancers like lymphoma and breast cancer, which most commonly precede t-MN (Allan & Travis, 2005; Nurgalieva et. al., 2011; McNerney et. al., 2017). The relative risk of developing a t-MN is significantly higher as compared to other tissues, presenting incidences

of t-MN diagnosis of approximately 0.06-2.6 per 100,000 cases (Allan & Travis, 2005; Lubeck et. al., 2016). The onset of t-MN can take several years after cytotoxic treatment (Godley & Larson, 2008) and is statistically correlated to the primary cancer, choice of agent, and therapeutic dose (Allan & Travis, 2005). Furthermore, the prognostic outlook for t-MN patients is worse compared to equivalent *de novo* MN due to the higher frequency of adverse-risk genetic aberrations and association with therapy resistance (Travis, 2006; Godley & Larson, 2008; Kuendgen et. al., 2021).

All genotoxic agents potentially drive the development of t-MN. Most cases are linked to exposure to alkylating agents and topoisomerase inhibitors (Pedersen-Bjergaard et. al., 2007; Godley & Larson, 2008). Alkylating agents cause unbalanced chromosomal translocations, particularly on chromosomes 5 and 7 leading to cancerous transformation through the inactivation of tumor suppressor genes typically within five to ten years. Topoisomerase inhibitors induce DNA double-strand breaks, frequently activating oncogenes through balanced translocations. In this case, leukemia manifests within one to four years post-treatment (Allan & Travis, 2005). These classical agents unselectively target proliferating cells, resulting in clonal mutations of the remaining healthy HSPC or surrounding tissue. The recognition of the potential role of the BM microenvironment in therapy-related leukemogenesis has grown within the last decades (McNerney et. al., 2017). Based on this, a novel potential therapeutic target to mitigate t-MN development or improve patient outcomes by implementing the relevance of the BM microenvironment might be offered. To achieve this, a deeper understanding of the BM microenvironment in t-MN development and potential therapy-induced damage is required.

In addition to the long-term side effect of t-MN development, hematopoiesis is acutely impaired during anticancer therapy leading to hematotoxicity in treated patients. In severe cases, therapy-induced hematotoxicity is dose-limiting and leads to attenuation of therapy and consequently to increased morbidity and mortality (Crawford et. al., 2008).

1.3.3. Hematopoietic Insufficiency as Dose-Limiting Side Effect of Anticancer Treatment

Hematopoietic insufficiency is not only a shared characteristic of hematological neoplasms but also a major adverse side effect of anticancer treatment (Wang et. al., 2006). Anticancer therapy is especially relevant in diseases like hematological neoplasms, since here no surgery or radiation therapy alone can cure the disease, due to its systemic nature. However, the unselective targeting of proliferative cells leads to undesired side effects by targeting

non-cancerous tissues. Hematopoietic insufficiency, also known as BM failure or myelosuppression, is the most severe acute side effect of anticancer treatment and causes the additional need for supportive care treatment. Therefore, blood transfusions or hematopoietic growth factors, such as granulocyte colony-stimulating factor (G-CSF), erythropoietin (EPO), or thrombopoietin (TPO) are used to stimulate the production of blood cells during treatment (Wang et. al., 2006; Griffiths et. al., 2022). However, these interventions are limited, and in severe cases, the therapy needs to be interrupted to allow the BM to recover. Consequently, increased morbidity and mortality among patients are reported, making severe hematotoxicity a dose-limiting side effect of oncological therapy (Wang et. al., 2006; Crawford et. al., 2008).

Dose-limiting myelosuppression is reported after various chemotherapeutics, especially unspecific alkylating agents like cyclophosphamide or temozolomide (TMZ) and topoisomerase inhibitors like doxorubicin or etoposide (ETO) (Gerson et. al., 1996; Barreto et. al., 2014), or radiation therapy (Green & Rubin, 2014). To mitigate therapy-related side effects, novel therapeutics were developed to more specifically target cancer cells and spare healthy tissues by their mode of action, which is not restricted to cellular proliferation. For instance, epigenetic regulation by azacitidine (AZA) or decitabine; as well as the selective inhibition of proteins that are specifically upregulated in cancer cells, like members of the BCL2 family (e.g. navitoclax or venetoclax (VEN)), present novel therapeutics. However, these particular agents are also associated with myelosuppression as an acute side effect, which is especially prominent when applied as a combination treatment (San Miguel Amigo et. al., 2011; DiNardo et. al., 2019).

The main reason for therapy-related hematotoxicity is considered to be the damage to HSPC and mature hematopoietic cells. However, the BM microenvironment is equally targeted by cytotoxic therapy, and damage to MSC as central regulators of hematopoiesis might contribute to myelosuppression. Data on MSC damage characterization and functionality are limited. A review from 2018 summarized available data on MSC alteration by various antineoplastic agents, including platinum-based compounds, antibiotics, topoisomerase inhibitors, alkylating agents, and antimetabolites (Rühle et. al., 2018). The most prominent effects on MSC viability were shown by antibiotics such as bleomycin or anthracyclines, which have negative impacts on growth, differentiation, and cell death. On the other hand, MSC were reported to confer efficient DNA damage repair in response to alkylating agents or topoisomerase inhibitors, thereby escaping cell death (Nifontova et. al., 2008; Nicolay et. al., 2016), although being more prone to cellular senescence after exposure (Qi et. al.,

2012). The effect of other antineoplastic agents on MSC are limited as well. For instance, epigenetic regulators affect differentiation capacity due to their expressional regulation; however, there are differential reports on whether differentiation potential is increased or inhibited (Rosca & Burlacu, 2011; Yan et. al., 2014; Bae et. al., 2017; Wenk et. al., 2018). Besides the fact that molecular and functional effects on MSC remain scarce and inconclusive, there is even less knowledge about a potential contribution to therapy-related myelosuppression.

Both, classical chemotherapeutics and more targeted novel therapies are implicated in therapy-related complications. Therefore, two substances of each category were investigated in this thesis on their effects on BM stromal cells and their hematopoietic support function, and are introduced in the next chapter.

1.4. Antineoplastic Substances Targeting the Bone Marrow

1.4.1. Classical Chemotherapeutics

1.4.1.1. Etoposide

The classical chemotherapeutic etoposide ETO is a semi-synthetic derivate of podophyllotoxin first synthesized in 1970 by scientists at Sandoz Laboratories in Switzerland (Keller-Juslen et. al., 1971). Since 1973, its antineoplastic activity has been investigated in clinical trials, and until today, ETO is a commonly administered cytostatic for a range of solid tumors and cancer types (e.g. bronchial carcinoma, malignant lymphomas, leukemia, etc.) (Sinkule, 1984). ETO is either administered orally or by intravenous injection. Dosage depends on the type and severity of the cancer as well as patient characteristics. Broadly, a range of 50-1000 mg/m^2 body surface is applied for 2-5 days (Kato et. al., 2003; Schroeder et. al., 2003; Duong et. al., 2018).

ETO inhibits the ligation activity of the enzyme topoisomerase II, thereby introducing DNA double-strand breaks during replication or transcription (Nitiss, 2009). During the induced G2/M arrest, DNA damage can be repaired by homologous recombination, or cells enter apoptosis if the damage is too high. This unselective targeting of cells is the main reason for ETO being implicated in severe hematotoxic effects (Barreto et. al., 2014). Additionally, persisting DNA double-strand breaks allow chromosomal aberrations, such as *MLL* translocations, which are a common consequence of ETO-induced DNA damage and typical for t-MN (Super et. al., 1997; Aplan, 2006).

1.4.1.2. Temozolomide

The alkylating agent TMZ is a pro-drug that is specifically applied for the treatment of glioblastomas due to its ability to pass the blood-brain barrier, but also for other diseases such as metastatic melanoma (Friedmann et. al., 2000; Cohen et. al., 2005). TMZ is administered orally or intravenously at an initiating dose of 75 mg/m^2 body surface in combination with radiotherapy for 42 days. Afterward, a higher dose of 150-200 mg/m^2 body surface is prescribed for five consecutive days, following a resting period of 23 days, which is repeated for six months (Friedmann et. al., 2000). TMZ generally exerts lower toxicity toward HSPC compared to other alkylating agents. However, a selection of patients, especially females and patients carrying distinct polymorphisms, carry an increased risk for dose-limiting hematotoxicity (Armstrong et. al., 2009; Lin et. al., 2018) as well as the severe delayed side effect of t-MN (Noronha et. al., 2006; Kim et. al., 2009).

Under physiological pH, the pro-drug TMZ is hydrolyzed to MTIC (5-(3-*N*-methyltriazen-1-yl)-imidazole-4-carboxamide), which introduces a methyl group at the DNA (Friedmann et. al., 2000). Initial repair of these lesions is achieved by single-step reversion repair through O6-methylguanine-DNA methyltransferase (MGMT), which contains a cytosine residue in its active core to which the methyl group from the alkylated guanosine is transferred. Thereby, the protein is inactivated irreversibly and subjected to proteasomal degradation (Christmann et. al., 2003). The sensitivity of cells to TMZ-induced damage is highly dependent on the presence of MGMT and the type of polymorphic variant, which differs significantly between cell types and patients (Altinoz et. al., 2017). Resistance against TMZ can be counteracted with the co-application of the MGMT inhibitor O6-benzyl guanine (O6BG). CD34+ myeloid precursors were shown to have comparably low levels of MGMT activity compared to other human tissues, making them particularly susceptible to TMZ (Gerson et. al., 1996). When MGMT is exhausted, the DNA mismatch repair machinery is activated after an initial mispairing and introduces a DNA single-strand break (Christmann et. al., 2003). Accumulating DNA nicks result in the eventual formation of DNA double-strand breaks, ultimately triggering apoptosis to circumvent initiating mutations (Wu J et. al., 1999). Cells deficient in mismatch repair capacity continue DNA replication, leading to transition mutations that contribute to the carcinogenicity of alkylating agents (Christmann et. al., 2003; Allan & Travis, 2005).

1.4.2. Novel Antineoplastic Substances

1.4.2.1. Azacitidine

AZA is a synthetic cytidine-analog first synthesized by Sorm and colleagues in 1964. Since its admission in 2004, AZA has been specifically used for the treatment of hematological neoplasms. Clinically, AZA is applied as a single treatment or combination treatment with other agents as a subcutaneous injection for six cycles of 75 mg/m^2 body surface for seven days with treatment breaks of 21 days. Besides gastrointestinal events and mild side effects such as insomnia or headaches, a more severe side effect of AZA treatment is myelosuppression (U.S. Food and Drug Administration, 2004; Kaminskas et. al., 2005).

As cytidine-analogs, AZA metabolites are incorporated into the DNA during replication or into RNA during transcription. RNA incorporation leads to the inhibition of protein synthesis, while integration into DNA leads to the covalent binding of DNA methyltransferase 1 (DNMT1), which functions as “maintenance methyltransferase”, and copies the methylation pattern onto daughter strands during replication. Due to the additional nitrogen atom at the C5 position of AZA (Figure 2B), the covalent bond cannot be released, and DNMT1 remains bound to the DNA, leading to the inactivation and proteasomal degradation of the enzyme (Stresemann & Lyko, 2008). As a consequence, daughter cells do not carry the methylation pattern and therefore confer expressional changes. Due to the reported aberrant hypermethylation, especially in abnormal hematopoietic cells, AZA was shown to confer clinical specificity against such diseases by reactivating tumor suppressor genes (Christman, 2002). At higher doses, the cytotoxic effects of AZA predominate (Kaminskas et. al., 2005).

1.4.2.2. Venetoclax

VEN (also known as ABT-199) is a selective BCL2 inhibitor (BH3 mimetic) and is generally applied as a combination treatment with other agents to circumvent therapy resistance (Scheffold et. al., 2018). VEN has been approved by the Food and Drug Administration (FDA) since 2018 and is mainly used in the treatment of hematological neoplasms. By selectively inhibiting the anti-apoptotic protein BCL2, the small molecule specifically targets cells with increased BCL2 content and decreases their threshold to enter apoptosis, which is often the case for cancer cells (Hanahan & Weinberg, 2011). For example, chromosomal translocations in lymphomas frequently affect the BCL2 location on chromosome 18, leading to overexpression of the anti-apoptotic protein (Pollyea et. al., 2019). VEN also exerts activity against myeloid blasts of high-risk MDS and AML that also confer increased BCL2 expression (Reidel et. al., 2018; Blum et. al., 2023). The high abundance of BCL2 in cancer

cells can cause resistance against conventional therapies (Guerra et. al., 2019). Therefore, VEN is used to overcome this challenge and is usually applied as a combination treatment with hypomethylating agents such as AZA or decitabine in MDS and AML. The recommended dose for an oral administration of the combination treatment is 400 mg (Koenig & Borate, 2022), while the maximal single agent dose is limited to 1200 mg for 28 days as the first treatment cycle, following shorter treatment cycles of 21 days. Due to the selective targeting of BCL2, heavy thrombocytopenia as seen in the precursor navitoclax is not as frequent anymore. However, common side effects of VEN still include gastrointestinal toxicity, pneumonia, hypokalemia, and hematotoxicity (Scheffold et. al., 2018; Pollyea et. al., 2019).

1.4.3. Radiation Therapy

Radiotherapy is one of the foundational treatments of contemporary anticancer therapy. Radiotherapy aims to shrink or eliminate solid tumors and cancer cells and can be applied in combination with other chemotherapeutic agents. Depending on cancer and patient characteristics, the accumulative dose varies between 20 and 80 Gray (Gy) over multiple weeks, with daily doses of around 2 Gy (Jaffray & Gospodarowicz, 2015). Irradiation-induced DNA strand breaks and oxidative stress are not exclusive to tumorous tissue but damage all exposed cells, including neighboring healthy tissue and remaining healthy HSPC, leading to apoptosis, proliferation arrest, or even the development of t-MN (Allan & Travis, 2005; Eriksson & Stigbrand, 2010).

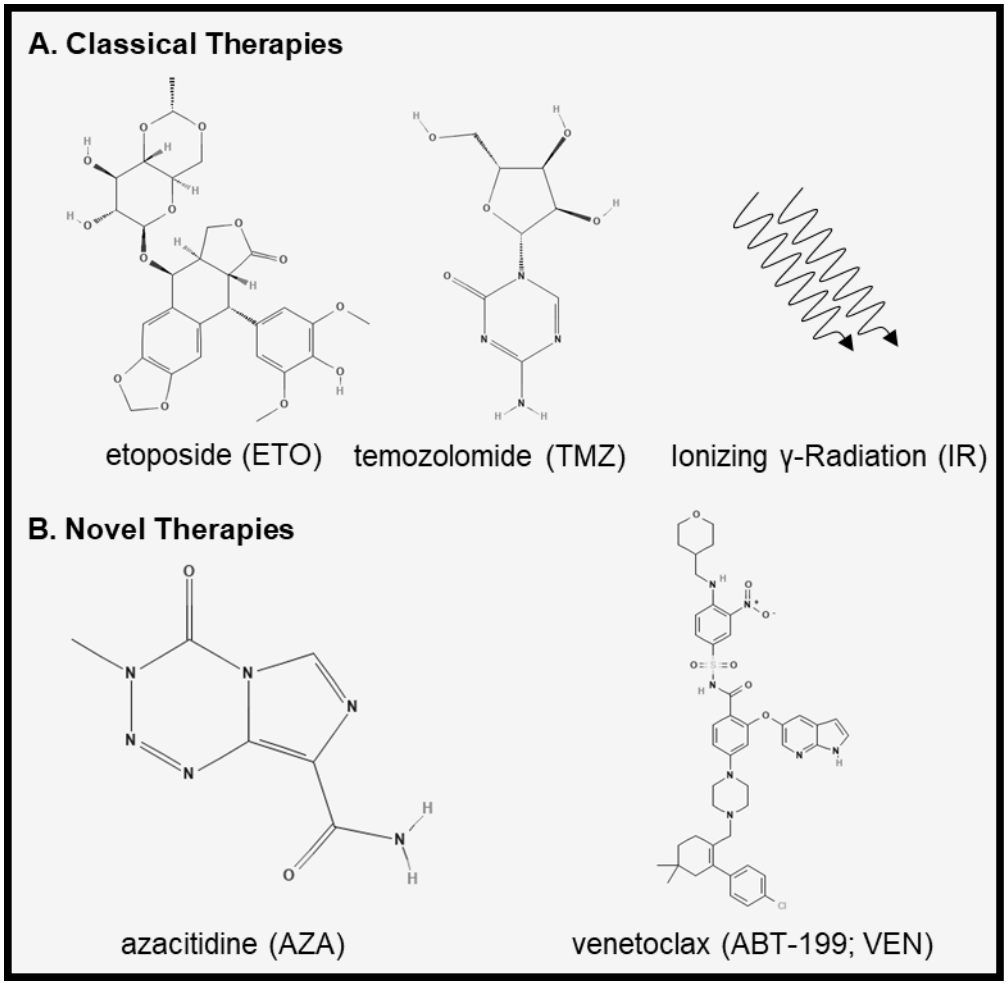

Figure 2. The structural formula of antineoplastic agents that are addressed in this thesis. A. The classical chemotherapeutic ETO is implicated in dose-limiting myelosuppression and the development of t-MN. The alkylating agent TMZ is assumed to be involved in therapy-induced myelosuppression and is often applied in combination treatment with radiotherapy. **B**. Novel therapeutics AZA and VEN are primarily applied in hematological neoplasms, the main reported side effect is hematotoxicity. Structural images were obtained from the National Center for Biotechnology Information using the database PubChem (National Center for Biotechnology Information, 2024a, 2024b, 2024c, 2024d). Images were adapted in MS PowerPoint 2013.

1.5. Scope and Aim of this Thesis

The BM niche harbors and regulates the hematopoietic system. Among the tightly controlled equilibrium, MSC play a central role in supporting HSPC survival, maintenance, migration, and differentiation. MSC interact with HSPC through ligand-receptor binding and paracrine signaling of cytokines and growth factors. Their multilineage differentiation supplies the niche with additional regulatory components. Given their crucial role, understanding MSC contributions to hematopoietic insufficiency in hematological neoplasms and therapy-related side effects is vital for elucidating the underlying mechanisms and improving therapeutic strategies.

This thesis summarizes the recent findings from our group regarding the significance of MSC in hematological pathological situations. MSC from patients with *de novo* myeloid (MDS, MPN, and AML) and lymphoid (NHL and ALL) neoplasms, as well as of patients with MM and precursor states (MGUS to SMM to MM) were extensively characterized to identify distinct or overlapping mechanisms involved in the pathogenesis of these diseases (Figure 3A). Furthermore, t-MN (t-MDS and t-AML), are myeloid neoplasms evolving due to previous antineoplastic treatment, also characterized by hematopoietic insufficiency, but with limited treatment options and poor clinical outcome. Still, the potential involvement of MSC is not clear so far. Therefore, MSC from patients suffering from t-MN were characterized functionally and molecularly, identifying similarities and differences to respective *de novo* MN. Additionally, the impact of pharmacological doses of common antineoplastic agents was investigated in healthy MSC to elucidate their potential direct damage to the BM and involvement in therapy-related side effects (Figure 3B).

A closer understanding of the role of MSC in the pathogenesis of hematological neoplasms, as well as their involvement in therapy-related adverse side effects might reveal novel therapeutic approaches that consider the role of the BM microenvironment and preserve their functionality.

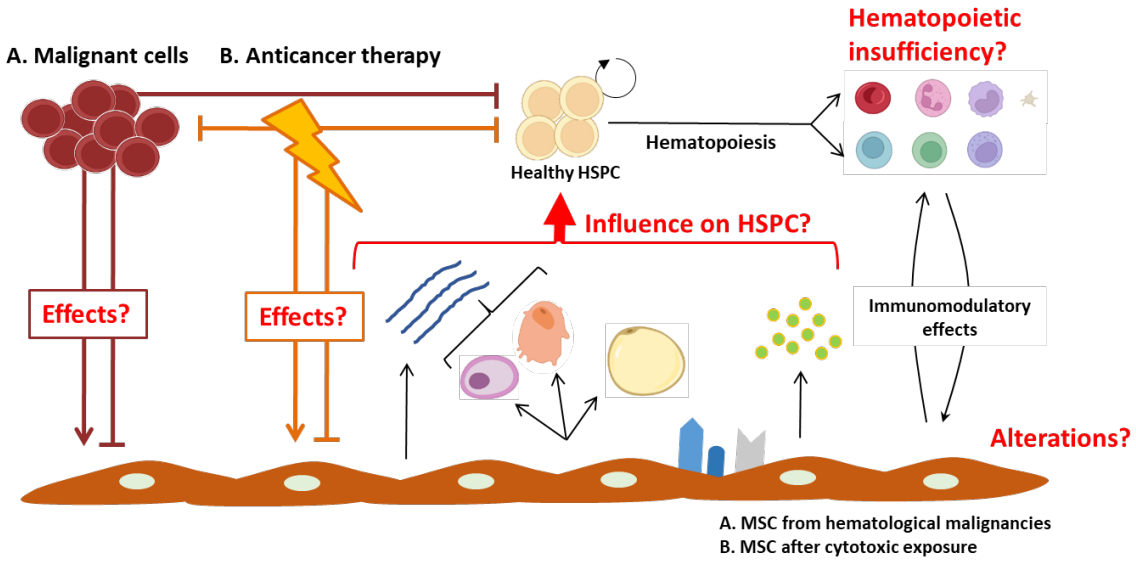

Figure 3. Schematic depiction of the research questions addressed in this thesis. A. Hematological neoplasms share the common characteristic of BM infiltration of malignant cells, accompanied by hematopoietic insufficiency. How malignant cells affect MSC in the BM, which potential alterations of MSC characteristics are induced, and whether this has an impact on the regulation of HSPC and hematopoietic insufficiency is investigated for myeloid and lymphoid neoplasms in manuscripts 2.1, 2.2 and 2.3. **B.** Anticancer therapies are associated with hematopoietic insufficiency and may contribute to the pathogenesis of t-MN. Whether direct effects of antineoplastic agents lead to molecular and functional alterations in BM-derived MSC resulting in hematopoietic insufficiency and t-MN development is investigated in manuscripts 2.3 and 2.4. Graphics were designed using Biorender.com and MS PowerPoint 2013.

2. Manuscripts

This thesis consists of four manuscripts. The first manuscript 2.1. “Overlapping stromal alterations in myeloid and lymphoid neoplasms” (Bogun et. al., 2024b) represents a comprehensive analysis of patient-derived MSC expanding the knowledge about the potential role of MSC in the pathogenesis of myeloid and lymphoid neoplasms, including MDS, MPN, AML, NHL, and ALL. Stromal alterations across these entities included decreased cellular growth and differentiation capacity towards the osteogenic-chondrogenic lineage and were inducible in healthy MSC by exposure to respective malignant cell supernatants. Molecular analyses showed overlapping dysregulation of signaling pathways involved in these cellular processes, namely BMP-, TGFB-, and WNT. Notably, alterations were mediated by SMAD-dependent TGFB signaling in myeloid neoplasms, while lymphoid neoplasms primarily involved non-canonical TGFB signaling.

The second manuscript 2.2. “Stromal alterations in patients with monoclonal gammopathy of undetermined significance, smoldering myeloma, and multiple myeloma” (Bogun et. al., 2024a) investigates MSC derived from premalignant MGUS over the course of asymptomatic SMM and progression to MM. Functional stromal alterations were already imprinted in MGUS and clearly progressed in SMM and MM. RNA sequencing analyses revealed BMP/TGFB-signaling as mediators of stromal alterations.

In the third manuscript 2.3. “Functional and molecular effects on the bone marrow stroma in patients with therapy-related myeloid neoplasms” (*submission planned*), MSC derived from patients with *de novo* and therapy-related MN MSC were investigated and showed overlapping functional and molecular deficits, including signaling pathways TGFB and WNT. Additionally, t-MN MSC exhibited distinct dysregulation of immunomodulatory genes, mainly affecting immune checkpoint signaling involving CD274, CD47, and Tumor necrosis factor (TNF) signaling, highlighting specific alterations potentially induced by anticancer therapy.

The last manuscript 2.4. “Antineoplastic therapy affects the *in vitro* phenotype and functionality of healthy human bone marrow-derived mesenchymal stromal cells” (Scherer *et. al.,* 2024), summarizes the therapy-induced damage of healthy MSC by antineoplastic therapy potentially contributing to therapy-related hematotoxicity. Indeed, ETO and AZA induced functional alterations in healthy MSC, including cellular growth and differentiation capacity respectively, while TMZ and VEN rather affected hematopoietic cells and spared BM-derived MSC.

2.1. Overlapping Stromal Alterations in Myeloid and Lymphoid Neoplasms

Lucienne Bogun, Annemarie Koch, Bo Scherer, Ulrich Germing, Roland Fenk, Uwe Maus, Felix Bormann, Karl Köhrer, Patrick Petzsch, Thorsten Wachtmeister, Guide Kobbe, Sascha Dietrich, Rainer Haas, Thomas Schroeder, Stefanie Geyh, and Paul Jäger

Abstract

Myeloid and lymphoid neoplasms share the characteristics of potential bone marrow infiltration as a primary or secondary effect, which readily leads to hematopoietic insufficiency. The mechanisms by which clonal malignant cells inhibit normal hematopoietic stem and progenitor cells (HSPCs) in the bone marrow (BM) have not been unraveled so far. Given the pivotal role of mesenchymal stromal cells (MSCs) in the regulation of hematopoiesis in the BM niche it is assumed that MSCs also play a relevant role in the pathogenesis of hematological neoplasms. We aimed to identify overlapping mechanisms in MSCs derived from myeloid and lymphoid neoplasms contributing to disease progression and suppression of HSPCs to develop interventions that target these mechanisms. MSCs derived from healthy donors (n = 44) and patients diagnosed with myeloproliferative neoplasia (n = 11), myelodysplastic syndromes (n = 16), or acute myeloid leukemia (n = 25) and B-Non-Hodgkin lymphoma (n = 9) with BM infiltration and acute lymphoblastic leukemia (n = 9) were analyzed for their functionality and by RNA sequencing. A reduced growth and differentiation capacity of MSCs was found in all entities. RNA sequencing distinguished both groups but clearly showed overlapping differentially expressed genes, including major players in the BMP/TGF and WNT-signaling pathway which are crucial for growth, osteogenesis, and hematopoiesis. Functional alterations in healthy MSCs were inducible by exposure to supernatants from malignant cells, implicating the involvement of these factors in disease progression. Overall, we were able to identify overlapping factors that pose potential future therapeutic targets.

Journal	Cancers
Impact factor	5.2 (2023)
Contribution to publication	10 %

The own contribution of this manuscript includes the partial conduction of experiments, and collection, assembly, analysis and interpretation of the obtained samples, as well as contribution to manuscript writing, proof reading and final approval.

Type of authorship	Co-author
Status of publication	Published 30.05.2024

cancers

MDPI

Article

Overlapping Stromal Alterations in Myeloid and Lymphoid Neoplasms

Lucienne Bogun [1], Annemarie Koch [1], Bo Scherer [1], Ulrich Germing [1], Roland Fenk [1], Uwe Maus [2], Felix Bormann [3], Karl Köhrer [4], Patrick Petzsch [4], Thorsten Wachtmeister [4], Guido Kobbe [1], Sascha Dietrich [1], Rainer Haas [1], Thomas Schroeder [1], Stefanie Geyh [1,*,†] and Paul Jäger [1,*,†]

[1] Department of Hematology, Oncology and Clinical Immunology, Medical Faculty, University of Duesseldorf, 40225 Duesseldorf, Germany; lucienne.bogun@uni-duesseldorf.de (L.B.); annemarie.koch@med.uni-duesseldorf.de (A.K.); bo.scherer@med.uni-duesseldorf.de (B.S.); germing@med.uni-duesseldorf.de (U.G.); fenk@med.uni-duesseldorf.de (R.F.); kobbe@med.uni-duesseldorf.de (G.K.); sascha.dietrich@med.uni-duesseldorf.de (S.D.); haas@med.uni-duesseldorf.de (R.H.); thomas.schroeder@uk-essen.de (T.S.)
[2] Department of Orthopedic Surgery and Traumatology, Medical Faculty, University of Duesseldorf, 40225 Duesseldorf, Germany; uwe.maus@med.uni-duesseldorf.de
[3] Bioinformatics.Expert UG, 12305 Berlin, Germany; f.bormann@bioinformatics.expert
[4] Biological and Medical Research Center (BMFZ), Medical Faculty, Heinrich-Heine-University, Universitätsstraße 1, 40225 Düsseldorf, Germany; koehrer@uni-duesseldorf.de (K.K.); patrick.petzsch@hhu.de (P.P.); thorsten.wachtmeister@uni-duesseldorf.de (T.W.)
* Correspondence: stefanie.geyh@med.uni-duesseldorf.de (S.G.); paulsebastian.jaeger@med.uni-duesseldorf.de (P.J.); Tel.: +49-211-8119606 (S.G. & P.J.); Fax: +49-211-8104296 (S.G. & P.J.)
† These authors contributed equally to this work.

Simple Summary: Myeloid and lymphoid malignant cells can become the dominant population in the bone marrow and thus inhibit healthy hematopoiesis. Patients suffer enormously as a result. In addition to the directly mediated inhibition of healthy hematopoietic stem and progenitor cells, indirect mechanisms via so-called mesenchymal stromal cells can also play a role. We are focusing our research on the latter and would like to identify functional and molecular overlapping mechanisms within the various myeloid and lymphoid neoplasms. In the future, it may be possible to block these mechanisms and thus prevent disease progression or improve healthy hematopoiesis.

Abstract: Myeloid and lymphoid neoplasms share the characteristics of potential bone marrow infiltration as a primary or secondary effect, which readily leads to hematopoietic insufficiency. The mechanisms by which clonal malignant cells inhibit normal hematopoietic stem and progenitor cells (HSPCs) in the bone marrow (BM) have not been unraveled so far. Given the pivotal role of mesenchymal stromal cells (MSCs) in the regulation of hematopoiesis in the BM niche it is assumed that MSCs also play a relevant role in the pathogenesis of hematological neoplasms. We aimed to identify overlapping mechanisms in MSCs derived from myeloid and lymphoid neoplasms contributing to disease progression and suppression of HSPCs to develop interventions that target these mechanisms. MSCs derived from healthy donors ($n = 44$) and patients diagnosed with myeloproliferative neoplasia ($n = 11$), myelodysplastic syndromes ($n = 16$), or acute myeloid leukemia ($n = 25$) and B-Non-Hodgkin lymphoma ($n = 9$) with BM infiltration and acute lymphoblastic leukemia ($n = 9$) were analyzed for their functionality and by RNA sequencing. A reduced growth and differentiation capacity of MSCs was found in all entities. RNA sequencing distinguished both groups but clearly showed overlapping differentially expressed genes, including major players in the BMP/TGF and WNT-signaling pathway which are crucial for growth, osteogenesis, and hematopoiesis. Functional alterations in healthy MSCs were inducible by exposure to supernatants from malignant cells, implicating the involvement of these factors in disease progression. Overall, we were able to identify overlapping factors that pose potential future therapeutic targets.

check for updates

Citation: Bogun, L.; Koch, A.; Scherer, B.; Germing, U.; Fenk, R.; Maus, U.; Bormann, F.; Köhrer, K.; Petzsch, P.; Wachtmeister, T.; et al. Overlapping Stromal Alterations in Myeloid and Lymphoid Neoplasms. *Cancers* **2024**, *16*, 2071. https://doi.org/10.3390/cancers16112071

Academic Editor: Orlando Guntinas-Lichius

Received: 19 April 2024
Revised: 27 May 2024
Accepted: 28 May 2024
Published: 30 May 2024

Keywords: myeloid neoplasms; lymphoid neoplasms; MPN; MDS; AML; ALL; NHL; MSC; bone marrow microenvironment; osteogenesis; hematopoietic insufficiency; RNA sequencing

1. Introduction

Myeloid neoplasms are mainly represented by myelodysplastic syndromes (MDSs), myeloproliferative neoplasia (MPN), or acute myeloid leukemia (AML), while lymphoid neoplasms comprise aggressive and indolent non-Hodgkin lymphoma (NHL) as well as acute lymphoblastic leukemia (ALL) [1,2]. Independent of the underlying specific genetic aberrations, these hematological neoplasms originate from hematopoietic cells at various differentiation stages, such as hematopoietic stem and progenitor cells (HSPCs) or line-determined progenitor cells. Irrespective of the molecular aberrations, in general, they confer growth and survival advantages to those cells over normal HSPCs [3–5].

A common feature of these neoplasms is the infiltration of the bone marrow (BM) by malignant cells, either primarily or secondarily, with a functional takeover resulting in hematopoietic insufficiency of various degrees. Consequently, patients experience cytopenia-related symptoms, including anemia, infections, and bleeding, which represent the major causes of morbidity and mortality [6,7].

The detailed underlying mechanisms by which clonal malignant cells functionally inhibit normal HSPCs in the BM are only partially understood. To some extent, the suppression of normal hematopoiesis certainly results from direct interactions between clonal malignant cells and healthy HSPCs [8]. The BM microenvironment, particularly of mesenchymal stromal cells (MSCs), plays a pivotal role in the regulation of normal hematopoiesis and their immunomodulatory potential and contributes to extracellular matrix formation. Recent work from our group, as well as other research groups, has shed some light on the pathophysiological role of the BM microenvironment in the progression and myelosuppression of hematological neoplasms [9–14].

For instance, MSCs derived from patients with AML and MDS show structural, functional, and epigenetic alterations, along with specific gene expression signatures resulting in inadequate stromal support for normal hematopoiesis [10,14–18].

Similar results have been reported in lymphoid malignancies. Indeed, MSCs derived from patients with multiple myeloma exhibit structural and functional abnormalities comparable to those observed in MDS and AML [9] and significantly contribute to hematopoietic insufficiency in these patients. Co-culture experiments of patient-derived ALL blasts with healthy MSCs resulted in an inhibition of osteogenic differentiation and a reduced number of osteoblastic cells [19].

In the light of potential overlaps in the phenotype, functionality, and molecular mechanisms of MSCs between myeloid and lymphoid neoplasms, we performed a comprehensive analysis including functional assessments and RNA sequencing (RNAseq) of MSCs from patients with both myeloid and lymphoid neoplasms. The identification of common pathological pathways could help to design a targeted therapy in the future to restore adequate stromal support of normal hematopoiesis.

2. Materials and Methods

2.1. Patients, Healthy Controls, and Cell Preparation

Bone marrow (BM) samples were obtained from 70 patients covering AML (n = 25), MDS (n = 16), MPN (n = 11), ALL (n = 9), and NHL ($\geq$10% BM infiltration) (n = 9) who received their initial diagnosis between 2019 and 2023. A total of 44 age- and sex-matched healthy donors served as a control group (HC, median age: 67 years, range: 33–86 years). Detailed patient characteristics are given in Table 1.

Table 1. Patient demographics and clinical characteristics.

	No.	%
Patients No.	**70**	
Sex		
Male	42	60
Female	28	40
AML No.	**25**	
Median age, years (Range)	61	(25–74)
Diagnosis WHO 2016 [1]		
Median BM infiltration, % (Range)	69	(35–95)
Median ANC, $\times 10^3/\mu L$ (Range)	16.50	(0.00–21.00)
Median platelets, $\times 10^3/\mu L$ (Range)	60	(6–279)
Median HB, g/dL (Range)	9.4	(4.2–11.9)
MDS No.	**16**	
Median age, years (Range)	68	(47–81)
Diagnosis WHO 2016 [2]		
Median BM infiltration, % (Range)	Dysplasia [2], blasts > 5% in 6	
Median ANC, $\times 10^3/\mu L$ (Range)	1.76	(0.20–6.89)
Median platelets, $\times 10^3/\mu L$ (Range)	69	(27–467)
Median HB, g/dL (Range)	9.2	6.6–11.2
MPN No.	**11**	
Median age, years (Range)	60	(22–75)
Diagnosis WHO 2016 [3]		
Median BM infiltration, % (Range)	Proliferation, blasts < 5%	
Median ANC, $\times 10^3/\mu L$ (Range)	16.10	(5.40–47.20)
Median platelets, $\times 10^3/\mu L$ (Range)	534	(54–1564)
Median HB, g/dL (Range)	13.6	(9.3–16.6)
ALL No.	**9**	
Median age, years (Range)	47	(22–69)
Diagnosis [4]		
Median BM infiltration, % (Range)	85	(40–95)
Median ANC, $\times 10^3/\mu L$ (Range)	2.35	(0.34–15.20)
Median platelets, $\times 10^3/\mu L$ (Range)	53	(9–138)
Median HB, g/dL (Range)	11.8	(8.5–16.7)
NHL No.	**9**	
Median age, years (Range)	63	(38–76)
Diagnosis [5]		
Median BM infiltration, % (Range)	25	(10–90)
Median ANC, $\times 10^3/\mu L$ (Range)	3.40	(0.33–8.90)
Median platelets, $\times 10^3/\mu L$ (Range)	193	(68–345)
Median HB, g/dL (Range)	12.5	(4.8–15.2)

[1] AML with rec. gen. abnormalities (n = 11), AML MRC (n = 7), AML NOS (n = 7). [2] MDS-MLD (n = 7), MDS-EB-I (n = 4), MDS-EB-II (n = 2), MDS-RS-MLD (n = 3). [3] PV (n = 2), ET (n = 2), PMF (n = 2), atyp. CML (n = 1), CML (n = 1), MPN-U (n = 1), post-PV-MF (n = 1), post-ET-MF (n = 1). [4] precursor-B-ALL (n = 6), precursor-T-ALL (n = 1), mature-T-ALL (n = 2). [5] LPL (n = 3), MCL (n = 2), HCL (n = 2), B-CLL (n = 1), MZL (n = 1). Abbreviations: AML, Acute Myeloid Leukemia; ANC, Absolute Neutrophil Count; ALL, Acute Lymphoblastic Leukemia; BM, Bone Marrow; CLL, Chronic Lymphatic Leukemia; CML, Chronic Myeloid Leukemia; EB-I, with Excess Blasts 5–9% in BM; EB-II, with Excess Blasts 10–19% in BM; ET, Essential Thrombocythemia; HB, Hemoglobin; HCL, Hairy Cell Leukemia; LPL, Lymphoplasmacytic Lymphoma; MCL, Mantle Cell Lymphoma; MF, Myelofibrosis; MDS, Myelodysplastic Syndrome; MLD, Multilineage Dysplasia; MRC, MDS Related Changes; MPN, Myeloproliferative Neoplasia; MZL, Marginal Zone Lymphoma; NOS, Not Otherwise Specified; PMF, Primary Myelofibrosis; PV, Polycythemia Vera; RS, Ringsideroblasts; U, Unclassified.

MSCs were derived from the mononuclear cell (MNC) fraction of these specimens and cultured as previously described [10]. All experiments were carried out using MSCs derived from passages 3–4. Furthermore, in 19 cases of these patients, MSCs as well as MNCs for generations of conditioned media were available.

2.2. Cell Culture Conditions and Reagents

MSCs were cultured as previously described [20]. MNC fractions were cultured in RPMI + 20% FBS (Sigma Aldrich, St. Louis, MO, USA) and supplemented with IL-3, IL-6, SCF (all 10 ng/mL), and FLT-3Ligand (20 ng/mL), all from Peprotech, Hamburg, Germany, as previously described [8].

2.3. Growth Properties and Cellular Senescence

The colony-forming unit fibroblast (CFU-F) activity was determined in primary culture under a light microscope. Cumulative population doublings (CPDs) were calculated after each passage. ß-galactosidase activity, as an indicator for senescent cells was measured using the Cellular Senescence Detection Kit (Biolabs, San Diego, CA, USA) in accordance with the manufacturers' instructions. Under a light microscope, visualization of senescent cells, as reflected by their blue staining through ß-galactosidase activity, was evaluated as previously described [10].

2.4. Conditioned Media

To generate conditioned media (CM), $2.7 \times 10^4/cm^2$ cells of the cell lines NALM-6, MAVER-1, MEC-1, HL-60, and K422 (all purchased from DSMZ, Braunschweig, Germany) were cultivated in T75 cm^2 culture flasks for 3 days following the manufacturers' instructions. For patient-derived CM, $2 \times 10^5/cm^2$ BM-derived MNCs from patients with myeloid neoplasms (MPN, MDS, and AML) and lymphoid neoplasms (ALL and NHL) and MNCs ($n = 16$) from healthy controls (HC) were cultivated in RPMI + 20% FBS medium supplemented with IL-3, IL-6, SCF (10 ng/mL), and FLT3-Ligand (20 ng/mL, all from Peprotech, Hamburg, Germany). Cells were cultured under humidified conditions at 37 °C and 5% CO_2. After incubation time, cell-free CM was harvested by filtration (Minisart® 0.45 µm, Sartorius AG, Göttingen, Germany) and stored at −80 °C for further experiments.

2.5. Differentiation Properties

Differentiation assays from native MSCs into adipocytes, chondroblasts, and osteoblasts were performed on Passage 3. For adipogenic differentiation, DMEM high glucose was supplemented with Insulin (0.1 mg/mL), Indomethacin (0.2 mM), Isobutylmethylxanthane (1 mM), and Dexamethasone (10^{-6} M) (all Sigma Aldrich), and differentiated for 21 days. Visualization of lipid vacuoles was performed using Oil Red O staining. Chondrogenic differentiation was induced with DMEM high glucose supplemented with TGF-ß3 (10 ng/mL, PeproTech Inc., Rocky Hill, CT, USA), L-Proline (40 µg/mL), ascorbate-2-phosphate (50 µg/mL), ITS+1 (1%) and Dexamethasone (10^{-7} M) (All from Sigma Aldrich). After 21 days, chondrogenic pellets were cut on a cryostate, and proteoglycane was stained with Safranin O. Alizarin Red staining was used to visualize osteogenic differentiation after 14 days of osteogenic induction in a medium consisting of DMEM low glucose ascorbic acid (50 µg/mL), ß-glycerol-phosphate (10 mM) and dexamethasone (10^{-7} M). Differentiation assays were performed as previously published [10,20]. Images were digitalized using SPOT Software version 4.7 (Diagnostic Instruments Inc., Sterling Heights, MI, USA) as previously described [10] and visualized using an Axiovert 25 microscope (Zeiss, Jena, Germany). We used a 5 objective-Zeiss CP-Achromat 5 Ph0 for native and osteogenic differentiated MSCs, a 10 objective-Zeiss CP-Achromat 10 Ph1 for adipogenic differentiated MSCs, and a 2.5 objective-Zeiss CP Achromat for chondrogenic differentiation.

2.6. Hematopoietic Support—Long-Term Culture-Initiating Cells (LTC-IC Assay)

A total of 0.8×10^6–1.0×10^6 MSCs were cultivated on 96-well plates (Costar, Corning, KS, USA) and irradiated with 30 Gray using Gulmay RS225 X-ray equipment. Subsequently, 6×10^3 healthy CD34+ cells were plated on these MSC feeder layers and then further processed using the same conditions and reagents as in our previous work [10,15].

2.7. Co-Culture with Conditioned Media and Blocking of TGFB1

To investigate which properties are mostly affected on healthy MSCs due to the malignant compartment, $1.4 \times 10^4/cm^2$ healthy MSCs were cultivated with primary MDS, MPN, AML, ALL or MM-derived MNCs, or cell line-derived CM (generated as described in 2.4) from INA-6, RPMI-8226, NALM-6, MEC-1, MAVER-1, SU-DHL-6, and K-422 on a 6-well plate. After 72 h (at 37 °C, 5% CO_2 under humidified conditions), viable cells were counted under a light microscope and were included in the following experiments.

Using SD208, an active ATP-competitive transforming growth factor-β receptor 1 (TGF-βRI) (ALK5) inhibitor (0.5 µM diluted in 10 mM DMSO, Biotechne/R&D systems, Minneapolis, Minnesota) to investigate the effects on TGFB1 signaling, healthy MSCs and MSCs derived from myeloid and lymphoid neoplasms were induced towards osteogenic differentiation and SD208 or DMSO (as control) was added to each medium change during the 14 days of osteogenic induction.

2.8. Quantitative Realtime-Polymerase Chain Reaction (qRT-PCR)

Total RNA was isolated using the RNeasy Micro Kit or Mini Kit (Qiagen, Hilden, Germany) with the optional DNase digestion, following the manufacturer's instructions. Using a StepOne Plus Realtime PCR cycler and Power SYBR Green PCR Mastermix (Applied Biosystem, Life Technologies, Carlsbad, CA, USA), qRT-PCR was performed in duplicate. GAPDH was used as reference control and differences in mRNA expression level were evaluated with the ΔΔCT method. Primer sequences can be provided on request.

2.9. RNA-Sequencing

For transcriptome analysis, total RNA was DNase digested and quality controlled before further use by quantifying them fluorometrically (Qubit RNA HS Assay, Thermo Fisher Scientific Inc., Waltham, MA, USA) and checking their integrity by capillary gel electrophoresis on the FragmentAnalyzer system using the "Total RNA Standard Sensitivity Assay" (Agilent Technologies, Inc., Santa Clara, CA, USA). Libraries were prepared using the VAHTS universal V6 RNA-seq library prep kit (Illumina, San Diego, CA, USA). Briefly, 500 ng total RNA was used for poly(A) RNA selection, fragmentation, cDNA generation, adapter ligation, strand selection, and library amplification. Bead-purified libraries were normalized and finally sequenced on the NextSeq 2000 system (Illumina Inc. San Diego, CA, USA) with a read setup of 1 × 151 bp. The bcl2fastq tool was used to convert the bcl files to fastq files and for adapter trimming and demultiplexing as previously described [8].

2.10. Bioinformatical Analysis

Bioinformatical analysis A: The fastq files were analyzed with CLC Genomics Workbench (version 20.0.3, QIAGEN, Venlo, The Netherlands). The reads of the samples were both adapter and quality trimmed. The default settings were used (bases < Q13 were trimmed from the end of the reads, ambiguous nucleotides max. 2). The reads were mapped against the human reference genome (hg38, GRCH38.103) (14 April 2021). Multi-group comparisons of the individual conditions (3 replicates each) were performed and statistically analyzed. The Empirical Analysis of DGE (version 1.1, cutoff = 5) algorithm implemented in CLC was used for this purpose. A p-value < 0.05 was considered significant after multiple test corrections for FDR. Using the Ingenuity Pathway Analysis software (Qiagen Inc., 2020, Venlo, The Netherlands), the data were further analyzed while maintaining the standard parameters ($|FC| \geq 1.5$, $p \leq 0.01$, P [FDR] ≤ 0.05).

Bioinformatical analysis B: Raw sequencing reads were cropped at their 5′ position by 12 bases using the Trimmomatic function "headcrop". The following analyses were initiated in the first quarter of 2023 using the online resources listed below. Alignment was then performed in a two-pass approach with STAR v2.7.2 [18] (adapted from https://docs.gdc.cancer.gov/Data/Bioinformatics_Pipelines/Expression_mRNA_Pipeline and described previously) [8]. New splice junctions were detected in the first pass and added to the reference human genome GRCh38.97 (hg38) to complement the second pass alignment.

Subsequently, featureCounts (1.6.5) and DESeq2 were applied to the aligned reads to identify differentially expressed genes. An FDR q-value of below 0.05 was used as the criterion to assign significance. Additionally, StringTie (2.0.3) [19] was applied to calculate fragments per kilobase of transcript per million mapped reads (FPKM-values). Further downstream analyses contained principal component analysis using the R package FactoMineR (1.42) and heatmaps created with pheatmap (1.0.12). Gene set enrichment analysis (GSEA, Broad Institute, Boston, MA, USA) was tested with FPKM values on custom gene sets or gene sets within the Molecular Signature Database (https://www.gsea-msigdb.org/gsea/msigdb). Gene Ontology analysis was conducted using a Panther over-representation test (https://amigo.geneontology.org/amigo) using the significantly differentially expressed genes as input. Significance was addressed by a Fisher's exact test followed by a Bonferroni correction.

2.11. Data Access

RNA sequencing expression data are currently being deposited in the NCBI Sequence Read Archive (SRA) with BioProject ID PRJNA1091937.

2.12. Statistical Analysis

GraphPad Prism 8.4.3 (GraphPad Software Inc., La Jolla, CA, USA) was used for statistical analyses. The Wilcoxon signed-rank test was used for intraindividual analysis, while a two-sided unpaired Student's *t*-test was performed for interindividual comparison. SEM and means are provided for every experiment and a statistically significant level of $p \leq 0.05$ was determined (* $p \leq 0.05$; ** $p \leq 0.01$; *** $p \leq 0.001$; **** $p \leq 0.0001$).

3. Results

3.1. MSCs from Myeloid and Lymphoid Neoplasms Showed Similar Alterations in Growth Capacity and Cellular Senescence

MSCs are usually characterized in vitro by a spindle-type morphology, their colony-forming unit fibroblast (CFU-F) activity, and plastic adherence, which results in the formation of a parallel growing feeder layer reaching 80% confluence after a few days in culture. Our group and others have previously reported deficits in morphology, which were accompanied by a diminished growth capacity as well as a higher percentage of cellular senescence, especially for MDS and AML-derived MSCs [10,15]. In contrast, MSCs derived from MPN, ALL, and NHL displayed a less atypical phenotype when compared to the disturbed morphology observed in MDS and AML-derived MSCs from new samples obtained for this comprehensive study (Figure 1A). Moreover, MDS and AML-derived MSCs were more prone to cellular senescence, as reflected by active ß-galactosidase in contrast to the relatively lower incidence observed in MPN, ALL, or NHL-derived MSCs (Figure 1B).

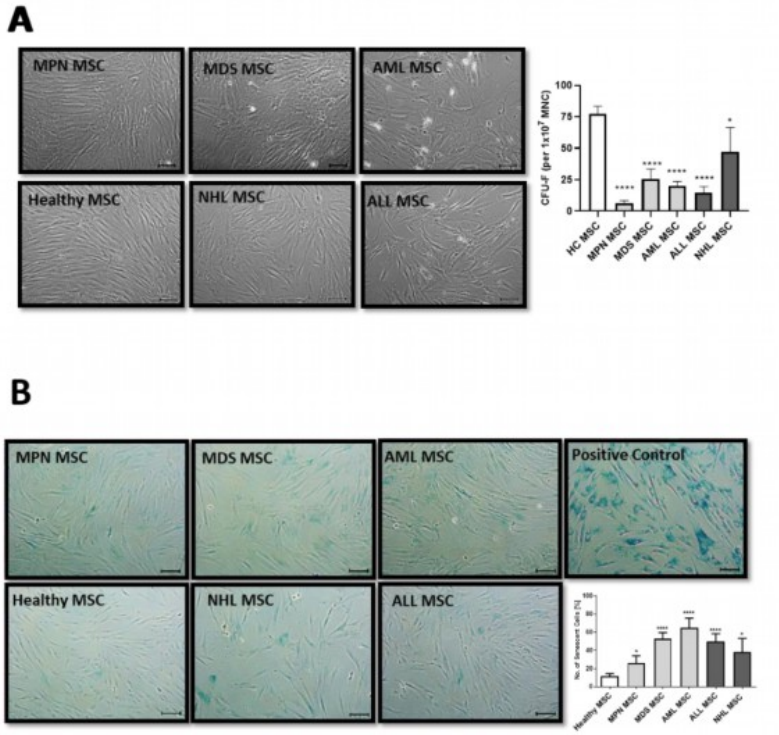

Figure 1. Growth capacity and cellular senescence of MSCs from myeloid and lymphoid neoplasms. (**A**) Representative micrographs of phenotype from Healthy-, MPN-, MDS-, AML-, ALL-, and NHL-derived MSCs with scale bars indicating 100 µm are shown. Bar charts of the CFU-F activity of MSCs from Healthy-, MPN-, MDS-, AML-, ALL-, and NHL-derived MSCs. (**B**) Representative micrographs of number of cellular senescence visualized in blue from native Healthy-, MPN-, MDS-, AML-, ALL-, and NHL-derived MSCs in Passage 3 after the ß-galactosidase staining. Scale bars indicating 100 µm are shown. Asterisks display *p*-values * $p < 0.05$, **** $p < 0.0001$.

3.2. MSCs from Myeloid and Lymphoid Neoplasms Showed Similar Reduced Chondrogenic-Osteogenic Differentiation Capacity

Patient-derived MSCs from all groups showed a reduced chondrogenic differentiation capacity, as evidenced by the pellet size and safranin O staining. In detail, MDS-derived MSCs showed the most severely reduced chondrogenic differentiation capacity, visualized by Safranin O and a very rough and cracking surface. MPN and AML-derived MSCs displayed a rather normal smooth chondrogenic surface structure, albeit with an uneven distribution of proteoglycan (Figure 2A). Conversely, ALL-derived MSCs exhibit the highest amount of proteoglycan despite their reduced pellet size, while NHL-derived MSCs showed a similar reduced chondrogenic differentiation capacity to that of MDS-derived MSCs (Figure 2A).

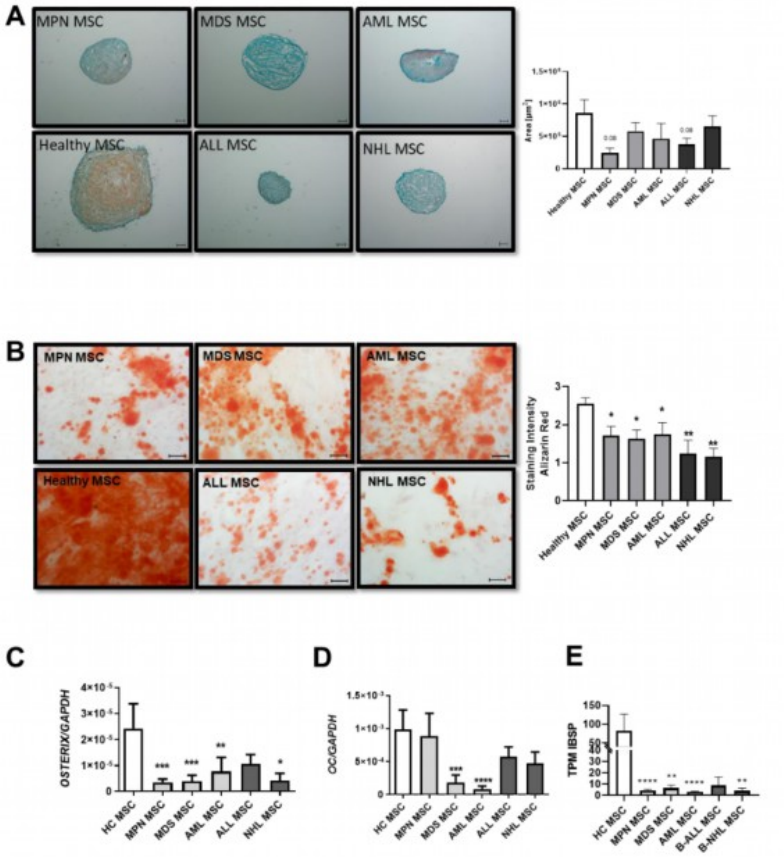

Figure 2. Chondrogenic and osteogenic differentiation capacity of MSCs derived from patients with myeloid and lymphoid neoplasms. (**A**) Representative micrographs of proteoglycan after Safranin O staining of chondrogenic-induced MSCs after 21 days. Scale bars indicating 100 µm are shown. Right side: area size in µm of chondrogenic pellets after 21 days of induction was measured and presented as bar charts of the respective MSC group in comparison to healthy MSCs (white bar). (**B**) Osteogenic differentiation was induced for 14 days and stained with Alizarin Red. Representative micrographs of the osteogenic potential of MSCs. Scale bars indicating 100 µm are shown. Right side: Bar charts represent staining intensity of observed osteogenic differentiation. Osteogenic differentiation capacity was graded according to the microscope as previously described [10]. Bar charts of the mRNA expression level of osteogenic factors *OSTERIX* (**C**), *OSTEOCALCIN* (**D**), and (**E**) TPM values from our sequencing data of Integrin Binding Sialoprotein (IBSP). For all other experiments, results are expressed as Mean ± SEM. Asterisks display *p*-values * $p < 0.05$, ** $p < 0.01$, *** $p < 0.001$, **** $p < 0.0001$.

MSCs derived from MDS and AML showed a 1.4-fold reduced osteogenic differentiation capacity (MDS: 1.8; AML: 1.75 vs. HC: 2.6, *p* value: ≤0.05), as already published. However, a significantly greater reduction of 2-fold with regard to osteogenic differentiation capacity was seen in MSCs derived from MPN patients (MPN: 1.3 vs. HC: 2.6 *p*-value ≤ 0.01). Even more pronounced, ALL-derived MSCs showed a 2.6-fold reduced

osteogenic capacity in comparison to MSCs derived from healthy individuals, while NHL-derived MSCs showed the greatest osteogenic impairment with a 3.2-fold diminished differentiation capacity (ALL: 1 and NHL: 0.8 vs. HC: 2.6, *p*-values $\leq$ 0.01) (Figure 2B). Molecular analysis revealed a correlation with decreased expression levels of osteogenic factors such as OSTERIX or OSTEOCALCIN in qRT-PCR analysis. A significantly decreased expression of OSTERIX was measured in all patient-derived MSCs (Figure 2C), while OSTEOCALCIN was strongly reduced in MPN, ALL, and NHL-derived MSCs, and significantly reduced in MDS and AML-derived MSCs (Figure 2D). Furthermore, TPM values of IBSP from our sequencing data were strongly decreased in derived MSCs (Figure 2E).

Using Oil Red O staining, no significant differences in adipogenic differentiation capacity could be observed in adipogenic-induced MSCs after 21 days of culture.

3.3. Insufficient Hematopoietic Support in Myeloid and Lymphoid Neoplasms

Crucial interactions governing the homing, proliferation, or differentiation of HSPCs with MSCs are well established. Stem Cell Factor (*SCF*), also known as *KITLG*, plays a pivotal role in the differentiation, proliferation, and survival of hematopoietic stem cells. Notably, *SCF* was found to be strongly downregulated in MSCs over all hematological neoplasms, and MSCs derived from myeloid neoplasms exhibited the most pronounced reduced mRNA expression of SCF (Figure 3A). The stromal cell-derived factor-1 (*SDF-1*, also known as *CXCL12*) is another key player in hematopoiesis, directing migrating HSPCs or activating lymphocytes. *SDF-1* mRNA expression was striking diminished in all MSCs from patients with hematological neoplasms, encompassing both myeloid and lymphoid (Figure 3B). In terms of functionality assessed in a long-term culture initiating cell (LTC-IC) assay, decreased expression of SCF and SDF-1 was associated with decreased hematopoietic supporting capacity. In detail, MDS and AML MSCs exhibited a 9.2-fold and a 7.6-fold reduced hematopoietic supporting capacity, while MPN MSCs showed a 1.2-fold, ALL-derived MSCs a 2.1-fold, and NHL-derived MSCs a 2.4-fold reduced hematopoietic supporting capacity (Figure 3C, LTC-IC frequency in %, HC: 0.55%; MPN: 0.31%, MDS: 0.05% *p*-value: $\leq$0.05; AML: 0.12% *p*-value: $\leq$0.05; ALL: 0.238; NHL: 0.19% *p*-values: $\leq$0.05).

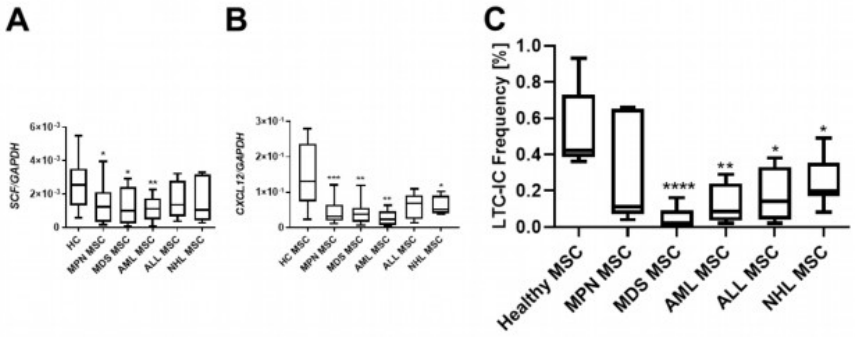

Figure 3. Hematopoietic supporting capacity of MSCs from myeloid and lymphoid neoplasms. Box plots of mRNA expression of hematopoietic factors SCF (**A**) and SDF-1 (*CXCL12*) (**B**) in healthy-, MPN-, MDS-, AML-, ALL-, and NHL-derived MSCs. mRNA expression was measured by qRT-PCR in healthy MSCs (n = 22), MPN MSCs (n = 14), MDS MSCs (n = 10), AML MSCs (n = 10), ALL MSCs (n = 7), and NHL MSCs (n = 4). (**C**) Box plots of long-term initiating cell (LTC-IC) assay frequency. Hematopoietic supporting capacity of MSCs derived from healthy and hematological neoplasms. Asterisks display *p*-values * $p < 0.05$, ** $p < 0.01$, *** $p < 0.001$, **** $p < 0.0001$.

3.4. Patient-Derived and Cell Line-Derived Conditioned Media-Induced Deficits in MSCs

Previous data from our group and others have indicated that conditioned media from AML cell lines could induce various alterations in MSCs related to growth and differentiation [4,20]. Building upon the hypothesis that soluble factors contribute to stromal alterations, we exposed healthy MSCs to conditioned Media (CM) derived from MNCs of healthy controls and patients with MDS, AML, ALL, and NHL. Additionally, we use CM from commercial cell lines covering AML HL-60, ALL NALM-6, and NHL cell lines MEC-1, MAVER-1, and K422.

After 3 days of cultivation, CM of the two NHL cell lines MAVER-1 and K422 induced phenotypical disorganization and reduced growth capacity in healthy MSCs. In contrast, CM from the MEC-1 NHL cell line and the NALM-6 ALL cell line did not induce these alterations in healthy MSCs (Figure 4A,B). Interestingly, CM derived from all cell lines induced a significantly reduced expression of *OSTEOCALCIN* in MSCs (Figure 4C).

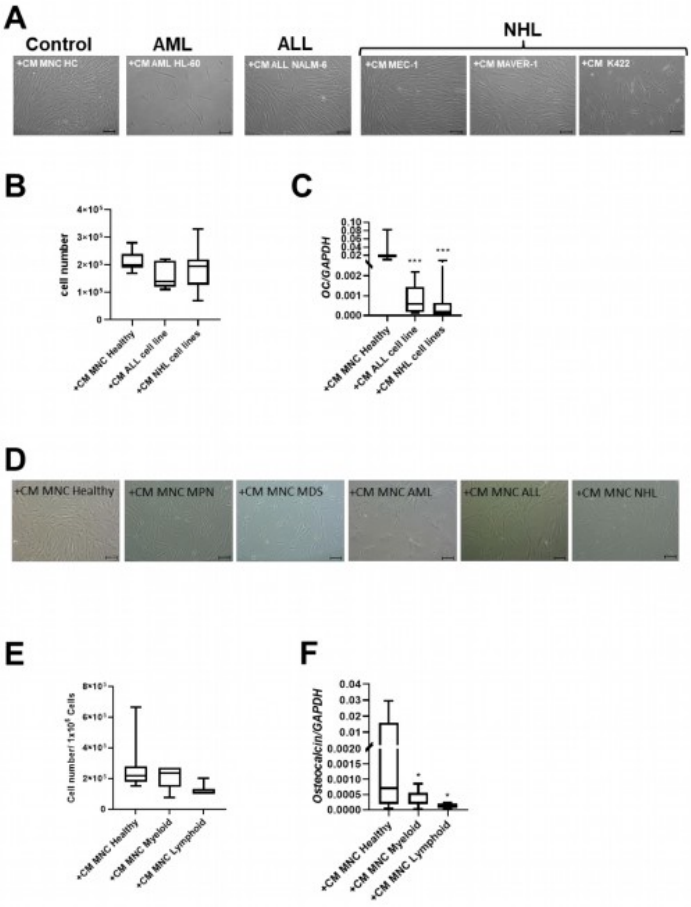

Figure 4. Exposure of healthy MSCs to conditioned media (CM) derived from cell lines and BM-MNCs from patients with myeloid and lymphoid neoplasms. (**A**) Representative micrographs of phenotype

of healthy MSCs after co-culture with CM from cell line HL-60 (AML), cell line NALM-6 (ALL), MEC-1, MAVER-1, and K422 (all three NHL). Scale bars indicating 100 µm are shown. (**B**) Box plots present cell numbers of healthy MSCs after 3 days of co-culture with CM derived from cell lines. (**C**) Box plots demonstrate mRNA expression of osteogenic factor *OSTEOCALCIN* measured by qRT-PCR. (**D**) Representative micrographs of phenotype of healthy MSCs after co-culture with patient-derived CM from BM-derived MNCs for 3 days. Scale bars indicating 100 µm are shown. Calculated cell numbers of manipulated healthy MSCs after 3 days of co-culture are given in box plots. (**E**) Box plots present cell numbers of healthy MSCs after 3 days of co-culture with CM derived from patients' BM MNCs. (**F**) mRNA expression of *OSTEOCALCIN* was measured in healthy MSCs after co-culture with respective patients BM-MNC CM by qRT-PCR. Asterisks display *p*-values * $p < 0.05$, *** $p < 0.001$.

Conditioned media (CM) derived from the MNCs of patients with myeloid neoplasms lead to significantly reduced growth capacity of MSCs (cell number: +CM MNC Healthy: 2.7×10^5; +CM MNC Myeloid: 2.2×10^5) after three days. A 2.2-fold reduced cell number of healthy MSCs after co-culture with CM derived from the MNCs from ALL and NHL patients was found and accompanied by a dramatically altered broad and flattened morphology (Figure 4D,E).

Consistent with experiments using cell line derived CM, the mRNA expression for *OSTEOCALCIN* was 22-fold significantly diminished after co-culture with CM derived from MNCs from patients with myeloid neoplasms, and 63-fold diminished after co-culture with CM derived from MNCs from patients with lymphoid neoplasms (Figure 4F).

3.5. RNA Sequencing Distinguish MSCs from Myeloid and Lymphoid Neoplasms

In order to obtain a better understanding of the observed functional and morphological alterations in MSCs across all entities at the molecular level and to identify common mechanisms, we performed RNA sequencing. As the respective entities are heterogeneous, we selected some representative samples from patients with B-cell neoplasms. In the case of myeloid neoplasms in AML, we concentrated on those with blasts, whereas in patients with MDS or MPN, we concentrated on those without blast proliferation. As a result, RNA sequencing data were available for MSCs from five healthy donors, four MDS, five MPN, four AML, four B-NHL, and five B-ALL. A detailed patient characteristic of the selected samples is shown in Figure 5A. In myeloid neoplasms (MDS, MPN, and AML), RNA sequencing revealed, in comparison to normal donors, 606 exclusively differentially expressed genes in MPN MSCs, 303 in MDS, and 413 in AML (FDR: $q \leq 0.05$). The greatest overlap, with 261 differential genes in MSCs, was noted between the pathophysiologically closely related myeloid stem cell diseases MDS and AML. This is reflected to some extent in the result of the Principal Component Analysis (PCA), which grouped the samples of MDS and AML closer to each other than to those of the other entities (Figure 5B). In contrast, the number of differentially expressed genes overlapping between MDS and MPN was 123, while the comparison of MPN and AML MSCs reveals a total overlap of 176 differentially expressed genes. Looking at the intersection of genes differentially expressed in all three entities, 263 overlapping differentially expressed genes were found. In lymphoid neoplasms of B-cell origin (B-ALL, B-NHL), RNA sequencing showed 972 differentially expressed genes exclusively in B-ALL derived MSCs and far fewer (193) exclusively differentially expressed in B-NHL-derived MSCs in comparison to healthy controls (FDR: $q \leq 0.05$). Meanwhile, there was an overlap of 196 differentially expressed genes in the MSCs of patients from both lymphoid entities.

A

No	Entity	Diagnosis	Age	Bone marrow infiltration	ANC (/µL)	platelets (x 10^3/µL)	HB (g/dL)	Karyotype	Molecularbiology	CRP (mg/dl)
1	AML	AML NOS[1]	74	blasts 73%	50	47	10.9	missing	missing	4.6
2	AML	AML MRC[1]	53	blasts 80%	1504	19	11.8	complex aberrant	missing	8.3
3	AML	AML with rec. gen. abnormalities[1]	66	blasts 80%	960	60	9.5	normal	biall. CEBPA	0.3
4	AML	AML with rec. gen. abnormalities[1]	68	blasts 78%	2212	120	11.9	normal	FLT3-ITD^{high}, NPM1	11.0
1	MDS	MDS with multilineage dysplasia (MLD)[1]	64	MLD (blasts <5%)	1836	127	7.9	normal	U2AF1	missing
2	MDS	MDS with multilineage dysplasia (MLD)[1]	56	MLD (blasts <5%)	1600	63	9,1	missing	missing	0.6
3	MDS	MDS-RS-MLD[1]	68	MDS-MLD (blasts <5%)	2499	461	9,2	normal	SF3B1	0.1
4	MDS	MDS with multilineage dysplasia (MLD)[1]	65	MLD blasts <5%	6890	467	9,2	missing	missing	2.5
1	MPN	atypical CML in chron. phase[1]	56	CML (blasts <5%)	47200	406	12.7	normal	BCR-ABL and JAK2 negativ	2.6
2	MPN	Primary Myelofibrosis (PMF)[1]	58	PMF (blasts <5%)	16100	158	13.4	der(1;7)(q10;p10)	JAK2 V617F positiv	0.8
3	MPN	post-PV-MF[1]	75	PV (blasts <5%)	10270	472	9.5	normal	JAK2 V617F positiv	0.5
4	MPN	Polycythemia Vera (PV)[1]	64	PV (blasts <5%)	23240	570	16.6	normal	JAK2 V617F positiv	0.1
5	MPN	Essential Thrombocythemia (ET)[1]	59	ET (blasts <5%)	17000	1546	13.6	normal	JAK2 V617F positiv	0.1
1	B-ALL	common-B-ALL	49	blasts 85%	340	9	8.5	normal	BCR-ABL negativ	2.2
2	B-ALL	common-B-ALL	49	blasts 95%	476	11	9.5	t(9;22)	BCR-ABL positiv	0.3
3	B-ALL	common-B-ALL	29	blasts 94%	1820	83	9.8	normal	BCR-ABL negativ	7.5
4	B-ALL	Pro-B-ALL	69	blasts 90%	2349	127	11.8	normal	BCR-ABL negativ	0.4
5	B-ALL	common-B-ALL	67	blasts 70%	7380	85	14.0	normal	BCR-ABL negativ	7.7
1	B-NHL	Lymphoplasmacytic Lymphoma (LPL)	70	lymphoma cells 70%	4440	330	10.3	del11q22.3	missing	6.6
2	B-NHL	Hairy Cell Leukemia (HCL)	45	lymphoma cells 90%	342	68	4.8	missing	B-RAF Exon 15	10.2
3	B-NHL	Mantle Cell Lymphoma (MCL)	76	lymphoma cells 25%	3395	193	12.1	trisomy 11	missing	0.5
4	B-NHL	Chronic Lymphatic Leukemia (CLL)	61	lymphoma cells 36%	4875	308	15.2	trisomy 12, del17p	IGHV unmutated	0.1

[1]according to WHO 2016 classification
MRC, MDS-related changes; NOS, not otherwise specified; RS, ringsideroblastic; CML, chronic myeloid leukemia

B

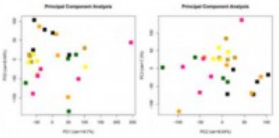

C

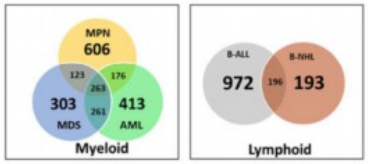

D

Meloid Neoplasms All regulated					
HOXB7	ELN	REXO1	MPPED2	SLC44A3	PHLDA2
ZNF703	FOXD1	INMT	EN1	CCDC85B	SNHG25
AC093849.2	MAOA	AC130371.2	HNRNPKP2	FGL2	ZNF414
RAB5IF	EXTL1	OSR2	COBL	AC304619.3	AC010327.1
HOXB4	LDHAP7	NUDT3	TCEA1	ATP13A2	SOCS2-AS1
NPIPA5	TNXB	ENC1	ZFPM1	GBP1P1	CACNA2D4
HOXB3	MTCO2P12	FADD	RIMS3	NUDT10	IL33
STEAP4	APOL3	TBX1B	BONF	POU2F2	RFX1
MOCOS	SERPINE2	LINC02328	PIAS4	SOCS2	ENDOG
HOXB2	CACNA2D3	FRAS1	TCF3	GSK3A	AKAP17A
HOXB6	HOXA3	FZD2	MMP24OS	PRDX2	CYP4V2
TIMP4	FOXP2	PI16	HOXA5	SLC25A26	SH3BP1
HAND2-AS1	LMO3	GIA1P1	AC080112.1	HS01181	AC010326.3
HAND2	LIMK1	SESN2	TSKS	IBSP	PLEC
LINC00900	HOXB-AS3	LBH	MTA1	MUPH	FAM129A
IQCJ-SCHIP1	ALDH1B1	FIBCD1	PSMA6	TMEM30B	PQLC3L
EEF1A1P5	C8ARP	RFLNB	WDR24	SLC47A1	AL137191.1
PNMA2	HIVEP3	G0S2	NR2F1-AS1	ANKRD1	RAB11B
BTG1	MIR137HG	AC117409.1	NRXN3	ZC3H18	MAP3K8
EEF1A1P11	HENMT1	ABCA2	ASPA	FASN	DCN
IRAK3	IL26	ATP1A2	AC022034.1	SHISA2	TGFBR3L
UQCRFS1P1	PTER	STX1B	PSAT1	UBTD1	NF2
PDE1A	PIP5KL1	SMURF2P1	SCAF1	AC008038.1	HOXA4
PTMAP4	SAMD5	SYBU	LINC01629	HTRA3	HOXA6
CNTNAP3B	CASP1	CERS3-AS1	IFIZ7	TNNT1	BMP5
MT-TY	MET	SPRED3	AC245100.3	TRIM67	AL133346.1
AL135905.2	FRMD5	SLC9A7	ATF5	PDGFD	PAK4
OLFML1	FBLN2	TLNRD1	C4orf48	DKK2	INHBA
HOXB5	HOXB8	PCGF2	OLFM4	SLC20A1	DOCK10
RP527A	ZNF628	ZNF579	SELENOP	ADAM19	RPLP0
PLPP4	AL590714.1	SLC14A1	FOXC2	MGST1	FOXCUT
RPL18AP3	SIPA1	TBX15	SLC22A17	ZNF771	EEF1A1
RPSA	ZNF865	HOXB-AS1	LRFN4	EEF1A1P19	IFNGR1
GYPE	LYPD1	HOXA2	FBRSL1	ABHD5	DEXI
EMILIN2	SLPI	ZNF787	MYH1	ITGA3	TBC1D8
TGFB1	ZBTB7A	DMGDH	TLE5	FHOC1	POU3F3
NR2F1	TPGS1	NETO2	AK5	ACKR3	GLDN
CRLS1	GNG5	SCAF4	RNF185	PTPRO-AS1	HOMER3
B3GALT2	IL20RB	PPP1R9B	MGRN1	HOAC30	SMOC2
PRR7	ALX1	PTPRE	PDF	MT-TL1	GMIP
PITX2	MYH13	LAMB3	AC055839.2	XPNPEP2	FBXO36
PSMB9	IL13RA2	MAGEL2	ZFP42	NKX6-1	ARHGAP22
CEBPG	HSP90AB2P	ERFE	GET4	GLCCI1	PITPNM8
HOXA-AS2	CITED4	PPDPF	SERP2	FZD9	

Lymphoid Neoplasms All regulated				
HOXB7	EXTL1	MSX2	AL844908.1	NFIB
HOXB4	DCDC1	HMOX1	FAT3	CLEC14A
MAB21L2	FURT3	MIR137HG	CNTNAP3B	SERPINE2
HOXB3	PTPRE	MKRN3	OLFML2A	IRAK1
HAND2	FYN	NKX6-1	SLC9A7	RABEP2
HAND2-AS1	DKK2	LINC01684	KCNS3	ABCA13
HOXB2	NRXN3	CITED4	CX3CL1	LRRN3
KYNU	C15orf54	SYNDIG1	BONF	ADAMTS12
HOXB5	IL33	TLR3	ALDH3B1	TNFRSF19
HOXB6	ADARB1	POU2F2	GASK1B	HIST1H2BC
ALX1	ICAM5	ADAMTS5	FBLN2	SALL1
MOCOS	HOXA-AS2	COL9A2	NR2F1	KRTAP1-1
TRIM67	CCNJL	LRIG1	SCRG1	CMAHP
SCARA5	RFLNB	PADI1	SPATA20P1	HAGHL
COX20P1	RPL10P9	GSC	GPR158	EN1
EMILIN2	MCF2L	COL8A2	MAP3K7CL	PLPP4
PITX2	BMP5	LINC01345	HOXA2	SCN2A
MYH13	LAMB3	TMEM30B	XPNPEP2	HIP1R
SFRP2	MGARP	AC093849.2	AL691420.1	LIMK1
C1QTNF1	THRB	ASPN	STX1B	RAP1GAP
HEY2	ADGRD1	PTPRO-AS1	IL17B	TGFB1
BMP8B	HIVEP3	AL121612.2	NUDT10	
MET	UBTD1	COL21A1	TMEM204	
LINC02432	SOCS2-AS1	TMTC1	SCN9A	
HOXB-AS3	PTPRD	STON2	IRX1	
IFIZ7	PLCB4	SYT12	KHDRBS3	
PARP15	INHBA	HOXA3	HPD	
LGI2	ITGA3	MYHAS	LTBP2	
IL13RA2	GPM6B	COL4A4	PDXK	
RSRC1	LYPD6B	HTRA3	PDE4D	
PRAG1	HOXA5	TNFRSF11B	CXCL16	
PHKA1	OLFM4	APCDD1	CADM3	
CBLB	PDE11A	MAPK10	TSKS	
LINC00623	TIMP4	KCNJ15	GPC5	
B3GALT2	ANKRD1	AC018697.1	SLC34A1	
FLG	SCN3A	TPM1	EMX2OS	
BCAS4	HOXB8	RUBCNL	WNT5B	
SOCS2	IQCJ-SCHIP1	KRT17	P2RX5	
PRG4	MOK	ZNF703	SMOC2	
HOXB-AS1	LMO3	COL4A2	MARCH4	
RAB39B	TNFAIP6	LYPD6	OTOF	
TBX15	LYPD1	TMEM30B	PCDH9	
EPGN	COBL	MYEF2	LINC00869	
CHL1	CA2	ZMYND15	CLDN14	

Figure 5. RNA Sequencing. (**A**) Clinical parameters of patients' characteristics, which were included in RNA sequencing. (**B**) Principal Component Analysis (PCA) of MSCs from Healthy (n = 5, black),

MPN MSCs (n = 5, purple), MDS (n = 4, brown), AML (n = 4, yellow), B-ALL (n = 5, orange), and B-NHL (n = 4, green). (**C**,**D**) Venn diagrams of differentially expressed genes (FDR q-value $\leq$ 0.05) for MSCs from myeloid (left: MPN, MDS, and AML) and for MSCs from lymphoid (right: B-ALL and B-NHL) neoplasms with tables of overlapping differentially expressed genes of 263 in MSCs of myeloid neoplasms (MPN, MDS, and AML MSCs; left) and 196 in MSCs of lymphoid (B-ALL and B-NHL; right) neoplasms. Green highlighted genes indicate overlapping genes in all hematological neoplasms and. black highlighted genes were exclusively found in the respective group (myeloid or lymphoid) (TGFB1*, was significant in p-value 0.005, FDR q-value 0.1, B-ALL sample 2 exhibited a lower Transcript per million (TPM) expression of TGFB1 than all other samples).

In the next step, we focused on differences and similarities between MSCs from myeloid and lymphoid neoplasms to unravel overlapping genes and pathways that may contribute to hematopoietic insufficiency. For that purpose, we performed a detailed examination of the differentially expressed genes (FC $\geq$ 1.5, FDR q $\geq$ 0.05) across all hematological neoplasms, encompassing 263 genes for the myeloid and 196 genes for the lymphoid entities. First, we concentrated on the subset of differentially expressed genes that we only found in the myeloid neoplasms. Among those are key players such as TGFBR3L, Integrin Binding Sialoprotein (IBSP), Frizzled-2 (FZD-2), and Frizzled-9 (FZD-9), which are essential for governing osteogenesis (Figure 5C,D). On the other hand, there were differentially expressed genes which we only overserved in patients with lymphoid neoplasms. Among them are BMP8B, WNT5B, TLR3, and TNFRSF19, which are pivotal for proliferation or apoptosis. This subset of genes also contained a substantial number of genes encoding collagens (COL9A2, COL8A1, COL21A1, COL4A4, and COL4A2), which are crucial for tissue development, osteogenesis, and cartilage formation (Figure 5C,D).

3.6. RNA Sequencing Revealed Overlapping Genetic Signatures Associated with Chondrogenic-Osteogenic Differentiation and Hematopoietic Supporting Capacity in MSCs from Myeloid and Lymphoid Neoplasms

Looking at the group of "overlapping genes" that were differentially expressed in all hematological neoplasms, we found candidates crucially involved in osteogenesis and hematopoiesis, such as BMP5 (Bone morphogenetic protein 5). This is a member of the TGF superfamily and a key player in osteogenesis, regulating several downstream processes including downregulated genes such as *HAND2*, the T-Box transcription factor *TBX15*, and *PITX2*, which are crucial for skeletal formation. The Dickkopf WNT signaling pathway inhibitor 2 (DKK-2) is another crucial factor for osteogenesis, with cross-talking to the BMP/TGF signaling pathway including PITX2 [21–23]. Furthermore, in MSCs from all hematological neoplasms, we observed an overexpression of *HOXA2* and *HOXA3* as well as *HOXB2-8* genes, which are crucial for hematopoietic cell fates and skeletal development. The group of overlapping genes also included proteins participating in the formation of extracellular matrix (ECM) such as *EMILIN2* or *TIMP4* (Metalloproteinase Inhibitor 4) (Figure 6A,B). Gene set enrichment analysis (GSEA) reveals a strong enrichment of genes for osteogenesis and hematopoiesis in MSCs derived from patients with myeloid and lymphoid neoplasms (Figure 6C). The differentially expressed genes were further corroborated through Reactome and Gene ontology (GO) analysis, encompassing processes as outlined in more detail in Supplementary Figure S1. Interestingly, looking for differences among the entities, Reactome analysis indicated a strong enrichment of genes involved in cell cycle regulation, particularly in the patients with MDS and AML. On the other hand, genes governing ECM processes were particularly affected in MSCs derived from lymphoid neoplasms. In line with this, GO analysis provides a similar tableau with a significant enrichment of genes involved in growth and cell death processes that were most affected in MDS- and AML-derived MSCs, and a strong enrichment of genes involved in skeletal system formation in MSCs from all groups (Supplementary Figure S2).

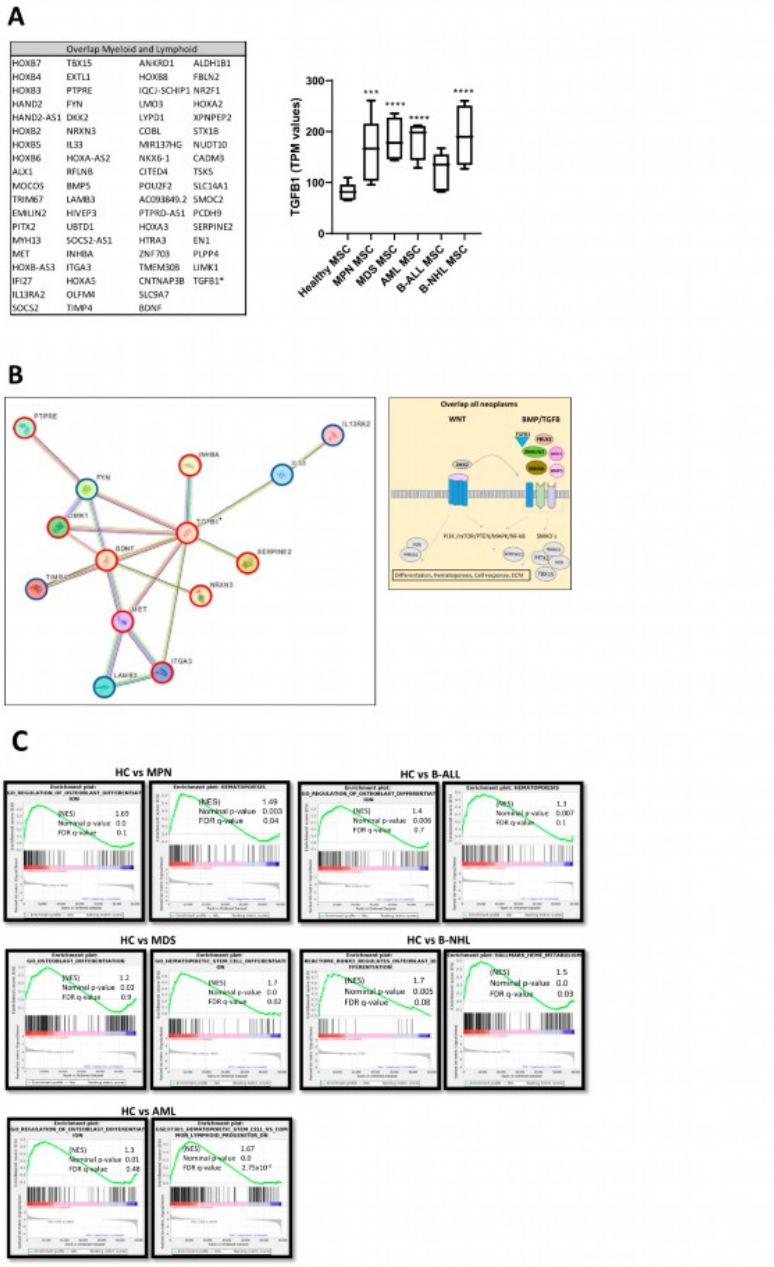

Figure 6. Overlapping differentially expressed genes in all hematological neoplasms affect cell processes. (**A**) Left side: Graphical overview of representative overlapping differentially expressed

genes that were found in MSCs from all hematological neoplasms from overlapping genes in the respective group from green highlighted in Figure 5D. A total of 74 differentially overlapping genes were identified in all hematological neoplasms. Right side: Transcript per million (TPM) values of TGFB1 in MSCs from our RNA sequencing data. Asterisks display adjusted *p*-values *** $p < 0.001$, **** $p < 0.0001$. (**B**) A total of 14 of these 74 genes are directly linked and form a potential theoretical protein network to TGFB signaling as visualized by using the STRING database (**B**, right side). A protein network was generated with the STRING database (Version 12.0) and adapted. Blue-circled genes indicate downregulation and red-circled genes indicate upregulation of these genes in our RNA sequencing. Visualization of further genes from the "overlap all neoplasms" group, that are regulators or related to the WNT and BMP/TGFB signaling pathways as well as downstream targets of these signaling pathways such as *PITX2*, *HAND2*, or *TBX15*, that were found in all hematological neoplasms, were contrasted with healthy MSCs. These genes play crucial roles in ECM, differentiation, or hematopoiesis (TGFB1*, was significant in *p*-value 0.005, FDR q-value 0.1, B-ALL sample 2 exhibited a lower Transcript per million (TPM) expression of TGFB1 than all other samples). (**C**) Strong enrichment in genes related to osteogenesis or hematopoiesis in all MSC groups reflected by gene set enrichment analysis (GSEA). Normalized enrichment score (NES), *p*-value, and false discovery rate (FDR) are given.

3.7. TGFB1 as Potential Overlapping Upstream Regulator

Ingenuity Pathway Analysis (IPA) predicted TNF or TGFB1 as potential upstream regulators in all patient-derived MSCs (Figure 7). Gene set enrichment analysis (GSEA) confirmed a strong enrichment for a TGFB signature but not for a TNFA signature in all patient-derived MSCs contrasted to healthy MSCs, except for B-NHL-derived MSCs. The latter showed a strong enrichment of an interferon signature (Figure 7).

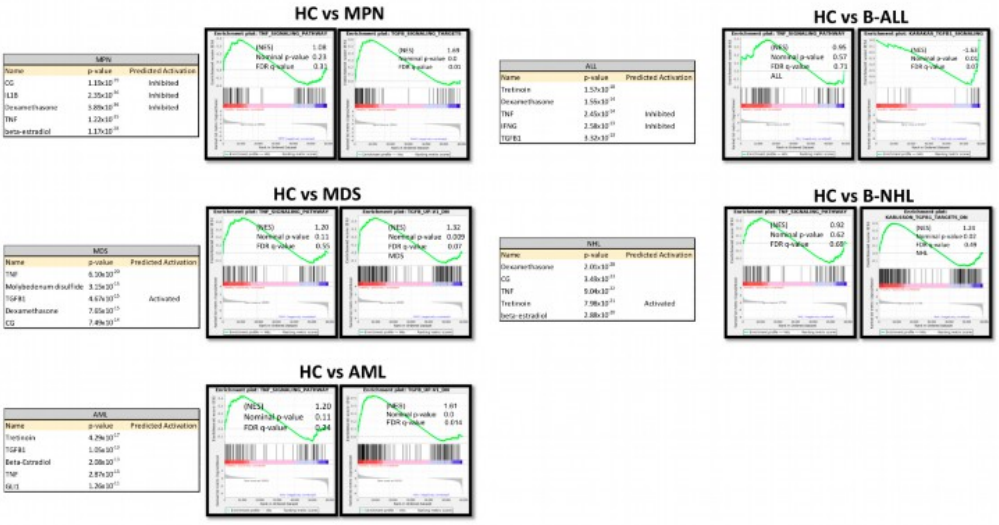

Figure 7. Ingenuity Pathway Analysis (IPA) and gene set enrichment analysis (GSEA) of native MSCs from Healthy, MPN, MDS, AML, ALL, and NHL MSCs. Tables of Ingenuity Pathway Analysis (IPA) and the prediction of potential upstream regulators from native MSCs from MPN, MDS, AML, B-ALL, and B-NHL contrasted to healthy and waterfall Plots from GSEA of native MSCs from Healthy, MPN, MDS, AML, B-ALL, and B-NHL MSCs. *p*-value, FDR q-value, and normalized enrichment score (NES) are included.

3.8. RNA Sequencing Revealed SMAD-Dependent and SMAD-Independent BMP/TGFB-Signaling in Myeloid and Lymphoid Neoplasms, Which Can Both Be Blocked as Potential Therapeutic Targets

We were able to detect overlapping differentially expressed genes in the myeloid and lymphoid groups that are related to growth, differentiation, and hematopoiesis. BMPs, INHBA, or DKK2 could be clearly assigned to the WNT and BMP/TGFB signaling pathways. Exclusively differentially expressed genes related to the BMP/TGFB signaling pathway in the respective group indicated a shift in the regulated signaling pathways. In the next step, we were interested in other genes related to these signaling pathways and whether we could find a group-specific signature. In the myeloid samples, a considerable number of genes integrated into or regulated by the canonical BMP/TGFB and WNT signaling pathways, as well as TGFB1, Frizzled, or GSK3A, were directly cross-talking and regulating downstream targets by SMAD- and beta-catenin signaling (Figure 8A,B). In comparison, the lymphoid group showed an impressive number of specifically differentially expressed collagens regulated by inflammatory programs, such as the MAPK pathway induced by TGFB (Figure 8A,B). A detailed view into our DESeq2 Data revealed a clear shift to canonical BMP/TGFB-signaling in MSCs from myeloid neoplasms, especially for MDS and AML, reflected by a respective number of genes such as TGFB1, TGFB3L, and a low number of detected genes for MAPK-signaling (via JNK and ERK). The heterogeneous MPN group exhibited a high number of both genes involved in SMAD-dependent and SMAD-independent BMP/TGFB signaling. A clear increase in differentially expressed genes involved in TGFB-inducible MAPK-signaling was detected in ALL and a higher number in NHL MSCs, as reflected by MAPK11 or MAPK10 (Figure 8C). Assuming that TGF/BMP-signaling acts as an overarching regulator of the canonical and non-canonical signaling pathway in varying degrees in the individual entities and is deregulated here, we wondered whether a blockade could reverse the observed effects. Since we saw overlapping impairments in the MSCs of various entities, particularly in osteogenic differentiation, we induced osteogenic differentiation in healthy MSCs and in MSCs derived from myeloid and lymphoid neoplasms, and added the active ATP-competitive transforming growth factor-β receptor 1 (TGF-βRI) (ALK5) inhibitor SD208 to each medium change within the osteogenic differentiation period. Interestingly, the addition of SD208 during the osteogenic differentiation period led to a significant restoration of osteogenic differentiation capacity (Figure 8D).

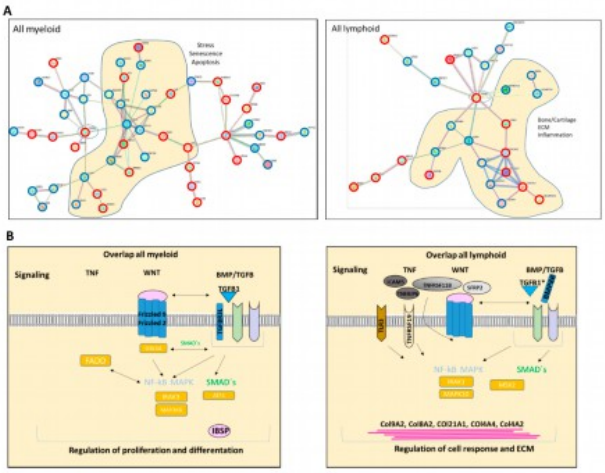

Figure 8. *Cont.*

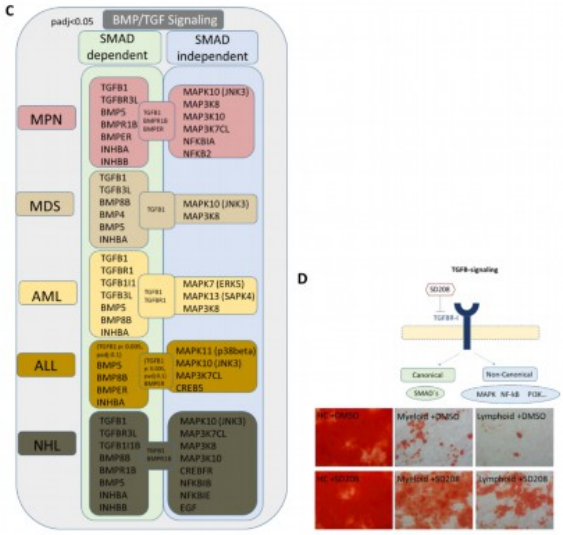

Figure 8. Graphical overview of representative exclusively differentially expressed genes from our RNA sequencing data in the myeloid and lymphoid group that are clearly assigned to the BMP/TGFB signaling pathway. (**A**) Illustration of representative and exclusively differentially expressed genes only in the "all myeloid group" (MPN, MDS, AML) and the exclusively overlapping differentially expressed genes only in the "all lymphoid group" (B-ALL, B-NHL) (from Figure 5D, black highlighted genes). Translation of differentially expressed genes from our mRNA sequencing data (FDR q-value < 0.05) from overlapping genes in all myeloid and separately in all lymphoid groups to a correlation and potential protein network of these genes as generated with STRING database (Version 12.0). STRING visualization was adapted starting from TGFB1 as is highlighted with a circle. In the "all myeloid group", 52 out of 192 exclusively differentially expressed genes in this group clearly show a direct correlation to the TGFB-signaling cascade based on current data in STRING (Version 12.0) (**B**, left side). In the "all lymphoid group", 26 out of 123 exclusively differentially expressed genes in this group clearly show a direct correlation to the TGFB-signaling cascade based on current data in STRING (Version 12.0) (**B**, right side). Overrepresented genes are red-circled, and underrepresented genes are blue-circled. (**B**) Graphical overview of further exclusively differentially expressed genes in the respective group, myeloid or lymphoid group (contrasted to healthy) that are regulators or related to the WNT and BMP/TGFB signaling pathways as well as downstream targets of these signaling pathways exclusively in the respective group. (TGFB1*, was significant in *p*-value 0.005, FDR q-value 0.1, B-ALL sample 2 exhibited a lower Transcript per million (TPM) expression of TGFB1 than all other samples). (**C**) Illustration of representative and exclusively overlapping differentially expressed genes in the "all myeloid group" and the "all lymphoid group" and the relationship to the canonical and non-canonical BMP/TGFB signaling pathway. Illustration of DESeq2 Data (*p*-adjusted < 0.05) reveals a clear shift to SMAD-dependent BMP/TGFB signaling in MDS and AML MSCs, while B-ALL, B-NHL, and the MPN group exhibit an increase and notable number of differentially expressed genes related to SMAD independent MAPK-signaling. (**D**) Representative pictures of MSCs from healthy, myeloid, and lymphoid groups after 14 days of osteogenic differentiation together with SD208. DMSO serves as an internal control. MSCs were induced for osteogenic differentiation and SD208 was added to each medium change within the osteogenic differentiation period. After 14 days of induction, MSCs were stained with Alizarin Red. Scale bars indicating 100 µm are shown.

4. Discussion

The major finding of this comprehensive study on the alterations inferred from the mesenchymal stromal cells of the bone marrow by infiltrating malignant cells of hematological neoplasms is diverse and dependent on the type of neoplasm. This is true with regard to the phenotypical changes as well as the molecular signature as reflected by the results of RNA sequencing of MSCs from myeloid and lymphoid neoplasms.

For instance, in MSCs derived from the myeloid neoplasms, a remarkable number of genes belonging to the TGF superfamily genes, such as TGFB-1, various BMPs, and INHBA as well as genes of the WNT signaling pathway, were differentially expressed. MPN-derived MSCs were the most heterogeneous group, showing a high number of additional differentially expressed genes related to inflammation or extracellular matrix (ECM) formation. In particular, the genes from the BMP/TGF signaling pathway are crucial for the regulation of proliferation, cell cycle, or differentiation of bone marrow MSCs. This finding may explain the profound functional deficits—significantly greater in comparison to the MSCs derived from the lymphoid group—such as structural integrity, cellular senescence, osteogenic differentiation capacity, and long-term culture initiating cell capacity. The latter deficit is characterized by a lack of *SDF-1* and *CXCL12* expression. These stroma-derived growth factors are essential for the maintenance of normal hematopoietic stem cells within their bone marrow niche. In accordance with these findings, it was shown by another group in myeloproliferative neoplasms that the hematopoietic cells induced a downregulation of the HSPC retention marker *CXCL12* [12]. The architecture of this particular niche also greatly depends on osteoblast and on a finely tuned osteogenic differentiation of MSCs which is significantly hampered in the myeloid-derived MSCs. These findings provide a reasonable explanation of the hematopoietic insufficiency observed with the strongest impairment encountered in patients with MDS and AML. On the other hand, in MSCs derived from lymphoid neoplasms, a remarkable number of genes involved in inflammatory processes like the TNF signaling pathway or the NFKB signaling pathway were observed. Different from the myeloid group, we found a high number of differentially expressed genes encoding proteins involved in the formation of the extracellular matrix (ECM), in particular members of the collagen family. Some studies have shown that MSCs from B-ALL patients have a pro-inflammatory genetic signature. The authors also found that MSCs from these patients were more prone to senescence and had a reduced osteogenic differentiation capacity, while their adipogenic and chondrogenic differentiation capacity was normal or increased [24–26]. In comparison, we found that the molecular disturbance with regard to growth and differentiation along the osteogenic and chondrogenic lineage was similar to ALL patients. In this context, other studies such as Medina et al. interestingly showed that MSCs from patients with mantle cell lymphoma protect the malignant cells from spontaneous and drug-induced apoptosis through the secretion of B-cell activating factor and activation of the canonical and non-canonical NFκB pathways [27]. Approaching the group of "overlap genes" which were in comparison to the healthy controls differentially expressed in all hematological neoplasms, we found candidates, such as *DKK2*, *PITX2*, and *TBX15*, various *HOXA2/3, HOXB2-B8* genes, and *BMP5,* that are crucially involved in the regulation of cell growth, osteogenesis, and hematopoiesis. For instance, BMP5 as a member of the TGF superfamily plays a pivotal role in the regulation of various processes, and is crucial for the stimulation of chondrogenesis and osteogenesis. Downstream targets such as *PITX2* or osteogenic transcription factors such as *OSTERIX* play an essential role in osteogenic differentiation. In addition, BMPs are known to regulate the expression of other factors such as *SERPINE2* involved in ECM formation, while, for example, HOXA2 inhibits *BMP5* expression in murine palatal MSCs. Altogether, alterations in gene expression and signaling pathways reflect a dysregulated osteogenesis contributing to a dysfunctional stem cell niche, irrespective of the underlying hematological disease [23,28,29].

Again, these molecular data are in accordance with the results of our in vitro cultures, demonstrating that MSCs derived from all hematologic neoplasms exhibit reduced osteogenic differentiation capacity, in particular going along with a reduced mRNA expres-

sion of the osteogenic marker *OSTEOCALCIN*. Assuming soluble factors have the potential to induce the observed functional alterations, we could show that exposure of healthy MSCs to patient-derived conditioned media led to a phenotypical disorganization and reduced growth capacity, and induced a reduced expression of *OSTEOCALCIN* in these MSCs. What are the mechanisms by which the BM-infiltrating cells confer their malignant imprint on the normal stroma cells? Based on the mRNA sequencing and functional data, we consider genes of the TGF family as dominant players in the pathophysiological network for hematopoietic insufficiency in all hematological neoplasm. In that respect, the findings of our comprehensive study confirm our previous findings of mRNA sequencing data from the MSCs of patients with MDS, AML, or multiple myeloma, and are in line with the results from other groups. These published data show that the structural and functional deficits greatly result from the secretion of soluble factors TGFB or CCL-3. They exert direct inhibitory and indirect effects resulting in the molecular reprogramming of the MSCs in myeloid and lymphoid neoplasms [9,10,13–18,30–32]. Accordingly, upon exposure to TGFB1, healthy MSCs developed functional deficits and adopted a phenotype reminiscent of that observed in patient-derived stromal cells, which could be reverted by the TGFB1 inhibitor SD208, especially towards their osteogenic differentiation capacity (Figure 4C,E) [9,16]. Despite the involvement of genes and pathways common for both groups of hematological malignancies, it appears that disturbances along the canonical signaling pathway are predominant in myeloid neoplasms, whereas alterations along the non-canonical signaling pathway are more prominent in lymphoid neoplasms as reviewed by other groups [33–36]. It was therefore not surprising that blocking TGFB signaling with SD208, which inhibits both the canonical and non-canonical pathways, led to an improvement in functionality, especially osteogenic differentiation in both groups.

5. Conclusions

In summary, mesenchymal stromal cells (MSCs) derived from patients with myeloid neoplasms (MPN, MDS, and AML) as well as lymphoid neoplasms (B-ALL and B-NHL) exhibit structural and functional alterations. Consequently, they play a crucial role in the pathophysiology of these conditions, significantly contributing to inadequate hematopoiesis. Our findings suggest the presence of overlapping mechanisms not only in the phenotype and functionality of MSCs but also in the underlying molecular pathways. Commonly involved factors, such as members of the TGF superfamily, have been identified across all neoplasms. Therefore, effectively blocking these pathways represents a promising strategy for improving hematopoiesis in affected patients.

Supplementary Materials: The following supporting information can be downloaded at: https://www.mdpi.com/article/10.3390/cancers16112071/s1, Figure S1: Reactome analysis of MSCs derived from MPN, MDS, AML, ALL, and NHL; Figure S2: Gene ontology (GO) analysis of MSCs derived from myeloid and lymphoid neoplasms contrasted to healthy MSCs.

Author Contributions: Conception and design, provision of study material or patients, collection and/or assembly of data, data analysis and interpretation, manuscript writing, final approval of manuscript: L.B., T.S., P.J. and S.G. Data analysis and interpretation, manuscript writing, final approval of manuscript: R.H. Provision of study material or patients, collection and/or assembly of data, data analysis and interpretation, manuscript writing, final approval of manuscript: U.G., R.F., B.S., A.K. and G.K. Resources, bioinformatical analysis: P.P., T.W., K.K. and F.B. Provision of study material or patients, collection and/or assembly of data, final approval of manuscript: U.M. and S.D. All authors have read and agreed to the published version of the manuscript.

Funding: This work was supported by a grant from the Leukämie Lymphom Liga e. V., Duesseldorf, Germany, and a grant (No. 2019-21) from the Research Committee of the Medical Faculty to SG and by the DFG 417677437/GRK2578.

Institutional Review Board Statement: The study was conducted in accordance with the Declaration of Helsinki, and approved by the Institutional Review Board Ethics Committee at the Faculty

of Medicine of Heinrich Heine University Düsseldorf (approval number: 4777, date of approval 02.09.2019).

Informed Consent Statement: Written informed consent was obtained from all subjects involved in the study.

Data Availability Statement: RNA-seq expression data are currently being deposited in the NCBI Sequence Read Archive (SRA) with BioProject ID PRJNA1091937.

Acknowledgments: We would like to thank Dennis Sohn from the Laboratory of Molecular Radio-oncology, Clinic and Polyclinic for Radiation Therapy and Radio-oncology for technical assistance regarding LTC-IC assays. The computational support of the Zentrum für Informations- und Medientechnologie, especially the HPC team (High-Performance Computing) at the Heinrich-Heine University, is acknowledged.

Conflicts of Interest: The authors declare that the research was conducted in the absence of any commercial or financial relationships that could be construed as a potential conflict of interest The author Felix Bormann is affiliated with Bioinformatics.Expert UG but has no potential interest relationship. The funder was not involved in the study design, collection, analysis, interpretation of data, the writing of this article or the decision to submit it for publication.

References

1. Alaggio, R.; Amador, C.; Anagnostopoulos, I.; Attygalle, A.D.; Araujo, I.B.O.; Berti, E.; Bhagat, G.; Borges, A.M.; Boyer, D.; Calaminici, M.; et al. The 5th edition of the World Health Organization Classification of Haematolymphoid Tumours: Lymphoid Neoplasms. *Leukemia* **2022**, *36*, 1720–1748. [CrossRef] [PubMed]
2. Arber, D.A.; Orazi, A.; Hasserjian, R.P.; Borowitz, M.J.; Calvo, K.R.; Kvasnicka, H.M.; Wang, S.A.; Bagg, A.; Barbui, T.; Branford, S.; et al. International Consensus Classification of Myeloid Neoplasms and Acute Leukemias: Integrating morphologic, clinical, and genomic data. *Blood* **2022**, *140*, 1200–1228. [CrossRef] [PubMed]
3. Will, B.; Zhou, L.; Vogler, T.O.; Ben-Neriah, S.; Schinke, C.; Tamari, R.; Yu, Y.; Bhagat, T.D.; Bhattacharyya, S.; Barreyro, L.; et al. Stem and progenitor cells in myelodysplastic syndromes show aberrant stage-specific expansion and harbor genetic and epigenetic alterations. *Blood* **2012**, *120*, 2076–2086. [CrossRef] [PubMed]
4. Weaver, C.J.; Tariman, J.D. Multiple Myeloma Genomics: A Systematic Review. *Semin. Oncol. Nurs.* **2017**, *33*, 237–253. [CrossRef] [PubMed]
5. Borkhardt, A.; Wuchter, C.; Viehmann, S.; Pils, S.; Teigler-Schlegel, A.; Stanulla, M.; Zimmermann, M.; Ludwig, W.D.; Janka-Schaub, G.; Schrappe, M.; et al. Infant acute lymphoblastic leukemia—Combined cytogenetic, immunophenotypical and molecular analy-sis of 77 cases. *Leukemia* **2002**, *16*, 1685–1690. [CrossRef] [PubMed]
6. van Beers, E.J.; Muller, M.C.; Vlaar, A.P.; Spanjaard, L.; van den Bergh, W.M.; Group, H.-I.S. Haematological malignancy in the intensive care unit: Microbiology results and mortality. *Eur. J. Haematol.* **2016**, *97*, 271–277. [CrossRef] [PubMed]
7. Franchini, M.; Frattini, F.; Crestani, S.; Bonfanti, C. Bleeding complications in patients with hematologic malignancies. *Semin. Thromb. Hemost.* **2013**, *39*, 94–100. [PubMed]
8. Jager, P.; Geyh, S.; Twarock, S.; Cadeddu, R.P.; Rabes, P.; Koch, A.; Maus, U.; Hesper, T.; Zilkens, C.; Rautenberg, C.; et al. Acute myeloid leukemia-induced functional inhibition of healthy CD34+ hematopoietic stem and progenitor cells. *Stem Cells* **2021**, *39*, 1270–1284. [CrossRef]
9. Bruns, I.; Cadeddu, R.P.; Brueckmann, I.; Frobel, J.; Geyh, S.; Bust, S.; Fischer, J.C.; Roels, F.; Wilk, C.M.; Schildberg, F.A.; et al. Multiple myeloma-related deregulation of bone marrow-derived CD34(+) hematopoietic stem and progenitor cells. *Blood* **2012**, *120*, 2620–2630. [CrossRef]
10. Geyh, S.; Oz, S.; Cadeddu, R.P.; Frobel, J.; Bruckner, B.; Kundgen, A.; Fenk, R.; Bruns, I.; Zilkens, C.; Hermsen, D.; et al. Insufficient stromal support in MDS results from molecular and functional deficits of mesenchymal stromal cells. *Leukemia* **2013**, *27*, 1841–1851. [CrossRef]
11. Sasaki, M.; Knobbe, C.B.; Munger, J.C.; Lind, E.F.; Brenner, D.; Brustle, A.; Harris, I.S.; Holmes, R.; Wakeham, A.; Haight, J.; et al. IDH1(R132H) mutation increases murine haematopoietic progenitors and alters epigenetics. *Nature* **2012**, *488*, 656–659. [CrossRef] [PubMed]
12. Schepers, K.; Pietras, E.M.; Reynaud, D.; Flach, J.; Binnewies, M.; Garg, T.; Wagers, A.J.; Hsiao, E.C.; Passegue, E. Myeloproliferative neoplasia remodels the endosteal bone marrow niche into a self-reinforcing leukemic niche. *Cell Stem Cell* **2013**, *13*, 285–299. [CrossRef] [PubMed]
13. Vallet, S.; Pozzi, S.; Patel, K.; Vaghela, N.; Fulciniti, M.T.; Veiby, P.; Hideshima, T.; Santo, L.; Cirstea, D.; Scadden, D.T.; et al. A novel role for CCL3 (MIP-1alpha) in myeloma-induced bone disease via osteocalcin downregulation and inhibition of osteoblast function. *Leukemia* **2011**, *25*, 1174–1181. [CrossRef] [PubMed]
14. Frisch, B.J.; Ashton, J.M.; Xing, L.; Becker, M.W.; Jordan, C.T.; Calvi, L.M. Functional inhibition of osteoblastic cells in an in vivo mouse model of myeloid leukemia. *Blood* **2012**, *119*, 540–550. [CrossRef] [PubMed]

15. Geyh, S.; Rodriguez-Paredes, M.; Jager, P.; Khandanpour, C.; Cadeddu, R.P.; Gutekunst, J.; Wilk, C.M.; Fenk, R.; Zilkens, C.; Hermsen, D.; et al. Functional inhibition of mesenchymal stromal cells in acute myeloid leukemia. *Leukemia* **2016**, *30*, 683–691. [CrossRef]
16. Geyh, S.; Rodriguez-Paredes, M.; Jager, P.; Koch, A.; Bormann, F.; Gutekunst, J.; Zilkens, C.; Germing, U.; Kobbe, G.; Lyko, F.; et al. Transforming growth factor beta1-mediated functional inhibition of mesenchymal stromal cells in myelodysplastic syndromes and acute myeloid leukemia. *Haematologica* **2018**, *103*, 1462–1471. [CrossRef] [PubMed]
17. Ferrer, R.A.; Wobus, M.; List, C.; Wehner, R.; Schonefeldt, C.; Brocard, B.; Mohr, B.; Rauner, M.; Schmitz, M.; Stiehler, M.; et al. Mesenchymal stromal cells from patients with myelodyplastic syndrome display distinct functional alterations that are modulated by lenalidomide. *Haematologica* **2013**, *98*, 1677–1685. [CrossRef] [PubMed]
18. Medyouf, H.; Mossner, M.; Jann, J.C.; Nolte, F.; Raffel, S.; Herrmann, C.; Lier, A.; Eisen, C.; Nowak, V.; Zens, B.; et al. Myelodysplastic cells in patients reprogram mesenchymal stromal cells to establish a transplantable stem cell niche disease unit. *Cell Stem Cell* **2014**, *14*, 824–837. [CrossRef] [PubMed]
19. Yang, G.C.; Xu, Y.H.; Chen, H.X.; Wang, X.J. Acute Lymphoblastic Leukemia Cells Inhibit the Differentiation of Bone Mesenchymal Stem Cells into Osteoblasts In Vitro by Activating Notch Signaling. *Stem Cells Int.* **2015**, *2015*, 162410. [CrossRef]
20. Bogun, L.; Koch, A.; Scherer, B.; Fenk, R.; Maus, U.; Bormann, F.; Köhrer, K.; Petzsch, P.; Wachtmeister, T.; Zukovs, R.; et al. Stromal alterations in patients with MGUS, smoldering myeloma and multiple myeloma. *Blood Adv.* **2024**. [CrossRef]
21. Frith, J.; Genever, P. Transcriptional control of mesenchymal stem cell differentiation. *Transfus. Med. Hemother.* **2008**, *35*, 216–227. [CrossRef] [PubMed]
22. Gage. The canonical Wnt signaling antagonist DKK2 is an essential effecotr of PITX2 function during normal eye development. *Dev. Biol.* **2008**, *317*, 310–324. [CrossRef] [PubMed]
23. Singh, M.K. The T-box transcription factor Tbx15 is required for skeletal development. *Mech. Dev.* **2005**, *122*, 131–144. [CrossRef] [PubMed]
24. Vanegas, N.P.; Ruiz-Aparicio, P.F.; Uribe, G.I.; Linares-Ballesteros, A.; Vernot, J.P. Leukemia-Induced Cellular Senescence and Stemness Alterations in Mesenchymal Stem Cells Are Reversible upon Withdrawal of B-Cell Acute Lymphoblastic Leukemia Cells. *Int. J. Mol. Sci.* **2021**, *22*, 8166. [CrossRef] [PubMed]
25. Balandran, J.C.; Davila-Velderrain, J.; Sandoval-Cabrera, A.; Zamora-Herrera, G.; Teran-Cerqueda, V.; Garcia-Stivalet, L.A.; Limon-Flores, J.A.; Armenta-Castro, E.; Rodriguez-Martinez, A.; Leon-Chavez, B.A.; et al. Patient-Derived Bone Marrow Spheroids Reveal Leukemia-Initiating Cells Supported by Mesenchymal Hypoxic Niches in Pediatric B-ALL. *Front. Immunol.* **2021**, *12*, 746492. [CrossRef] [PubMed]
26. Iwamoto, S.; Mihara, K.; Downing, J.R.; Pui, C.H.; Campana, D. Mesenchymal cells regulate the response of acute lymphoblastic leukemia cells to asparaginase. *J. Clin. Investig.* **2007**, *117*, 1049–1057. [CrossRef] [PubMed]
27. Medina, D.J.; Goodell, L.; Glod, J.; Gelinas, C.; Rabson, A.B.; Strair, R.K. Mesenchymal stromal cells protect mantle cell lymphoma cells from spontaneous and drug-induced apoptosis through secretion of B-cell activating factor and activation of the canonical and non-canonical nuclear factor kappaB pathways. *Haematologica* **2012**, *97*, 1255–1263. [CrossRef] [PubMed]
28. Hayashi, M.; Maeda, S.; Aburatani, H.; Kitamura, K.; Miyoshi, H.; Miyazono, K.; Imamura, T. Pitx2 prevents osteoblastic transdifferentiation of myoblasts by bone morphogenetic proteins. *J. Biol. Chem.* **2008**, *283*, 565–571. [CrossRef] [PubMed]
29. Lefort, S.; Maguer-Satta, V. Targeting BMP signaling in the bone marrow microenvironment of myeloid leukemia. *Biochem. Soc. Trans.* **2020**, *48*, 411–418. [CrossRef]
30. Ame-Thomas, P.; Maby-El Hajjami, H.; Monvoisin, C.; Jean, R.; Monnier, D.; Caulet-Maugendre, S.; Guillaudeux, T.; Lamy, T.; Fest, T.; Tarte, K. Human mesenchymal stem cells isolated from bone marrow and lymphoid organs support tumor B-cell growth: Role of stromal cells in follicular lymphoma pathogenesis. *Blood* **2007**, *109*, 693–702. [CrossRef]
31. Purroy, N. Co-culture of primary CLL cells with bone marrow mesenchymal cells, CD40 ligand and CpG ODN promotes proliferation of chemoresistant CLL cells phenotypically comparable to those proliferating in vivo. *Oncotarget* **2015**, *6*, 7632–7643. [CrossRef] [PubMed]
32. Xu, S.; De Veirman, K.; De Becker, A.; Vanderkerken, K.; Van Riet, I. Mesenchymal stem cells in multiple myeloma: A therapeutical tool or target? *Leukemia* **2018**, *32*, 1500–1514. [CrossRef] [PubMed]
33. Chen, G.; Deng, C.; Li, Y.P. TGF-beta and BMP signaling in osteoblast differentiation and bone formation. *Int. J. Biol. Sci.* **2012**, *8*, 272–288. [CrossRef] [PubMed]
34. Shi, X.; Yang, J.; Deng, S.; Xu, H.; Wu, D.; Zeng, Q.; Wang, S.; Hu, T.; Wu, F.; Zhou, H. TGF-beta signaling in the tumor metabolic microenvironment and targeted therapies. *J. Hematol. Oncol.* **2022**, *15*, 135. [CrossRef] [PubMed]
35. Yao, J.C.; Oetjen, K.A.; Wang, T.; Xu, H.; Abou-Ezzi, G.; Krambs, J.R.; Uttarwar, S.; Duncavage, E.J.; Link, D.C. TGF-beta signaling in myeloproliferative neoplasms contributes to myelofibrosis without disrupting the hematopoietic niche. *J. Clin. Investig.* **2022**, *132*, e154092. [CrossRef]
36. Timmins, M.A.; Ringshausen, I. Transforming Growth Factor-Beta Orchestrates Tumour and Bystander Cells in B-Cell Non-Hodgkin Lymphoma. *Cancers* **2022**, *14*, 1772. [CrossRef]

cancers

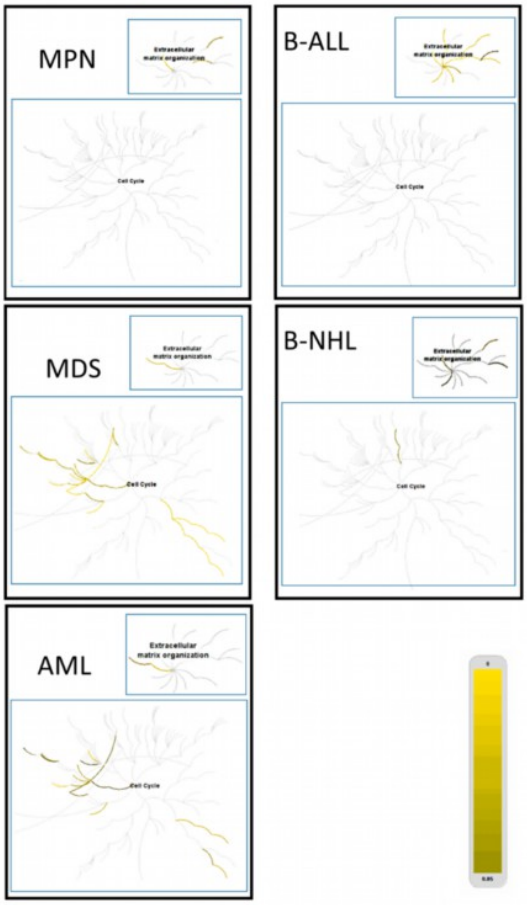

Supplementary Figure S1. Reactome analysis of MSCs derived from MPN, MDS, AML, ALL, and NHL. A strong enrichment of cell cycle was detected in MDS- and AML-derived MSCs from the myeloid group, while MPN, B-ALL, and B-NHL-derived MSCs exhibited a strong enrichment for extracellular matrix (ECM).

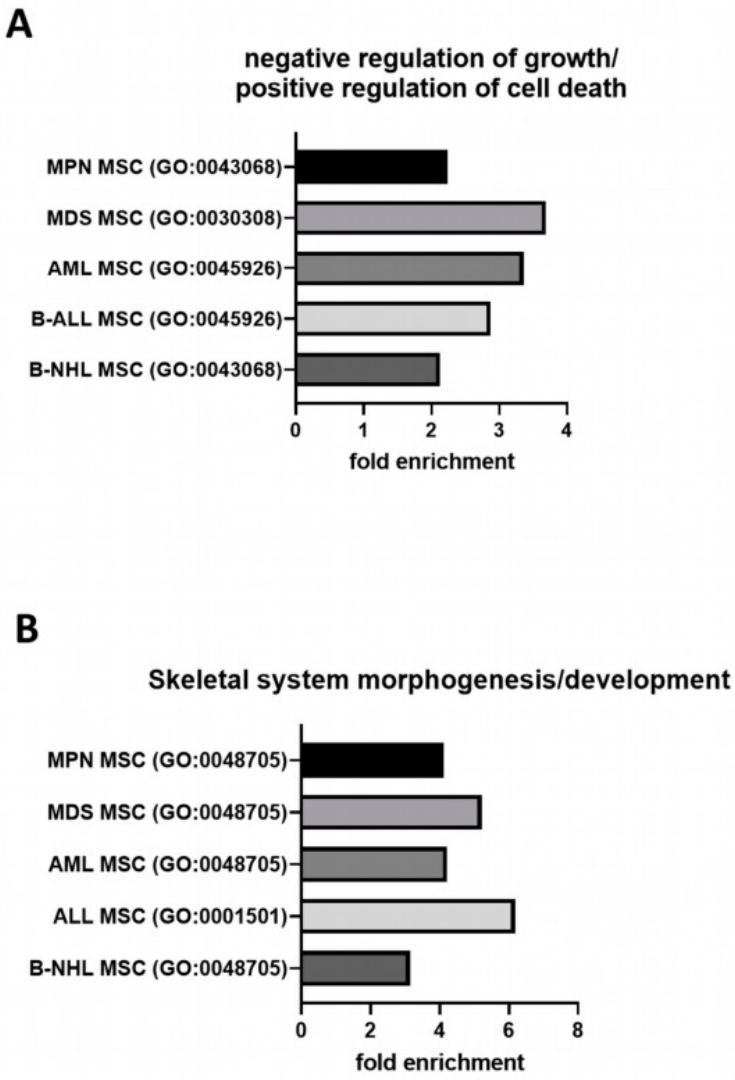

Supplementary Figure S2. Gene ontology (GO) analysis of MSCs derived from myeloid and lymphoid neoplasms contrasted to healthy MSCs. (A) Representative GO analysis for enriched cell processes such as overrepresented negative regulation of growth/positive regulation of cell death (GO:0043068 regulation of cell death; GO:0030308 negative regulation of cell growth; GO0045926 negative regulation of growth) were strongly enriched in all patient groups, with the highest fold-change in MDS and AML MSCs. (B) Representative GO analysis for underrepresented skeletal system morphogenesis/development (GO:0048705 skeletal system morphogenesis; GO:0001501 skeletal system development). MSCs from both myeloid and lymphoid patient groups exhibit a significant strong enrichment in the skeletal system.

2.2. Stromal Alterations in Patients with Monoclonal Gammopathy of Undetermined Significance, Smoldering Myeloma, and Multiple Myeloma

Lucienne Bogun, Annemarie Koch, Bo Scherer, Roland Fenk, Uwe Maus, Felix Bormann, Karl Köhrer, Patrick Petzsch, Thorsten Wachtmeister, Romans Zukovs, Sascha Dietrich, Rainer Haas, Thomas Schroeder, Paul Jäger, and Stefanie Geyh

Abstract

The hallmark of multiple myeloma (MM) is a clonal plasma cell infiltration in the bone marrow accompanied by myelosuppression and osteolysis. Premalignant stages such as monoclonal gammopathy of undetermined significance (MGUS) and asymptomatic stages such as smoldering myeloma (SMM) can progress to MM. Mesenchymal stromal cells (MSCs) are an integral component of the bone marrow microenvironment and play an important role in osteoblast differentiation and hematopoietic support. Although stromal alterations have been reported in MM contributing to hematopoietic insufficiency and osteolysis, it is not clear whether alterations in MSC already occur in MGUS or SMM. In this study, we analyzed MSCs from MGUS, SMM, and MM regarding their properties and functionality and performed messenger RNA sequencing to find underlying molecular signatures in different disease stages. A high number of senescent cells and a reduced osteogenic differentiation capacity and hematopoietic support were already present in MGUS MSC. As shown by RNA sequencing, there was a broad spectrum of differentially expressed genes including genes of the BMP/TGF-signaling pathway, detected already in MGUS and that clearly increases in patients with SMM and MM. Our data may help to block these signaling pathways in the future to hinder progression to MM.

Journal	Blood Advances
Impact factor	7.4 (2023)
Contribution to publication	10 %

The own contribution of this manuscript includes the partial conduction of experiments, collection, assembly, analysis and interpretation of the obtained samples, as well as contribution to manuscript writing, proof reading and final approval.

Type of authorship	Co-author
Status of publication	Published 28.05.2024

REGULAR ARTICLE

blood advances

Stromal alterations in patients with monoclonal gammopathy of undetermined significance, smoldering myeloma, and multiple myeloma

Lucienne Bogun,[1] Annemarie Koch,[1] Bo Scherer,[1] Roland Fenk,[1] Uwe Maus,[2] Felix Bormann,[3] Karl Köhrer,[4] Patrick Petzsch,[4] Thorsten Wachtmeister,[4] Romans Zukovs,[1] Sascha Dietrich,[1] Rainer Haas,[5] Thomas Schroeder,[1] Paul Jäger,[1,*] and Stefanie Geyh[1,*]

[1]Department of Hematology, Oncology and Clinical Immunology, and [2]Department of Orthopedic Surgery and Traumatology, University Hospital Duesseldorf, Medical Faculty, Duesseldorf, Germany; [3]Bioinformatics.Expert UG, Berlin, Germany; [4]Biological and Medical Research Center, Medical Faculty, Heinrich-Heine-University, Duesseldorf, Germany; and [5]Institute of Medical Microbiology and Hospital Hygiene, University of Duesseldorf, Medical Faculty, Duesseldorf, Germany

Key Points

- Stromal alterations are already imprinted in patients with asymptomatic stages that further progress in patients with MM.
- The BMP/TGF-signaling pathway can play a role in progression and may become a potential therapeutic target to prevent end-organ damage.

The hallmark of multiple myeloma (MM) is a clonal plasma cell infiltration in the bone marrow accompanied by myelosuppression and osteolysis. Premalignant stages such as monoclonal gammopathy of undetermined significance (MGUS) and asymptomatic stages such as smoldering myeloma (SMM) can progress to MM. Mesenchymal stromal cells (MSCs) are an integral component of the bone marrow microenvironment and play an important role in osteoblast differentiation and hematopoietic support. Although stromal alterations have been reported in MM contributing to hematopoietic insufficiency and osteolysis, it is not clear whether alterations in MSC already occur in MGUS or SMM. In this study, we analyzed MSCs from MGUS, SMM, and MM regarding their properties and functionality and performed messenger RNA sequencing to find underlying molecular signatures in different disease stages. A high number of senescent cells and a reduced osteogenic differentiation capacity and hematopoietic support were already present in MGUS MSC. As shown by RNA sequencing, there was a broad spectrum of differentially expressed genes including genes of the BMP/TGF-signaling pathway, detected already in MGUS and that clearly increases in patients with SMM and MM. Our data may help to block these signaling pathways in the future to hinder progression to MM.

Introduction

Multiple myeloma (MM) is characterized by an infiltration of clonal plasma cells in the bone marrow (BM) accompanied by end-organ damage such as hematopoietic insufficiency and/or osteolysis. The latter is a result of increased osteoclast and impaired osteoblast function.[1-3] MM with indication for treatment is present when either end-organ damage is present, and thus, at least 1 of the CRAB (calcium elevation, renal insufficiency, anemia, and bone lesions) criteria is met, or clinical predictive biomarkers like 60% bone marrow plasma cells, involved:uninvolved serum free light chain ratio ≥100 or >1 focal lesions on MRI studies (SLiM-CRAB) are present that make progression of the disease highly likely.

Submitted 12 September 2023; accepted 9 January 2024; prepublished online on *Blood Advances* First Edition 19 January 2024; final version published online 28 May 2024. https://doi.org/10.1182/bloodadvances.2023011632.

*P.J. and S.G. contributed equally to this study.

Parts of this study have been presented at the annual meeting of the German-Austrian-Suisse Society of Hematology and Oncology (DGHO), Vienna, Austria, October 2022.

RNA-seq expression data are deposited in NCBI Sequence Read Archive (SRA) with BioProject (ID PRJNA1015628).

Data are available upon reasonable request from corresponding authors, Paul Jäger (paulsebastian.jaeger@med.uni-duesseldorf.de) and Stefanie Geyh (stefanie.geyh@med.uni-duesseldorf.de).

The full-text version of this article contains a data supplement.

Smoldering myeloma (SMM) does not clinically show CRAB or SLiM CRAB criteria and therefore does not need to be treated initially, but it can, with a significant probability of 10% per year, progress into a full blown MM.

This also applies to monoclonal gammopathie of undetermined significance (MGUS), which is present in ~3% of those aged >50 years and has a probability of transformation into MM of ~1% per year.[4,5]

The underlying mechanisms of how these asymptomatic or premalignant stages evolve to MM await further clarification, particularly because there are limited valid biomarkers reliably predicting the likelihood of progression.[2,6,7] In the BM microenvironment, mesenchymal stromal cells (MSCs) are important components and are characterized by their capacity to differentiate into adipocytes, chondroblasts, and osteoblasts.[8] MSCs are particularly relevant for the support of hematopoietic stem and progenitor cells with regard to proliferation, migration, and differentiation. These processes are governed and mediated via cross talk by direct cell-cell contact or secretion of a great variety of cytokines.[9,10]

Based on earlier findings of alterations in MSC in MM,[11] we were interested in a better understanding of the mechanisms underlying disease progression from premalignant and asymptomatic stages to the final stage of MM. In addition, it is of major clinical interest to identify possible factors involved in progression, for example, the development of osteolysis, which can be blocked with already available drugs that are applied in other hematological diseases. To address this, we investigated for the first time MSCs from healthy donors (HD) and patients with MGUS, SMM, and MM toward functionality and performed RNA sequencing.

Material and methods

Patients, healthy controls, and cell preparation

BM samples were obtained from a total of 40 patients (MGUS, n = 11; SMM, n = 7; MM, n = 22). Healthy BM samples were derived from 41 healthy individuals (median age, 78 years; range, 33-90 years) undergoing orthopedic surgery. Detailed patient characteristics with typical features of the respective disease entity documented progression or pre-phase, fluorescence in situ hybridization data; high risk was defined according to revised international staging score[12] and International Myeloma Working Group[13] and C-reactive protein values, which could indicate inflammatory processes as potential confounders (Table 1).

MSCs were derived from the mononuclear cell (MNC) fraction, after density gradient centrifugation of BM aspirates of these specimens, and were directly cultured as previously described.[14,15] All experiments were carried out using MSC derived from passages 3 to 4. The study was approved by our local institutional review board (approval number: 4777) and all patients gave written informed consent.

Cell culture conditions and reagents

Healthy MSCs were cultured in Dulbecco's modified eagle medium low glucose supplemented with 30% fetal bovine serum and 1% penicillin/streptomycin/L-glutamine (PSG; all from Sigma-Aldrich Chemie GmbH, Taufkirchen, Germany), given in the legends of the respective figures.

CM and coculture

To generate cell line–derived conditioned media (CM), $2.7 \times 10^5/cm^2$ cells of the MM cell line INA-6 (purchased DSMZ) were cultivated in RPMI with 10% fetal bovine serum and 1% PSG (all from Sigma Aldrich, Taufkirchen Germany) as previously described. To generate patient-derived CM, $2 \times 10^5/cm^2$ BM-derived MNC from patients with MGUS, SMM, or MM and from healthy controls were used freshly or from short time frozen storage in liquid nitrogen and thawed afterward. Cell number and cell viability were measured by CASY cell counter system and showed no differences in viability. Cells were then cultivated and further cocultivated with healthy MSCs as previously described.[15,16] To investigate effects on the transforming growth factor beta 1 (TGFB1) signaling, we used the active adenosine triphosphate (ATP)-competitive transforming growth factor beta receptor 1 (TGF-βRI) (ALK5) inhibitor SD208 (0.5 μM; Biotechne/R&D systems, Minneapolis, MN), diluted in DMSO (10 mM). Healthy MSC were cocultured with respective CM with and without SD208 (DMSO served as control) for 3 days and subsequently after 14 days of osteogenic induction, Alizarin Red staining visualized osteogenic differentiation. DMSO served as control.

Phenotypic characterization of MGUS-, SMM- and MM-derived MSCs

Primarily patients-derived MSCs were characterized regarding their morphology and growth properties by light microscopy. Quantification of growth was determined as described elsewhere.[14,15]

Differentiation properties

Differentiation assays into osteoblasts, chondroblasts, and adipocytes were performed on Passage 3. Adipogenic and chondrogenic differentiation were induced as previously described.[14] For osteogenic differentiation, Dulbecco's modified eagle medium low glucose were supplemented with dexamethasone (10^{-7} M), ascorbic acid (50 μg/mL), and β-glycerolphosphate (10 mM; all Sigma-Aldrich) and, after 14 days of differentiation, visualized by Alizarin Red staining. All images were visualized using Axiovert 25 microscope (Zeiss, Jena, Germany; 5 objective Zeiss CP-Achromat 5 Ph0, for native and osteogenic differentiated MSC or a 10 objective-Zeiss CP-Achromat 10 Ph1, for adipogenic differentiation, Zeiss EC Plan-Neofluar, 2.5×/0.075, for chondrogenic differentiation) and digitalized with the SPOT Software (Diagnostic Instruments Inc, Sterling Heights, MI).

Long-term culture-initiating cells assay

A total of 0.8×10^6 to 1.2×10^6 MSCs were cultivated on 96-well plates (Costar, Corning) and irradiated with 30 Gray using Gulmay RS225 X-ray equipment. Subsequently, 6×10^3 healthy $CD34^+$ cells were plated on these MSC feeder layers and then further proceeded using the same conditions and reagents as in our previous work.[14,15]

Cellular senescence assay by β-galactosidase staining

β-galactosidase activity is an indicator for cellular senescence and was determined by using the Cellular Senescence Detection Kit (Biolabs, San Diego, CA), following manufacturer's instructions. Cells were visualized under light microscope and senescent cells reflected blue staining through β-galactosidase activity were assessed.

Enzyme-linked Immunosorbent Assay

Filtered conditioned media from MSC were harvested in passage 3 and frozen at −20°C. Human CXCL12/SDF-1 alpha

Table 1. Patients demographics and clinical characteristics

	No.	%
Patients no.	40	
Sex		
Male	22	55
Female	18	45
MGUS no.	11	27
Median age, y (range)	65	(44-78)
Type		
Heavy chain leading*[1]	10	91
Light chain leading*[2]	1	9
FISH		
Standard risk	3	27
High risk§	2	18
Missing	6	55
Mean CRP, mg/dL (range)	0.65	(0.1-2.8)
Documented SMM progression	2	18
SMM no.	7	18
Median age, y (range)	60	(51-80)
Type		
Heavy chain leading*[3]	6	86
Light chain leading*[4]	1	14
FISH		
Standard risk	4	57
High risk	3	43
Missing	0	0
Mean CRP, mg/dL (range)	0.4	(0.1-1.0)
Documented MGUS pre-phase	2	29
Documented MM progression	5	71
MM no.	22	55
Median age, y (range)	58	(50-76)
Type/Paraprotein		
Heavy chain leading*[5]	18	82
Light chain leading*[6]	4	18
CRAB (see below)		
Hyper calcaemia	1	5
Renal failure	3	14
Anaemia*	8	36
Bone lesions	17	77
SLiM CRAB (see below)		
Sixty-percent bone marrow plasma cells†	11	50
Light chain ratio ≥100	6	27
>1 focal lesions on MRI studies	1	5
FISH		
Standard risk	11	50
High risk	9	41
Missing	2	9
Mean CRP, mg/dL (range)	0.56	(0.1-3.7)
Documented SMM or MGUS pre-phase	8	36

Scatter Plot for Infiltration [%], Scatter Plot for hemoglobin (HB) [g/dl] of MGUS, SMM and MM patients included in this study at time of diagnosis shown on the right side.

MGUS, monoclonal gammopathy of undetermined significance; SMM, smoldering myeloma; MM, multiple myeloma; CRP, C-reactive protein; FISH, fluorescence in situ hybridization.

*[1]IgG kappa n = 7, IgG lambda n = 2, IgM lambda n = 1.

*[2]LC kappa n = 1.

*[3]IgG kappa n = 3, IgG lambda n = 2, IgA kappa n = 1.

*[4]LC kappa n = 1.

*[5]IgG kappa n = 9, IgG lambda n = 4, IgA kappa n = 3, IgA lambda n = 1, IgG lambda n = 1.

*[6]LC kappa n = 3, LC lambda n = 1.

*Plot shows the HB values of the individual patients.

†Plot shows the infiltration rate by plasma cells of the individual patients.

§According to revised-international staging score and International Myeloma Working Group: del(17p), t(4;14), t(14;16), +1q21.

Enzyme-Linked Immunosorbent Assay–Quantikine was performed according to the manufacturers' instructions (R&D systems, Minneapolis, Minnesota).

Quantitative real-time PCR

RNA was isolated using the RNeasy Micro Kit or Mini Kit (Qiagen, Hilden, Germany) with the optional DNase digestion, according the manufacturer's instruction.

All quantitative real-time PCR were performed in duplicates on a StepOne Plus Realtime PCR Cycler using SYBR Green PCR Master Mix (Applied Biosystems, Life Technologies, Carlsbad, CA). All primer sequences can be provided on request. GAPDH serves as reference control, and differences in the expression on messenger RNA level were calculated with the ΔCT method.

RNA-sequencing

DNase digested total RNA samples used for transcriptome analyses were quantified (Qubit RNA HS Assay, Thermo Fisher Scientific Inc, Waltham, MA) and quality measured by capillary electrophoresis using the fragment analyzer and the "Total RNA Standard Sensitivity Assay" or the bioanalyzer assay "Eukaryote Total RNA Pico" (Agilent Technologies, Inc, Santa Clara, CA). The library preparation was performed according to the manufacturer's protocol using the VAHTS universal V6 RNA-seq library prep kit (Illumina, San Diego, CA). Briefly, 10 ng total RNA was used for poly(A) RNA selection, fragmentation, complementary DNA generation, adapter ligation, strand selection, and library amplification. Bead purified libraries were normalized and finally sequenced on the NextSeq 2000 system (Illumina Inc, San Diego, CA) with a read setup of 1 × 150bp. The bcl2fastq tool was used to convert the bcl files to fastq files as well for adapter trimming and demultiplexing as previously described.[16]

Bioinformatical analysis

Data analyses on fastq files were conducted with CLC Genomics Workbench (version 20.0.3, QIAGEN, Venlo, The Netherlands). Reads of all probes were adapter trimmed and quality trimmed

(using the default parameters: bases below Q13 were trimmed from the end of the reads, ambiguous nucleotides maximal 2). Mapping was done against the Homo sapiens (hg38) (Mai 25, 2017) genome sequence. After grouping of samples (3 biological replicates each) according to their respective experimental condition, multigroup comparisons were made and statistically determined using the empirical analysis of differential gene expression (version 1.1, cutoff = 5). The resulting *P* values were corrected for multiple testing by false discovery rate (FDR) correction. A *P* value ≤ .05 was considered significant. The data were further evaluated with the Ingenuity-Pathway analysis software (Qiagen Inc 2020, Venlo, The Netherlands) using the core analysis with default parameters (|FC| ≥ 1.5; $P \leq .01$; *P* [FDR] ≤ .05).

After quality control, the sequencing raw data were trimmed by removing the first 12 bases from each read. Alignment was performed using the program STAR v2.7.2a[17] against the reference human genome GRCh38.97 (hg38). Alignment was performed as a 2-pass experiment, which means that in a first step new splice junctions were detected, which were added in the second step to the initial reference. The analysis pipeline was adapted from an NIH protocol.

After applying the program featureCounts (1.6.5) to the aligned reads, DESeq2 (1.24.0) was used to calculate the differential expression of patients-derived samples in contrast to healthy individuals. Genes with an FDR q-value <0.05 were considered differentially expressed. StringTie (2.0.3)[18] was applied to calculate fragments per kilobase of transcript per million mapped reads (FPKM values). Principal component analysis plots were created in R using the FactoMineR (2.3) and pheatmap (1.0.12) packages. For gene set enrichment analysis (GSEA) (Broad Institute, Boston, MA), the fragments per kilobase of transcript per million mapped reads values obtained from StringTie (2.0.3) for the different samples and the healthy controls were compared either with the gene sets contained in the Molecular Signature database or with self-made gene lists. The parameter metric was set to Signal2Noise, and 1000 gene set–based permutations were applied to all analyses.

Gene Ontology analysis was performed with differentially expressed genes using the panther overrepresentation test, which is accessible via the AmiGO 2 webpage (https://amigo.geneontology.org/amigo). A Fisher's exact test was performed, and the results were Bonferroni-corrected as previously reported.[16]

Statistical analysis

Statistical analyses were performed using Prism 8.4.3 (GraphPad Software Inc, La Jolla, CA). For interindividual comparison, the 2-sided unpaired Student *t* test was used, whereas for intra-individual analysis, the Wilcoxon signed rank test was used. For all experiments, means and standard error of the mean (SEM) are given. Statistical significance was established at $P \leq .05$ (* $P \leq 0.05$; ** $P \leq .01$; *** $P \leq .001$; **** $P \leq .0001$).

Results

MSC transition from MGUS to SMM to MM - RNA-sequencing revealed a genetic signature

RNA-sequencing data were obtained for MSC from 5 healthy donors, 4 patients with MGUS, 4 patients with SMM, and 5 patients with MM (median age in years: HC, 72; MGUS, 65; SMM, 58; and MM, 57). Detailed patient characteristics of the samples we used for RNA sequencing with additional information such as documented progression or documented preliminary phase are shown in Figure 1A. Principal component analysis illustrated the distribution of the groups we analyzed, showing a closer relationship between MGUS and SMM MSC (Principal components 1 vs 3, Figure 1B, blue and dark blue dots). In comparison to MSC from normal donors, RNA-sequencing data revealed 1539 differentially expressed genes in MGUS-derived MSCs, 1513 in SMM-derived MSCs, and 4696 in MM-derived MSCs (FDR q-value ≤ 0.05). The most overlapping differentially expressed genes of 747 were found between MGUS and SMM MSC (Figure 1C).

By contrasting MGUS and MM or SMM and MM MSCs, 505 and 549 genes were revealed differentially expressed, respectively (Figure 1C).

Subtracting the 296 genes that were overlapping differentially expressed by all 3 groups, MGUS and SMM MSCs have the highest number of an overlapping signature, with 451 differentially expressed genes only detected in this comparison. These genes include, for example, *TGFBR3L*, *CD274*, *DKK2*, *MMP9*, or *S100A9* (Figure 1D; supplemental Figure 1). An overlap of 253 differentially expressed genes were found only between SMM and MM MSC (Figure 1D; supplemental Figure 1), which includes *TGFBR1*, *WNT2*, *S100A6*, *S100A4*, or *TNFRSF25* (*Death Receptor3*). Moreover, the lowest number of 209 overlapping differentially expressed genes were found by comparing only MGUS and MM MSC, with, for example, the cell cycle markers *CDKN2A* and *CDKN2B* or *NOTCH1*, which were only detected in this comparison (Figure 1D; supplemental Figure 1). The aforementioned 296 differentially expressed genes that were overlapping in all 3 MSC groups, includes genes from the BMP/TGF (*BMP8B*, *TGFB1*) or WNT-signaling Pathway (*WNT5B*, *FZD8*) and downstream targets of these pathways that are involved in skeletal development (*Integrin Binding Sialoprotein; IBSP*, *Msh Homeobox 2; MSX2*), proliferation (TNF receptor superfamily member 19; *TNFRSF19*), or extracellular matrix (ELN; Elastin) (Figure 1D). This was confirmed by gene ontology analysis, demonstrating enriched cell processes such as proliferation, skeletal system, or apoptosis in all 3 groups contrasted to the healthy samples. Moreover, cell processes such as mesenchymal differentiation or mesenchymal development arises in SMM and remain to the progression in myeloma (Figure 2).

RNA-sequencing revealed a unique genetic signature in MSC transition from MGUS to SMM to MM

Apart from that overlapping signature of all 3 MSC groups, we also focused on genes that were uniquely expressed in the MSC for that entity alone. MGUS MSCs exhibit a unique signature of 583 differentially expressed genes such as *MAPK7*, *FZD9*, *FZD7*, *TFGB1I1*, and *TGFB2* and downstream targets such as *SPP1* (Secreted Phosphoprotein 1, Osteopontin) (Figure 3A, supplemental Table 1). A unique signature of 513 differentially expressed genes in SMM MSC revealed *CCND2* (Cyclin D2), *CDK15* (Cyclin dependent kinase 15), or *WNT7B*, *EMILIN1*, or *CXCL2* (Figure 3A; supplemental Table 1).

MM MSCs exhibit the highest number of unique differentially expressed genes of 3938. Here, *MAPK14* (p38), *SMAD5*, *SMAD6*, *TGFA*, *TGFB3*, *TGFBR3*, *WNT9A*, or several genes involved in cell cycle such as cyclin dependent kinases (CDKs) (4, 6, 7, 10, 12, and

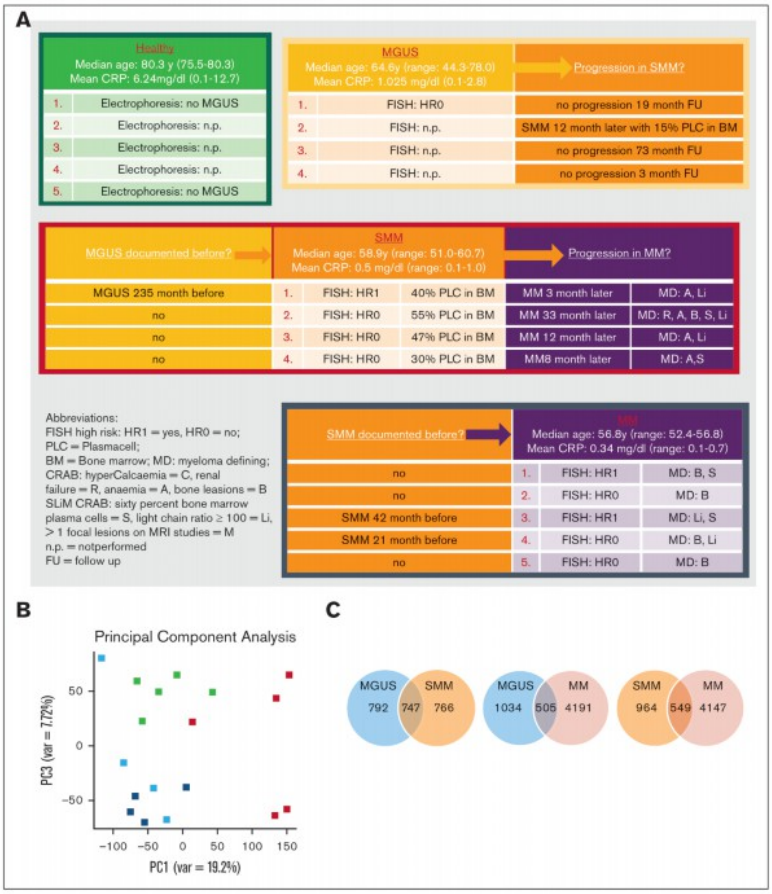

Figure 1. RNA sequencing analysis of MSCs derived from patients with MGUS, SMM, and MM revealed a genetic signature in the respectively stages. (A) Patient characteristics of included samples in RNA sequencing analysis. Table shows clinical parameters including prestages and/or progression status of MGUS (n = 4), SMM (n = 4), and MM (n = 5) samples in comparison to healthy (n = 5) samples. (B) Principal component analysis of MGUS, SMM and MM MSC. PC1 vs PC3 is shown. Green squares depict healthy MSC, dark blue squares depict MGUS MSC, light blue squares depict SMM MSC, and red squares depict MM MSC. (C) Venn diagrams of all differentially expressed genes, unique genes, and overlapping genes (FDR q-value ≤ 0.05) between the groups to be compared. (D) Top: graphical summary of representative overlapping genes from all 3 groups and between the groups to be compared. Several genes from that total overlap such as TGFB1, BMP8B, or WNT5B are represented by red framing. Unique overlapping genetic signature between MGUS and SMM MSC (such as TGFBR3L, RPSA or RPS27A) or the unique overlapping genetic signature between MGUS and MM (such as CDKN2A, CDKN2B) or between SMM and MM MSC (such as TGFR1, WNT2 or SFRP2) are represented by black framing. Bottom: graph table of the overlapping 296 differentially expressed genes by contrasting MGUS, SMM and MM MSC (FDR q-value ≤ 0.05).

19) were detected (Figure 3A; supplemental Table 1). For additional information regarding ribosomal, mitochondrial and apoptotic processes see GSEA results in supplemental Figure 3.

Ingenuity pathway analysis predicted *TGFB1* (Transforming Growth Factor-β1) or *CG* (Calycosin-7-O-β-d-glucopyranoside) in MGUS and SMM derived MSC and *DAP3* (death associated protein 3) or *ESR1* (estrogen receptor 1) in MM derived MSCs as potential top 5 upstream regulators (Figure 3B).

BMP/TGF-signaling as potential key pathway contributing to MSC transition from MGUS to SMM to MM

As predicted by Ingenuity pathway analysis, gene set enrichment analysis (GSEA) confirmed a clear transition to affected BMP/TGF-signaling in all 3 MSC groups. The bone morphogenetic protein 2 (*BMP2*) is a major regulator for osteogenesis and can be

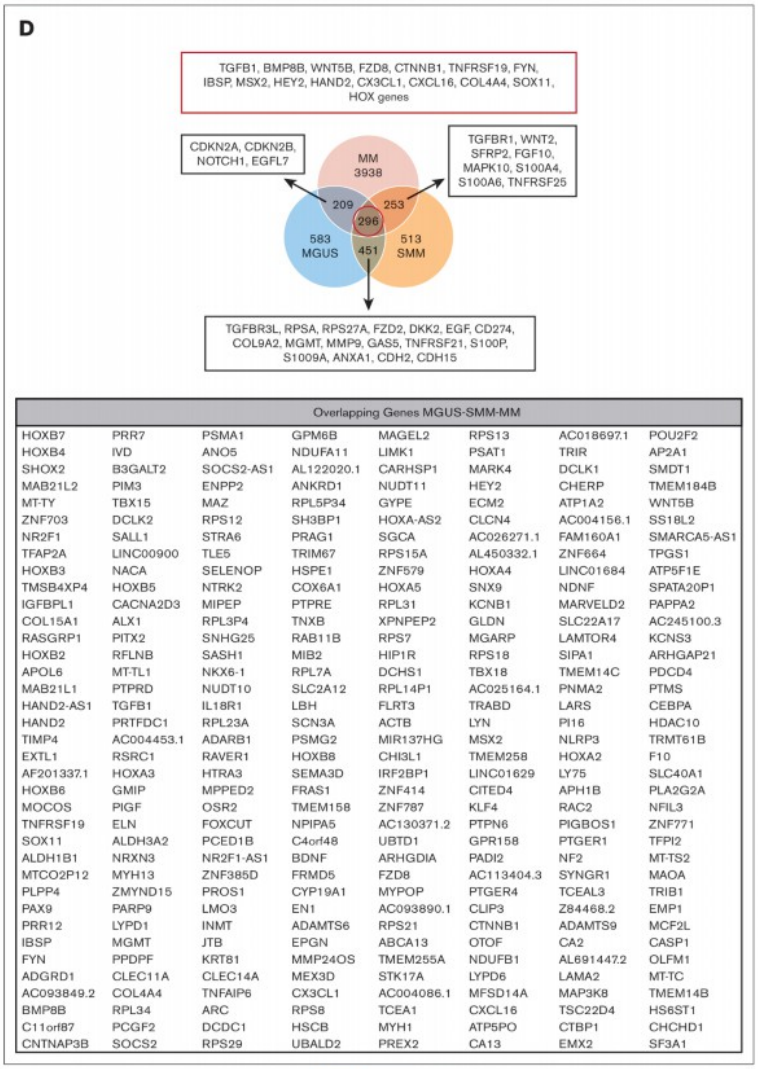

Overlapping Genes MGUS-SMM-MM							
HOXB7	PRR7	PSMA1	GPM6B	MAGEL2	RPS13	AC018697.1	POU2F2
HOXB4	IVD	ANO5	NDUFA11	LIMK1	PSAT1	TRIR	AP2A1
SHOX2	B3GALT2	SOCS2-AS1	AL122020.1	CARHSP1	MARK4	DCLK1	SMDT1
MAB21L2	PIM3	ENPP2	ANKRD1	NUDT11	HEY2	CHERP	TMEM184B
MT-TY	TBX15	MAZ	RPL5P34	GYPE	ECM2	ATP1A2	WNT5B
ZNF703	DCLK2	RPS12	SH3BP1	HOXA-AS2	CLCN4	AC004156.1	SS18L2
NR2F1	SALL1	STRA6	PRAG1	SGCA	AC026271.1	FAM160A1	SMARCA5-AS1
TFAP2A	LINC00900	TLE5	TRIM67	RPS15A	AL450332.1	ZNF664	TPGS1
HOXB3	NACA	SELENOP	HSPE1	ZNF579	HOXA4	LINC01684	ATP5F1E
TMSB4XP4	HOXB5	NTRK2	COX6A1	HOXA5	SNX9	NDNF	SPATA20P1
IGFBPL1	CACNA2D3	MIPEP	PTPRE	RPL31	KCNB1	MARVELD2	PAPPA2
COL15A1	ALX1	RPL3P4	TNXB	XPNPEP2	GLDN	SLC22A17	AC245100.3
RASGRP1	PITX2	SNHG25	RAB11B	RPS7	MGARP	LAMTOR4	KCNS3
HOXB2	RFLNB	SASH1	MIB2	HIP1R	RPS18	SIPA1	ARHGAP21
APOL6	MT-TL1	NKX6-1	RPL7A	DCHS1	TBX18	TMEM14C	PDCD4
MAB21L1	PTPRD	NUDT10	SLC2A12	RPL14P1	AC025164.1	PNMA2	PTMS
HAND2-AS1	TGFB1	IL18R1	LBH	FLRT3	TRABD	LARS	CEBPA
HAND2	PRTFDC1	RPL23A	SCN3A	ACTB	LYN	PI16	HDAC10
TIMP4	AC004453.1	ADARB1	PSMG2	MIR137HG	MSX2	NLRP3	TRMT61B
EXTL1	RSRC1	RAVER1	HOXB8	CHI3L1	TMEM258	HOXA2	F10
AF201337.1	HOXA3	HTRA3	SEMA3D	IRF2BP1	LINC01629	LY75	SLC40A1
HOXB6	GMIP	MPPED2	FRAS1	ZNF414	CITED4	APH1B	PLA2G2A
MOCOS	PIGF	OSR2	TMEM158	ZNF787	KLF4	RAC2	NFIL3
TNFRSF19	ELN	FOXCUT	NPIPA5	AC130371.2	PTPN6	PIGBOS1	ZNF771
SOX11	ALDH3A2	PCED1B	C4orf48	UBTD1	GPR158	PTGER1	TFPI2
ALDH1B1	NRXN3	NR2F1-AS1	BDNF	ARHGDIA	PADI2	NF2	MT-TS2
MTCO2P12	MYH13	ZNF385D	FRMD5	FZD8	AC113404.3	SYNGR1	MAOA
PLPP4	ZMYND15	PROS1	CYP19A1	MYPOP	PTGER4	TCEAL3	TRIB1
PAX9	PARP9	LMO3	EN1	AC093890.1	CLIP3	Z84468.2	EMP1
PRR12	LYPD1	INMT	ADAMTS6	RPS21	CTNNB1	ADAMTS9	MCF2L
IBSP	MGMT	JTB	EPGN	ABCA13	OTOF	CA2	CASP1
FYN	PPDPF	KRT81	MMP24OS	TMEM255A	NDUFB1	AL691447.2	OLFM1
ADGRD1	CLEC11A	CLEC14A	MEX3D	STK17A	LYPD6	LAMA2	MT-TC
AC093849.2	COL4A4	TNFAIP6	CX3CL1	AC004086.1	MFSD14A	MAP3K8	TMEM14B
BMP8B	RPL34	ARC	RPS8	TCEA1	CXCL16	TSC22D4	HS6ST1
C11orf87	PCGF2	DCDC1	HSCB	MYH1	ATP5PO	CTBP1	CHCHD1
CNTNAP3B	SOCS2	RPS29	UBALD2	PREX2	CA13	EMX2	SF3A1

Figure 1 (continued)

stimulated by estrogen signaling. We observed a significantly shifted enrichment score of signatures describing BMP2 and TGFB1 signaling and target genes already in the analysis with MGUS-derived MSC contrasted to healthy samples, while the gene set for TNFA/NFKB signaling was not affected in GSEA. The BMP2 signature was clearly conserved when contrasting healthy and SMM MSC while WNT signature was not strongly affected. GSEA results from MM MSC contrasted to healthy revealed a strong enrichment of genes related to TGFB1 signaling signature and expanded with a strong enriched TNF/p38 and Estrogen-signature (Figure 3C). BMP's, TGF und ESR are known to be involved in several cell processes such as osteogenesis and multiple myeloma progression and we already have seen in MGUS MSC a marked enrichment of genes that could be assigned to multiple myeloma in the later course of progression. This was confirmed by a strong enrichment of processes such as

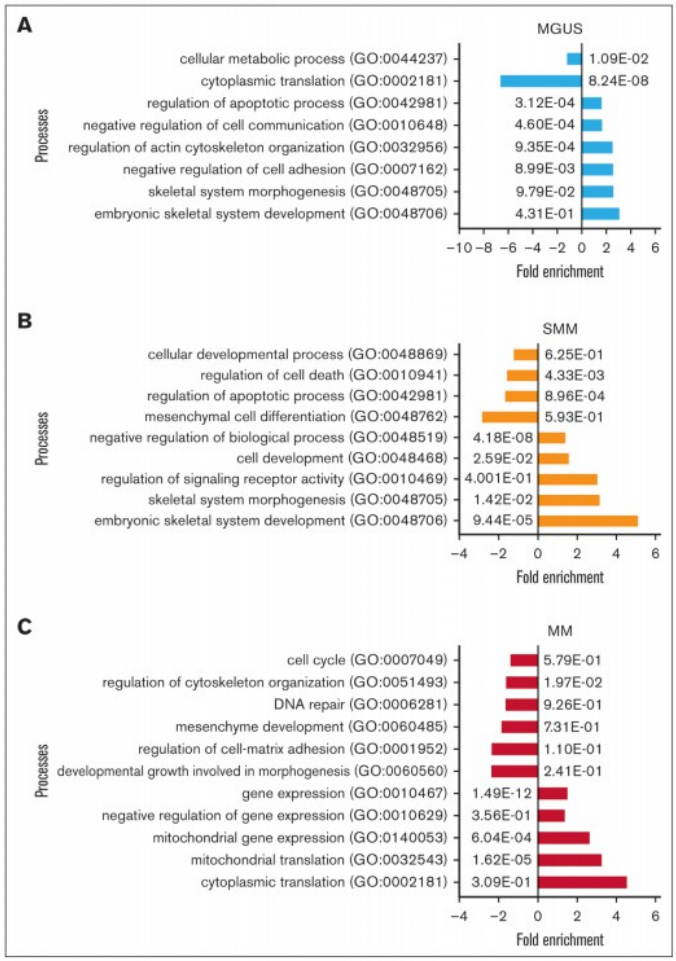

Figure 2. Gene Ontology (GO) of MGUS, SMM and MM MSC contrasted to healthy individuals revealed contributed cell processes Representative overview of GO representing contributed processes such as skeletal system, cell communication or apoptotic processes in MGUS MSC. (A) Developmental processes, cell death, or mesenchymal cell differentiation were enriched in SMM (B) and in MM MSC processes such as DNA repair, mesenchyme development, or regulation of cell-matrix adhesion (C) were strongly enriched. For all GO terms, fold enrichment and *P*-values of overrepresented and underrepresented processes are given.

hematopoiesis, osteogenesis or cell cycle regulation by GSEA analysis in all 3 groups (supplemental Figure 2).

Differential gene expression translates to functional alterations

To address the question whether programmatic alterations detected on molecular level underlying the transition from MGUS to MM are also seen in MSCs concerning their functionality, we performed different in vitro assays.

Typical characteristics of in vitro MSCs are a spindle type morphology and the formation of fibroblast colonies (Colony Forming Unit-Fibroblast; CFU-F). We already found a significantly reduced CFU-F activity of MGUS-derived MSC (mean, MGUS: 31.94; HC: 91.2, *P*-value: 0.002). SMM-derived MSC showed a 2.6-fold reduced CFU-F activity (mean, SMM: 34.6; HC: 91.2, *P*-value: 0.01) and MM-derived MSC showed the most reduced CFU-F activity (mean, MM: 22.7; HC: 91.2 *P*-value: ≤0.0001). We observed a heterogeneous morphology in MGUS-derived MSC, ranging from no relevant to single alterations, while a more disorganized and broad shaping

A

MGUS	SMM	MM
MAPK7	*CCND2*	*CDK's (4, 6, 7, 10, 12, 19)*
SPP1 (Osteopontin)	*WNT7B*	*MAPK14 (p38)*
FGF11	SESN2	*BMP2K*
FZD9	*EMILIN1*	*BMPR2*
TGFB1I1	*CXCL2*	*BMP5*
FZD7	TGIF1	*SMAD5*
FGF18	*FZR1*	*SMAD6*
TGFB2	*CEMIP2*	*TGFA*
VCAM	*CASP2*	*TGFB3*
CCL7	*CCPG1*	*TGFBR3*
FZD6	*CDK15*	*WNT9A*

B

MGUS		
Name	*P*-value	Predicted Activation
Lipopolysaccharide	8.62E-50	Activated
Dexamethasone	1.14E-49	
TNF	2.78E-47	Activated
Tretinoin	3.54E-41	Activated
TGFB1	5.79E-36	Activated

SMM		
Name	*P*-value	Predicted Activation
TGFB1	1.59E-19	
CG	8.10E-18	Inhibited
WNT3A	3.99E-16	
Tretinoin	4.89E-16	
Dexamethasone	2.24E-15	

MM		
Name	*P*-value	Predicted Activation
DAP3	2.44E-16	Activated
ESR1	7.34E-16	Inhibited
Beta-Estradiol	1.85E-14	
KRAS	4.66E-13	
Dexamethasone	7.49E-13	Inhibited

C

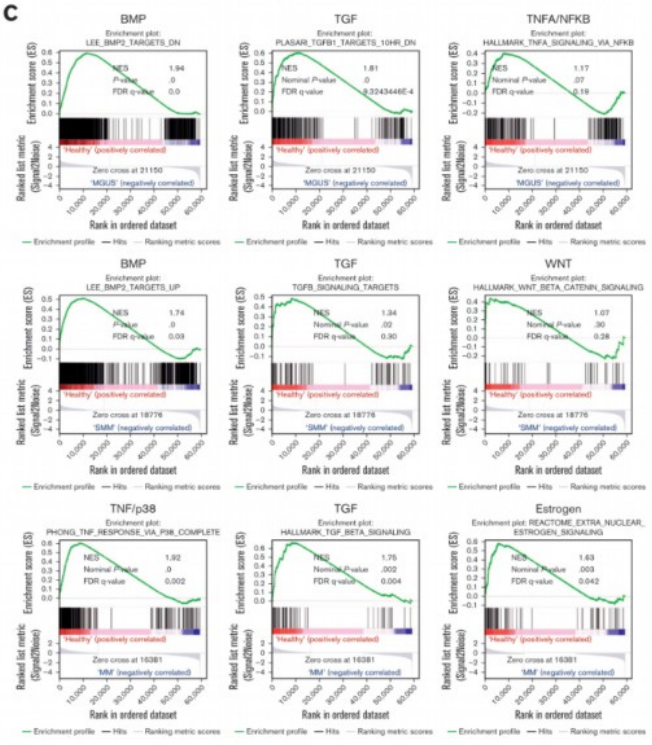

Figure 3. Ingenuity pathway analysis and GSEA in MSC from patients with MGUS, SMM and MM revealed a unique genetic signature in MSC transition. (A) Table overview of unique differentially expressed genes from DESeq2 output such as MAPK7, SPP1 or FGF11 in MGUS MSC, CCND2, WNT7B or SESN2 in SMM MSC as well as several CDK's, MAPK14 or BMP2K in MM MSC within the comparison of all 3 groups (FDR q-value ≤0.05). (B) Ingenuity pathway analysis predicted the top 5 most probable upstream regulators in MGUS, SMM and MM MSC. (C) GSEA contrasting healthy samples to MGUS, SMM and MM samples. The results confirmed a strong enrichment for the BMP/TGFB-signaling pathway signature. Neither TNFA/NFKB nor WNT are strongly enriched. MM MSC to healthy MSC confirmed a strong enrichment of a gene set also for TNF/p38 and Estrogen signaling signature. For all plots, the normalized enrichment score, *P*-values and (FDR q-value) are given.

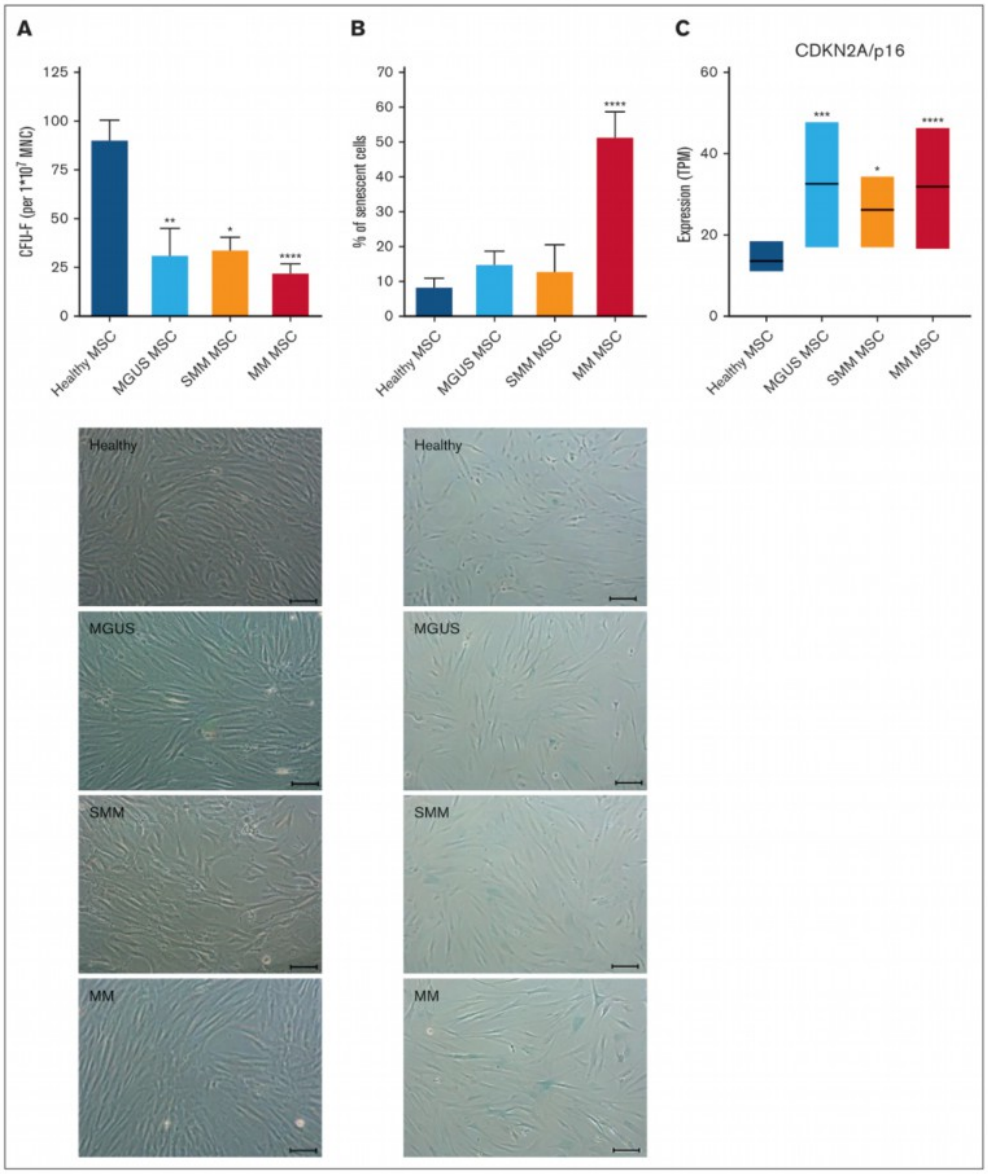

Figure 4. Alteration in morphology and reduced growth capacity of MGUS, SMM and MM MSC. (A) Bar charts of CFU-F were normalized to 1 × 10^7 plated BM-MNC and representative micrograph of the phenotype of MGUS-, SMM- and MM-derived MSC with scale bars indicating 100 µm. (B) Bar charts of the number of senescent cells in native MGUS-, SMM- and MM-derived MSC in passage 3 cells after the β-galactosidase staining and representative micrographs to visualize senescent cells in blue (scale bars indicating 100 µm). For all experiments results are expressed as mean ± SEM. Asterisks indicate *P*-values **P* < .05, ***P* < .01, ****P* < .001. (C) Box plot of the TPM (Transcripts per Kilobase Million) values for CDKN2A (p16) from our RNA sequencing data of healthy (n = 5), MGUS (n = 4), SMM (n = 4) and MM (n = 5) MSC. Significances were included from the DESeq2 results of CDKN2A of MGUS, SMM and MM MSC contrasted to healthy MSC. Asterisks indicate *P*-values **P* < .05, ***P* < .01, ****P* < .001, *****P* < .0001.

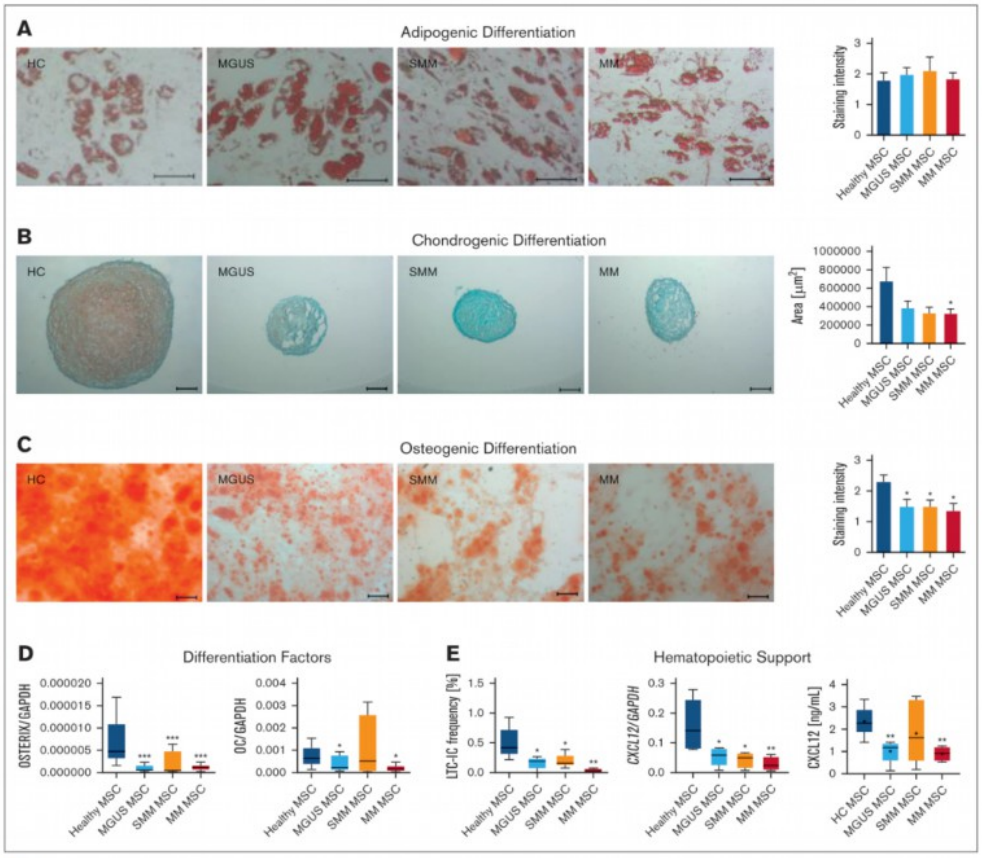

Figure 5. Reduced differentiation capacity and hematopoietic support of MGUS, SMM and MM MSC. (A) Representative micrographics of lipid vacuoles after Oil Red O staining of adipogenic differentiated MGUS-, SMM- and MM-derived MSC after 21 days of differentiation. Scale bars indicating 100 µm are shown. (B) Bar charts of measured cartilage area of chondrogenic differentiated MGUS-, SMM- and MM-derived MSC after 21 days of differentiation, stained with Safranin O and representative micrographics of orange proteoglycan after staining. Scale bars indicating 100 µm are shown. Chondrogenic differentiation capacity was graded according to the area of chondrogenic pellets and according to microscopic analysis. (C) Osteogenic differentiation was induced for 14 days and stained with Alizarin Red. Differences of the osteogenic potential between healthy MSC and MGUS-, SMM- and MM-derived MSC were quantified and are shown in bar charts. Representative micrographics of healthy and MGUS-, SMM- and MM-derived MSC with scale bars indicating 100 µm. For quantification, adipogenic, chondrogenic and osteogenic differentiation capacity was graded according to microscopic analysis of staining intensity as: 0 = absent; 1 = weak; 2 = moderate; 3 = intensive as previously described.[14] (D) mRNA expression level of osteogenic factors as *OSTERIX* and *OSTEOCALCIN* were measured by quantitative Realtime-PCR in healthy MSC and MGUS-, SMM- and MM-derived MSC. (E) Hematopoietic Support of MGUS, SMM and MM MSC. Left side: Bar charts showing LTC-IC frequency of healthy CD34+ HSPC cultured on healthy-, MGUS-, SMM- or MM-derived MSC. Colonies were calculated under light microscope and visualized in graph. Right side: mRNA expression level of *CXCL12* was measured by quantitative Realtime-PCR in healthy MSC, MGUS-, SMM- and MM-derived MSC. CXCL12 protein level in conditioned media (CM) from healthy (n = 5), MGUS (n = 5), SMM (n = 6), MM (n = 4) were assessed by Enzyme-Linked Immunosorbent Assay. For all experiments, results are expressed as mean ±SEM. Asterisks display *P*-values $*P \leq .05$; $** P \leq .01$; $*** P \leq .001$.

structure in SMM-derived MSC was observed which was even more apparent in MM derived MSC (Figure 4A). Cellular senescence was up to 1.7-fold increased in MGUS- and SMM-derived MSC (mean, MGUS: 15.2%, SMM 13.2%, HC: 8.7%), whereas it was 5.9-fold increased in MM-derived MSC compared to healthy MSC (mean, MM: 51.8%, HC: 8.7%, $P \leq .0001$, Figure 4B) and in line with this, RNA sequencing data show an upregulation of CDKN2A (p16), as a marker for senescent cells (Figure 4C).

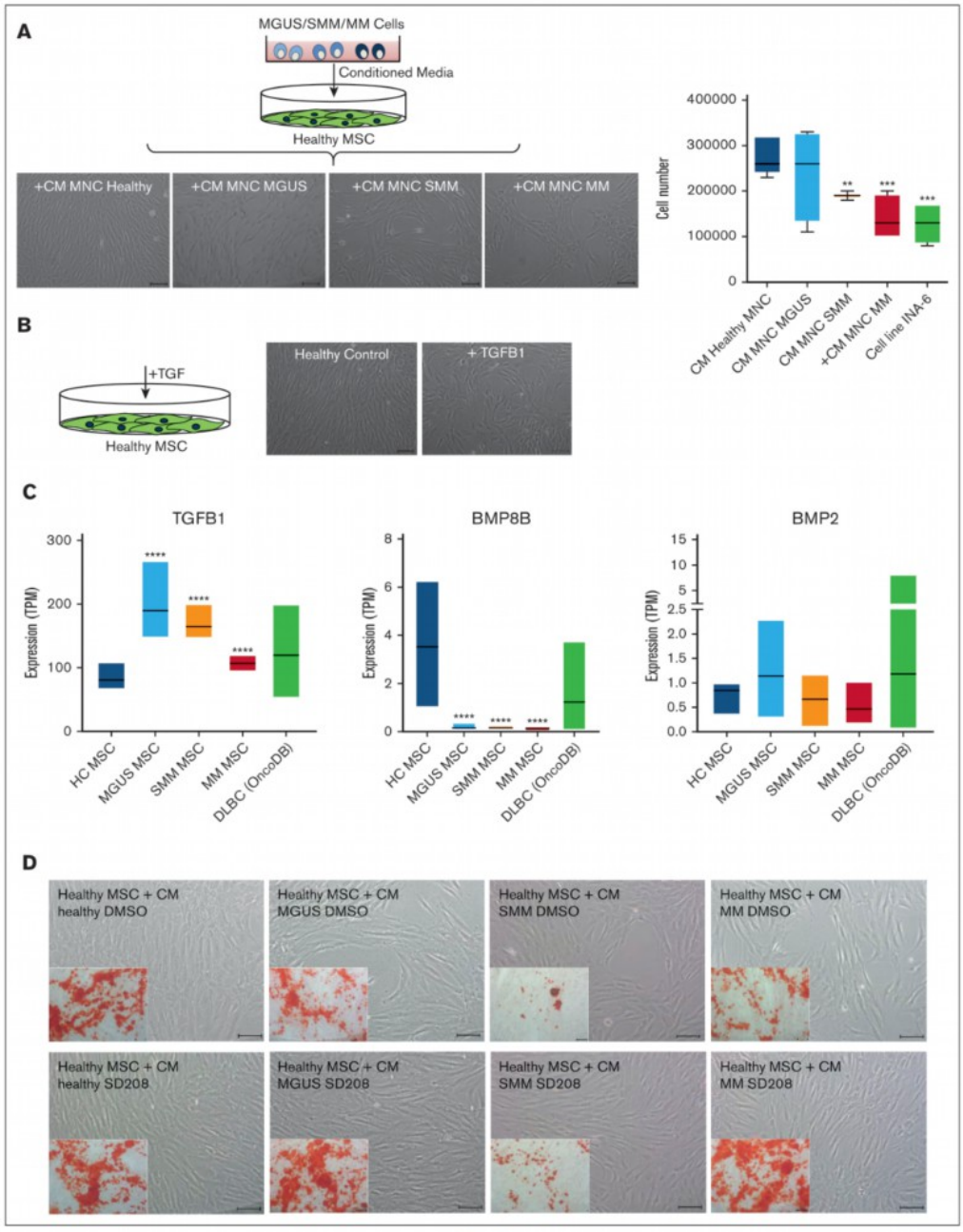
A
MGUS/SMM/MM Cells
Conditioned Media
Healthy MSC
+CM MNC Healthy
+CM MNC MGUS
+CM MNC SMM
+CM MNC MM
Cell number
400000
300000
200000
100000
0
CM Healthy MNC
CM MNC MGUS
CM MNC SMM
+CM MNC MM
Cell line INA-6
B
+TGF
Healthy MSC
Healthy Control
+ TGFB1
C
TGFB1
BMP8B
BMP2
Expression (TPM)
HC MSC
MGUS MSC
SMM MSC
MM MSC
DLBC (OncoDB)
D
Healthy MSC + CM healthy DMSO
Healthy MSC + CM MGUS DMSO
Healthy MSC + CM SMM DMSO
Healthy MSC + CM MM DMSO
Healthy MSC + CM healthy SD208
Healthy MSC + CM MGUS SD208
Healthy MSC + CM SMM SD208
Healthy MSC + CM MM SD208

Figure 6.

MGUS, SMM and MM derived MSC show a diminished osteogenic-chondrogenic differentiation capacity

In the next step, we investigated patients-derived MSC in their capacity to differentiate into the osteogenic, chondogenic, or adipogenic lineage. No relevant differences could be observed in adipogenic differentiation in MGUS, SMM or in MM MSC (Figure 5A), but the chondrogenic differentiation was reduced in all 3 groups, indicated by reduced area size of cartilage pellets and Safranin O staining (Figure 5B). Since we know about the clinical relevance of osteoblast impairment in MM, we were interested in the question whether osteogenic differentiation is already impaired in MGUS and SMM. We observed a significantly reduced osteogenic differentiation capacity already in MGUS and SMM derived MSC as well as in MM derived MSC in comparison to healthy MSC (mean, HC: 2.28, MGUS: 1.33, *P-value: .02* SMM: 1.25, *P*-value: .03; MM: 1.3, *P*-value: .009, Figure 5C). The early osteogenic marker *OSTERIX* was significantly reduced in all groups and the late osteogenic factor *OSTEOCALCIN* was significantly reduced in MGUS and MM MSC, but not in SMM MSC. For the latter the limited size of the samples analyzed must be noted.

Impaired hematopoietic support is already diminished in MGUS- and SMM-derived MSC and progresses in MM-derived MSC

To investigate hematopoietic supporting capacity of MGUS-, SMM- and MM-derived MSC we performed Long Term Culture Initiating Cell (LTC-IC) assays. Already MGUS and SMM-derived MSC exhibited a twofold reduced hematopoietic supporting capacity and in line with the clinical presentation we observed a 12-fold reduced hematopoietic supporting capacity in MM-derived MSC. On a molecular level, the expression of *CXCL12*, also known as Stromal-derived factor-1 (*SDF-1*), a crucial player for several cell processes such as migration of stem cells, bone formation, inflammation, or cancer association, was significantly downregulated in MGUS, SMM and MM derived MSC (Figure 5E). This was validated on protein level by measuring SDF-1 (CXCL12) in supernatants of cultured MGUS, SMM, MM MSC (Figure 5E).

Soluble factors from TGF beta family as potential candidates to induce the observed alterations

Finally we wanted to test whether these observed MSC alterations are inducible and whether this could be responsible due to soluble factors. For this we co-cultured healthy MSC with supernatants from MGUS, SMM, and MM patients. Inducible effects on morphology and growth properties of healthy MSC after exposure to supernatants from MGUS, SMM, and MM patients could be observed, similar to those observed in patients-derived MSC from our aforementioned functional analysis (Figure 6A). Previous data from our group [19] show, that TGF could be a potential candidate for inducing alterations in healthy MSC as representative shown in Figure 6B. Furthermore, the database OncoDB shows, that a dysregulated expression of *TGFB1*, *BMP8B* and *BMP2* is noted in other mature B-cell neoplasia like diffuse large B-cell lymphoma (DLBC, 48 samples), comparable to those expression data in our Multiple Myeloma MSC (Figure 6C) and may suggest a potential contribution to disease progression to multiple myeloma. Assuming TGFβ1 as a soluble factor in CM derived from patients' cells have the potential to induce the observed alterations in healthy MSC we wondered whether blocking by the active ATP-competitive transforming growth factor-β receptor 1 (TGF-βRI) (ALK5) inhibitor SD208 can revert the effects.

Therefore, we incubated healthy MSC with CM from patients-derived MNCs (MGUS, SMM, or MM) and blocked TGFB1 signaling by SD208 (Figure 6D). In line with our previous findings, coculture with patient derived MNC lead to a dysregulated phenotype, reduced cell number, and diminished osteogenic differentiation capacity of healthy MSCs. The addition of SD208 restores the phenotype and osteogenic differentiation capacity (Figure 6D).

Discussion

The hallmark of MM is a clonal plasma cell infiltration in the BM accompanied by end-organ damage such as hematopoietic insufficiency and/or osteolysis. MM is often considered to be preceded by a sequence of premalignant stages such as MGUS and asymptomatic stages such as SMM. Although there are studies showing this sequence within the malignant cell itself, it is unclear whether this sequence is also found in MSC.[20] Some studies have addressed the pathophysiological contribution in disease development of MSC within the BM microenvironment but mainly focused on MM.[11,21]

In this study, we could show that alterations of MSC are already imprinted in MGUS and further progresses in SMM and finally in MM. Within this sequence, we were able to show both structural and functional alterations of MSC, with reduced osteogenic differentiation capacity and impaired hematopoietic support. In part, these alterations showed a significant progression to full blown MM. In line with this, PCR analyses showed reduced expression of *CXCL12*, which is known as a crucial player for several cell processes; for example, for migration of stem cells, bone formation,

Figure 6. Blocking of the potential candidate TGFB in supernatants derived from MGUS, SMM and MM restores differentiation capacity of co-cultured healthy MSC. (A) Study design for coculture of healthy MSC with conditioned media (CM) from MGUS, SMM, and MM patients. MSC were cultured with CM from healthy, MGUS, SMM, or MM MNC for 3 days. Representative micrographics of the phenotype of healthy MSC after exposure to supernatants from MGUS-, SMM-, and MM-derived MNC for 3 days with scale bars indicating 100 μm. Bar charts of cell number after exposure to supernatants from MGUS, SMM, and MM MNC as well as the MM cell line INA-6. (B) Healthy MSC were treated 3 days with TGFB1 and representative pictures show phenotype of untreated healthy control and after exposure to TGFB1. Scale bars indicating 100 μm. (C) Expression TPM-values (transcripts per kilobase million) from our RNA sequencing data for TGFB1, BMP8B, and BMP2 from our MGUS, SMM, and MM MSC samples in comparison to 48 patients samples with diffuse large B-cell lymphoma from the database OncoDB. (D) Coculture of healthy MSC with CM from healthy, MGUS, SMM, and MM MNC. To analyze and inhibit potential TGFB1 inducing effects, the potent ATP-competitive TGF-βRI inhibitor SD208 was added to CM from healthy, MGUS, SMM, and MM-derived MNC. DMSO containing CM served as control group. Healthy MSC were co-cultured with respective CM for 3 days. Representative micrographs of the morphology of healthy MSC cocultured with CM supplemented with DMSO or SD208 are shown. Inner pictures show Alizarin Red staining of 14 days osteogenic induced healthy MSC after the period of 3 days of exposure to respective condition (CM MGUS, SMM, MM + DMSO, or +SD208). Scale bars indicating 100 μm.

and inflammation.[20,21] The deletion of *CXCL12* in murine MSC leads to a dysregulated bone formation in the number of osteoclasts and osteoblasts and increased adipocytes.[22]

Physiologically TGF/BMP signaling plays a crucial role in several cell processes,[19,22,23] and it has been shown to play a role in MM progression.[11] Although the role of BMPs in the development of osteolysis in myeloma is controversial, blocking these signaling pathways has already been considered.[24,25]

RNA sequencing revealed that MSC from all 3 groups exhibited activation of BMP/TGF signaling. This may lead to dysregulation of downstream targets such as the osteogenic-chondrogenic transcription factor *RUNX2*, which in turn led to dysregulation of induction factors for osteogenesis such as *OSTERIX* or *IBSP*.[26] With the knowledge of the osteoblast's crucial role in normal BM and MM, it has been reported that osteoblasts directly inhibit MM cells in vitro.[27] We and other groups consistently show overrepresented *TGFB-1*, which was described in correlation with bone lesions in patients with MM and other WNT-regulators or reduced osteogenic differentiation.[11,21,28-30] Blocking of TGB1-signaling by SD208 restores functionality of MSC as shown by our group and others for other entities.[11,19]

Surprisingly, osteogenic capacity of MGUS MSC was already diminished and reflected by a reduced *OSTERIX* and *OSTEOCALCIN* level.

This imbalance, with impaired osteoblastic differentiation as shown in this study and the clinically known activation of osteoclasts, may contribute to defective bone remodeling that is implicated in early disease stages.

In addition, immunologic dysfunction of MSCs became a greater focus of interest and has been reported by other groups, because activation of an immunosuppressive microenvironment by MSCs may contribute to the transition from MGUS to MM.[29,31] Furthermore, *TGFB* plays a role here, which can create an immunosuppressive milieu and lead to drug resistance of modern immunotherapeutics.[32] In addition, our group has already shown that extrinsic *TGF-β* is capable of generating functional deficits in MSC.[19] In conclusion, our data lead to a broader understanding of the impact of the microenvironment on the progression of MGUS and SMM to MM, and MSCs are a potential therapeutic target. This would provide a treatment that not only targets the malignant clone and tumor-associated immunosuppression but also addresses the remodeling of the microenvironment by altered MSCs as a third pillar. We, therefore, consider blocking the BMP/TGF signaling pathway as a future approach to prevent end-organ damage and to avoid progression to MM.

Acknowledgments

The authors thank Dennis Sohn from the Laboratory of Molecular Radio-Oncology for technical assistance regarding LTC-IC assay.

This work was supported by the Leukämie Lymphom Liga e. V., Duesseldorf, Germany and a grant (2019-21) from the Research Committee of the Medical Faculty, Heinrich-Heine-University, Duesseldorf (S.G.), and the German Research Foundation (417677437/GRK2578).

The funders had no role in the design of the study, the collection, analyses, or interpretation of data, the writing of the manuscript, or in the decision to publish the results.

Authorship

Contribution: L.B., T.S., P.J., and S.G. contributed to conception and design, provision of study material or patients, collection and/or assembly of data, data analysis and interpretation, manuscript writing, and final approval of the manuscript; R.F. contributed to provision of study material or patients, collection and/or assembly of data, data analysis and interpretation, manuscript writing, and final approval of the manuscript; U.M. and R.Z. contributed to provision of study material or patients, collection and/or assembly of data, and final approval of the manuscript; A.K., B.S., P.P., T.W., K.K., and F.B. contributed to collection and/or assembly of data, data analysis and interpretation, and final approval of the manuscript; and S.D. and R.H. contributed to data analysis and interpretation, manuscript writing, and final approval of the manuscript.

Conflict-of-interest dislosure: The authors declare no competing financial interests.

ORCID profiles: B.S., 0000-0003-3738-4979; F.B., 0000-0002-5919-3375; K.K., 0000-0003-3644-2022; P.P., 0000-0002-8355-5524; T.W., 0000-0002-6760-2458; R.Z., 0000-0002-3721-6820; P.J., 0000-0001-9250-2064.

Correspondence: Paul Jäger, Department of Hematology, Oncology and Clinical Immunology, University of Duesseldorf, Medical Faculty, Moorenstr. 5, 40225 Düsseldorf, Germany; email: paul-sebastian.jaeger@med.uni-duesseldorf.de; and Stefanie Geyh, Department of Hematology, Oncology and Clinical Immunology, University of Duesseldorf, Medical Faculty, Moorenstr. 5, 40225 Düsseldorf, Germany; email: Stefanie.geyh@med.uni-duesseldorf.de.

References

1. Kyle RA. Multiple myeloma. *N Engl J Med*. 2004;351(18):1860-1873.
2. Kyle RA. Multiple myeloma. *Blood*. 2007;111(6):2962-2972.
3. Medical Masterclass, e.b.J.F. Haematology: multiple myeloma. *Clin Med (Lond)*. 2019;19(1):58-60.
4. Dispenzieri A, Katzmann JA, Kyle RA, et al. Prevalence and risk of progression of light-chain monoclonal gammopathy of undetermined significance: a retrospective population-based cohort study. *Lancet*. 2010;375(9727):1721-1728.
5. Kyle RA. Prevalence of monoclonal gammopathy of undetermined significance. *N Engl J Med*. 2006;354(13):1362-1369.
6. Rodriguez-Otero P, Paiva B, San-Miguel JF. Roadmap to cure multiple myeloma. *Cancer Treat Rev*. 2021;100:102284.
7. Michels T, Petersen KE. Multiple myeloma: diagnosis and treatment. *Am Fam Physician*. 2017;95(6):373-383.

8. Dominici M, Le Blanc K, Mueller I, et al. Minimal criteria for defining multipotent mesenchymal stromal cells. The International Society for Cellular Therapy position statement. *Cytotherapy*. 2006;8(4):315-317.
9. Anthony BA, Link DC. Regulation of hematopoietic stem cells by bone marrow stromal cells. *Trends Immunol*. 2014;35(1):32-37.
10. Morrison SJ, Scadden DT. The bone marrow niche for haematopoietic stem cells. *Nature*. 2014;505(7483):327-334.
11. Bruns I, Cadeddu RP, Brueckmann I, et al. Multiple myeloma-related deregulation of bone marrow-derived CD34(+) hematopoietic stem and progenitor cells. *Blood*. 2012;120(13):2620-2630.
12. Palumbo A, Avet-Loiseau H, Oliva S, et al. Revised International staging system for multiple myeloma: a report from International Myeloma Working Group. *J Clin Oncol*. 2015;33(26):2863-2869.
13. Chng W J, Dispenzieri A, Chim C-S, et al. IMWG consensus on risk stratification in multiple myeloma. *Leukemia*. 2014;28(2):269-277.
14. Geyh S, Oz S, Cadeddu RP, et al. Insufficient stromal support in MDS results from molecular and functional deficits of mesenchymal stromal cells. *Leukemia*. 2013;27(9):1841-1851.
15. Geyh S, Rodríguez-Paredes M, Jäger P, et al. Functional inhibition of mesenchymal stromal cells in acute myeloid leukemia. *Leukemia*. 2016;30(3): 683-691.
16. Jager P, Geyh S, Twarock S, et al. Acute myeloid leukemia-induced functional inhibition of healthy CD34+ hematopoietic stem and progenitor cells. *Stem Cells*. 2021;39(9):1270-1284.
17. Dobin A, Davis CA, Schlesinger F, et al. STAR: ultrafast universal RNA-seq aligner. *Bioinformatics*. 2013;29(1):15-21.
18. Pertea M, Pertea GM, Antonescu CM, Chang TC, Mendell JT, Salzberg SL. StringTie enables improved reconstruction of a transcriptome from RNA-seq reads. *Nat Biotechnol*. 2015;33(3):290-295.
19. Geyh S, Rodríguez-Paredes M, Jäger P, et al. Transforming growth factor beta1-mediated functional inhibition of mesenchymal stromal cells in myelodysplastic syndromes and acute myeloid leukemia. *Haematologica*. 2018;103(9):1462-1471.
20. van Nieuwenhuijzen N, Spaan I, Raymakers R, Peperzak V. From MGUS to multiple myeloma, a paradigm for clonal evolution of premalignant cells. *Cancer Res*. 2018;78(10):2449-2456.
21. Jurczyszyn A, Zebzda A, Czepiel J, et al. The analysis of the relationship between multiple myeloma cells and their microenvironment. *J Cancer*. 2015; 6(2):160-168.
22. Chen G, Deng C, Li YP. TGF-beta and BMP signaling in osteoblast differentiation and bone formation. *Int J Biol Sci*. 2012;8(2):272-288.
23. Batlle E, Massague J. Transforming growth factor-beta signaling in immunity and cancer. *Immunity*. 2019;50(4):924-940.
24. Ghosh-Choudhury N, Windle JJ, Koop BA, et al. Immortalized murine osteoblasts derived from BMP 2-T-antigen expressing transgenic mice. *Endocrinology*. 1996;137(1):331-339.
25. Gooding S, Olechnowicz SWZ, Morris EV, et al. Transcriptomic profiling of the myeloma bone-lining niche reveals BMP signalling inhibition to improve bone disease. *Nat Commun*. 2019;10(1):4533.
26. Bruderer M, Richards RG, Alini M, Stoddart MJ. Role and regulation of Runx2 in osteogenesis. *Eur Cell Mater*. 2014;28:269-286.
27. Reagan MR, Ghobrial IM. Multiple myeloma mesenchymal stem cells: characterization, origin, and tumor-promoting effects. *Clin Cancer Res*. 2012; 18(2):342-349.
28. Todoerti K, Lisignoli G, Storti P, et al. Distinct transcriptional profiles characterize bone microenvironment mesenchymal cells rather than osteoblasts in relationship with multiple myeloma bone disease. *Exp Hematol*. 2010;38(2):141-153.
29. Garcia-Gomez A, De Las Rivas J, Ocio EM, et al. Transcriptomic profile induced in bone marrow mesenchymal stromal cells after interaction with multiple myeloma cells: implications in myeloma progression and myeloma bone disease. *Oncotarget*. 2014;5(18):8284-8305.
30. Tian E, Zhan F, Walker R, et al. The role of the Wnt-signaling antagonist DKK1 in the development of osteolytic lesions in multiple myeloma. *N Engl J Med*. 2003;349(26):2483-2494.
31. Giallongo C, Tibullo D, Camiolo G, et al. TLR4 signaling drives mesenchymal stromal cells commitment to promote tumor microenvironment transformation in multiple myeloma. *Cell Death Dis*. 2019;10(10):704.
32. Rana PS, Soler DC, Kort J, Driscoll JJ. Targeting TGF-beta signaling in the multiple myeloma microenvironment: steering CARs and T cells in the right direction. *Front Cell Dev Biol*. 2022;10:1059715.

Supplementary Material can be accessed using the following URLs:

1) https://pmc.ncbi.nlm.nih.gov/articles/instance/11145751/bin/BLOODA_ADV-2023-011632-mmc1.xlsx
2) https://pmc.ncbi.nlm.nih.gov/articles/instance/11145751/bin/BLOODA_ADV-2023-011632-mmc2.pdf

2.3. Functional and Molecular Effects on the Bone Marrow Stroma in Patients with Therapy-Related Myeloid Neoplasms

Bo Scherer, Lucienne Bogun, Annemarie Koch, Paul Jäger, Ulrich Germing, Uwe Maus, Felix Bormann, Thorsten Wachtmeister, Patrick Petzsch, Karl Köhrer, Rainer Haas, Thomas Schroeder and Stefanie Geyh

Abstract

Therapy-related myeloid neoplasms (*t*-MN) are serious late complications of anticancer treatment and have been mainly attributed to genotoxic alterations of hematopoietic stem and progenitor cells (HSPC) in the bone marrow (BM). Mesenchymal stromal cells (MSC) are a key component of the BM niche and are recognized as key regulator of normal hematopoiesis and contributor in the pathogenesis of *de novo* MDS and AML. MSC are also exposed to genotoxic stress during anticancer therapy; however, their contribution to *t*-MN development has not been elucidated so far. For this purpose, we compared MSC from patients with *t*-MN and *de novo* myeloid neoplasm (MN). Phenotypical alterations along with an altered differentiation capacity and diminished hematopoietic supporting capacity was similar, but more pronounced in t-MN compared MN MSC. This was also confirmed by their genetic signature as mRNA sequencing revealed affected genes related to MSC development and extracellular matrix organization. A comparison of *t*-MN (*t*-MDS and *t*-AML) with MN (*de novo* MDS and AML) samples revealed 91 overlapping genes in all groups, which clearly show a relevance regarding the skeletal system and hematopoiesis. Moreover, a specific molecular signature including de regulated pathways involved in inflammation and angiogenesis was determined only in *t*-MN MSC, hinting on distinct therapy-induced alterations in the stromal compartment.

Journal	Blood Advances *(planned submission)*
Impact factor	7.4 (2023)
Contribution to publication	65 %

The own contribution of this manuscript includes the main provision of study material, the main bulk of collection and assembly of experiment data, as well as analysis and interpretation of obtained data. The conceptualization, manuscript writing and figure design was mainly conducted by the first author.

Type of authorship	First author
Status of publication	Manuscript draft

Functional and molecular effects on the bone marrow stroma in patients with therapy-related myeloid neoplasms

Bo Scherer[1], Lucienne Bogun[1], Annemarie Koch[1], Paul Jäger[1], Ulrich Germing[1], Uwe Maus[2], Felix Bormann[3], Thorsten Wachtmeister[4], Patrick Petzsch[4], Karl Köhrer[4], Rainer Haas[1], Thomas Schroeder[5*] and Stefanie Geyh[1*]

[1]Department of Hematology, Oncology and Clinical Immunology, University Hospital Duesseldorf, Medical Faculty, Heinrich Heine University Duesseldorf, Germany

[2]Department of Orthopedic Surgery and Traumatology, University Hospital Duesseldorf, Medical Faculty, Heinrich Heine University Duesseldorf, Germany

[3]Bioinformatics.expert, Berlin

[4]Biologological and Medical Research Center (BMFZ), Department Genomics & Transcriptomics Laboratory Heinrich Heine University, Universitätsstr.1, 40225 Duesseldorf, Germany

[5]Department of Hematology and Stem Cell Transplantation, University Hospital Essen, Essen, Germany

*These authors contributed equally

Short title: MSC in therapy related myeloid neoplasms

Corresponding authors: Thomas Schroeder (Department of Hematology and Stem Cell Transplantation, University Hospital Essen, Germany, Hufelandstraße 55, D-45147 Essen, phone: +49 201 / 723-7165, FAX: +49 201 / 723-5463), thomas.schroeder@uk-essen.de and Stefanie Geyh (Department of Hematology, Oncology and Clinical Immunology, University of Duesseldorf, Medical Faculty, Moorenstr. 5, 40225 Düsseldorf, phone: +49 211 / 8119606, Fax: +49 211 / 8104296), stefanie.geyh@med.uni-duesseldorf.de

Keywords: Mesenchymal stromal cells, MSC, bone marrow microenvironment, therapy-related myeloid neoplasms, inflammation, differentiation, hematopoiesis support

Parts of this study have been presented at the EACR-AACR-IACR Conference in Dublin, Ireland, in February 2024.

29 **Graphical abstract**

30

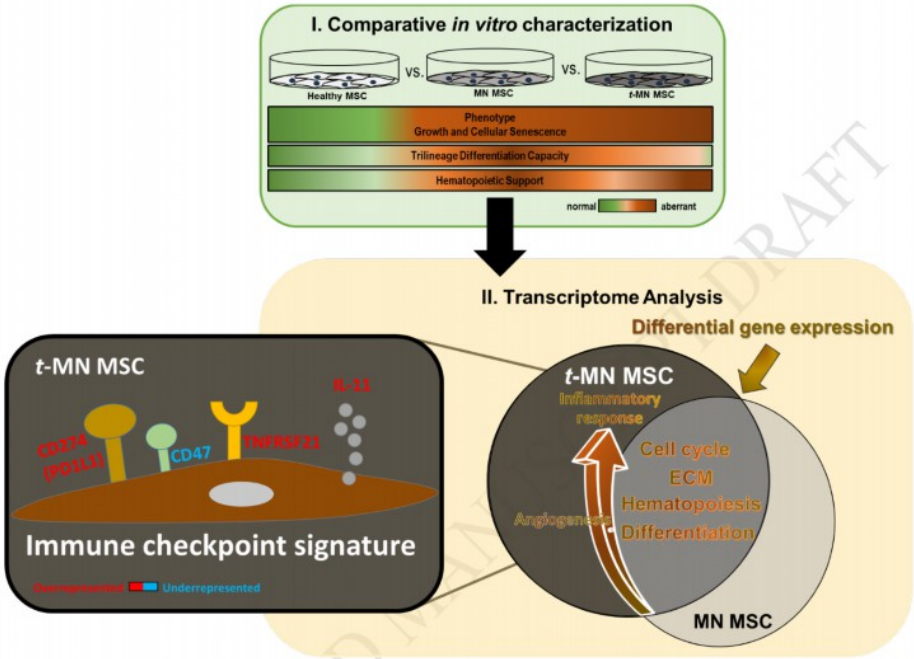

31

32

Abstract

Therapy-related myeloid neoplasms (*t*-MN) are serious late complications of anticancer treatment and have been mainly attributed to genotoxic alterations of hematopoietic stem and progenitor cells (HSPC) in the bone marrow (BM). Mesenchymal stromal cells (MSC) are a key component of the BM niche and are recognized as key regulators of normal hematopoiesis and contributors to the pathogenesis of *de novo* MDS and AML. MSC are also exposed to genotoxic stress during anticancer therapy; however, their contribution to *t*-MN development has not been elucidated so far. For this purpose, we compared MSC from patients with *t*-MN and *de novo* myeloid neoplasm (MN). Phenotypical alterations along with an altered differentiation capacity and diminished hematopoietic supporting capacity were similar, but more pronounced in t-MN compared to MN MSC. This was also confirmed by their genetic signature as mRNA sequencing revealed affected genes related to MSC development and extracellular matrix organization. A comparison of *t*-MN (*t*-MDS and *t*-AML) with MN (*de novo* MDS and AML) samples revealed 91 overlapping genes in all groups, which clearly show relevance regarding the skeletal system and hematopoiesis. Moreover, a specific molecular signature including deregulated pathways involved in inflammation and angiogenesis was determined only in *t*-MN MSC, hinting at distinct therapy-induced alterations in the stromal compartment.

Introduction

Therapy-related cancers are a long-term side effect of major concern following modern anti-cancer treatment. Especially hematological malignancies in the form of myelodysplastic syndromes (MDS) or acute myeloid leukemia (AML) are recurrently diagnosed as therapy-related myeloid neoplasm (*t*-MN) [1]. Depending on the primary tumor and its treatment, the cumulative incidence of *t*-MN varies broadly, with most cases establishing up to ten years after breast cancer [2]. Patients with primitive lymphoma and Hodgkin- or non-Hodgkin disease carry a particular high risk to develop *t*-MN eventually [3]. Unlike *de novo* malignancies, which develop inherently due to

germline predisposition or a consecutive series of mutations leading to blast transformation, *t*-MN incidence directly correlates to the exposure to cytotoxic or genotoxic agents in the course of anti-cancer therapy [4]. Therapies especially correlated with an increased relative risk of *t*-MN are radiation therapy, alkylating agents and topoisomerase II inhibitors. These treatments cause DNA damage and allow balanced or unbalanced chromosomal translocations, driving leukemic transformation [5-7]. Although presenting similar clinical features, *de novo* and therapy-related malignancies differ particularly in their clinical outcome highlighted by the considerably shorter overall survival for *t*-MN patients and lack of treatment strategies [8, 9].

Genetic predisposition and clonal selection of mutated blasts are well-established drivers for the development of *t*-MN after cytotoxic exposure [2]. Recognized as key hematopoietic regulator in healthy individuals, and relevant in the pathogenesis of *de novo* MDS and AML [10-14], the bone marrow microenvironment may also have a role in the development of *t*-MN. Mesenchymal stromal cells (MSC) originate from the mesenchyme and play a regulatory role in immunomodulation and hematopoiesis through their functional properties and differentiation potential. Expression and secretion of several factors are essential to form a unique niche for homing and activating hematopoietic cells [15, 16]. With this knowledge, it was of high interest during the last years to analyze the role of MSC in the pathogenesis of hematological neoplasms by our group and others [14, 17-19] and open a new view to the effects on bone marrow stroma and their probable contribution to disease progression. On the one hand, *t*-MN has been suggested a result of DNA damage induced in normal hematopoietic cells by exposure to cytotoxic therapy [20, 21]. MSC from *t*-MN are functionally and molecularly affected and the underlying mechanisms which might contribute to hematopoietic insufficiency and leukemogenesis are not clarified conclusively.

Moreover, it opens the question of an overlapping molecular signature to *de novo* MDS and AML or distinct features of *t*-MN due to cancer etiology. The unraveling of potentially common or distinct signaling pathways may help to establish more targeted therapy strategies in the future. Therefore, we characterized MSC from the bone marrow of *t*-MN patients and found phenotypical and

functional similarities to *de novo* myeloid neoplasms (MN, MDS or AML) MSC in contrast to healthy MSC. Additionally, transcriptome analysis revealed overlapping regulation of cell cycle, extracellular matrix (ECM) organization, differentiation and hematopoiesis in MN and *t*-MN MSC. Strikingly, a distinct molecular signature of *t*-MN MSC was found. A notable number of genes involved in blood vessel development and inflammatory response were only dysregulated in *t*-MN, but not MN MSC, indicating distinct alterations in the bone marrow stroma following genotoxic exposure in anti-cancer therapy, favoring the development of an inflammatory environment in the etiology of the disease.

Materials and Methods

Patients characteristics

Bone marrow samples were obtained from patients with *t*-MN (*t*-MDS n=5; *t*-AML n=8) and patients with MN (MDS n=12, AML n=11). Healthy bone marrow samples were derived from 28 healthy age and sex matched donors undergoing orthopedic hip replacement. Detailed patient characteristics are given in Table 1. The primary cancer diagnosis with corresponding anti-cancer therapy applied and time to diagnosis of a *t*-MN are shown in Supplementary Figure 1. The study was approved by local institutional review board (approval number 4777) and all patients and donors gave written informed consent.

Table 1. Patient characteristics and clinical parameters of included patients. Abbreviations are found below.

Patients	*de novo* MN (MDS and AML)		*t*-MN (*t*-MDS and *t*-AML)	
No.	**23**		**13**	
Sex				
Male	**14**		**5**	
Female	**9**		**8**	
Median age, years (Range)	**64**	(44-83)	**60**	(40-71)
Median BM infiltration, % (Range)	**30**	(1-85)	**49**	(2-90)
Median Leukocytes/µL (Range)	**3800**	(1100-48700)	**6800**	(500-21900)
Median Hemoglobin g/dL (Range)	**9.5**	(6.6-11.3)	**8.3**	(7.3-10.8)
Median Thrombocytes/µL (Range)	**66000**	(2300-483000)	**4900**	(2400-142000)
MDS No.	**12**		**5**	
Median age, years (Range)	65	(44-73)	**60**	(53-73)
Median BM infiltration, % (Range)	5	(1-15)	16	(2-20)
Diagnosis WHO 2016				
MDS MLD	8		2	
MDS EB I / EB II	6		3	
Karyotype				
Normal	3		1	
Aberrant	6		3	
Missing	3		1	
Genetic abnormalities, No.	9		1	
AML No.	**11**		**8**	
Median age, years (Range)	60	(48-83)	47	(40-71)
Median BM infiltration, % (Range)	79	(30-85)	80	(32-90)
Diagnosis WHO 2016				
AML with rec. gen. abnormalities	2			
AML MRC	1			
AML NOS	8			
Karyotype				
Normal	3		1	
Aberrant	6		5	
Missing	2		2	
Genetic abnormalities, No.	5		4	

Abbreviations: No., number; MN, myeloid neoplasms; t-MN, therapy-related myeloid neoplasms; MDS, myelodysplastic syndromes; AML, acute myeloid leukemia; MLD, multilineage dysplasia; EB, excessive blasts; rec. gen., recurrent genetic; MRC, myelodysplasia-related changes; NOS, not otherwise specified; BM, bone marrow; WHO, world health organization; EB, excess blasts; MLD, multilineage dysplasia

Isolation and cultivation of bone marrow derived MSC

The mononuclear cell (MNC) fraction was isolated from bone marrow aspirates using density-gradient centrifugation. Mesenchymal stromal cells (MSC) were thereafter derived and cultivated as described previously [11] in Dulbecco's Modified Eagle Medium (DMEM) low glucose supplemented with 25 % FBS and 1 % penicillin/streptomycin/L-glutamine (Sigma-Aldrich Chemie GmbH, Darmstadt, Germany). Growth characteristics were assessed by colony-forming unit fibroblast (CFU-F) activity and cumulative population doublings (CPD). All experiments were performed with MSC in passage 3-4.

Cellular senescence measured by β-galactosidase activity

β-galactosidase activity was determined by Cellular Senescence Detection Kit (Merck KGaA, Darmstadt, Germany). Stained cells were enumerated using the Axiovert 25 light microscope (Zeiss, Jena, Germany) and the proportion of positive cells was calculated.

Differentiation of MSC

Trilineage differentiation capacity of patient-derived and healthy MSC was performed as previously described [11, 22]. Shortly, adipogenic differentiation was induced for 21 days in DMEM high glucose (10 % FBS; 1 % penicillin/streptomycin/L-glutamine) supplemented with 0.1 mg/mL insulin, 0.1 µM dexamethasone, 0.2 mM indomethacine and 1 mM IBMX, or alternating with 0.01 mg/mL insulin only. Lipid vacuoles were histochemically stained with Oil-Red O. Osteogenesis was induced for 14 days supplemented with 50 µg/mL ascorbic acid, 10 mM β-glycerolphosphate and 0.1 µM dexamethasone and afterwards stained with Alizarin Red. Chondrogenesis was performed as three dimensional culture in DMEM high glucose (1 % penicillin/streptomycin/L-glutamine, 1 % ITS+1, 1 µM dexamethasone, 50 µg/mL ascorbate-2-phosphate, 40 µg/mL L-prolin and 10 ng/mL TGFβ3) for 21 days. 6 µm slices were prepared at

the Leica Cryostat CM3050 (Leica, Wetzlar, Germany) and stained with Safranin O. All stainings were microscopically documented using Axiovert 25 light microscope (Zeiss, Jena, Germany) and SPOT Software (Diagnostic Instruments Inc., Sterling Heights, MI, USA).

Isolation and culture conditions of CD34+ cells from bone marrow

CD34+ cells were isolated from MNC fraction of bone marrow aspirates using the Midi Magnetic Cell Separation (MACS) technology (Miltenyi, Bergisch Gladbach, Germany). Cell number and viability was determined using CASY® Cell Counter TTC (Roche, Mannheim, Germany) or by Trypan Blue staining. CD34+ cells were immediately cryoconserved in equal parts of 80 % FBS and 20 % DMSO. Frozen vials were stored at minus 196 °C and freshly thawed for use.

Co-Culture experiments with MSC and CD34+ cells

MSC were plated at a density of $3x10^4$ per cm^2 on tissue culture-treated plates. $1.5x10^4$ CD34+ cells per cm^2 were added 24 hours afterwards as direct culture and co-cultivated for three days. A monoculture of CD34+ cells was prepared under equal conditions with medium containing 10 ng/mL IL3, IL6 and SCF and 20 ng/mL FLT3-L (all Peprotech Inc., London, UK). Afterwards, 1000 CD34+ cells were plated in semi-solid clonogenic medium containing erythropoietin (MethoCult™ H4434 Classic, Stem Cell Technologies, Vancouver, Canada) for colony forming units (CFU) assay. After 14 days, differentiated colonies were enumerated and distinguished between CFU-GM, CFU-G, CFU-M, and CFU-E, BFU-E, and CFU-GEMM.

For Long-Term Culture-Initiating Cell (LTC-IC) assay, MSC were plated as a feeder layer on a 96-well tissue-culture cell culture plate and irradiated with 30 Gray with Gulmay RS225. 6000 CD34+ cells were added in a dilution series in MyeloCult H15000 medium containing 1 µM Hydrocortisone (all from Stem Cell Technologies, Vancouver, Canada). Medium was refreshed weekly. After five

weeks, the medium was replaced by clonogenic methylcellulose (MethoCult™ H4534 Classic, Stem Cell Technologies, Vancouver, Canada) supplemented with 10 U/mL Epoietin and cultivated for 14 days. Enumeration of colonies for both assays was performed microscopically (Axiovert 25 light microscope, Zeiss, Jena, Germany).

RNA Sequencing

Total RNA was quantified using the Qubit RNA HS Assay (Thermo Fisher Scientific Inc., Waltham Massachusetts) and quality control was performed by capillary electrophoresis using the Fragment Analyzer and the "Total RNA Standard Sensitivity Assay" (Agilent Technologies, Inc., Santa Clara, California). The library preparation was performed according to the manufacturer's protocol using the VAHTS Universal V6 RNA-seq Library Prep Kit for Illumina (Illumina, San Diego, CA, USA). 500 ng total RNA were prepared as previously described [22] and sequenced on the NextSeq2000 system (Illumina Inc. San Diego, California) with a read setup of 1 x 100 bp. The bcl2fastq tool was used to convert the bcl files to fastq files as well for adapter trimming and demultiplexing as previously described [17].

Bioinformatical analysis of transcriptome data

After quality control, the sequencing raw data was trimmed by removing the first 12 bases from each read. Alignment was performed using the program STAR v2.7.2a [23] against the reference human genome GRCh38.97 (hg38). Alignment was performed as a two-pass experiment, which means that in a first step new splice junctions were detected, which were added in the second step to the initial reference. After applying the program featureCounts (1.6.5) to the aligned reads, DEseq2 (1.24.0) was used to calculate differential expression. Genes with an FDR q-value <0.05 were considered differentially expressed. StringTie (2.0.3) [24] was applied to calculate fragments per kilobase of transcript per million mapped reads (FPKM-values). Principal component analysis plots were created in R using the FactoMineR (1.42) and pheatmap (1.0.12) packages,

respectively. For gene set enrichment analysis (GSEA, Broad Institute, Boston, MA, USA), the FPKM values obtained from StringTie (2.0.3) for the different samples were compared either with the gene sets contained in the Molecular Signature Database or with self-made gene lists. The Signal2Noise metric and 1000 gene set-based permutations were applied to all analyses.

Gene Ontology (GO) analysis was performed with differentially expressed genes using the panther over-representation test, which is accessible via the amigo 2 webpage (https://amigo.geneontology.org/amigo). A Fisher's exact test was performed and the results were Bonferroni-corrected. The analysis pipeline was adapted from an NIH-protocoll (https://docs.gdc.cancer.gov/Data/Bioinformatics_Pipelines/Expression_mRNA_Pipeline. Analyses strategies were carried out as previously described [25]. Additionally, the open source online platform https://www.metascape.org [26] was used to identify enriched GO from gene term lists from DESeq2 data.

Data access

RNA sequencing expression data will be deposited in NCBI Sequence Read Archive (SRA). RNA sequencing data from *de novo* MDS and AML samples for a new bioinformatic analysis were used from the NCBI Sequence Read Archive (SRA) with BioProject ID PRJNA1091937 [17].

Statistical analysis

All statistical analyses were performed using Prism 8.4.3 (GraphPad Software Inc., La Jolla, USA) using the two-sided unpaired student's t-test for parametric data, or Mann-Whitney test for non-parametric data. Data graphs show mean and SEM unless stated otherwise. Significance was determined at $P < 0.05$ and is indicated by asterisks.

Results

MSC derived from therapy-related myeloid neoplasms show alteration in growth capacity

Mesenchymal stromal cells (MSC) display a spindle-like phenotype and plastic adherence *in vitro*. We characterized MSC from therapy-related MN (*t*-MN, *t*-MDS and *t*-AML) according to their phenotypically properties and growth kinetics in comparison to MSC derived from *de novo* myeloid neoplasms (MN, MDS and AML). Compared to healthy controls, MN- and *t*-MN derived MSC share pronounced deficits as reflected by their broad morphology and disorganized structure (Figure 1A) and equal diminished proliferation capacity as represented by colony forming unit-fibroblast (CFU-F) activity (mean CFU-F/1x10^7 MNC, HC: 106, MN: 22, *t*-MN: 22, $P < 0.001$). This was accompanied by a prolonged culture duration to reach similar cumulative population doublings (CPD) as healthy MSC until passage 3 (mean days, HC: 23, MN: 31, *t*-MN: 30, $P < 0.001$). Accompanied, an increased proportion of senescent cells as shown by β-galactosidase staining (mean % positive cells, HC: 9, MN: 26, *t*-MN: 23) and an increased expression of senescence-associated marker *CDKN2A* on mRNA level was determined in both, MN and *t*-MN MSC (Figure 1B).

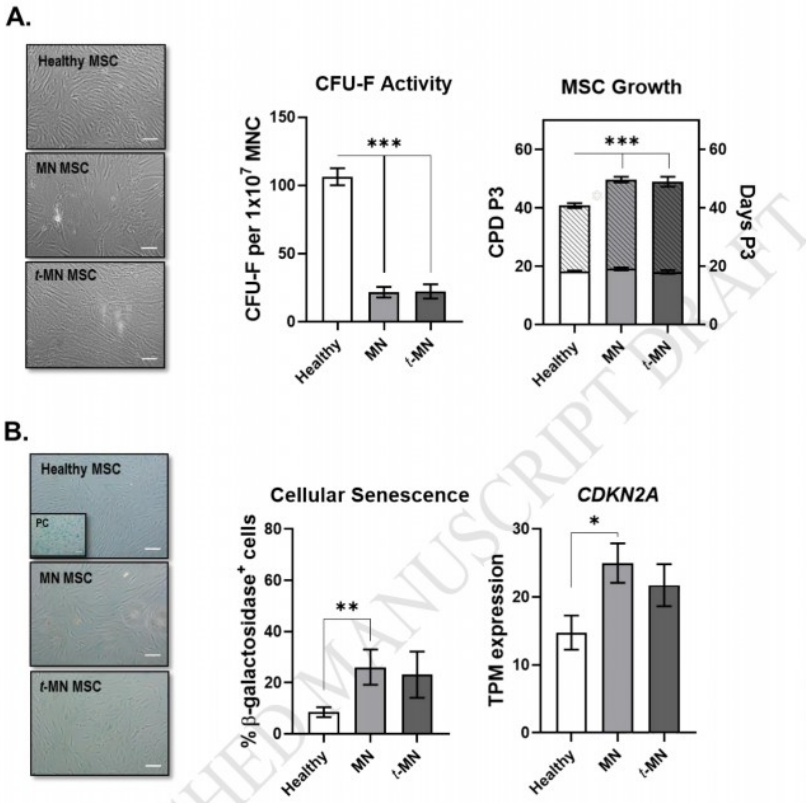

233

234 **Figure 1. Comparative analysis of growth properties in *t*-MN derived MSC and MN MSC vs.**
235 **healthy MSC.** (A.) *Left*: Representative micrographs of phenotype from healthy MSC and MSC
236 derived from MN and *t*-MN patients. *Middle*: CFU-F activity in MN (n=23) and *t*-MN (n=13) MSC
237 contrasted to healthy controls (n=22). *Right*: CPD and respective days in culture (shaded bars)
238 were calculated for healthy (n=21), MN (n=21) and *t*-MN (n=13) MSC in passage 3. (B.)
239 *Left/Middle*: Representative micrographs of blue stained senescent cells after β-galactosidase
240 staining in MSC derived from healthy (n=10), MN (n=7) and *t*-MN (n=8) MSC in passage 3 and
241 graphical depiction of the calculated mean percentage of β-galactosidase positive cells. *Right*:
242 TPM (Transcripts per million) values from RNA sequencing data for the senescent-associated
243 marker *CDKN2A* (p16) in healthy (n=4), MN (n=8) and *t*-MN (n=8) MSC are given. For all
244 micrographs, scale bars indicate 100 µm. For all graphs, asterisks indicate statistical significance
245 after student's t-test versus healthy controls **P <0.05, **P <0.01, ***P <0.001*. MN versus t-MN
246 MSC was not significant.
247

MSC derived from therapy-related myeloid neoplasms exhibit deficits in trilineage differentiation capacity

MSC are further characterized by their trilineage differentiation capacity into adipogenic, chondrogenic and osteogenic lineage *in vitro*. Previous work from our group and others [14, 17, 18] showed deficits in MN derived MSC, especially regarding the differentiation capacity towards the chondrogenic-osteogenic lineage. This was confirmed in an independent cohort in this study and a direct comparison to *t*-MN MSC exhibited similar results with a trend to a pronounced impairment of the trilineage differentiation capacity. This was underlined by a more consistently decreased adipogenic differentiation in *t*-MN MSC in comparison to MN, as reflected by Oil-Red O staining (mean Oil-Red O staining intensity; HC: 2.3, MN: 1.9, t-MN: 1.7) and accompanied by a stringent underrepresented mRNA expression level of adipogenic marker *PPARγ* (Figure 2A). Chondrogenic differentiation capacity of *t*-MN MSC was diminished in contrast to healthy MSC but not as dramatically as in MN MSC, as indicated by reduced pellet area (mean pellet area μm^2, HC: $1.1x10^6$, MN: $0.46x10^6$, *t*-MN: $0.81x10^6$) and proteoglycan staining, together with a significant downregulation of Aggrecan (*ACAN*) on mRNA level (Figure 2B). Moreover, osteogenic differentiation capacity was diminished in both, *t*-MN MSC and MN MSC (mean Alizarin Red staining intensity; HC: 2.3, MN: 1.5, t-MN: 1.8) accompanied with decreased mRNA level of Integrin Binding Sialoprotein (*IBSP*), mostly underrepresented in *t*-MN MSC (Figure 2C).

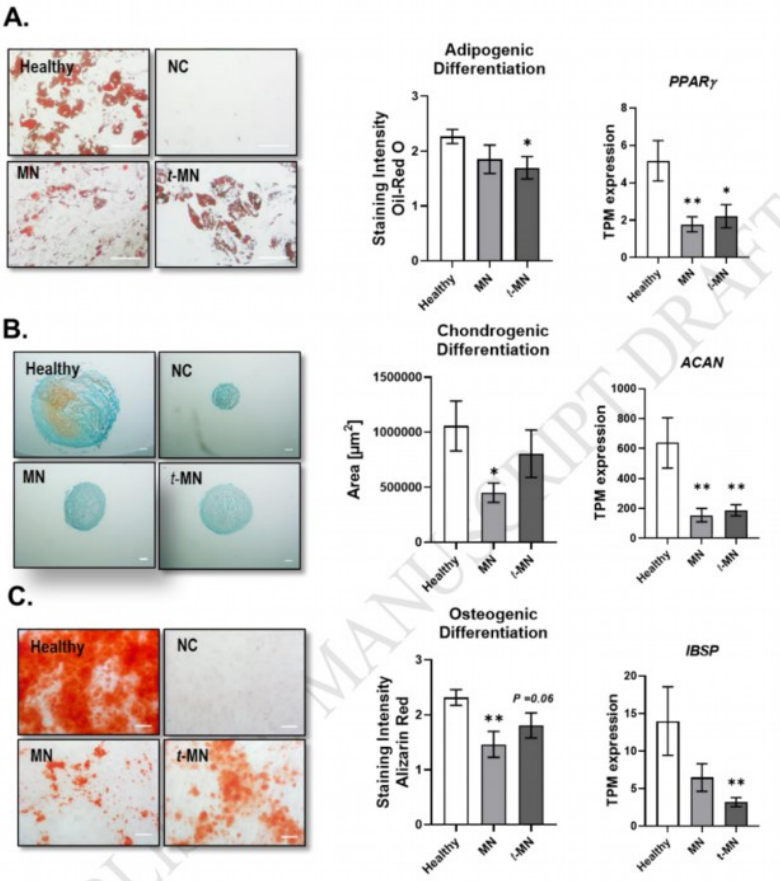

266

Figure 2. Trilineage differentiation capacity of *t*-MN derived MSC. (A.) Adipogenic differentiation capacity of MSC after 21 days of differentiation lipid vacuoles were stained with Oil-Red O (Healthy n=10, MN n=10, t-MN n=9). TPM expression values from RNA sequencing data of adipogenic marker *PPARγ* are shown. (B.) Safranin O staining of chondrogenic induced MSC. Pellets were cryosectioned and proteoglycan was visualized by Safranin O staining (Healthy n=8, MN n=7, t-MN n=7). TPM expression values for chondrogenic marker Aggrecan (*ACAN*) are given. (C.) Osteogenic differentiation was induced for 14 days and visualized with Alizarin Red staining (Healthy n=20, MN n=14, t-MN n=9). TPM (transcripts per million) expression values from our RNA sequencing data for the osteogenic marker Integrin-binding sialoprotein (*IBSP*) are shown. Representative images are given with scale bars indicating 100 µm, NC= negative control. Asterisks indicate statistical significance after student's t-test vs healthy MSC **P <0.05, **P <0.01.* MN versus t-MN MSC was not significant.

Therapy-related myeloid neoplasm derived MSC confer decreased hematopoiesis support

MSC play a crucial role in regulating hematopoietic cell fate. To investigate whether the hematopoietic support capacity of *t*-MN MSC was affected, as already observed in MN MSC [17], we conducted long-term and short-term functional assays (Figure 3A). In long-term culture initiating cell (LTC-IC) assay, MSC derived from *t*-MN showed a similar diminished supporting capacity comparable to those observed in MN derived MSC (mean LTC-IC frequency %, HC: 0.44, MN:0.14, *t*-MN: 0.22), as reflected here in an independent group (Figure 3B). Short-term supporting capacity after three days of co-culture with healthy CD34+ HSPC was investigated by colony forming unit (CFU) assay to determine CD34+ differentiation potential. Cell numbers of CD34+ cells after co-culture with *t*-MN MSC or MN derived was not notably altered compared to healthy MSC (mean cell number % to mono-culture, HC: 70.3 , MN: 88.9, *t*-MN: 75.0). However, CFU of these co-cultured healthy hematopoietic CD34+ cells revealed decreased number of lineage differentiated cells towards the erythroid progenitors, granulocyte-macrophage progenitor cells and the multipotential (GEMM) progenitor cells in both MN- and *t*-MN derived MSC. But, a clear and more dramatically, significant diminished differentiation capacity towards all blood lineages were evaluated after co-culture with *t*-MN derived MSC as reflected in Figure 3C (mean number of total colonies, HC: 167.1, MN: 105.8, *t*-MN: 41.1).

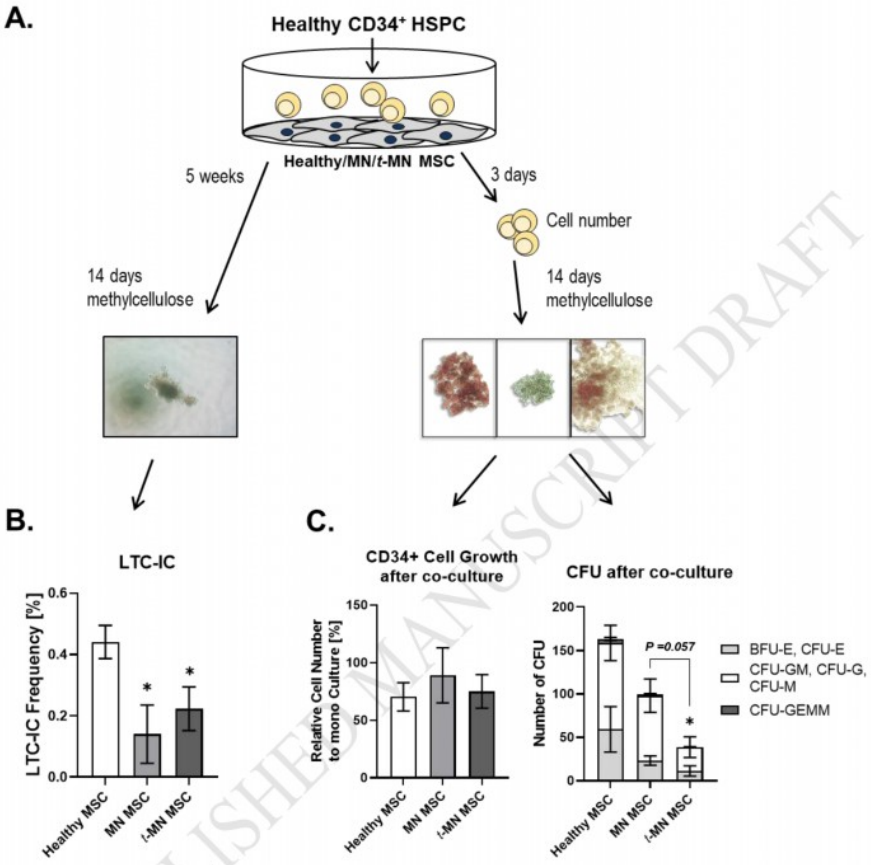

Figure 3. Hematopoietic support capacity of *t*-MN derived MSC. (A.) Graphical study design. MSC from healthy, MN and *t*-MN were co-cultured with healthy CD34+ cells for five weeks for long-term analysis (LTC-IC assay) or for three days for short-term analysis (CFU assay) and afterwards cultured in methylcellulose for 14 days to evaluate hematopoietic supporting capacity. (B.) LTC-IC frequency was calculated for healthy (n=9), MN (n=5) and *t*-MN (n=9) MSC (C.) *Left*: Cell number of CD34+ cells after three days co-culture with healthy (n=7), MN (n=6) and t-MN (n=7) MSC relative to mono-cultured CD34+ cells. *Right*: CFU assay of co-cultured healthy CD34+ cells was performed and colonies were enumerated differentially between white (CFU-GM, CFU-G, CFU-M), red (CFU-E, BFU-E) and multipotential (CFU-GEMM) colonies. Asterisks indicate statistical significance of total CFU using student's t-test versus healthy MSC **P <0.05*. MN and t-MN MSC were significantly different regarding white colonies only (*P =0.049*).

RNA sequencing revealed molecular alterations in therapy-related myeloid neoplasms that reflect functional deficits in vitro

In our *in vitro* analysis, *t*-MN MSC showed alterations along phenotypical and functional deficits, partially comparable to those in *de novo* MN MSC. We were interested whether these *in vitro* observations resulted from molecular dysregulation of genes and signaling pathways and, if there are potentially overlapping underlying mechanisms to MN derived MSC, or whether *t*-MN derived MSC exhibited a distinct molecular signature. Therefore, we performed RNA sequencing to unravel transcriptomic alterations for four *t*-MDS- and four *t*-AML derived MSC in comparison to four healthy controls. As first step in our comprehensive data analysis, principal component analysis (PCA) of healthy, *t*-MDS and *t*-AML derived MSC showed a familiar relationship between *t*-MDS and *t*-AML as depicted by the comparison in PC1 vs PC2 and in second level PC2 vs PC3 (Figure 4A). Differential expression analysis revealed 617 genes in *t*-MDS and respectively 324 exclusively differentially expressed in this group, that were primarily involved in cell cycle, cell response or ECM such as *CDK15* (cyclin dependent kinase 15), Collagens or *CXCL1* (FDR q-value ≤ 0.05). 824 differentially expressed genes were detected in *t*-AML derived MSC, whereby a number of 531 differentially expressed genes were exclusively found in this group. This includes a notable number of genes related to inflammation or ECM such as *MMP2* or *S100P* or collagens (Figure 4B). The comparison of *t*-MDS and *t*-AML derived MSC revealed an overlap of 293 differentially expressed genes including several HOX genes and genes related to growth, differentiation or ECM and signaling pathways such as inflammation via MAPK/NFkB or WNT (Figure 4B). Reactome analysis identified a strong enrichment of these differentially expressed genes related to cell processes such as ECM, manifested already in *t*-MDS MSC and progressing more dramatically in *t*-AML MSC (Figure 4C). Moreover, gene ontology (GO) confirmed a strong enrichment in cell processes such as mesenchymal differentiation and skeletal system in both, *t*-MDS and *t*-AML derived MSC (Figure 4D).

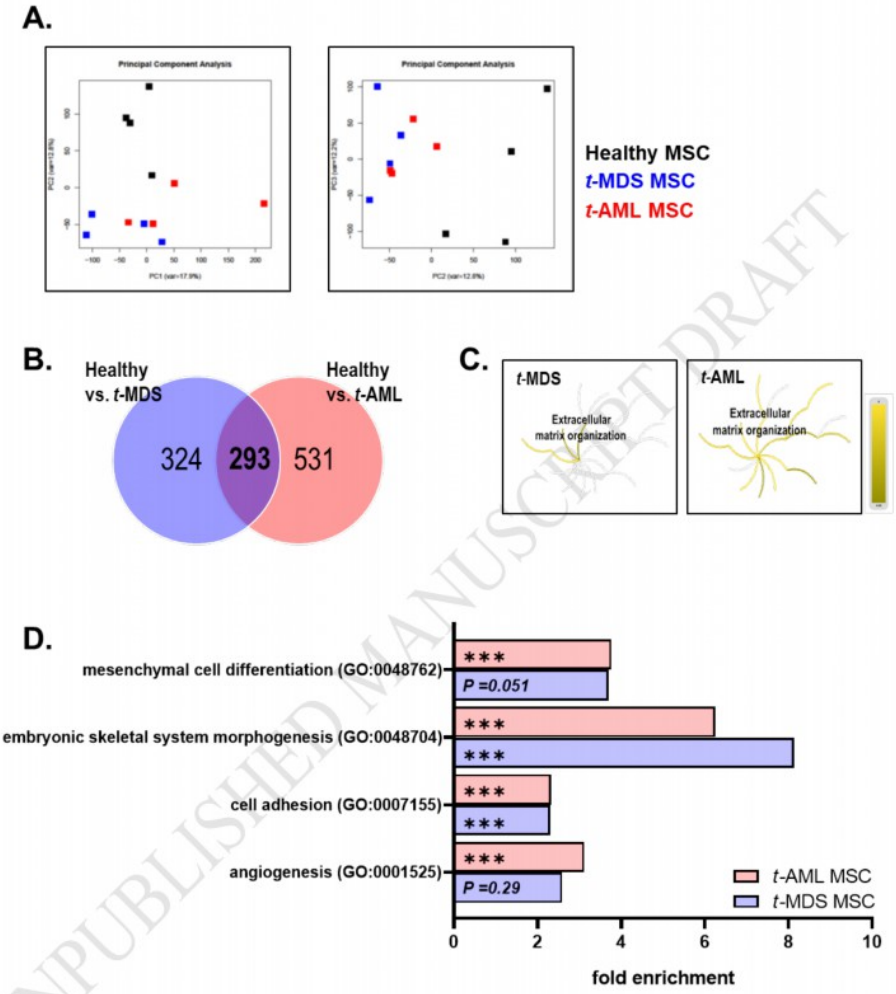

Figure 4. RNA sequencing analysis of *t*-MDS and *t*-AML derived MSC. (A.) Principal component analysis (PCA) of MSC from healthy controls (black), *t*-MDS (blue) and *t*-AML (red) patients. PC1 vs PC2 and PC2 vs PC3 are shown. (B.) Venn diagram of differentially expressed genes in *t*-MDS and *t*-AML (FDR q-value ≤0.05). (C.) Reactome analysis revealed a strong enrichment of the detected genes for ECM organization, with an increased enrichment from *t*-MDS to *t*-AML. (D.) Representative overview of GO identified with significant enrichment in MSC related processes in *t*-MDS and *t*-AML. Fold enrichment is given, asterisks indicate statistical significance *(***P <0.001)*.

MSC from therapy-related myeloid neoplasms share overlapping molecular signatures to de novo MN neoplasms

As next step, we wanted to compare *t*-MN MSC directly to *de novo* MN MSC, due to the results in our *in vitro* assays as both MSC groups (MN and t-MN) showed similar phenotypical and functional deficits. Overall, these assays alone do not reflect the etiology of exogenous stimuli or trigger factors, like therapies, to induce *t*-MN. However, notable differences between both groups are reflected by more pronounced deficits in *t*-MN MSC. This opened the question, whether there is a molecular signature exclusively found in *t*-MN MSC but not in MN MSC and whether there are overlapping mechanisms, potentially explaining similarities and differences in MN and *t*-MN we found in our *in vitro* analyses.

Following the question of an overlapping signature, analyses of four healthy, four *t*-MDS and four *t*-AML-derived MSC were compared to available RNA sequencing data from four MDS and four AML derived MSC at first diagnosis (project ID PRJNA1015628 [17]) to compare expressional signatures of *de novo* and therapy-related myeloid neoplasms. Details on patients characteristics included in RNA sequencing are given in Suppl. Table 2.

PCA revealed clusters, neighboring MN and *t*-MN towards healthy MSC (PC1 vs PC2). A more detailed comparison of PC2 vs PC3 clearly showed a familiar relationship of MN (MDS, AML) and *t*-MN (*t*-MDS, *t*-AML) in comparison to healthy MSC (Figure 5A). DESeq2 analysis revealed 91 differentially expressed genes that overlap in all, MN and *t*-MN MSC (FDR q-value<*0.05*; Figure 5B). These included a notable number of genes related to growth and cell cycle, hematopoiesis regulation, differentiation and ECM organization, such as Cyclin D2 (*CCND2*), *EMILIN2* or *TBX15*. Interestingly, both *t*-MN and MN MSC showed a strong regulation of HOX genes, however, only in *t*-MN MSC the HOX-C cluster is differentially expressed. Using STRING database, we found that 30 out of that 91 overlapping genes in all groups form a network and are related to MSC development, hematopoiesis, cell cycle and skeletal system (Figure 5C). Gene set enrichment

371 analysis (GSEA) and GO analysis confirmed a strong enrichment these gene sets for cell
372 processes such as skeletal system development, cell communication, apoptosis or hematopoiesis
373 (Figure 5D, E).

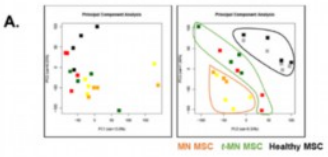

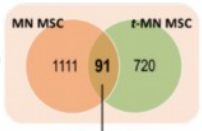

Overlapping genes* in MDS, *t*-MDS, AML, *t*-AML

ACKR3	EMILIN2	HOXB5	MET	PTPRD-AS1
ADAM19	EN1	HOXB6	MOCOS	RFLNB
ADAMTS5	EPHB2	HOXB7	MYH13	SCARA5
AKR1C1	ETV5	HOXB-AS3	NFIB	SELENOP
ALDH1B1	EXTL1	IL13RA2	NR2F1	SLC44A3
ALX1	FYN	IL20RB	NR2F1-AS1	SLC9A7
APH1B	GLCCI1	IL33	NRXN3	SLPI
APOL3	GLDN	INMT	NT5DC2	SOCS2
ATF5	HAND2	IQCJ-SCHIP1	OLFM1	SOCS2-AS1
ATP13A2	HAND2-AS1	IRAK3	OLFM4	STX1B
B3GALT2	HOXA2	ITGA5	PDE1A	TBX15
BCAR3	HOXA3	LIMK1	PI16	TFAP2A
BDNF	HOXA5	LMO3	PITX2	TIMP4
CCDC85C	HOXA-AS2	LYPD1	PNMA2	TNFRSF19
CCND2	HOXB2	MAB21L2	POU2F2	TNNT1
CD55	HOXB3	MAGEL2	PPP1R18	TNXB
DLGAP1	HOXB4	MAP3K8	PREX2	TPPP3

*RNA genes not included

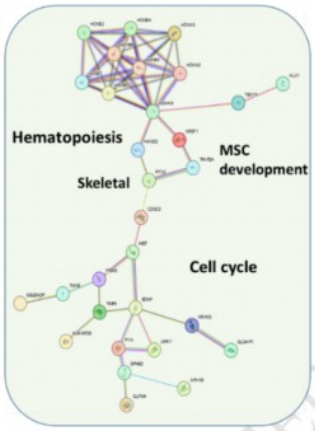

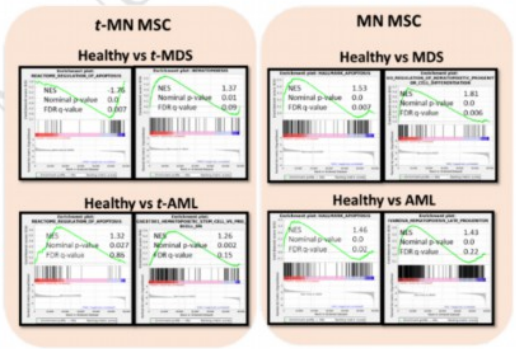

E.

Gene ontology (GO): fold enrichment vs healthy MSC	*t*-MDS	*t*-AML	MDS	AML
skeletal system development (GO:0001501)	3.77	2.87	2.23	2.65
cell differentiation (GO:0030154)	1.63	1.52	1.40	1.44
cartilage development (GO:0051216)	3.58#	3.21#	2.32	3.48
regulation of cell communication (GO:0010646)	1.56	1.48	1.49	1.33#
cell adhesion (GO:0007155)	2.30	2.33	1.32	1.30
regulation of cell migration (GO:0030334)	2.50	2.30	1.39	1.43
angiogenesis (GO:0048468)	1.71	1.62	1.33	1.50
vasculature development (GO:0001944)	2.52	2.65	1.47	1.76
cellular response to chemical stimulus (GO:0070887)	1.56#	1.50	1.31	1.34

374

Figure 5. Overlapping transcriptomic signature in MDS, *t*-MDS, AML and *t*-AML derived MSC. (A.) PCA shows clustering of healthy controls (black), MDS (yellow), *t*-MDS (green), AML (orange) and *t*-AML (red). PC1 vs PC2 and PC 2 vs PC3 are given. (B.) Venn diagram of differentially expressed genes in all entities (MDS, AML, *t*-MDS and *t*-AML versus healthy MSC revealed 91 genes overlapping in *t*-MN and MN MSC versus healthy controls. (C.) Using STRING database (Version 12.0), 30 out of the 91 overlapping differentially expressed genes form a network. Genes are involved in hematopoiesis, skeletal system, MSC development or cell cycle. (D.) GSEA confirmed these overlapping differentially expressed genes involved in cell processes such as apoptosis or hematopoiesis. Normalized enrichment score (NES), nominal *P-value* and FDR *q-value* are given. (E.) GO enrichment of regulation in both *t*-MN and MN MSC versus healthy MSC. The table shows the fold enrichment of GO processes identified for the respective group. Depicted fold enrichments were significant when colored (*P <0.05*), except when marked (*# P <0.08)*.

A distinct molecular signature distinguishes therapy-related myeloid neoplasm derived MSC from de novo neoplasms: t-MN MSC exhibit immunomodulatory gene expression

Apart from the overlapping differentially expressed genes related to affected cell processes in all groups (MN and t-MN), we finally wanted to check, if *t*-MN MSC exhibit a therapy-related molecular signature that is exclusively reflected by the clinical cytostatic exposure. The direct bioinformatic comparison of MN and *t*-MN MSC revealed distinct molecular signatures that are indicated by the differential gene expression depicted as Venn diagram in Figure 6A. MSC derived from *t*-MN revealed 720 differentially genes exclusively for this group. This includes a notable number of genes that are related to e.g. cell adhesion, angiogenesis or inflammatory response. Next to the differentially genes exclusive in *t*-MDS (212) or *t*-AML (385), we identified 123 differentially genes that are shared by both *t*-MDS and *t*-AML, but were not found in MN derived MSC (FDR q-value <0.05, Figure 6A right side). This signature contains genes that are related to cell adhesion such as or *CADM1* (Cell Adhesion Molecule 1) or inflammatory response and immunoregulatory genes such as *IL-11* (Interleukin-11) or *CD274* (programmed cell death 1 Ligand 1, PD1L1) (Figure 6A right side). GO analysis (from Metascape.org [26], last access 10.06.2024) of these 123 overlapping differentially expressed genes confirmed a strong and significant enrichment for these cell processes, especially to cell motility, tissue remodeling, inflammatory response or T-cell

407 regulation only in *t*-MN derived MSC, but not in *de novo* MN derived MSC (Figure 6B). Using
408 STRING database (Version 12.0), 25 out of these 123 genes were found to directly interact and
409 form a network correlated to these cell processes as mentioned above (Figure 6C left side).
410 Especially CD274, also known as programmed cell death 1 ligand 1, plays a critical role in immune
411 response or tumorigenesis and is essential for T-cell regulation. Furthermore also CD47, an
412 Integrin associated protein (IAP), is described as "don´t eat me" signal and plays a crucial role in
413 immune response. CD47 is often highly expressed on tumor cells, which is why its relationship
414 with clinical pathogenic features in hematological neoplasms is a major focus.

415 A detailed view in our DESeq2 data show that CD274 was strongly and significantly increased
416 (log2foldchange >2), while CD47 was significantly downregulated only in *t*-MN MSC but not in MN
417 derived MSC. This lead us to check, whether more immunomodulatory involved genes could be
418 identified only in *t*-MN MSC. We identified differentially expressed genes related to these
419 signalings, such as *SERPINE1*, a regulator for cell adhesion or tumor growth, *IL-11,* or the tumor
420 necrosis factor (TNF) family member *TNFRSF21* (Figure 6C, right side). All these genes have in
421 common to be members of the immune checkpoints and are of high interest in cancer
422 development.

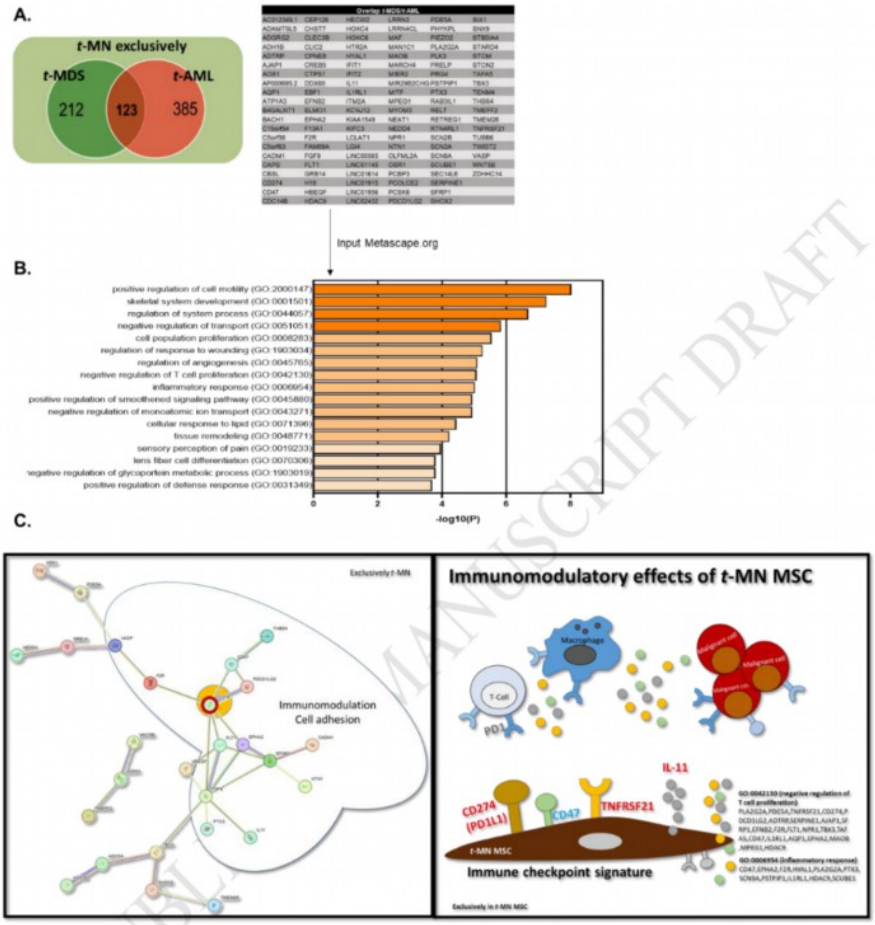

Figure 6. Differentially expressed genes and cellular processes exclusively regulated in *t*-MN MSC. (A.) Venn diagram of 720 differentially expressed genes exclusively in *t*-MN MSC (*t*-MDS and *t*-AML versus healthy MSC) (FDR *q-value <0.05*) and depiction of 123 overlapping genes in *t*-MDS and *t*-AML MSC. (B.) Representative overview for related cell processes of these 123 differentially genes by GO using Metascape.org [26]. The graph was adapted from Metascape.org results. GO and the respective -log10(p) values of gene input are shown. (C.) STRING database (Version 12.0) revealed 25 genes that interact and form a network correlated with cell adhesion and immunomodulation. *Right*: Schematic overview of potential immunomodulatory effects of *t*-MN MSC affecting the bone marrow niche. Colored genes indicate exclusive dysregulation in *t*-MN MSC (red= overrepresented, blue= underrepresented).

Discussion

Our comprehensive analysis of MSC derived from *t*-MN patients towards MN compared to healthy controls, revealed notable functional alterations in *t*-MN MSC, partially comparable to those observed in MN. Deficits in growth and cellular aging were similar to those found in MN derived MSC [11] and cannot distinguish the respective etiologies of *t*-MN or *de novo* MN. However, MN derived MSC showed deficits especially regarding the chondrogenic-osteogenic differentiation lineage, while *t*-MN MSC exhibited differentiation capacity deficiency along all three lineages. All patient-derived MSC (MN and *t*-MN) showed significantly decreased molecular levels of common differentiation markers on mRNA level, independent of their disease etiology. MSC differentiation capacity accompanied with expression and secretion of regulatory factors are the most crucial functions to maintain or regulate hematopoietic cells. Indeed, hematopoietic support assays revealed significant decrease in the maintenance capacity of MN- and *t*-MN MSC as shown by LTC-IC assays with healthy CD34+ HSPC. Interestingly, short-term support capacity was more dramatically affected in *t*-MN MSC in comparison to MN MSC as shown by diminished capacity of healthy CD34+ HSPC to differentiate into the erythroid progenitors, granulocyte-macrophage progenitor cells and the multipotential progenitor cells reflected in CFU assay.

We and other studies have shown that MSC from hematological neoplasms exhibit functional and molecular deficits as reflected by alterations in mRNA expression or secretion of hematopoiesis regulating factors, activation of inflammatory response and dysregulation of hematopoiesis [10, 11, 27]. The underlying mechanisms and genes that contribute to leukemogenesis were more highlighted in the last years by our group and others [14, 17-19], but limited to primary diseases. Therefore, we were interested to identify overlapping genes and signaling pathways that are shared by all myeloid neoplasms including MDS and AML, and might indicate similar underlying mechanisms. Further, we identified a specific signature in *t*-MN MSC, which potentially explain

460 the dramatic *in vitro* findings for this group and reveal pathogenic mechanisms induced specifically
461 by clinical cytostatic exposure.

462 RNA sequencing analysis of *t*-MN MSC and comparative analysis to MN MSC revealed that
463 exclusive genes were differentially expressed in all groups, which were however involved in similar
464 cell processes such as cell cycle, proliferation or differentiation, as reflected by GSEA. We and
465 other studies have shown that MSC derived from myeloid neoplasms such as AML patients exhibit
466 molecular signatures that could reflect functional deficits [28-30]. Additionally, *t*-MN MSC showed
467 similar functional deficits to *de novo* MN patients, but with more dramatic alterations regarding
468 their hematopoietic support function. We identified a distinct regulation of genes in *t*-MN derived
469 MSC that are clearly involved in inflammation. These exclusive genes include *IL-11*, *TNFRSF21*,
470 *CD274* or *CD47*. All these genes play a crucial as immune checkpoints for immunoregulation and
471 cancer immunotherapy [31, 32]. Especially CD274, also known as programmed cell death ligand 1
472 is a major player in immunoregulation. It has been described as the “don’t find me” signal and
473 interacts with the receptor PD-1 on T-cells. Within the last years, CD274 was found to be highly
474 expressed in tumor cells and became focus in clinical pathogenic features for immunotherapy due
475 to its relevance to escape cancer cells from the immune response by inhibiting T-cell functionality
476 [33-35]. Interestingly, significantly increased levels of CD274 were found exclusively in *t*-MN MSC.
477 Moreover, CD47, an Integrin associated protein (IAP) is another crucial regulator for adhesion,
478 apoptosis or immune response and functions together with the receptor SIRP-α (signal-regulatory
479 protein alpha) as an important immune checkpoint, better known as “don’t eat me signal”. CD47
480 is expressed in all myeloid cells as well as in tumor cells and gained clinical relevance to establish
481 immunotherapeutic strategies within the last years, also in hematological neoplasms [36-38].
482 Interestingly, our RNA sequencing data showed significantly downregulated levels of CD47 in *t*-
483 MN MSC, but not MN MSC. The immunoregulatory role of MSC and their contribution to
484 hematological neoplasms such as MDS has arisen in the last decade due to their functional
485 properties and their expression and secretion of regulatory factors [27]. It is of high interest that

the bone marrow stroma of t-MN show an immune exhaustion signature and opens the questions: How might MSC contribute to t-MN development? Which underlying mechanisms are responsible, and act malignant cells as inducers of stromal immundysregulation?

Conclusion

Taken together, mesenchymal stromal cells from therapy-related myeloid neoplasms (*t*-MN MSC) exhibit structural and functional alterations. This consequently contributes to inadequate hematopoiesis, similar to stromal alterations in *de novo* MN. RNA sequencing revealed a specific immunosuppressive signature exclusively in *t*-MN MSC. Their contribution and their role in t-MN has not been understood so far. This is of high interest, especially with a view to immunotherapeutic strategies in myeloid pathologies, and may open a new view on bone marrow damage by chemotherapeutic agents.

Supplementary Material

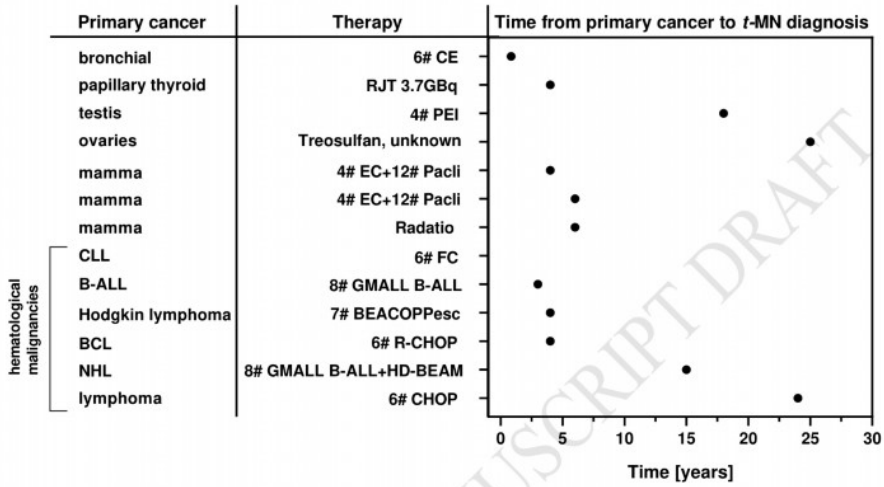

Supplementary Figure 1. Graphical depiction of primary cancer diagnosis, received therapy, and time passed until a *t*-MN was diagnosed. The graphs shows the primary cancer classification, the type of therapy the patient received (numbers before # indicates the number of cycles) and the time between primary cancer and t-MN diagnosis.

Abbreviations: CLL=chronic lymphocytic leukemia; B-ALL=B-lymphoblastic acute lymphocytic leukemia; BCL= B-cell lymphoma; NHL=non-hodgkin lymphoma; CE=cyclophosphamide and etoposide; RJT=radioiodinetherapy; PEI=cisplatin, etoposide, and ifosfamide; EC=epirubicin and cyclophosphamide; Pacli=paclitaxel; FC=fludarabine and cyclophosphamide; GMALL B-ALL=treatment protocol for leukemia; BEACOPPesc=bleomycin, etoposide, adriamcyin (doxorubicin), cyclophosphamide, oncovin, procarbazine, prednisone; R-CHOP=rituximab, cyclophosphamide, hydrocydaunorubicin, oncovin, and prednisone; HD-BEAM=high dose carmusine, etoposide, cytarabine, and melphalan; CHOP= cyclophosphamide, hydrocydaunorubicin, oncovin, and prednisone.

Supplementary Table 2. Detailed patient characteristics of the patients included in the RNA sequencing analysis. *MDS and AML (MN) data from project ID PRJNA1015628 [17] were re-analyzed for comparison with newly acquired t-MN MSC data. Abbreviations are found below.

No	Entity	WHO 2016	Therapy	Age	Blast infiltration	ANC (/µL)	Platelets (x10^3/µL)	HB (g/dL)	Karyotype	Molecularbiology
1	t-MDS	MDS-RS-MLD	4# PEI	55	8%	2670	71	8.2	Deletion 5q31 57	
2	t-MDS	MDS MLD	6# CHOP	73	2%	12700	557	7.5	normal	JAK2
3	t-MDS	EB I/EB II	8# GMALL B-ALL	60	13%	1500	41	7.9	complex	
4	t-MDS	EB II	4# EC + 12# Pacli	53	20%	1300	153	10.8	normal	MLL translocation
1	t-AML		RJT 3.7GBq	43	76%	26300	25	8.3	normal	FLT3- TKD
2	t-AML		7# BEACOPPesc	41	66%	9500	24	8.4	47,XX,+11	FLT3
3	t-AML		8# GMALL B-ALL + HD-BEAM	58	80%	21900	49	7.3	normal	
4	t-AML		6# R-CHOP	60	90%	500	25	7.5	47, XY, +8[22]/46, XY[2]	IDH1 Mutation
1	MDS*	MDS MLD	none	64	< 5%	1836	127	7.9	normal	U2AF1
2	MDS*	MDS MLD	none	58	< 5%	1600	63	9.1	missing	missing
3	MDS*	MDS-RS-MLD	none	68	< 5%	2499	461	9.2	normal	SF3B1
4	MDS*	MDS MLD	none	65	< 5%	6890	467	9.2	missing	missing
1	AML*	AML NOS	none	74	73%	50	47	10.9	missing	missing
2	AML*	AML MRC	none	53	80%	1504	19	11.8	complex	missing
3	AML*	AML with rec. gen. abnormalities	none	66	80%	960	60	9.5	normal	biall. CEBPA
4	AML*	AML with rec. gen. abnormalities	none	68	78%	2212	120	11.9	normal	FLT3-ITDhigh, NMP1

Abbreviations: No, number; ANC, absolute neutrophil count; HB, hemoglobin; CRP, c-reactive protein; #, number of therapeutic cycles; PEI, cisplatin, etoposide, and ifosfamide; (R)-CHOP, (rituximab), cyclophosphamide, hydrocydaunorubicin, oncovin, and prednisone; GMALL B-ALL=treatment protocol for leukemia; ; EC=epirubicin and cyclophosphamide; Pacli=paclitaxel; RJT=radioiodinetherapy; BEACOPPesc=bleomycin, etoposide, adriamcyin (doxorubicin), cyclophosphamide, oncovin, procarbazine, prednisone, escalated; HD-BEAM=high dose carmusine, etoposide, cytarabine, and melphalan

Author Contributions

Conceptualization, B.S., T.S., S.G.; methodology, B.S., L.B., A.K., T.W., P.P., K.K., S.G.; validation, B.S., L.B., A.K., S.G.; formal analysis, B.S., S.G.; investigation, B.S., L.B., A.K., P.J., S.G., T.S.; resources, B.S., L.B., A.K., P.J., U.M., U.G., S.G.; data curation, B.S., L.B., A.K., P.J., S.G.; writing—original draft preparation, B.S., S.G., T.S.; writing—review and editing, B.S., L.B., A.K., P.J., U.M., T.W., P.P., K.K., F.B., R.H., U.G., S.G. T.S.; visualization, B.S., S.G., T.S.; supervision, S.G., T.S.; project administration, B.S., S.G., T.S..; funding acquisition, T.S. All authors have read and agreed to the published version of the manuscript.

Acknowledgments

This work was supported by the Deutsche Forschungsgemeinschaft (DFG) 417677437/GRK2578 (to T.S.). We would like to thank Dennis Sohn from the Laboratory of Molecular Radio-oncology, Clinic and Polyclinic for Radiation Therapy and Radiooncology for technical assistance regarding LTC-IC assays and the contributing groups within the GRK2578. We thank Maria Grandoch of the Institute of Translational Pharmacology, Sören Twarock, and Katharina Bottermann of the Institute of Pharmacology at the Heinrich-Heine University Düsseldorf for using the cryostat. Computational support of the Zentrum für Informations- und Medientechnologie, especially the HPC team (High Performance Computing) at the Heinrich-Heine University is acknowledged.

Conflicts of Interest: The authors declare no conflict of interest. The funders had no role in the design of the study; in the collection, analyses, or interpretation of data; in the writing of the manuscript, or in the decision to publish the results.

Funding

Deutsche Forschungsgemeinschaft, 417677437/GRK2578, Thomas Schroeder

Declarations

The authors declare no conflict of interest. The funders had no role in the design of the study; in the collection, analyses, or interpretation of data; in the writing of the manuscript, or in the decision to publish the results.

References

1. Allan, J.M. and L.B. Travis, *Mechanisms of therapy-related carcinogenesis.* Nat Rev Cancer, 2005. **5**(12): p. 943-55.
2. McNerney, M.E., L.A. Godley, and M.M. Le Beau, *Therapy-related myeloid neoplasms: when genetics and environment collide.* Nat Rev Cancer, 2017. **17**(9): p. 513-527.
3. Godley, L.A. and R.A. Larson, *Therapy-Related Myeloid Leukemia.* Seminars in Oncology, 2008. **35**(4): p. 418-429.
4. Stoddart, A., et al., *Cytotoxic Therapy–Induced Effects on Both Hematopoietic and Marrow Stromal Cells Promotes Therapy-Related Myeloid Neoplasms.* Blood Cancer Discovery, 2020. **1**(1): p. 32-47.
5. Blanco, J.G., M. Edick, J. , and M.V. Relling, *Etoposide induces chimeric Mll gene fusions.* FASEB Journal, 2004. **18**(1).
6. Escobar, P.A., et al., *Leukaemia-specific chromosome damage detected by comet with fluorescence in situ hybridization (comet-FISH).* Mutagenesis, 2007. **22**(5): p. 321-7.
7. Lomax, M.E., L.K. Folkes, and P. O'Neill, *Biological consequences of radiation-induced DNA damage: relevance to radiotherapy.* Clin Oncol (R Coll Radiol), 2013. **25**(10): p. 578-85.
8. Rogers, H.J., et al., *Comparison of therapy-related and de novo core binding factor acute myeloid leukemia: A bone marrow pathology group study.* Am J Hematol, 2020. **95**(7): p. 799-808.
9. Kuendgen, A., et al., *Therapy-related myelodysplastic syndromes deserve specific diagnostic sub-classification and risk-stratification-an approach to classification of patients with t-MDS.* Leukemia, 2021. **35**(3): p. 835-849.
10. Wu, Y., et al., *Impaired Expression of Focal Adhesion Kinase in Mesenchymal Stromal Cells from Low-Risk Myelodysplastic Syndrome Patients.* Front Oncol, 2017. **7**: p. 164.
11. Geyh, S., et al., *Insufficient stromal support in MDS results from molecular and functional deficits of mesenchymal stromal cells.* Leukemia, 2013. **27**(9): p. 1841-51.
12. Kitagawa, M., et al., *Overexpression of tumor necrosis factor (TNF)-alpha and interferon (IFN)-gamma by bone marrow cells from patients with myelodysplastic syndromes.* Leukemia, 1997. **11**(12): p. 2049-54.
13. Cogle, C.R., et al., *Bone marrow niche in the myelodysplastic syndromes.* Leuk Res, 2015. **39**(10): p. 1020-7.
14. Geyh, S., et al., *Transforming growth factor beta1-mediated functional inhibition of mesenchymal stromal cells in myelodysplastic syndromes and acute myeloid leukemia.* Haematologica, 2018. **103**(9): p. 1462-1471.
15. Mendez-Ferrer, S., et al., *Mesenchymal and haematopoietic stem cells form a unique bone marrow niche.* Nature, 2010. **466**(7308): p. 829-34.
16. Anthony, B.A. and D.C. Link, *Regulation of hematopoietic stem cells by bone marrow stromal cells.* Trends Immunol, 2014. **35**(1): p. 32-7.

17. Bogun, L., et al., *Overlapping Stromal Alterations in Myeloid and Lymphoid Neoplasms.* Cancers, 2024. **16**(11).
18. Falconi, G., et al., *Impairment of PI3K/AKT and WNT/beta-catenin pathways in bone marrow mesenchymal stem cells isolated from patients with myelodysplastic syndromes.* Exp Hematol, 2016. **44**(1): p. 75-83 e1-4.
19. Falconi, G., et al., *Impairment of FOXM1 expression in mesenchymal cells from patients with myeloid neoplasms, de novo and therapy-related, may compromise their ability to support hematopoiesis.* Sci Rep, 2022. **12**(1): p. 21231.
20. Pich, O., et al., *The evolution of hematopoietic cells under cancer therapy.* Nat Commun, 2021. **12**(1): p. 4803.
21. Bertrums, E.J.M., et al., *Elevated Mutational Age in Blood of Children Treated for Cancer Contributes to Therapy-Related Myeloid Neoplasms.* Cancer Discov, 2022. **12**(8): p. 1860-1872.
22. Bogun, L., et al., *Stromal alterations in patients with MGUS, smoldering myeloma and multiple myeloma* Blood Adv, 2024.
23. Dobin, A., et al., *STAR: ultrafast universal RNA-seq aligner.* Bioinformatics, 2013. **29**(1): p. 15-21.
24. Pertea, M., et al., *StringTie enables improved reconstruction of a transcriptome from RNA-seq reads.* Nat Biotechnol, 2015. **33**(3): p. 290-5.
25. Jäger, P., et al., *Acute myeloid leukemia-induced functional inhibition of healthy CD34+ hematopoietic stem and progenitor cells.* Stem Cells, 2021. **39**(9): p. 1270-1284.
26. Zhou, Y., et al., *Metascape provides a biologist-oriented resource for the analysis of systems-level datasets.* Nat Commun, 2019. **10**(1): p. 1523.
27. Zheng, L., et al., *The immunological role of mesenchymal stromal cells in patients with myelodysplastic syndrome.* Front Immunol, 2022. **13**: p. 1078421.
28. Geyh, S., et al., *Functional inhibition of mesenchymal stromal cells in acute myeloid leukemia.* Leukemia, 2016. **30**(3): p. 683-91.
29. Plakhova, N., et al., *Mesenchymal stromal cell senescence in haematological malignancies.* Cancer Metastasis Rev, 2023. **42**(1): p. 277-296.
30. Yehudai-Resheff, S., et al., *Abnormal morphological and functional nature of bone marrow stromal cells provides preferential support for survival of acute myeloid leukemia cells.* Int J Cancer, 2019. **144**(9): p. 2279-2289.
31. Sharpe, A.H., *Introduction to checkpoint inhibitors and cancer immunotherapy.* Immunol Rev, 2017. **276**(1): p. 5-8.
32. Ge, S., et al., *Molecular imaging of immune checkpoints in oncology: Current and future applications.* Cancer Lett, 2022. **548**: p. 215896.
33. Fang, X., et al., *CD274 promotes cell cycle entry of leukemia-initiating cells through JNK/Cyclin D2 signaling.* J Hematol Oncol, 2016. **9**(1): p. 124.
34. Zajac, M., et al., *Expression of CD274 (PD-L1) is associated with unfavourable recurrent mutations in AML.* Br J Haematol, 2018. **183**(5): p. 822-825.
35. Gou, Q., et al., *PD-L1 degradation pathway and immunotherapy for cancer.* Cell Death Dis, 2020. **11**(11): p. 955.
36. Eladl, E., et al., *Role of CD47 in Hematological Malignancies.* J Hematol Oncol, 2020. **13**(1): p. 96.
37. Jia, X., et al., *CD47/SIRPalpha pathway mediates cancer immune escape and immunotherapy.* Int J Biol Sci, 2021. **17**(13): p. 3281-3287.
38. Logtenberg, M.E.W., F.A. Scheeren, and T.N. Schumacher, *The CD47-SIRPalpha Immune Checkpoint.* Immunity, 2020. **52**(5): p. 742-752.

2.4. Antineoplastic Therapy Affects the in vitro Phenotype and Functionality of Healthy Human Bone Marrow-Derived Mesenchymal Stromal Cells

Bo Scherer, Lucienne Bogun, Annemarie Koch, Paul Jäger, Uwe Maus, Laura Schmitt, Karina S. Krings, Sebastian Wesselborg, Rainer Haas, Thomas Schroeder and Stefanie Geyh

Abstract

While antineoplastic therapies aim to specifically target cancer cells, they may also exert adverse effects on healthy tissues, like healthy hematopoietic stem and progenitor cells (HSPC), leading to hematotoxicity as a common side effect. Mesenchymal stromal cells (MSC) are a major component of the bone marrow (BM) microenvironment, regulating normal hematopoiesis, while their susceptibility to anticancer therapies and contribution to therapy-related hematotoxicity remains largely unexplored. To address this, we investigated the effects of etoposide, temozolomide, 5-azacitidine, and venetoclax on healthy BM-derived MSC functionality. Doses below therapeutic effects of etoposide (0.1-0.25 µM) inhibited cellular growth and induced cellular senescence in healthy MSC, accompanied by an increased mRNA expression of *CDKN1A*, decreased trilineage differentiation capacity, and insufficient hematopoietic support. Pharmacological doses of 5-azacitidine (2.5 µM) shifted MSC differentiation capacity by inhibiting osteogenic capacity but enhancing the chondrogenic lineage, as demonstrated by histochemical staining and on mRNA level. At the highest clinically relevant dose, neither venetoclax (40 nM) nor temozolomide (100 µM) exerted any effects on MSC but clearly inhibited cellular growth of cancer cell lines and primary healthy HSPC, pointing to damage to hematopoietic cells as a major driver of hematotoxicity of these two compounds. Our findings show that besides HSPC, also MSC are sensitive to certain antineoplastic agents, resulting in molecular and functional alterations that may contribute to therapy-related myelosuppression. Understanding these interactions could be helpful for the development of strategies to preserve BM MSC functionality during different kinds of anticancer therapies.

Journal	Archives of Toxicology
Impact factor	4.8 (2023)
Contribution to publication	70 %

The own contribution of this manuscript includes the main provision of study material, the main bulk of collection and assembly of experiment data, as well as analysis and interpretation of obtained data. The conceptualization, manuscript writing and figure design was mainly conducted by the first author.

Type of authorship	First author
Status of publication	Published online 12.11.2024

Archives of Toxicology
https://doi.org/10.1007/s00204-024-03898-w

GENOTOXICITY AND CARCINOGENICITY.

Antineoplastic therapy affects the in vitro phenotype and functionality of healthy human bone marrow-derived mesenchymal stromal cells

Bo Scherer[1] · Lucienne Bogun[1] · Annemarie Koch[1] · Paul Jäger[1] · Uwe Maus[2] · Laura Schmitt[3] · Karina S. Krings[3] · Sebastian Wesselborg[3] · Rainer Haas[1] · Thomas Schroeder[4] · Stefanie Geyh[1]

Received: 1 October 2024 / Accepted: 17 October 2024

Abstract

While antineoplastic therapies aim to specifically target cancer cells, they may also exert adverse effects on healthy tissues, like healthy hematopoietic stem and progenitor cells (HSPC), leading to hematotoxicity as a common side effect. Mesenchymal stromal cells (MSC) are a major component of the bone marrow (BM) microenvironment, regulating normal hematopoiesis, while their susceptibility to anticancer therapies and contribution to therapy-related hematotoxicity remains largely unexplored. To address this, we investigated the effects of etoposide, temozolomide, 5-azacitidine, and venetoclax on healthy BM-derived MSC functionality. Doses below therapeutic effects of etoposide (0.1–0.25 µM) inhibited cellular growth and induced cellular senescence in healthy MSC, accompanied by an increased mRNA expression of *CDKN1A*, decreased trilineage differentiation capacity, and insufficient hematopoietic support. Pharmacological doses of 5-azacitidine (2.5 µM) shifted MSC differentiation capacity by inhibiting osteogenic capacity but enhancing the chondrogenic lineage, as demonstrated by histochemical staining and on mRNA level. At the highest clinically relevant dose, neither venetoclax (40 nM) nor temozolomide (100 µM) exerted any effects on MSC but clearly inhibited cellular growth of cancer cell lines and primary healthy HSPC, pointing to damage to hematopoietic cells as a major driver of hematotoxicity of these two compounds. Our findings show that besides HSPC, also MSC are sensitive to certain antineoplastic agents, resulting in molecular and functional alterations that may contribute to therapy-related myelosuppression. Understanding these interactions could be helpful for the development of strategies to preserve BM MSC functionality during different kinds of anticancer therapies.

Keywords MSC · Bone marrow microenvironment · Antineoplastic therapy · Hematotoxicity · Differentiation

Introduction

Anticancer therapy, in particular cytotoxic chemotherapy, is often associated with adverse side effects on healthy tissues, resulting in increased morbidity and mortality

Thomas Schroeder and Stefanie Geyh have contributed equally.

(1) Annual Meeting of the German-Austrian-Suisse Societies of Hematology and Medical Oncology (DGHO), Vienna, Austria, October 2022
(2) 9th German Pharm-Tox Summit, Munich, Germany, March 2024 (Award: best poster in the field of General Toxicology)

✉ Thomas Schroeder
thomas.schroeder@uk-essen.de

✉ Stefanie Geyh
stefanie.geyh@med.uni-duesseldorf.de

[1] Department of Hematology, Oncology and Clinical Immunology, Medical Faculty and University Hospital Duesseldorf, Heinrich Heine University Duesseldorf, Moorenstraße 5, 40225 Düsseldorf, Germany

[2] Department of Orthopedic Surgery and Traumatology, Medical Faculty and University Hospital Duesseldorf, Heinrich Heine University, Moorenstraße 5, 40225 Duesseldorf, Germany

[3] Institute for Molecular Medicine 1, Medical Faculty and University Hospital Duesseldorf, Heinrich Heine University, Universitätsstraße 1, 40225 Duesseldorf, Germany

[4] Department of Hematology and Stem Cell Transplantation, University Hospital Essen, Hufelandstraße 55, 45147 Essen, Germany

Published online: 12 November 2024

(Crawford et al. 2008). Cytostatic drugs such as the topoisomerase II inhibitor etoposide (ETO) or the alkylating agent temozolomide (TMZ) target proliferating cells by intervening with the cell cycle, inducing DNA double-strand breaks, and eventually leading to apoptosis (Friedmann et al. 2000; Sinkule 1984). Other antineoplastic compounds, such as 5-azacitidine (AZA) or venetoclax (VEN), target cancer cells by interfering with epigenetic regulation and apoptosis mechanisms, respectively (Kaminskas et al. 2005; Scheffold et al. 2018). Hematotoxicity is a major side effect of most conventional and targeted therapies and has mainly been attributed to the effects of these drugs on cycling hematopoietic stem and progenitor cells (HSPC). Physiologically, HSPC reside within the bone marrow (BM) microenvironment. Mesenchymal stromal cells (MSC) are an integral component of the BM microenvironment and have an indispensable role in the regulation and support of HSPC by expression and secretion of regulatory factors, such as CXCL12, KITLG, or ANGPT1. Thereby, MSC are involved in orchestrating the balance of HSPC self-renewal and differentiation, helping to ensure the life-long supply of mature blood cells. In addition, MSC exhibit immunoregulatory properties and can differentiate into adipocytes, chondrocytes, and osteoblasts (Anthony and Link 2014; Mendez-Ferrer et al. 2010). Besides a direct effect of antineoplastic agents on HSPC, antineoplastic drugs may also exert effects on non-hematopoietic cells of the BM microenvironment, such as MSC, and thereby contribute to cancer therapy-related myelosuppression. So far, reports on the effects of conventional cytostatic drugs and novel therapies on MSC are relatively rare (Li et al. 2004; Qi et al. 2012; Rosca and Burlacu 2011; Ruhle et al. 2018), thus not allowing a definitive conclusion of their contribution to hematotoxicity. To address their potential role in therapy-related myelosuppression, we exposed healthy BM-derived MSC to conventional cytostatic drugs, as well as novel, more targeted therapies, and subsequently analyzed their phenotype and functionality.

Materials and methods

Donor characteristics, cell isolation of MSC and CD34 + cells and cell culture conditions

BM samples were collected from 25 healthy donors (median age: 69.6 years, range 39–88 years) undergoing orthopedic surgery. This study was conducted in accordance with the ethical standards with the 1964 Helsinki Declaration and was approved by the ethics committee of the Heinrich Heine University, Düsseldorf (approval number 4777). All donors gave written informed consent.

MSC were derived from the mononuclear cell fraction as described previously (Geyh et al. 2013) and cultivated in Dulbecco´s Modified Eagle Medium (DMEM) low glucose with 25% FBS and 1% penicillin/streptomycin/L-glutamine (Sigma-Aldrich Chemie GmbH, St. Louis, MO, USA). All treatment experiments were performed in Passage 3–4. CD34 + cells were isolated from the mononuclear cell fraction of healthy donors using the Midi Magnetic Cell Separation (MACS) technology (Miltenyi, Bergisch Gladbach, Germany), cryopreserved, or directly cultured in Iscove's Modified Dulbecco's Medium (20% FBS and 1% penicillin/streptomycin/L-glutamine) supplemented with 10 ng/µL IL3, IL6, SCF, and 20 ng/µL FLT3L (all from Preprotech Inc., London, UK). Cell lines (THP-1, KG-1a, MV4-11, HL-60, K422, and SU-DHL-6) were purchased from the DSMZ (German collection of microorganisms and cell culture GmbH, Braunschweig, Germany) and cultivated according to the manufacturer's instructions.

Anticancer drug exposure

BM-derived MSC were plated at a density of 4×10^3 cells per cm^2, or in the case of ETO at a density of 6×10^3 cells per cm^2. Simultaneously, MSC were exposed to 2.5 µM AZA (#A2385, Sigma-Aldrich Chemie GmbH, St. Louis, MO, USA), 0.04 µM VEN (#S8048, Selleck Chemicals, Houston, USA), 0.1 and 0.25 µM ETO (#E1383, Sigma-Aldrich Chemie GmbH, St. Louis, MO, USA) or 100 µM TMZ (#T2577, Sigma-Aldrich Chemie GmbH, St. Louis, MO, USA), with and without pre-treatment with 1 µM O6-benzylguanine (O6BG; #73,762, STEMCELL technologies, Vancouver, Canada) to block the activity of reversal repair protein O6-methylguanine methyltransferase (MGMT). To mimic the clinical treatment duration, AZA treatment was continued until day seven, ETO was exposed for 48 h, and TMZ with or without O6BG and VEN were exposed for five days. VEN was repeatedly added every other day throughout the differentiation process. Details of the treatment scheme for MSC are depicted in Fig. 1A.

Primary CD34 + cells were treated with maximal doses of TMZ (with or without pre-treatment with 1 µM O6BG) and VEN at a density of 1.4×10^4 cells per cm^2 for five days. AML cell lines THP-1, KG-1a, MV4-11, and HL-60 were treated at a density of 5.2×10^4 cells per cm^2 for three days with TMZ and O6BG. Lymphoma cell lines SU-DHL-6 and K422 were treated at a density of 5.2×10^4 cells per cm^2 for five days with repeated exposure to VEN. Cell numbers were determined using the CASY® Cell Counter TTC (Roche, Basel, Schweiz) or by Trypan Blue staining.

Analysis of cellular senescence by β-galactosidase staining

MSC were harvested after the respective treatment period and re-plated on a new culture plate. After 24 h, β-galactosidase activity was investigated using the Cellular Senescence Detection Kit (Merck KGaA, Darmstadt, Germany) following the manufacturer's instructions. Stained cells were enumerated using the Axiovert 25 light microscope (Zeiss, Jena, Germany), and the fraction of senescent cells (β-galactosidase-positive) was assessed.

Cell Cycle analysis and measurement of apoptosis

Cell cycle distribution and hypodiploid nuclei after exposure were determined using the Nicoletti assay (Nicoletti et al. 1991) by lysis of MSC with 100 µL of hypotonic buffer (1% sodium citrate, 0.1% Triton X-100) containing 50 µg/mL propidium iodide (#81845, Sigma-Aldrich Chemie GmbH, St. Louis, MO, USA). Analysis was performed by flow cytometry at the LSR-Fortessa™ and evaluated using BDFACSuite software (Becton Dickinson, Heidelberg, Germany).

MSC differentiation

Trilineage differentiation of healthy MSC was initiated 24 h after treatment as previously described (Geyh et al. 2013). Adipogenesis was induced in DMEM high glucose medium (10% FBS and 1% penicillin/streptomycin/L-glutamine) with 0.1 mg/mL insulin, 0.1 µM dexamethasone, 0.2 mM indomethacin, and 1 mM IBMX, and cultivated with 0.01 mg/mL insulin for 21 days. Fat vacuoles were visualized with Oil Red O staining. Chondrogenesis was performed as 3D culture for 21 days in DMEM high glucose (1% penicillin/streptomycin/L-glutamine) supplemented with 1% ITS + 1, 1 µM dexamethasone, 50 µg/mL ascorbate-2-phosphate, 40 µg/mL L-proline, and 10 ng/mL TGFβ3 (all from Peptrotech, Inc., London, UK). Pellets were embedded in freezing medium and cryosectioned in 6 µm slices at the Leica Cryostat CM3050 (Leica, Wetzlar, Germany). Visualization of proteoglycan was performed by Safranin O staining. Osteogenesis was induced for 14 days with DMEM low glucose (25% FBS and 1% penicillin/streptomycin/L-glutamine) supplemented with 50 µg/mL ascorbic acid, 10 mM β-glycerol phosphate, and 0.1 µM dexamethasone. Calcium deposition was visualized by Alizarin Red staining. All reagents and supplements were obtained from SIGMA-Aldrich Chemie GmbH (St. Louis, MO, USA), unless otherwise stated. Images were captured at the Axiovert 25 microscope (Zeiss, Jena, Germany) and digitalized with the SPOT Software (Diagnostic Instruments Inc., Sterling Heights, MI, USA).

Hematopoietic support analysis of MSC

MSC were plated at a density of 3×10^4 per cm^2 on tissue culture-treated 12-well plates and exposed to chemical agents. After indicated exposure times, medium was exchanged to agent-free medium. After 24 h, 1.5×10^4 CD34 + cells per cm^2 were added as direct co-culture for three days. Afterward, 1000 CD34 + cells were transferred to 1 mL methylcellulose containing erythropoietin (MethoCult™ H4434 Classic, STEMCELL technologies, Vancouver, Canada), plated in duplets and cultivated at 37 °C and 5% CO_2 for 14 days for colony-forming units (CFU) assay. Colonies were enumerated using the Axiovert 25 microscope (Zeiss, Jena, Germany) and differentiated between white (CFU-GM, CFU-G, CFU-M), red (CFU-E, BFU-E) and mixed (CFU-GEMM) colonies as previously described (Jager et al. 2021).

Quantitative real-time PCR (qPCR)

RNA was purified directly after treatment exposure using the RNase Micro or Mini Kit (QIAGEN, Hilden, Germany) including optional DNase digestion. Transcription to cDNA was performed by Superscript II TM Reverse transcriptase (Invitrogen, Darmstadt, Germany). qPCR was performed in duplicates on a StepOne Plus Real-time PCR Cycler or QuantStudio™3 System using SYBR Green PCR Master Mix (all from Applied Biosystem, Life Technologies, Carlsbad, CA, USA). Primer sequences can be provided on request. *GAPDH* served as reference control. Differences in mRNA expression levels were calculated as fold change by the ΔΔCT method.

Statistical analysis

Statistical analysis was performed using Prism 8.4.3 (GraphPad Software Inc., La Jolla, USA) using the two-sided paired Student's t test for parametric data, or Wilcoxon matched-pairs signed-rank test of non-parametric data. Data graphs show mean and SEM unless otherwise stated. Significance was determined at $P < 0.05$ and is indicated by asterisks ($*P \leq 0.05$, $**P \leq 0.01$, $***P \leq 0.001$).

Results

Exposure to antineoplastic agents affect phenotype, growth and differentiation capacity of healthy MSC

In vitro cultured healthy MSC are usually characterized by a spindle-like phenotype, plastic adherence and trilineage

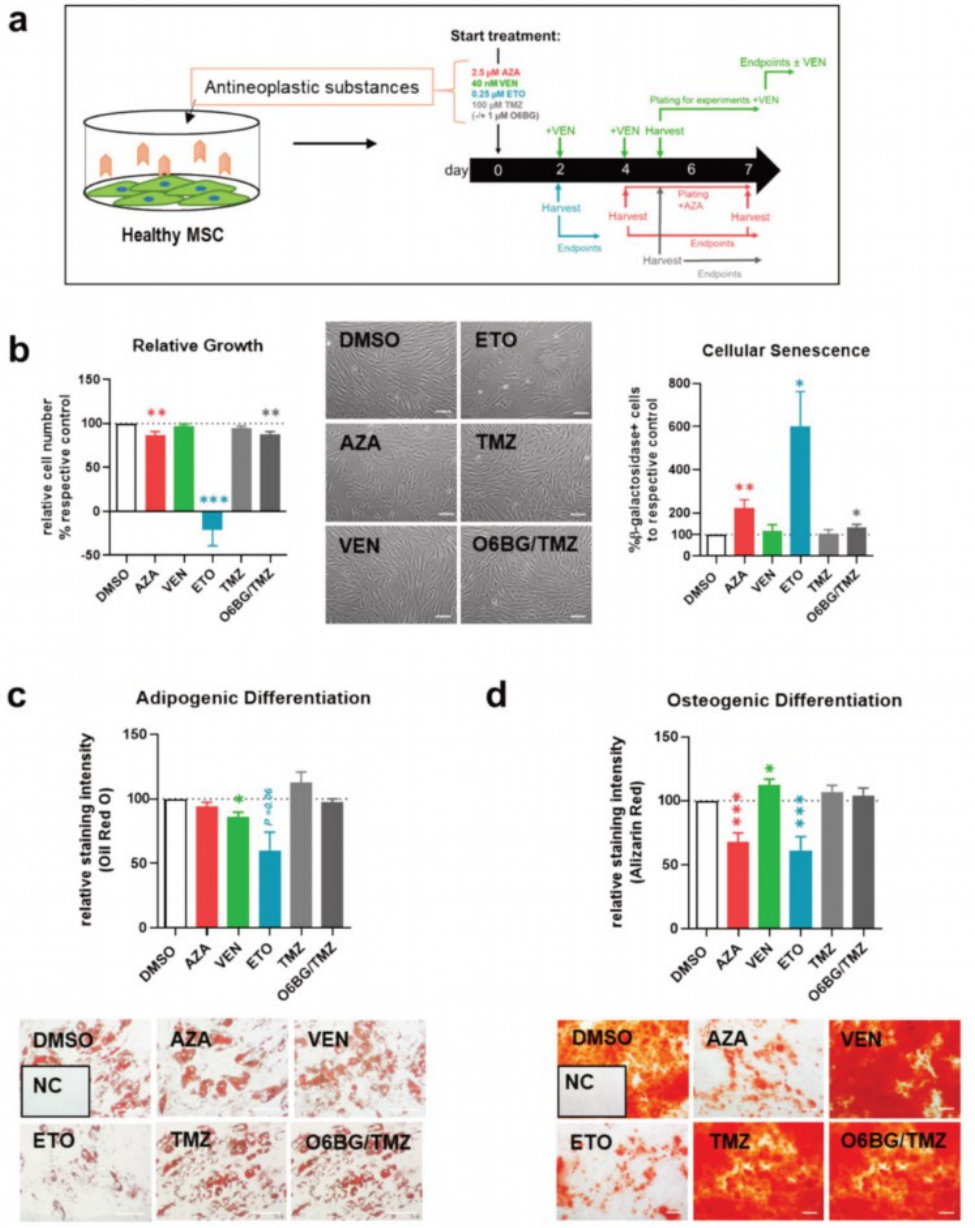
a
Start treatment:
Antineoplastic substances
Healthy MSC
Endpoints ± VEN
Plating for experiments +VEN
+VEN
+VEN Harvest
day 0 2 4 6 7
Harvest
Endpoints
Plating +AZA
Harvest
Endpoints
Harvest
Endpoints
b
Relative Growth
relative cell number % respective control
DMSO AZA VEN ETO TMZ O6BG/TMZ
DMSO
ETO
AZA
TMZ
VEN
O6BG/TMZ
Cellular Senescence
%β-galactosidase+ cells to respective control
c
Adipogenic Differentiation
relative staining intensity (Oil Red O)
d
Osteogenic Differentiation
relative staining intensity (Alizarin Red)
NC

◂**Fig. 1** Phenotype, growth and differentiation of healthy, exposed MSC **a** Healthy MSC were exposed to antineoplastic agents or DMSO. Growth, cellular senescence and differentiation capacity were analyzed. **b** *Left side*: Relative cell numbers to the DMSO control were calculated and representative micrographs of MSC phenotype after exposure are given. *Right side*: Percentage of senescent cells as shown by β-galactosidase activity was calculated and normalized to the respective DMSO control. **c** Differentiation intensity of adipogenic induction of exposed healthy MSC was determined based on lipid vacuoles, stained with Oil Red O after 21 days. Representative micrographs are given. DMSO served as control and an un-induced negative control (NC) was included. **d** Alizarin Red staining intensity of exposed and osteogenic-induced MSC after 14 days are represented in comparison to the DMSO control. Bar charts display mean values and SEM. Statistical significance was determined by two-sided paired Student's *t* test indicated by asterisks for at least four independent experiments ($n \geq 4$; *$P < 0.05$ **$P < 0.01$ ***$P < 0.001$). Scale bars indicate 100 µm

differentiation capacity. MSC were cultivated in the presence of clinical doses of 5-azacitidine (AZA), venetoclax (VEN), etoposide (ETO), or temozolomide (TMZ) alone or co-treated with the MGMT inhibitor O6-benzylguaine (O6BG/TMZ) following the scheme depicted in Fig. 1a. Neither VEN nor TMZ induced phenotypical alterations in MSC or altered growth behavior or differentiation capacity (Fig. 1b-d). Slight phenotypical and proliferative alterations of MSC were found after AZA with decreased cumulative population doublings (CPD) by 13% ($P < 0.0001$) and a roughly doubled cellular senescence ($P < 0.01$). Functionally, AZA exposure inhibited osteogenic differentiation in healthy MSC as shown by decreased Alizarin Red staining ($P < 0.001$), but not adipogenesis. After ETO exposure, MSC displayed a broad and disorganized morphology and the proliferative activity of MSC diminished completely after 48 h exposure (mean population doublings (PD), DMSO: 1.0, ETO: -0.2, $P < 0.001$) accompanied by a sixfold increase in β-galactosidase-positive cells ($P < 0.05$), indicating cellular senescence. Differentiation into adipocytes and osteoblasts was substantially inhibited following ETO exposure (Fig. 1b-d).

Etoposide induces irreversible cell cycle arrest in MSC

ETO prominently affected phenotype and growth of healthy MSC after 48 h of exposure already at sub-clinical concentrations. Therefore, we tested an even lower concentration of 0.1 µM ETO and found similar effects regarding phenotypical alterations and decreased PD in a dose-dependent manner, which were not recovered after four days without exposure (Fig. 2a; mean PD recovery, DMSO: 2.2, 0.1 µM ETO: 1.1, 0.25 µM ETO: − 0.5, $P < 0.01$). Similarly, increased cellular senescence and selective induction of cell cycle marker *CDKN1A* were already determined at 0.1 µM and more prominent at the higher dose. Downregulation of hematopoiesis-relevant factors *CXCL12* and *KITLG* after two days of culture was determined (Fig. 2b, c). Cell cycle arrest in the absence of apoptosis was shown by Nicoletti assay with the majority of ETO-exposed MSC remaining in S–G_2 phase (mean proportion of cells in S–G_2, DMSO: 17.3%, 0.25 µM ETO: 50%) (Fig. 2d).

5-Azacitidine inhibits osteogenic potential, but enhances chondrogenic differentiation capacity in healthy MSC

We found that AZA clearly inhibited osteogenic potential of healthy MSC (Fig. 1d). Knowing that osteoblasts share a common progenitor with chondroblasts and osteogenic–chondrogenic lineage factors, alterations in chondrogenic differentiation were assumed. Therefore, AZA-exposed MSC were differentiated into the chondrogenic lineage. However, Safranin O staining of chondrogenic differentiated cell pellets revealed no differences to the control group, but even showed a tendency to a more robust and concentrated proteoglycan disposition (Fig. 3a, II). To investigate differentiation regulation after AZA exposure on the molecular level, mRNA expression of early and late osteogenic and chondrogenic markers in exposed, but still un-differentiated MSC, was determined (Fig. 3b). Interestingly, the late osteogenic marker Osteocalcin (*OCN*) was clearly upregulated, while not stained by Alizarin Red in osteoblastic-differentiated MSC after AZA (Fig. 3a, I) On the other hand, early osteogenic marker *RUNX2* was downregulated, while early chondrogenic marker *SOX9* was upregulated. However, *ACAN*, a late marker of chondrogenesis, was downregulated. To elucidate this diverse dysregulation of differentiation markers in MSC after AZA, we more closely investigated the regulation of common markers on mRNA level during the course of osteogenic differentiation (induction phase (days 1–7) and maturation phase (days 10–14). Strikingly, we found upregulation of early and late osteogenic markers after AZA exposure. However, at the same time, Dickkopf-2 (*DKK2*), a WNT regulator and inhibitor of osteogenesis, and late chondrogenic marker aggrecan (*ACAN*) were upregulated as well (Fig. 3d). These findings, together with an increased expression of early chondrogenic inducer *SOX9* in un-differentiated AZA-exposed MSC, as well as increased *OCN* levels after AZA treatment, suggest that AZA may skew the differentiation of MSC toward the chondrogenic lineage, at the expense of the osteoblastic lineage.

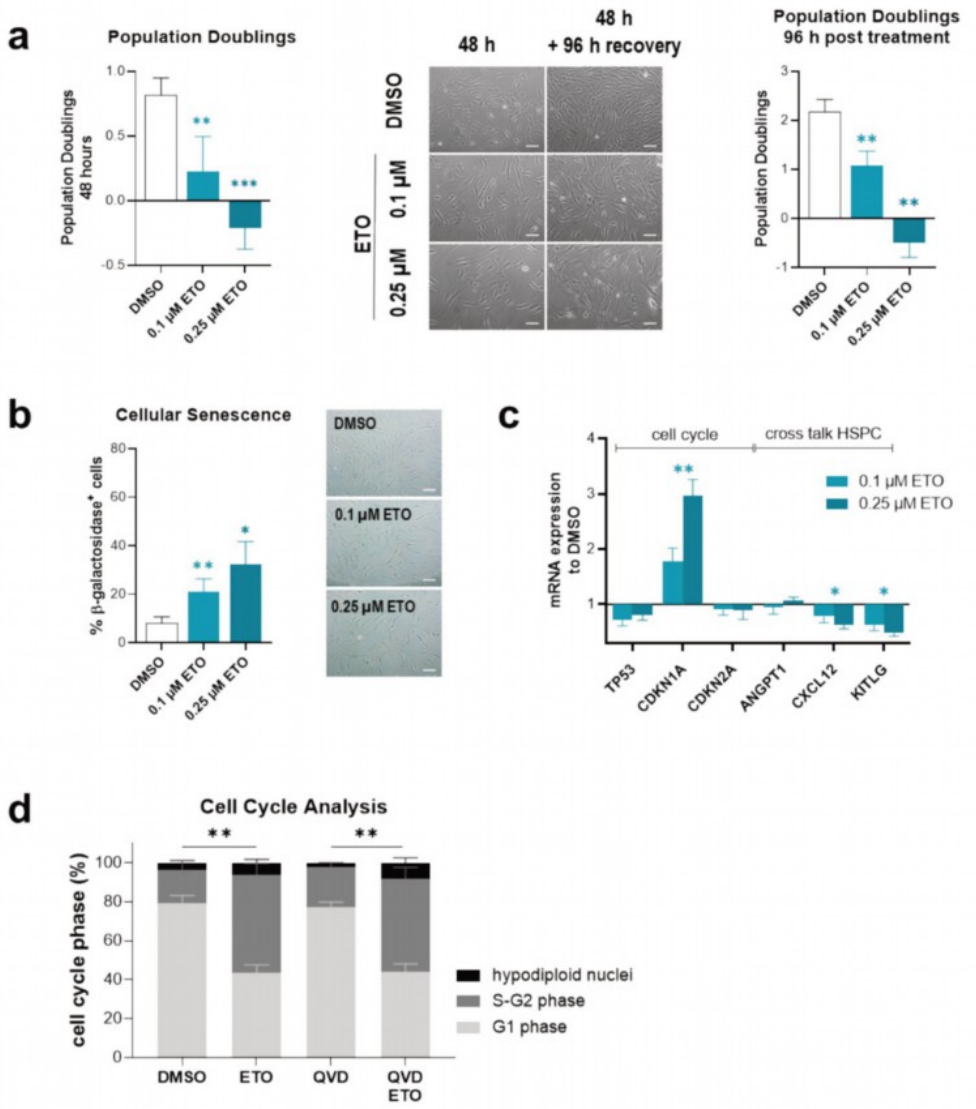

Fig. 2 Cellular senescence and cell cycle arrest after exposure to ETO Healthy MSC were exposed to 0.1 or 0.25 µM ETO for 48 h. **a** *Left side*: PD were calculated after 48 h of exposure to 0.1 µM and 0.25 µM ETO. DMSO served as solvent control. *Middle*: representative micrographs of MSC phenotype after 48 h exposure or additional 96 h recovery period. Scale bars indicate 100 µm. *Right side*: PD of exposed MSC with a recovery period of 96 h. **b** Percentage of β-galactosidase-positive cells after exposure to 0.1 µM and 0.25 µM ETO. **c** Exposed MSC were analyzed by qPCR for cell cycle marker *TP53*, *CDKN1A*, *CDKN2A* on mRNA level as well as for microenvironment regulatory factors *ANGPT1*, *CXCL12* and *KITLG*. Dose-dependent dysregulation of *CDKN1A*, *CXCL12* and *KITLG* was determined. **d** Flow cytometry of Nicoletti staining revealed absence of apoptosis in ETO-exposed MSC, but showed a clear shift of cell cycle stage to S–G_2. Mean values and SEM are shown for at least three independent experiments ($n \geq 3$). Asterisks indicate statistical significance using Student's t test vs DMSO (*$P < 0.05$, **$P < 0.01$, ***$P < 0.0001$)

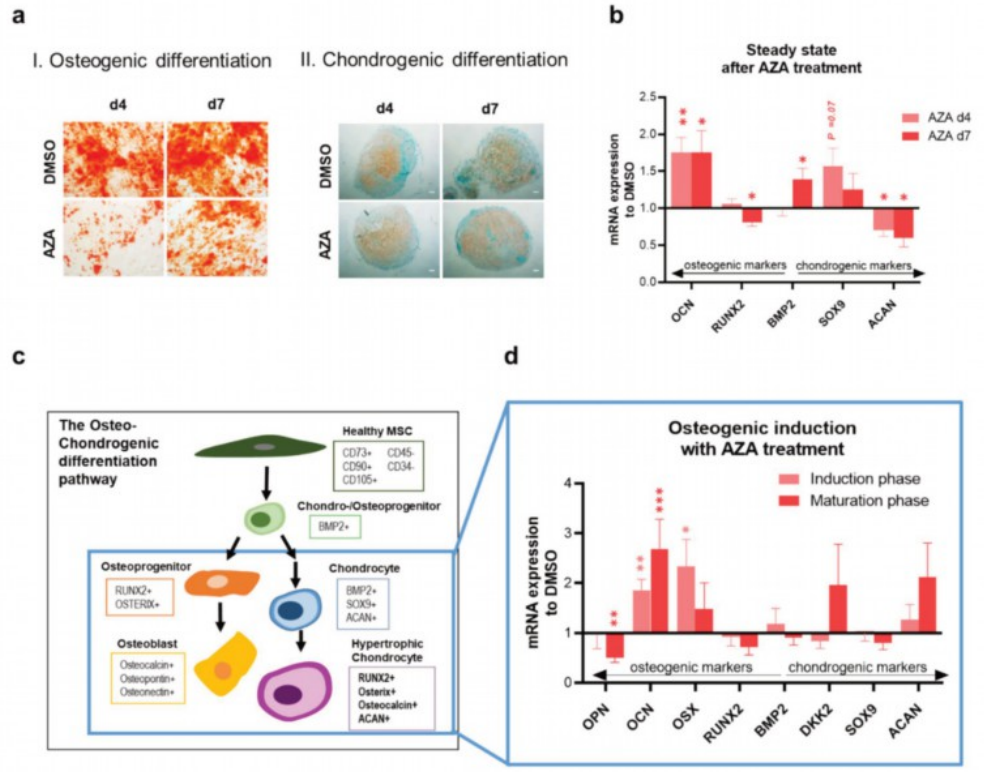

Fig. 3 5-Azacitidine induces differentiation shift from osteogenic to preferentially chondrogenic differentiation **a** MSC were exposed to AZA for four and seven days and afterward induced for osteogenic or chondrogenic differentiation. AZA exposure led to inhibition of calcium disposition after osteogenic induction for 14 days as shown by Alizarin Red staining, while proteoglycan was robustly incorporated during chondrogenic induction as visualized by Safranin O staining after 21 days of differentiation. Representative images are shown. Scale bars indicate 100 µm. **b** Steady-state transcriptional regulation after AZA exposure showed upregulation of osteo-chondrogenic factor *bone morphogenetic protein-2* (*BMP2*), but differential regulation of specific osteogenic and chondrogenic markers. **c** Schematic depiction of the osteo-chondrogenic differentiation pathway and involved regulating factors. Graphics were generated using Microsoft PowerPoint 2013. **d** qPCR results of mRNA expression levels of osteogenic–chondrogenic factors (*BMP2, RUNX2, DKK2, OSX, OCN, SOX9, ACAN*) during 14 days of osteogenic induction and simultaneous AZA treatment. Fold changes of the respective expression related to the control group (normalized as 1) are given for induction phase (days 1–7) and maturation phase (days 10–14) of osteogenic differentiation. Mean values and SEM are shown for at least four independent experiments ($n \geq 4$). Asterisks indicate statistical significance using Student's t test (*$P < 0.05$, **$P < 0.01$, ***$P < 0.0001$)

Temozolomide and venetoclax specifically target malignant cells, but do not affect healthy MSC

Having observed no effects on the growth or functionality of healthy exposed MSC after maximal doses of TMZ and VEN, we investigated the efficacy of TMZ and VEN on AML and lymphoma cell lines respectively. For this purpose, four AML cell lines (HL-60, THP-1, KG-1a, MV4-11) were exposed to increasing concentrations ranging from 1 µM up to 100 µM of TMZ. THP-1 and KG-1a showed no response to TMZ, while a decreased cell number of MV4-11 was observed at the highest concentration of TMZ. HL-60 cell numbers decreased in a dose-dependent manner, already at the lowest TMZ concentration (Fig. 4a, I). Sensitivity of AML cell lines toward TMZ concentration correlated with the mRNA expression of the DNA damage repair enzyme *MGMT* with the sensitive cell line HL-60 exhibiting low mRNA levels of *MGMT* compared to other AML cell

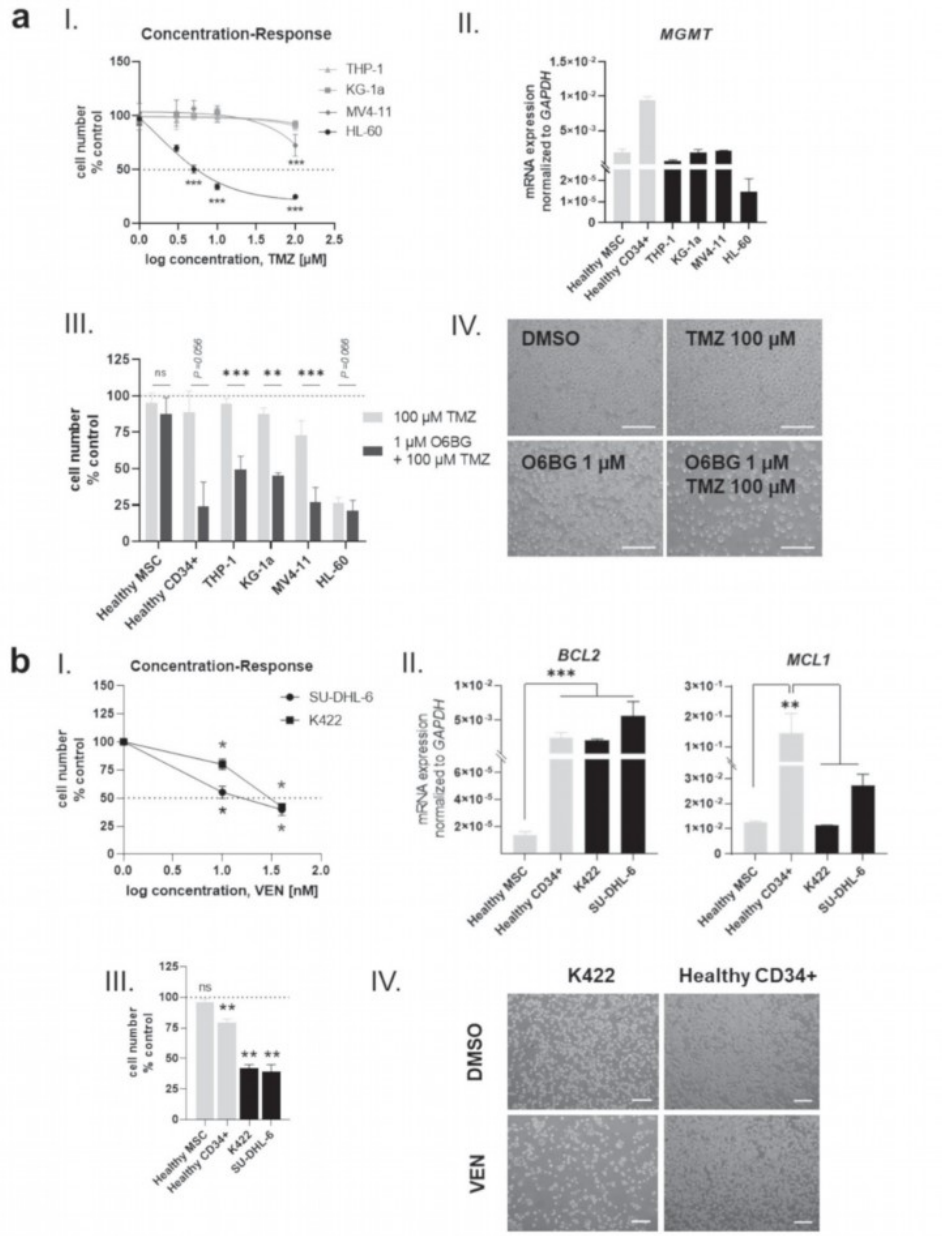
a
I.
Concentration-Response
THP-1
KG-1a
MV4-11
HL-60
cell number % control
log concentration, TMZ [µM]
II.
MGMT
mRNA expression normalized to GAPDH
Healthy MSC
Healthy CD34+
THP-1
KG-1a
MV4-11
HL-60
III.
cell number % control
100 µM TMZ
1 µM O6BG + 100 µM TMZ
IV.
DMSO
TMZ 100 µM
O6BG 1 µM
O6BG 1 µM TMZ 100 µM
b
I.
Concentration-Response
SU-DHL-6
K422
cell number % control
log concentration, VEN [nM]
II.
BCL2
MCL1
mRNA expression normalized to GAPDH
III.
cell number % control
IV.
K422
Healthy CD34+
DMSO
VEN

◂**Fig. 4** Temozolomide and venetoclax target hematopoietic cells, but not healthy MSC **a** I: Concentration response curve of AML cell lines THP-1, KG-1a, MV4-11 and HL-60 after three days exposure to increasing concentrations from 1 to 100 µM of alkylating TMZ are shown. II: qPCR of *MGMT* mRNA expression in native MSC, CD34 + cells and AML cell lines. III: Relative cell growth after co-treatment of AML cell lines and healthy MSC and CD34 + cells with TMZ and O6BG. IV: Representative images of AML cell line MV4-11 with TMZ with or without MGMT inhibitor O6BG are shown. DMSO served as control. **b** I: Concentration response of lymphoma cell lines SU-DHL6 and K422 to VEN after seven days of culture. II: qPCR of *BCL2* and *MCL1* mRNA expression in native MSC, CD34 + and lymphoma cell lines SU-DHL6 and K422. III: Cell lines, MSC and CD34 + were exposed to VEN for 5 days and subsequently cell numbers were determined. IV: Representative micrographs of lymphoma cell line K422 and healthy CD34 + cells after exposure to VEN for five days are shown. DMSO served as control. Scale bars indicate 100 µm. Mean values and SEM are shown for at least three independent experiments ($n \geq 3$). Asterisks indicate statistical significance using Student's t test vs DMSO (*$P < 0.05$, **$P < 0.01$, ***$P < 0.0001$)

lines. In agreement with this, healthy MSC showed mRNA expression levels of *MGMT* comparable to resistant AML cell lines, while healthy CD34 + HSPC exhibited a 4.5-fold higher mRNA expression level of *MGMT* than AML cell lines (Fig. 3a, II). Co-treatment of TMZ and MGMT inhibitor O6BG showed significantly diminished cell numbers of all AML cell lines, as well as healthy CD34 + cells. MSC were not sensitive to the combination of TMZ with O6BG (Fig. 4a, III).

Regarding VEN, two lymphoma cell lines (SU-DHL-6, K422) were exposed to clinically relevant doses ranging from 10 to 40 nM and showed dose-dependent decrease in cell number, with SU-DHL-6 being more sensitive (Fig. 4b, I). On mRNA level, *BCL2* expression was similar in healthy CD34 + cells, K422 and SU-DHL-6, while healthy MSC exhibited low *BCL2* expression. On the other hand, *MCL1* expression was significantly higher in healthy CD34 + cells compared to healthy MSC and lymphoma cell lines (Fig. 4b, II). Accordingly, exposure of 40 nM VEN led to significantly diminished cell numbers in both lymphoma cell lines, while healthy MSC and CD34 + HSPC were not as drastically affected (Fig. 4b, III, IV).

Antineoplastic agents affect hematopoietic support capacity of healthy MSC

Given the pivotal role for hematopoiesis under physiological circumstances, which are mediated by secreted factors as well as ligand–receptor interactions, we investigated the hematopoietic support capacity of MSC after exposure to antineoplastic agents next. For this purpose, healthy CD34 + cells were co-cultivated with MSC, which were previously exposed to the cytostatic drugs, and subsequently subjected to CFU assays (Fig. 5a). After three days of co-culture with exposed MSC, relative cell numbers of MSC were comparable to findings in Fig. 1b. CD34 + cell numbers were not altered by antineoplastic agents, however showed a clear tendency to an increased cell number after co-culture with ETO-exposed MSC (Fig. 5b). Regarding CFU assays, only MSC previously exposed to ETO showed a significantly diminished hematopoietic support capacity as indicated by a lower number of total colonies, while the distribution along the different colony subtypes was not altered significantly (Fig. 5c, d).

Discussion

The majority of anticancer therapies is associated with an impairment of healthy hematopoietic progenitor cells, leading to dose-limiting hematotoxicity or the development of therapy-related neoplasms (Bertrums et al. 2022; Diamond et al. 2023; McNerney et al. 2017). So far, the main focus of chemotherapy-induced hematotoxicity has been on HSPC with elaborate research on cytoprotective strategies for HSPC to mitigate myelosuppressive effects (Fakhrabadi et al. 2020; List et al. 1996; Sawai et al. 2001). Despite the regulatory role of MSC in the hematopoietic system, the impact of different anticancer therapies on MSC and specifically their contribution to hematotoxicity remain incompletely understood. Therefore, we investigated this using human BM-derived MSC from healthy donors with a corresponding age of cancer patients for clinical relevance. It has to be noted that age-related clonal hematopoiesis and accompanying bone marrow alterations were not tested in this cohort and therefore the significance of clonal hematopoiesis regarding MSC sensitivity toward anticancer therapy cannot be derived here (Hecker et al. 2021; Winter et al. 2024). Nevertheless, our comprehensive *in vitro* analyses show that MSC are directly affected by some antineoplastic agents (ETO, AZA) and thereby contribute to hematotoxicity, demonstrating the relevance of MSC and their therapeutic response for further investigations.

ETO induced cellular senescence in MSC already at concentrations below clinical plasma levels of 0.1–0.25 µM, which was not reversible, neither in proliferative medium nor by induction of differentiation. Nicoletti assay revealed efficient cell cycle inhibition by ETO in the absence of apoptosis. Similar findings were reported by other groups, showing that MSC are largely resistant to apoptosis but undergo cellular changes, e.g., cellular senescence (Lutzkendorf et al. 2017; Nicolay et al. 2016; Qi et al. 2012). Increased proportion of β-galactosidase-positive cells, accompanied by the induction of senescent-associated markers as shown here, suggests the induction of the senescence-associated secretory phenotype (SASP). This phenotype is pro-inflammatory

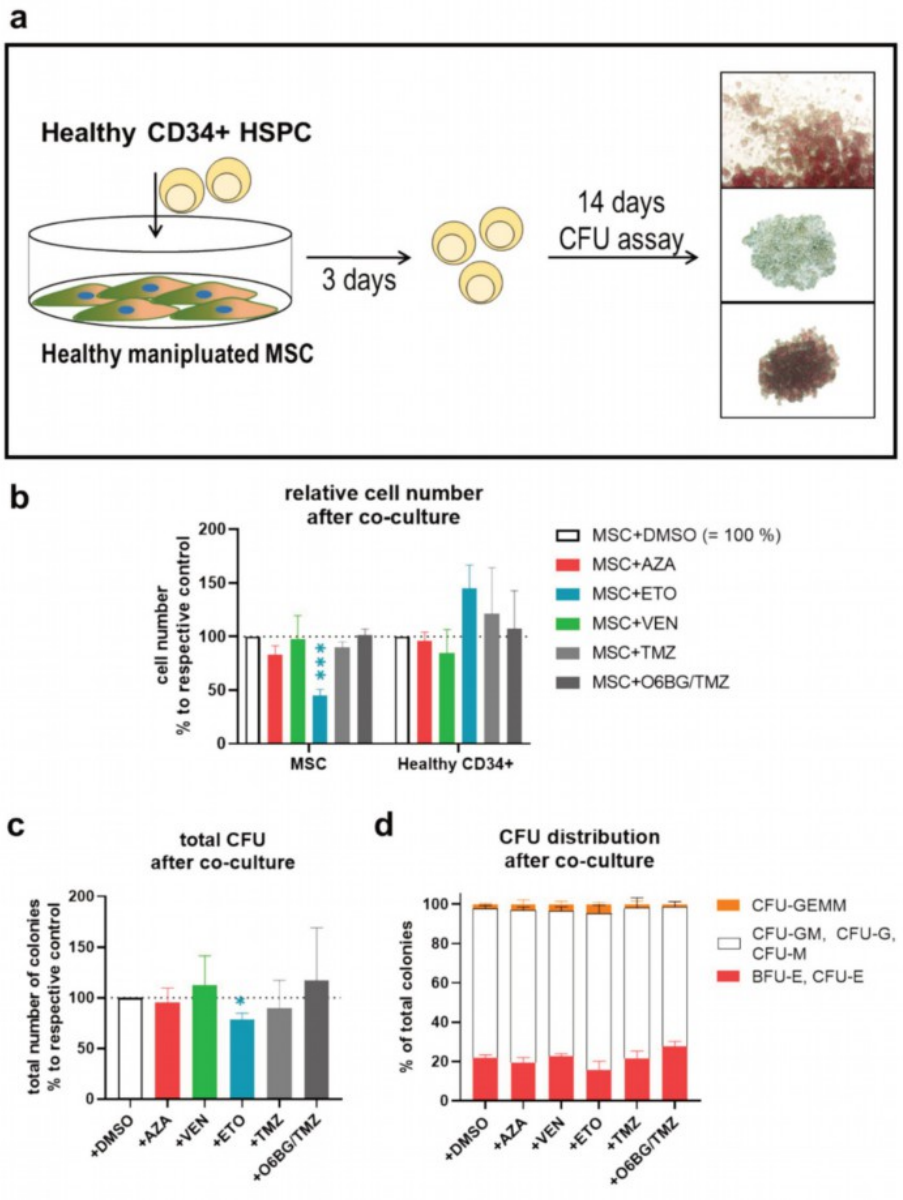

and shown to lower the viability and differentiation capacity of HSPC (Demaria et al. 2017; Tchkonia et al. 2013). Although we did not analyze the SASP of ETO-exposed MSC, together with our findings, this may explain the insufficient hematopoietic support of MSC exposed to topoisomerase II inhibitors. Within a clinical setting, the

◂**Fig. 5** Hematopoietic support capacity of exposed MSC **a** Study design: MSC were pre-treated for 24 h with AZA or ETO, or six days with VEN and TMZ (±O6BG) and subsequently co-cultured for three days with healthy CD34 + cells in medium without antineoplastic agents. Afterward, CFU assay was performed for 14 days with co-cultured CD34 + HSPC to investigate their differentiation potential toward CFU-GEMM, BFU-E, CFU-E, CFU-G, CFU-M, CFU-GM. Colonies were enumerated under a light microscope. **b** Cell numbers of MSC and CD34 + were determined after three days of co-culture. **c** Total number of colonies of co-cultured CD34 + cells after 14 days of CFU assay. **d** CFU-GEMM, BFU-E, CFU-E, CFU-G, CFU-M, CFU-GM MSC were counted and are depicted in respective colors. CD34 + cells co-cultured with MSC supplemented with DMSO served as control. Mean values and SEM are shown for at least three independent experiments ($n \geq 3$). Asterisks indicate statistical significance using Student's t test vs DMSO (*$P < 0.05$; ***$P < 0.001$)

application of senolytics to manage therapy-induced senescence might help preserve a healthy microenvironment during treatment (Kirkland and Tchkonia 2020), a view that is supported by studies in mice showing that senolytics enhance MSC differentiation capacity (Zhou et al. 2021). Hence, the modulation of MSC by senolytics or molecular manipulation, e.g., by retroviral transfection, may help maintain the niche equilibrium and support healthy hematopoiesis (Halim et al. 2020; Sawai et al. 2001).

On the other hand, AZA led to a differentiation shift of MSC, clearly inhibiting osteogenic differentiation of healthy MSC and favoring differentiation toward the chondrogenic and adipogenic lineage. As hypomethylating agent, AZA was reported to reverse the hypermethylation patterns in MDS stroma and affect epigentically regulated differentiation processes (Bhagat et al. 2017). However, described effects of AZA on the differentiation capacity of MSC are controversial and range from enhanced potential (Bae et al. 2017; Yan et al. 2014) to decreased potential in individual lineages of differentiation (Rosca and Burlacu 2011; Wenk et al. 2018) and are most likely dependent on the cellular origin and treatment scheme. Clinically, patients are exposed to 75 mg/m^2 body surface with a bioavailability of around 89% (Derissen et al. 2014; Kaminskas et al. 2005). In this study, we have chosen a low concentration (2.5 µM) within patient plasma levels, which can range from 1 to 50 µM, and mimicked the treatment duration of seven days (Kaminskas et al. 2005). Moreover, we used cells derived directly from human BM, while other studies were conducted in mice (Rosca and Burlacu 2011) or with MSC derived from adipose tissue (Yan et al. 2014). Although we did not observe effects on the hematopoietic support function, the essence of osteoblasts in hematopoietic homing is well known (Neiva et al. 2005) and might implicate the initiation of a dysbalance in niche equilibrium, potentially indirectly affecting HSPC crosstalk and regulation (Raaijmakers et al. 2010). Due to the epigenetic mode of action of AZA, dose escalation might reveal differential effects. Wenk and colleagues (2018) used a fourfold higher concentration with a lower exposure time (48 h) and found osteogenic-enhancing effects on healthy MSC and MSC from patients with MDS, while adipogenic differentiation was inhibited. In this set-up, the hematopoietic support function was increased as well, demonstrating the importance of osteogenic potential on the one hand and dose selection on the other.

In our analysis, TMZ and VEN clearly targeted hematopoietic cells but not MSC. We did not find notable alterations in MSC at the highest clinically relevant dose of 100 µM TMZ (Meany et al. 2009; Ostermann et al. 2004) or 40 nM VEN (Scheffold et al. 2018). On the one hand, TMZ effectively targeted malignant cells, as reflected by decreased growth after exposure, which was dependent on *MGMT* expression level. The overall response of cancer patients treated with TMZ is dependent on their MGMT activity, with patients conferring high activity being resistant to TMZ treatment (Marrari et al. 2011; Trillo Aliaga et al. 2021). Resistant cells usually become sensitized by MGMT inhibition, as shown here and by others (Chen et al. 2022), but this does not apply to healthy MSC in our experiments. The slow proliferative activity of MSC compared to cancer cell lines must be noted; however, TMZ exerts its effects after two cell cycles according to its mode of action, which was given in each tested cell population. Studies have shown that myelosuppression by TMZ correlates with *MGMT* expression in leukocytes (Stokes et al. 2012). On the other hand, primitive CD34 + HSPC were exposed to TMZ and showed clear sensitivity when exposed in combination with the MGMT inhibitor. This points to the fact that the origin of TMZ-induced myelosuppression is probably also caused by the suppression of HSPC. Although HSPC already present with the relative highest *MGMT* expression in our cohort, alkylating agents are often combined with O6BG to potentiate TMZ effects, thereby also targeting HSPC. To protect HSPC reservoirs, MGMT expression and activity could be artificially increased in these cells to ensure selective elimination of cancer cells (Pollok 2003; Reese et al. 1999).

Similarly, VEN specifically inhibits the anti-apoptotic protein BCL2, which is mainly increased in cancer cells. Mainly hematological neoplasms, such as acute myeloid leukemia or lymphomas are treated with VEN as part of a combination therapy. In lymphomas, for example, the common chromosomal translocation t(14;18)(q32;q21) leads to a constitutive overexpression of BCL2, allowing apoptotic escape for malignant cells (Miyashita and Reed 1993; Weiss et al. 1987). Therefore, VEN selectively targets these cells and induces apoptosis. Compared to cancer cell lines and HSPC, the expression of *BCL2* is much lower in healthy MSC, explaining their lack of alterations after VEN exposure. In fact, CD34 + cells have similar levels of *BCL2* to lymphoma cell lines due to their immaturity (Delia et al. 1992) but were not as dramatically affected by VEN.

Following this, we detected a tenfold increased expression of the alternative anti-apoptotic *MCL1* in healthy CD34 + cells compared to lymphoma cell lines, protecting the progenitor cells from long-lasting abolishment of BCL2 by VEN. Consequently, only cells conferring both, high *BCL2* and low *MCL1* levels are specifically and durably targeted by VEN (Warren et al. 2019). While it was shown that VEN spares hematopoietic cells in peripheral blood (Chen et al. 2020; Shi et al. 2021; Souers et al. 2013), knowledge about alterations in hematopoietic progenitors and their potential contribution to myelosuppression does not exist. To determine the etiology of VEN-related myelosuppression, functional effects on healthy CD34 + HSPC should be investigated in future.

Conclusion

The new insights into direct MSC alterations provided by this study emphasize the critical need to consider the entire BM microenvironment in the context of anticancer therapies. While not all antineoplastic agents mediate their myelosuppressive effects via BM stromal cells, substance-specific effects directly affecting MSC were found after ETO and AZA exposure, potentially contributing to therapy-related hematotoxicity. These results open a new perspective on the management of myelosuppressive side effects during anticancer therapy and should be further investigated for developing novel strategies implementing the relevance of BM MSC.

Acknowledgements This work was supported by grants from the Deutsche Forschungsgemeinschaft (DFG) 417677437/GRK2578 (to S.W. and T.S.). We would like to thank the contributing groups within the GRK2578, especially the group of Sebastian Wesselborg for excellent support of apoptosis assays. We thank Maria Grandoch of the Institute of Translational Pharmacology, Sören Twarock, and Katharina Bottermann of the Institute of Pharmacology at the Heinrich Heine University Düsseldorf for using the cryostat.

Author contribution Conceptualization: Bo Scherer, Thomas Schroeder, Stefanie Geyh; Methodology: Bo Scherer, Annemarie Koch, Sebastian Wesselborg, Laura Schmitt, Karina S. Krings, Stefanie Geyh; Validation: Bo Scherer, Lucienne Bogun, Annemarie Koch, Stefanie Geyh; Formal analysis: Bo Scherer, Stefanie Geyh; Investigation: Bo Scherer, Lucienne Bogun, Annemarie Koch, Stefanie Geyh; Resources: Bo Scherer, Lucienne Bogun, Annemarie Koch, Paul Jäger, Uwe Maus, Stefanie Geyh, Thomas Schroeder; Data curation: Bo Scherer, Lucienne Bogun, Annemarie Koch, Stefanie Geyh, Paul Jäger; Writing—original draft preparation: Bo Scherer, Thomas Schroeder, Stefanie Geyh; Writing—review and editing: Bo Scherer, Laura Schmitt, Karina S. Krings, Sebastian Wesselborg, Paul Jäger, Thomas Schroeder, Stefanie Geyh; Visualization: Bo Scherer, Karina Krings, Stefanie Geyh; Supervision: Sebastian Wesselborg, Rainer Haas, Thomas Schroeder, Stefanie Geyh.; Project administration: Bo Scherer, Thomas Schroeder, Stefanie Geyh.; Funding acquisition: Sebastian Wesselborg, Thomas Schroeder. Final approval of manuscript: All authors have read and agreed to the published version of the manuscript.

Funding Open Access funding enabled and organized by Projekt DEAL. Deutsche Forschungsgemeinschaft, 417677437/GRK2578, Thomas Schroeder.

Data availability The data that support the findings of this study are available from the corresponding author upon reasonable request.

Declarations

Conflict of interest The authors declare that they have no conflict of interest. The funders had no role in the design of the study; in the collection, analyses, or interpretation of data; in the writing of the manuscript; or in the decision to publish the results.

References

Anthony BA, Link DC (2014) Regulation of hematopoietic stem cells by bone marrow stromal cells. Trends Immunol 35(1):32–37. https://doi.org/10.1016/j.it.2013.10.002

Bae YJ, Kwon YR, Kim HJ, Lee S, Kim YJ (2017) Enhanced differentiation of mesenchymal stromal cells by three-dimensional culture and azacitidine. Blood Res 52(1):18–24. https://doi.org/10.5045/br.2017.52.1.18

Bertrums EJM, Rosendahl Huber AKM, de Kanter JK et al (2022) Elevated mutational age in blood of children treated for cancer contributes to therapy-related myeloid neoplasms. Cancer Discov 12(8):1860–1872. https://doi.org/10.1158/2159-8290.CD-22-0120

Bhagat TD, Chen S, Bartenstein M et al (2017) Epigenetically aberrant stroma in MDS propagates disease via Wnt/beta-Catenin activation. Cancer Res 77(18):4846–4857. https://doi.org/10.1158/0008-5472.CAN-17-0282

Chen K, Yang Q, Zha J et al (2020) Preclinical evaluation of a regimen combining chidamide and ABT-199 in acute myeloid leukemia. Cell Death Dis 11(9):778. https://doi.org/10.1038/s41419-020-02972-2

Chen TC, Minea RO, Swenson S, Yang Z, Thein TZ, Schonthal AH (2022) NEO212, a Perillyl alcohol-temozolomide conjugate, triggers macrophage differentiation of acute myeloid leukemia cells and blocks their tumorigenicity. Cancers (Basel). https://doi.org/10.3390/cancers14246065

Crawford J, Dale DC, Kuderer NM et al (2008) Risk and timing of neutropenic events in adult cancer patients receiving chemotherapy: the results of a prospective nationwide study of oncology practice. J Natl Compr Canc Netw 6(2):109–118. https://doi.org/10.6004/jnccn.2008.0012

Delia D, Aiello A, Soligo D et al (1992) bcl-2 proto-oncogene expression in normal and neoplastic human myeloid cells. Blood 79(5):1291–1298. https://doi.org/10.1182/blood.V79.5.1291.1291

Demaria M, O'Leary MN, Chang J et al (2017) Cellular senescence promotes adverse effects of chemotherapy and cancer relapse.

Cancer Discov 7(2):165–176. https://doi.org/10.1158/2159-8290.CD-16-0241

Derissen EJ, Hillebrand MJ, Rosing H et al (2014) Quantitative determination of azacitidine triphosphate in peripheral blood mononuclear cells using liquid chromatography coupled with high-resolution mass spectrometry. J Pharm Biomed Anal 90:7–14. https://doi.org/10.1016/j.jpba.2013.11.010

Diamond B, Zicchedda B, Maclachlan K et al (2023) Tracking the evolution of therapy-related myeloid neoplasms using chemotherapy signatures. Blood 141(19):2359–2371. https://doi.org/10.1182/blood.2022018244

Fakhrabadi HG, Rabbani-Chadegani A, Ghadam P, Amiri S (2020) Protective effect of bleomycin on 5-azacitidine induced cytotoxicity and apoptosis in mice hematopoietic stem cells via Bcl-2/Bax and HMGB1 signaling pathway. Toxicol Appl Pharmacol 396:114996. https://doi.org/10.1016/j.taap.2020.114996

Friedmann HS, Kerby T, Calvert H (2000) Temozolomide and treatment of malignant glioma. Clin Cancer Res 6:2585–2597

Geyh S, Oz S, Cadeddu RP et al (2013) Insufficient stromal support in MDS results from molecular and functional deficits of mesenchymal stromal cells. Leukemia 27(9):1841–1851. https://doi.org/10.1038/leu.2013.193

Halim A, Ariyanti AD, Luo Q, Song G (2020) Recent progress in engineering mesenchymal stem cell differentiation. Stem Cell Rev Rep 16(4):661–674. https://doi.org/10.1007/s12015-020-09979-4

Hecker JS, Hartmann L, Riviere J et al (2021) CHIP and hips: clonal hematopoiesis is common in patients undergoing hip arthroplasty and is associated with autoimmune disease. Blood 138(18):1727–1732. https://doi.org/10.1182/blood.2020010163

Jager P, Geyh S, Twarock S et al (2021) Acute myeloid leukemia-induced functional inhibition of healthy CD34+ hematopoietic stem and progenitor cells. Stem Cells 39(9):1270–1284. https://doi.org/10.1002/stem.3387

Kaminskas E, Farrell AT, Wang Y-C, Sridhara R, Pazdur R (2005) FDA drug approval summary: azacitidine (5-azacytidine, VidazaTM) for injectable suspension. Oncologist 10:176–182

Kirkland JL, Tchkonia T (2020) Senolytic drugs: from discovery to translation. J Intern Med 288(5):518–536. https://doi.org/10.1111/joim.13141

Li J, Law HK, Lau YL, Chan GC (2004) Differential damage and recovery of human mesenchymal stem cells after exposure to chemotherapeutic agents. Br J Haematol 127(3):326–334. https://doi.org/10.1111/j.1365-2141.2004.05200.x

List AF, Heaton R, Glinsmann-Gibson B, Capizzi RL (1996) Amifostine protects primitive hematopoietic progenitors against chemotherapy cytotoxicity. Semin Oncol 23(4 Suppl 8):58–63

Lutzkendorf J, Wieduwild E, Nerger K et al (2017) Resistance for genotoxic damage in mesenchymal stromal cells is increased by hypoxia but not generally dependent on p53-regulated cell cycle arrest. PLoS ONE 12(1):e0169921. https://doi.org/10.1371/journal.pone.0169921

McNerney ME, Godley LA, Le Beau MM (2017) Therapy-related myeloid neoplasms: when genetics and environment collide. Nat Rev Cancer 17(9):513–527. https://doi.org/10.1038/nrc.2017.60

Meany HJ, Warren KE, Fox E, Cole DE, Aikin AA, Balis FM (2009) Pharmacokinetics of temozolomide administered in combination with O6-benzylguanine in children and adolescents with refractory solid tumors. Cancer Chemother Pharmacol 65(1):137–142. https://doi.org/10.1007/s00280-009-1015-8

Mendez-Ferrer S, Michurina TV, Ferraro F et al (2010) Mesenchymal and haematopoietic stem cells form a unique bone marrow niche. Nature 466(7308):829–834. https://doi.org/10.1038/nature09262

Miyashita T, Reed JC (1993) Bcl-2 oncoprotein blocks chemotherapy-induced apoptosis in a human leukemia cell line. Blood 81(1):151–157. https://doi.org/10.1182/blood.V81.1.151.151

Neiva K, Sun Y-X, Taichman RS (2005) The role of osteoblasts in regulating hematopoeitic stem cell activity and tumor metastasis. Braz J Med Biol Res 38:1449–1454

Nicolay NH, Ruhle A, Perez RL et al (2016) Mesenchymal stem cells exhibit resistance to topoisomerase inhibition. Cancer Lett 374(1):75–84. https://doi.org/10.1016/j.canlet.2016.02.007

Nicoletti I, Migliorati G, Pagliacci MC, Grignani F, Riccardi C (1991) A rapid and simple method for measuring thymocyte apoptosis by propidium iodide staining and flow cytometry. J Immunol Methods 139(2):271–279. https://doi.org/10.1016/0022-1759(91)90198-o

Ostermann S, Csajka C, Buclin T et al (2004) Plasma and cerebrospinal fluid population pharmacokinetics of temozolomide in malignant glioma patients. Clin Cancer Res 10(11):3728–3736. https://doi.org/10.1158/1078-0432.CCR-03-0807

Pollok KE (2003) In vivo protection of hematopoietic cells from alkylator-mediated DNA damage. Curr Hematol Rep 2(4):341–347

Qi Z, Zhang Y, Liu L, Guo X, Qin J, Cui G (2012) Mesenchymal stem cells derived from different origins have unique sensitivities to different chemotherapeutic agents. Cell Biol Int 36(9):857–862. https://doi.org/10.1042/CBI20110637

Raaijmakers MH, Mukherjee S, Guo S et al (2010) Bone progenitor dysfunction induces myelodysplasia and secondary leukaemia. Nature 464(7290):852–857. https://doi.org/10.1038/nature08851

Reese JS, Davis BM, Liu L, Gerson SL (1999) Simultaneous protection of G156A methylguanine DNA methyltransferase gene-transduced hematopoietic progenitors and sensitization of tumor cells using O6-benzylguanine and temozolomide. Clin Cancer Res 5(1):163–169

Rosca AM, Burlacu A (2011) Effect of 5-azacytidine: evidence for alteration of the multipotent ability of mesenchymal stem cells. Stem Cells Dev 20(7):1213–1221. https://doi.org/10.1089/scd.2010.0433

Ruhle A, Huber PE, Saffrich R, Lopez Perez R, Nicolay NH (2018) The current understanding of mesenchymal stem cells as potential attenuators of chemotherapy-induced toxicity. Int J Cancer 143(11):2628–2639. https://doi.org/10.1002/ijc.31619

Sawai N, Zhou S, Vanin EF, Houghton P, Brent TP, Sorrentino BP (2001) Protection and in vivo selection of hematopoietic stem cells using temozolomide, O6-benzylguanine, and an alkyltransferase-expressing retroviral vector. Mol Ther 3(1):78–87. https://doi.org/10.1006/mthe.2000.0223

Shi Y, Ye J, Yang Y et al (2021) The Basic Research of the Combinatorial Therapy of ABT-199 and Homoharringtonine on Acute Myeloid Leukemia. Front Oncol 11:692497. https://doi.org/10.3389/fonc.2021.692497

Sinkule JA (1984) Etoposide: a semisynthetic epipodophyllotoxin. Chemistry, pharmacology, pharmacokinetics, adverse effects and use as an antineoplastic agent. Pharmacotherapy 4(2):61–73. https://doi.org/10.1002/j.1875-9114.1984.tb03318.x

Souers AJ, Leverson JD, Boghaert ER et al (2013) ABT-199, a potent and selective BCL-2 inhibitor, achieves antitumor activity while sparing platelets. Nat Med 19(2):202–208. https://doi.org/10.1038/nm.3048

Stokes JE, Bobola MS, Chamberlain MC, Silber JR (2012) Low leukocyte MGMT accompanies temozolomide induced myelotoxicity in brain tumor patients. J Cancer Res Updat 1:44–48

Tchkonia T, Zhu Y, van Deursen J, Campisi J, Kirkland JL (2013) Cellular senescence and the senescent secretory phenotype: therapeutic opportunities. J Clin Invest 123(3):966–972. https://doi.org/10.1172/JCI64098

Trillo Aliaga P, Spada F, Peveri G et al (2021) Should temozolomide be used on the basis of O(6)-methylguanine DNA methyltransferase

status in patients with advanced neuroendocrine tumors? A systematic review and meta-analysis. Cancer Treat Rev 99:102261. https://doi.org/10.1016/j.ctrv.2021.102261

Warren CFA, Wong-Brown MW, Bowden NA (2019) BCL-2 family isoforms in apoptosis and cancer. Cell Death Dis 10(3):177. https://doi.org/10.1038/s41419-019-1407-6

Weiss LM, Warnke RA, Sklar J, Cleary ML (1987) Molecular analysis of the t(14;18) chromosomal translocation in malignant lymphomas. N Engl J Med 317(19):1185–1189. https://doi.org/10.1056/NEJM198711053171904

Wenk C, Garz AK, Grath S et al (2018) Direct modulation of the bone marrow mesenchymal stromal cell compartment by azacitidine enhances healthy hematopoiesis. Blood Adv 2(23):3447–3461. https://doi.org/10.1182/bloodadvances.2018022053

Winter S, Gotze KS, Hecker JS et al (2024) Clonal hematopoiesis and its impact on the aging osteo-hematopoietic niche. Leukemia 38(5):936–946. https://doi.org/10.1038/s41375-024-02226-6

Yan X, Ehnert S, Culmes M et al (2014) 5-azacytidine improves the osteogenic differentiation potential of aged human adipose-derived mesenchymal stem cells by DNA demethylation. PLoS ONE 9(6):e90846. https://doi.org/10.1371/journal.pone.0090846

Zhou Y, Xin X, Wang L et al (2021) Senolytics improve bone forming potential of bone marrow mesenchymal stem cells from aged mice. NPJ Regen Med 6(1):34. https://doi.org/10.1038/s41536-021-00145-z

Marrari A, Hornick JL, Ramaiya NH, Manola A, Wagner AJ (2011) Expression of MGMT and response to treatment with temozolomide in patients with leiomyosarcoma. Paper presented at the ASCO, Atlanta, Georgia, June 2–6, United States, 2011

Scheffold A, Jebaraj BMC, Stilgenbauer S (2018) Venetoclax: targeting BCL2 in hematological cancers. recent results in cancer research Fortschritte der Krebsforschung Progres dans les recherches sur le cancer 212:215-242 https://doi.org/10.1007/978-3-319-91439-8_11

3. Discussion

Hematological neoplasms represent a significant global health burden with increasing incidences worldwide driven by increasing age (Zhang N et. al., 2023). A common hallmark of these diverse neoplasms is hematopoietic insufficiency, irrespective of their *de novo* or therapy-related etiology (Hoffbrand & Moss, 2015). The proportion of t-MN diagnoses among AML diagnoses makes up 10-20 %, with an upward trend due to the increase in cancer survivors (Leone et. al., 2007; Fianchi et. al., 2013; Zhang N et. al., 2023). This demonstrates the advancements in oncology on the one hand, but challenges like dose-limiting myelosuppression and increased risk to develop t-MN persist (Allan & Travis, 2005; Barreto et. al., 2014).

Clinically, t-MN patients present with more severe cytopenias and chromosomal abnormalities than equivalent *de novo* MN, and are usually less responsive to conventional anticancer therapy (Godley & Larson, 2008; Larson, 2009). For this reason, t-MN patients confer a worse clinical prognosis and overall outcome (Wang et. al., 2006; Larson, 2009). Increasing evidence, including the findings from manuscripts 2.1 and 2.2, underscore the relevance of the BM stroma in disease progression across both myeloid and lymphoid neoplasms (Geyh et. al., 2013; Geyh et. al., 2016; von der Heide et. al., 2016; Bhagat et. al., 2017; Wu Y et. al., 2017). Based on this, the main focus of this thesis is to expand this knowledge to a potential role of MSC in secondary hematological neoplasms following anticancer therapies. Further, the hematotoxic effects of oncological therapies were investigated in the context of therapy-related hematopoietic insufficiency.

We showed that functional stromal alterations were not only overlapping in primary myeloid and lymphoid neoplasms (manuscript 2.1 and 2.2), but also found in t-MN MSC (manuscript 2.3) with even more pronounced deficits regarding differentiation capacity and hematopoiesis support. On a molecular level, all hematological neoplasms displayed dysregulation of pleiotropic signaling pathways TGFB and WNT. Beyond that, t-MN MSC additionally conferred a unique immunomodulatory signature, possibly representing a therapy-related origin that could be utilized for novel therapeutic strategies.

Insights into the direct stromal damage induction by oncological therapies are addressed in manuscript 2.4. Healthy MSC were exposed to pharmacological doses of four antineoplastic agents that present with hematotoxic effects in the clinic. Alkylating agent TMZ and BCL2 inhibitor VEN spared MSC and rather affected hematopoietic cells. However, phenotypical

and functional alterations were induced in healthy MSC after exposure to ETO or AZA and impacted their hematopoietic support function. These findings demonstrate the potential of certain therapeutic agents to damage MSC and contribute to therapy-related hematotoxicity.

Together, these studies provide a comprehensive characterization of the molecular and functional alterations in MSC following antineoplastic therapy and expand our knowledge of MSC as a contributor to therapy-related adverse side effects besides *de novo* pathogenesis of hematological neoplasms.

3.1. Stromal Alterations in Therapy-related Myeloid Neoplasms Resemble de novo Hematological Neoplasms

Primary (*de novo*) and secondary hematological neoplasms differ in their etiologies. *De novo* neoplasms develop as a consequence of aging, genetic predisposition, and/or exposure to environmental- or lifestyle toxins, such as tobacco smoke. In contrast, therapy-related neoplasms arise from the preceding exposure to oncological therapies and are associated with higher frequencies of cytogenetic abnormalities and worse overall survival compared to equivalent MN patients (Godley & Larson, 2008).

Our comprehensive characterization of t-MN-derived MSC revealed phenotypical and functional alterations of t-MN MSC compared to healthy MSC (manuscript 2.3). Remarkably, these alterations were similar to previous findings of BM-derived MSC from patients with *de novo* hematological neoplasms (manuscript 2.1 and 2.2) in terms of morphology, growth characteristics, cellular senescence, and differentiation capacity. This suggests a common dysregulation of underlying mechanisms in MSC from patients with differential hematological neoplasms and was investigated using RNA sequencing. Indeed, all MSC from *de novo* hematological neoplasms, as well as therapy-related neoplasms displayed a common dysregulation of pleiotropic pathways such as Notch, WNT, and BMP/TGFB signaling, confirming and expanding the previous data by others (Kitagawa et. al., 1997; Schepers et. al., 2013; Bhagat et. al., 2017). These pathways are implicated in the regulation and differentiation of MSC and other cell types (Jian et. al., 2006; Grafe et. al., 2018) and likely reflect the *in vitro* observed deficits. Constitutive WNT activation and aberrant Notch signaling have been already reported in the literature as potential mediators of stromal alterations (Kode et. al., 2014; Bowers et. al., 2015). However, we found that the gene *TGFB1* was consistently upregulated across all sequenced entities in our cohorts, including t-MN MSC (Appendix Figure 1). In addition, Ingenuity Pathway Analysis (IPA) and Gene Set Enrichment Analysis (GSEA) confirmed TGFB signaling as a common potential mediator.

To confirm a functional relevance in patient-derived MSC, the small molecule inhibitor SD208 was used to block the TGFB cascade and restored insufficient osteogenesis in MSC derived from myeloid and lymphoid neoplasms. It has to be noted that this was not experimented in t-MN MSC and is therefore limited to *de novo* hematological neoplasms. Still, the indication is given by the similar regulation of *TGFB1* on mRNA basis and offers an interesting possibility for future investigations. Nevertheless, the common molecular and functional relevance of TGFB1 in aberrant MSC suggests TGFB signaling as a potential central mediator of stromal alterations. Utilizing the TGFB pathway clinically remains challenging due to the diverse functions of TGFB in tumor suppression, tumor promotion, or chemotherapy resistance (Colak & Ten Dijke, 2017; Liu et. al., 2021). However, targeting downstream pathways of TGFB offers intriguing targets, as myeloid and lymphoid neoplasms can be differentiated by dysregulation of canonical and non-canonical TGFB signaling. Indeed, the inhibition of canonical SMAD2/3 signaling by novel agent luspatercept demonstrated effectiveness by enhancing erythropoiesis in MDS patients (Cappellini & Taher, 2021). Expanding on these studies and the effects on MSC could further contribute to minimizing the adverse side effects of conventional therapies.

Concluding that stromal alterations are likely regulated by TGFB raises the question of the origin of dysregulations that mediate stromal alterations and ultimately lead to hematopoietic insufficiency. The findings of manuscripts 2.1 and 2.2, together with those of other groups (Vallet et. al., 2011; Schepers et. al., 2013; Arranz et. al., 2014; Huan et. al., 2015; Yang et. al., 2015; Cui et. al., 2019), suggest the instructive role of malignant cell signaling to transform BM-derived MSC to build a leukemia-endorsing niche. While this was not tested in t-MN MSC, a similar mechanism can be assumed due to the presence of t-MN blasts that seem to be similar to MN blasts (Godley & Larson, 2008). In addition to malignant cell signaling, the BM stroma of t-MN patients was exposed to oncological therapies. Whether additional aberrations are induced by this exposure was suggested by the identification of a unique molecular signature in t-MN MSC, beyond the similar regulation of TGFB, WNT, and Notch signaling.

3.2. Unique Alterations in Bone Marrow-derived MSC from Patients with Therapy-related Myeloid Neoplasms

Ongoing advancements in the understanding of pathological situations have enabled more specific treatment strategies tailored to the cancer's genetic and molecular features, as well as patient-specific characteristics, such as age, disease progression, and comorbidities (Koenig & Borate, 2022; Totiger et. al., 2023). However, many oncological therapies still rely on the application of genotoxic agents, accepting the undesired targeting of healthy surrounding tissue (Moon et. al., 2023; National Cancer Institute, 2024) and an increased relative risk of patients to develop a therapy-related neoplasm later in life (Allan & Travis, 2005). The role of MSC in the pathogenesis and hematopoietic insufficiency of t-MN patients was investigated by focusing on the unique alterations of t-MN MSC in comparison to *de novo* neoplasms.

Although MSC from *de novo* and therapy-related neoplasms show clear similarities, t-MN MSC exhibited more profound impairments regarding differentiation capacity and hematopoietic support in direct comparison to equivalent MN MSC. This possibly reflects the more severe clinical parameters of t-MN patients and could result from the additional induced stromal damage by preceding oncological therapy besides malignant cell signaling. Indeed, a unique immunomodulatory signature was identified in t-MN MSC. This transcriptomic signature involved the dysregulation of immune checkpoint genes, including *CD274* (also known as Programmed Cell Death 1 Ligand 1, PD-L1), *CD47* (leucocyte surface antigen, also known as integrin-associated protein), and immunomodulatory *IL11.* Additionally, it encompassed numerous genes from the TNF signaling family, which were not dysregulated in respective MN MSC. Particularly, CD274 and CD47 are involved in the inactivation of cytotoxic T-cells and macrophages respectively, rendering them unable to eliminate malignant transformed cells (Sharpe, 2017; Eladl et. al., 2020). Dysregulation of this tumor-suppressive immune function in MSC indicates that malignant cell evasion from the immune system might be actively supported by t-MN MSC. To investigate the functional relevance of this signature in t-MN MSC, the uniquely expressed immune checkpoint genes could be manipulated to derive a functional dependency between these genes or pathways and the t-MN phenotype. If the t-MN phenotype is correlated with dysregulation of immunomodulatory mechanisms, therapeutic agents targeting these mechanisms might enhance current therapy strategies for the poor outcome group of t-MN.

The targeting of immune checkpoints is a current subject of clinical research in hematological neoplasms and exhibits potential. However, current studies are primarily focused on the treatment of *de novo* malignancies (Salik et. al., 2020). Research on t-MN remains scarce, not at least because of its relatively low incidence, compared to other hematological neoplasms (Fianchi et. al., 2013). The presented findings here potentially offer new approaches for otherwise unsuccessful agents. For example, the inhibition of CD47 was already explored in clinical trials for MDS treatment (Koenig & Borate, 2022) but was discontinued prematurely due to lacking efficiency. In view of the apparent dysregulation of CD47 in stromal cells of t-MN patients, CD47 inhibition might come into a new light with potentially increased efficacy because of the additional targeting of the stroma. This however requires extensive research on both, the efficacy against t-MN blasts, as well as the stroma.

3.3. Substance-specific Effects on Bone Marrow-derived MSC Contribute to Therapy-related Hematotoxicity

In view of the observed distinct stromal alterations in t-MN-derived MSC, it would be interesting to discern whether these effects were distinctly induced by oncological therapies, or are a result of the aberrant signaling of t-MN cancer cells in the BM. Whether and how different antineoplastic agents might impact the molecular or functional characteristics of MSC, as well as their potential contribution to therapy-related hematotoxicity was investigated comprehensively in manuscript 2.4.

The presented results indicated substance-specific sensitivity of MSC towards antineoplastic agents. The potential damage to healthy MSC during therapy was especially demonstrated by ETO, which as a single agent treatment induced persistent cellular senescence in healthy MSC, accompanied by the inhibition of their differentiation capacity and insufficient hematopoietic support. This implicates MSC as a contributor to therapy-related myelosuppression in this case. Similar findings were found in preliminary data of MSC exposure to ionizing radiation (IR) (Appendix Figure 2), highlighting DNA double-strand breaks as the driving force of such alterations. Also, other groups reported the induction of cellular changes like cellular senescence by ETO and other DNA-damaging agents, while conferring resistance towards apoptosis (Qi et. al., 2012; Nicolay et. al., 2016; Lutzkendorf et. al., 2017). The substantial induction of cellular senescence, and possibly the senescence-associated secretory phenotype (SASP) in stromal cells thereby contributes to a pro-inflammatory environment that drives disease progression (Zhou P et. al., 2021).

These findings coincide with the dysregulated inflammatory processes in stromal cells from t-MN patients and suggests an involvement of ETO-induced stromal damage in the immunomodulatory transformation of the BM in t-MN patients. Indeed, ETO is one of the substances directly correlated to the development of t-MN by inducing DNA double-strand breaks and allowing chromosomal translocation, specifically in the *MLL* gene of HSPC (Allan & Travis, 2005; Libura et. al., 2005). Whether ETO induces genetic alterations also in MSC, in addition to cellular changes remains unclear but offers a possibility for further exploration to establish a connection between t-MN stromal alterations and ETO exposure.

Another interesting substance-specific effect on MSC was found after AZA exposure. AZA is so far not implicated as a risk factor for t-MN development. However, the hypomethylating agent was reported to be associated with therapy-related myelosuppression (U.S. Food and Drug Administration, 2004; Kaminskas et. al., 2005). *In vitro* reports demonstrated that the epigenetic mode of action of AZA enhanced the differentiation capacity and hematopoietic support capacity of MDS-derived stromal cells (Bhagat et. al., 2017; Xu et. al., 2023), indicating a different origin of hematotoxic side effects besides MSC. To explore this in our model, the direct effects of AZA were examined on healthy MSC (manuscript 2.4), as well as MN- and t-MN-derived MSC (Appendix Figure 3, preliminary data). Interestingly, pharmacological doses of AZA resulted in a shift of differentiation potential in healthy MSC, inhibiting osteogenic potential, while enhancing chondrogenic differentiation. A shift in BM components potentially affects the structural integrity of the BM, as well as the cell type-specific signaling within the micro milieu. The introduction of changes in the tightly regulated equilibrium indicates that AZA exposure could contribute to therapy-related myelosuppression by affecting the hematopoietic support function of the BM. Contrary to healthy MSC, the characteristics of patient-derived MSC were not considerably affected by AZA exposure (Appendix Figure 3), which might be partially contributed to the lower proliferative activity of patient-derived MSC, or the dose selection. Using a lower dose (0.5 µM AZA for five days), Bhagat *et. al.* (2017) reported enhanced osteogenic potential and hematopoietic support capacity of MDS-derived MSC. Our analyses confirmed the enhanced hematopoietic support of MN MSC after exposure, but no effects on their differentiation capacity. This discrepancy demonstrates the importance of exploring different treatment schemes to fully elucidate the effect of AZA on MSC and emphasizes the need for further investigations, comparing the drug response between healthy, *de novo* MN and t-MN MSC.

Interestingly, the induced deficits in healthy MSC by AZA or ETO were similar to the aberrations found in t-MN MSC regarding prolonged growth, increased cellular senescence, and decreased osteogenic capacity. It cannot be definitively established that anticancer therapy alone causes the observed stromal alterations. However, it is noteworthy that different stimuli, including antineoplastic exposure and the interaction with malignant cells, appear to affect similar processes in MSC that impair the stromal support for HSPC. Answering the question of the exact origin of stromal alterations in t-MN MSC remains difficult because both factors, antineoplastic exposure and/or malignant cell interaction might have led to the observed aberrations. A better understanding of the underlying mechanisms of MSC alterations specifically induced by anticancer therapy could result from transcriptome analysis of healthy MSC exposed to anticancer therapies and comparing them to the transcriptome of t-MN MSC in the future.

Contrary to AZA and ETO, MSC proved highly resilient against the other antineoplastic agents, namely the BCL2 inhibitor VEN and alkylating agent TMZ. At the same time, both agents inhibited the growth of hematological cancer cell lines and primary healthy HSPC. This indicates that the therapy-related hematotoxicity in these cases is a result of hematopoietic cell damage and negates the involvement of MSC in therapy-related myelosuppression. In the case of TMZ, the activity of MGMT in MSC poses a possible explanation for the cell-specific resistance. This study did not comprise methylation or activity analyses and there is no clear information on this in the literature so far. Therefore, this reasoning can only be hypothesized. Interestingly, MSC were not sensitized towards the alkylating agent by inhibiting MGMT, in contrast to other resistant cell lines (Marrari et. al., 2011; Chen TC et. al., 2022; manuscript 2.4). To elucidate the mechanism of MSC resistance against TMZ, more studies regarding the DNA repair machinery and long-term effects should be conducted.

In the case of VEN, the resistance of MSC is most likely attributed to the relatively low abundance of target protein BCL2 and alternative protein MCL1 in MSC, which determine the sensitivity of cells towards VEN (Warren et. al., 2019). This also explains the sensitivity of lymphoma cell lines and intermediate sensitivity of healthy HSPC as discussed in manuscript 2.4. Clinically, VEN is usually applied in a combination treatment. In the standard care treatment for AML patients, AZA and VEN presented with synergistic combination effects (Derissen et. al., 2013; DiNardo et. al., 2019). While this led to an increase in the response rates, it also presented an increased risk for acute therapy-related myelosuppression (Bogenberger et. al., 2015; DiNardo et. al., 2019). Synergistic effects in

this case are likely caused by the MCL1 inhibition through AZA that potentiates the efficacy of VEN (Tsao et. al., 2012). Further explanation is given in manuscript 2.4, which showed that the effects of AZA on MSC might contribute to myelosuppressive effects. In combination with the targeting of hematopoietic cells by VEN, this explains the increased risk for hematotoxicity in the combination treatment.

Overall, manuscript 2.4 gives an overview of the substance-specific effects on healthy MSC. These were partly overlapping with observations made in t-MN MSC and demonstrated the potential of direct therapy-induced stromal damage contributing to therapy-related hematotoxicity. By taking the preservation of stromal functions in the BM into account, myelosuppressive effects during oncological therapy could be minimized in the future.

3.4. Limitations of in vitro Cultured MSC as a Model to Study the Bone Marrow Microenvironment

MSC as a model cannot recapitulate the whole BM niche with its complex cellular and non-cellular interactions. This is one reason why the stromal alterations induced by antineoplastic agents in healthy MSC cannot be directly translated to the observed alterations in t-MN MSC of manuscript 2.3, although substantial overlaps were noted. T-MN MSC were exposed to both, antineoplastic agents during primary treatment, as well as the aberrant signaling of t-MN blasts during disease onset and only afterward transferred into an *in vitro* setting. On the other hand, healthy MSC were directly exposed to the antineoplastic agents in cell culture and did not take the interaction with surrounding niche components, including malignant cells into account.

Additionally, conventional therapy strategies almost always feature the application of drug combinations in order to maximize therapeutic efficacy. The effects of single substances can be enhanced by additive or synergistic effects, or be weakened by antagonistic effects when combined (Humphrey et. al., 2011; Foucquier & Guedj, 2015). Most of the patients of manuscript 2.3 were treated with more than four agents at the same time, making the observed stromal alterations a result of combination effects, rather than deriving from a single substance. In addition to that, the patient histories in terms of primary cancer and treatment regimen were vastly diverse. Therefore, we could not derive a relation between specific drug combinations and MSC effects, as visualized in Appendix Figure 4. To conclude how combinations of anticancer drugs specifically affect surrounding healthy tissue, a larger cohort with uniform patient histories and the consideration of malignant cell signaling should be tested. Additionally, comparative transcriptome analyses of t-MN MSC

and healthy MSC exposed to one or more substances used in the combination therapy of the respective t-MN patients could be performed. This might help to identify underlying therapy-induced mechanisms in the stromal alterations of MSC. Another possibility to study combination effects on the BM stroma offer animal models. *In vivo* models take the interplay of cells within a tissue and circulating factors into account. Additionally, the metabolism of substances is considered and combination therapy can be more easily recreated, although the human relevance might be a shortcoming of this approach (Chen et. al., 2012; Balderman et. al., 2016). In the end, the integration of both *in vivo* and *in vitro* models is required to draw clearer conclusions before clinical explorations can be initiated.

When studying the *in vitro* BM stroma of patients conferring a hematological disease, healthy samples are analyzed in parallel as biological control. To represent a suitable control, the healthy samples must be sex- and age-matched. Control matching was performed in the cohort of each manuscript individually. Merely in the case of manuscript 2.2, healthy controls were older by over ten years in median compared to the patient-derived samples. Despite the age difference, patient-derived MSC showed striking differences in phenotype, functionality, and transcriptome in each stage of disease progression from MGUS to SMM and MM when compared to healthy samples. This suggests the overall fitness of the healthy cohort in this case and their suitability for the study.

To warrant age matching between healthy controls and patients with age-related diseases, the applicability of MSC from donors undergoing hip surgery is considered to be suitable due to the similar age. Although these donors did not exhibit any sign of an underlying hematological disorder, age-related and asymptomatic clonal hematopoiesis in the donor cohort may be present in some healthy controls and needs to be considered when interpreting these results (Genovese et. al., 2014; Jaiswal et. al., 2014; Hecker et. al., 2021; Hartmann et. al., 2022; Winter et. al., 2024). While this condition was not tested in our control groups, exclusively healthy controls that fulfilled the minimal criteria for MSC definition were used (Dominici et. al., 2006). These control MSC were characterized by a healthy phenotype and proliferative capacity, low cellular senescence (below 25 %), trilineage differentiation capacity, and hematopoietic support *in vitro.* The same criteria were applied for the antineoplastic exposure of healthy MSC in manuscript 2.4. Still, further investigations regarding the influence of clonal hematopoiesis on MSC characteristics are of high interest for future studies to enhance the informative value of this *in vitro* model. Until now, BM-derived MSC represent a well-established and suitable model with human relevance that

contributes to the advancing knowledge about the relevance of the BM microenvironment in normal hematopoiesis.

3.5. Conclusion and Perspective

The collective findings of the four presented manuscripts emphasize the role of BM stroma in the pathogenesis of hematological neoplasms and in mediating the hematotoxic effects of oncological therapy. A simplified, visualized summary of the findings presented here is shown in Figure 4. Shortly, MSC from *de novo* (manuscripts 2.1 and 2.2) as well as therapy-related hematological neoplasms (manuscript 2.3) display resembling phenotypical and functional alterations, which are mainly mediated by TGFB and WNT signaling. On top of that, t-MN-derived MSC confer a unique molecular immunomodulatory signature, possibly demonstrating anticancer therapy-induced stromal alterations. Similar functional alterations as observed in patient-derived MSC were induced in healthy MSC by ETO and AZA (manuscript 2.4), and possibly contribute to therapy-related side effects. Ultimately, the functional and molecular stromal alterations induced by malignant cell signaling and/or antineoplastic agents negatively impact the hematopoietic support function of MSC and contribute to clinically observed hematopoietic insufficiency. Understanding the overlapping and distinct mechanisms that lead to this inadequate hematopoietic support can pave the way for more targeted therapies that preserve normal BM function during oncological therapy.

To achieve this goal, the application of appropriate and standardized models for investigating the BM microenvironment is helpful for data comparability across research groups. Still, animal models remain critical, especially when assessing the therapeutic effects of drug combinations, while single-cell *in vitro* models from human samples have proven adequate for human relevance. For example, the identification of mediating signaling pathways might offer novel therapeutic ideas to target MSC and preserve BM function to mitigate disease progression.

The insights of this thesis further emphasize the necessity of both, the creation of targeted and efficient therapies as well as an ongoing investigation into the complex interactions within the BM microenvironment. By incorporating these discoveries into clinical practice in the future, the management of hematological neoplasms and patient outcomes can be enhanced, and therapy-related complications can be minimized.

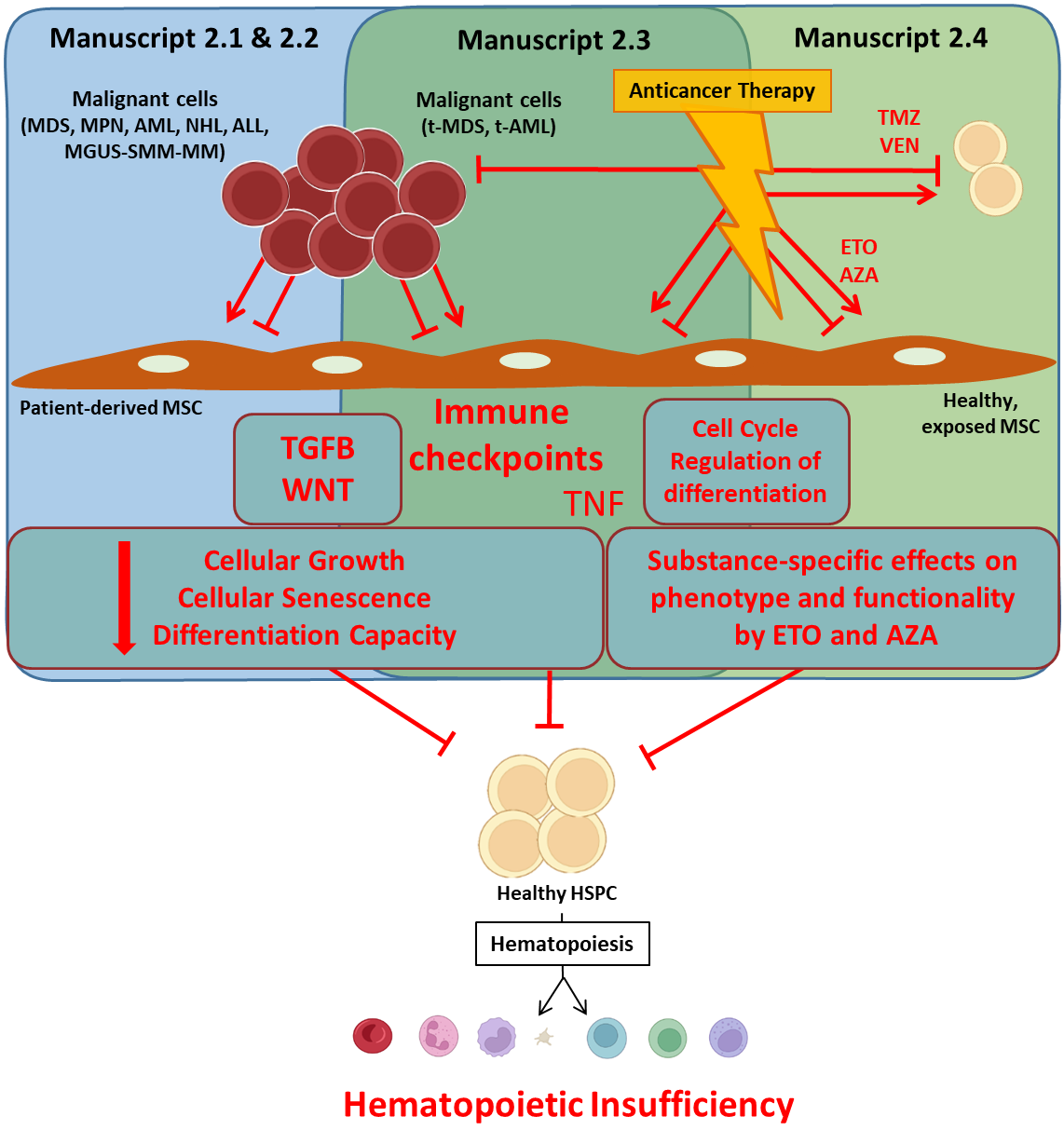

Figure 4. Simplified summary of overall findings in the discussed manuscripts. The first two manuscripts 2.1 and 2.2 demonstrate significant overlapping alteration in MSC from myeloid and lymphoid neoplasms regarding growth and differentiation capacity with prominent molecular dysregulation of TGFB and WNT signaling. Alterations are induced by malignant cell signaling and result in insufficient hematopoietic support. Manuscript 2.3 finds overlapping MSC alteration of growth and differentiation in t-MN and MN patients, highlighting similar underlying mechanisms involving TGFB and WNT signaling. Additionally, a unique dysregulation of immune checkpoint molecules and TNF signaling was determined in t-MN MSC, suggesting distinct alterations induced by anticancer therapy. The last manuscript 2.4 shows direct stromal damage by ETO and AZA in healthy MSC, affecting cellular growth and differentiation as shown functionally and molecularly, and contributing to hematotoxicity. Functional and molecular alterations were partly overlapping with t-MN-derived MSC. Malignant cells and healthy HSPC are also targeted by distinct substances (TMZ and VEN). Overall, stromal alteration in different hematological neoplasms and as a consequence of cytotoxic exposure are partially overlapping and contribute to hematopoietic insufficiency. The schematic was designed by Biorender.com and MS PowerPoint 2013.

4. Bibliography

Aiuti A, Webb IJ, Bleul C, Springer T, Gutierrez-Ramos JC (1997). The Chemokine SDF-1 Is a Chemoattractant for Human CD34 + Hematopoietic Progenitor Cells and Provides a New Mechanism to Explain the Mobilization of CD34+ Progenitors to Peripheral Blood. *Journal of Experimental Medicine,* **185**, 111-120

Akashi K, Traver D, Miyamoto T, Weissman IL (2000). A clonogenic commonmyeloid progenitor that gives rise to all myeloid lineages. *Nature,* **404**, 193-197

Alaggio R, Amador C, Anagnostopoulos I, Attygalle AD, Araujo IBO, Berti E, Bhagat G, Borges AM, Boyer D, Calaminici M, Chadburn A, Chan JKC, Cheuk W, Chng WJ, Choi JK, Chuang SS, Coupland SE, Czader M, Dave SS, de Jong D, Du MQ, Elenitoba-Johnson KS, Ferry J, Geyer J, Gratzinger D, Guitart J, Gujral S, Harris M, Harrison CJ, Hartmann S, Hochhaus A, Jansen PM, Karube K, Kempf W, Khoury J, Kimura H, Klapper W, Kovach AE, Kumar S, Lazar AJ, Lazzi S, Leoncini L, Leung N, Leventaki V, Li XQ, Lim MS, Liu WP, Louissaint A, Jr., Marcogliese A, Medeiros LJ, Michal M, Miranda RN, Mitteldorf C, Montes-Moreno S, Morice W, Nardi V, Naresh KN, Natkunam Y, Ng SB, Oschlies I, Ott G, Parrens M, Pulitzer M, Rajkumar SV, Rawstron AC, Rech K, Rosenwald A, Said J, Sarkozy C, Sayed S, Saygin C, Schuh A, Sewell W, Siebert R, Sohani AR, Tooze R, Traverse-Glehen A, Vega F, Vergier B, Wechalekar AD, Wood B, Xerri L, Xiao W (2022). The 5th edition of the World Health Organization Classification of Haematolymphoid Tumours: Lymphoid Neoplasms. *Leukemia,* **36**, 1720-1748

Allan JM, Travis LB (2005). Mechanisms of therapy-related carcinogenesis. *Nature Reviews: Cancer,* **5**, 943-955

Altinoz MA, Elmaci I, Bolukbasi FH, Ekmekci CG, Yenmis G, Sari R, Sav A (2017). MGMT gene variants, temozolomide myelotoxicity and glioma risk. A concise literature survey including an illustrative case. *Journal of Chemotherapy,* **29**, 238-244

Ankrum JA, Ong JF, Karp JM (2014). Mesenchymal stem cells: immune evasive, not immune privileged. *Nature Biotechnology,* **32**, 252-260

Anthony BA, Link DC (2014). Regulation of hematopoietic stem cells by bone marrow stromal cells. *Trends in Immunology,* **35**, 32-37

Aplan P (2006). Chromosomal translocations involving the MLL gene: molecular mechanisms. *DNA Repair,* **5**, 1265-1272

Arai F, Hirao A, Ohmura M, Sato H, Matsuoka S, Takubo K, Ito K, Koh GY, Suda T (2004). Tie2/angiopoietin-1 signaling regulates hematopoietic stem cell quiescence in the bone marrow niche. *Cell,* **118**, 149-161

Arber DA, Orazi A, Hasserjian R, Thiele J, Borowitz MJ, Le Beau MM, Bloomfield CD, Cazzola M, Vardiman JW (2016). The 2016 revision to the World Health Organization classification of myeloid neoplasms and acute leukemia. *Blood,* **127**, 2391-2405

Armstrong TS, Cao Y, Scheurer ME, Vera-Bolanos E, Manning R, Okcu MF, Bondy M, Zhou R, Gilbert MR (2009). Risk analysis of severe myelotoxicity with temozolomide: the effects of clinical and genetic factors. *Neuro-Oncology,* **11**, 825-832

Arranz L, Sanchez-Aguilera A, Martin-Perez D, Isern J, Langa X, Tzankov A, Lundberg P, Muntion S, Tzeng YS, Lai DM, Schwaller J, Skoda RC, Mendez-Ferrer S (2014). Neuropathy of haematopoietic stem cell niche is essential for myeloproliferative neoplasms. *Nature,* **512**, 78-81

Asada N (2018). Regulation of Malignant Hematopoiesis by Bone Marrow Microenvironment. *Frontiers in Oncology,* **8**, 119

Aust G (2017). Blut und lymphatische Organe – Grundlagen. In: *Duale Reihe Anatomie (Editor:* Georg Thieme Verlag, Deutschland, ISBN: 9783132417526, pages 165-192

Baccin C, Al-Sabah J, Velten L, Helbling PM, Grunschlager F, Hernandez-Malmierca P, Nombela-Arrieta C, Steinmetz LM, Trumpp A, Haas S (2020). Combined single-cell and spatial transcriptomics reveal the molecular, cellular and spatial bone marrow niche organization. *Nature Cell Biology,* **22**, 38-48

Bae Y-J, Kwon Y-R, Kim HJ, Lee S, Kim Y-J (2017). Enhanced differentiation of mesenchymal stromal cells by three-dimensional culture and azacitidine. *Blood Research,* **52**, 18

Balderman SR, Li AJ, Hoffman CM, Frisch BJ, Goodman AN, LaMere MW, Georger MA, Evans AG, Liesveld JL, Becker MW, Calvi LM (2016). Targeting of the bone marrow microenvironment improves outcome in a murine model of myelodysplastic syndrome. *Blood,* **127**, 616-625

Barreto JN, McCullough KB, Ice LI, Smith JA (2014). Antineoplastic Agents and the Associated Myelosuppressive Effects: A Review. *Journal of Pharmacy Practice,* **27**, 440-446

Barwick BG, Gupta VA, Vertino PM, Boise LH (2019). Cell of Origin and Genetic Alterations in the Pathogenesis of Multiple Myeloma. *Frontiers in Immunology,* **10**, 1121

Bhagat TD, Chen S, Bartenstein M, Barlowe AT, Von Ahrens D, Choudhary GS, Tivnan P, Amin E, Marcondes AM, Sanders MA, Hoogenboezem RM, Kambhampati S, Ramachandra N, Mantzaris I, Sukrithan V, Laurence R, Lopez R, Bhagat P, Giricz O, Sohal D, Wickrema A, Yeung C, Gritsman K, Aplan P, Hochedlinger K, Yu Y, Pradhan K, Zhang J, Greally JM, Mukherjee S, Pellagatti A, Boultwood J, Will B, Steidl U, Raaijmakers MHGP, Deeg HJ, Kharas MG, Verma A (2017). Epigenetically Aberrant Stroma in MDS Propagates Disease via Wnt/β-Catenin Activation. *Cancer Research,* **77**, 4846-4857

Bieback K, Kern S, Klüter H, Eichler H (2004). Critical parameters for the isolation of mesenchymal stem cells from umbilical cord blood. *Stem Cells,* **22**, 625-634

Blank U, Karlsson G, Karlsson S (2008). Signaling pathways governing stem cell fate. *Blood,* **11**, 492-503

Blum S, Tsilimidos G, Bresser H, Lubbert M (2023). Role of Bcl-2 inhibition in myelodysplastic syndromes. *International Journal of Cancer,* **152**, 1526-1535

Bodo M, Baroni T, Tabilio A (2009). Haematopoietic and stromal stem cell regulation by extracellular matrix components and growth factors *Journal of Stem Cells,* **4**, 57-69

Bogenberger JM, Delman D, Hansen N, Valdez R, Fauble V, Mesa RA, Tibes R (2015). Ex vivo activity of BCL-2 family inhibitors ABT-199 and ABT-737 combined with 5-azacytidine in myeloid malignancies. *Leukemia & Lymphoma,* **56**, 226-229

Bogun L, Koch A, Scherer B, Fenk R, Maus U, Bormann F, Kohrer K, Petzsch P, Wachtmeister T, Zukovs R, Dietrich S, Haas R, Schroeder T, Jager P, Geyh S (2024a). Stromal alterations in patients with monoclonal gammopathy of undetermined significance, smoldering myeloma, and multiple myeloma. *Blood Advances,* **8**, 2575-2588

Bogun L, Koch A, Scherer B, Germing U, Fenk R, Maus U, Bormann F, Kohrer K, Petzsch P, Wachtmeister T, Kobbe G, Dietrich S, Haas R, Schroeder T, Geyh S, Jager P (2024b). Overlapping Stromal Alterations in Myeloid and Lymphoid Neoplasms. *Cancers,* **16**, 2071

Bowers M, Zhang B, Ho Y, Agarwal P, Chen CC, Bhatia R (2015). Osteoblast ablation reduces normal long-term hematopoietic stem cell self-renewal but accelerates leukemia development. *Blood,* **125**, 2678-2688

Boyd AL, Campbell CJ, Hopkins CI, Fiebig-Comyn A, Russell J, Ulemek J, Foley R, Leber B, Xenocostas A, Collins TJ, Bhatia M (2014). Niche displacement of human leukemic stem cells uniquely allows their competitive replacement with healthy HSPCs. *Journal of Experimental Medicine,* **211**, 1925-1935

Bradford GB, Williams B, Rossi R, Bertoncello I (1997). Quiescence, cycling, and turnover in the primitive hematopoietic stem cell compartment. *Experimental Hematology,* **25**, 445-453

Butler JM, Nolan DJ, Vertes EL, Varnum-Finney B, Kobayashi H, Hooper AT, Seandel M, Shido K, White IA, Kobayashi M, Witte L, May C, Shawber C, Kimura Y, Kitajewski J, Rosenwaks Z, Bernstein ID, Rafii S (2010). Endothelial cells are essential for the self-renewal and repopulation of Notch-dependent hematopoietic stem cells. *Cell Stem Cell,* **6**, 251-264

Calvi LM, Adams GB, Welbrecht KW, Weber JM, Olson DP, Knight MC, Martin RP, Schipani E, Divieti P, Bringhurst FR, Milner LA, Kronenberg HM, Scadden DT (2003). Osteoblastic cells regulate the haematopoietic stem cell niche. *Nature,* **425**, 836-841

Campagnoli C, Roberts IAG, Kumar S, Bennett PR, Bellantuono I, Fisk NM (2001). Identification of mesenchymal stem/progenitor cells in human first-trimester fetal blood liver and bone marrow. *Blood,* **98**, 2396-2402

Caplan AI (1991). Mesenchymal stem cells. *Journal of Orthopaedic Research,* **9**, 641-650

Cappellini MD, Taher AT (2021). The use of luspatercept for thalassemia in adults. *Blood Advances,* **5**, 326-333

Casanova-Acebes M, Pitaval C, Weiss LA, Nombela-Arrieta C, Chevre R, N AG, Kunisaki Y, Zhang D, van Rooijen N, Silberstein LE, Weber C, Nagasawa T, Frenette PS, Castrillo A, Hidalgo A (2013). Rhythmic modulation of the hematopoietic niche through neutrophil clearance. *Cell,* **153**, 1025-1035

Celebi B, Pineault N, Mantovani D (2012). The Role of Collagen Type I on Hematopoietic and Mesenchymal Stem Cells Expansion and Differentiation. *Advances in Materials Research,* **402**, 111-116

Cesarman E (2014). Gammaherpesviruses and lymphoproliferative disorders. *Annual Review of Pathology,* **9**, 349-372

Chadburn A, Abdul-Nabi AM, Teruya BS, Lo AA (2013). Lymphoid proliferations associated with human immunodeficiency virus infection. *Archives of Pathology and Laboratory Medicine,* **137**, 360-370

Chen Y, Jacamo R, Shi YX, Wang RY, Battula VL, Konoplev S, Strunk D, Hofmann NA, Reinisch A, Konopleva M, Andreeff M (2012). Human extramedullary bone marrow in mice: a novel in vivo model of genetically controlled hematopoietic microenvironment. *Blood,* **119**, 4971-4980

Cheng H, Hao S, Liu Y, Pang Y, Ma S, Dong F, Xu J, Zheng G, Li S, Yuan W, Cheng T (2015). Leukemic marrow infiltration reveals a novel role for Egr3 as a potent inhibitor of normal hematopoietic stem cell proliferation. *Blood,* **126**, 1302-1313

Chow A, Lucas D, Hidalgo A, Mendez-Ferrer S, Hashimoto D, Scheiermann C, Battista M, Leboeuf M, Prophete C, van Rooijen N, Tanaka M, Merad M, Frenette PS (2011). Bone marrow CD169+ macrophages promote the retention of hematopoietic stem and progenitor cells in the mesenchymal stem cell niche. *Journal of Experimental Medicine,* **208**, 261-271

Christman JK (2002). 5-Azacytidine and 5-aza-2′-deoxycytidine as inhibitors of DNA methylation: mechanistic studies and their implications for cancer therapy. *Oncogene,* **21**, 5483-5495

Christmann M, Tomicic MT, Roos WP, Kaina B (2003). Mechanisms of human DNA repair: an update. *Toxicology,* **193**, 3-34

Cohen MH, Johnson JR, Pazdur R (2005). Food and Drug Administration Drug approval summary: temozolomide plus radiation therapy for the treatment of newly diagnosed glioblastoma multiforme. *Clinical Cancer Resarch,* **11**, 6767-6771

Colak S, Ten Dijke P (2017). Targeting TGF-beta Signaling in Cancer. *Trends Cancer,* **3**, 56-71

Colmone A, Amorim M, Pontier AL, Wang S, Jablonski E, Sipkins DA (2008). Leukemic Cells Create Bone Marrow Niches That Disrupt the Behavior of Normal Hematopoietic Progenitor Cells. *Science,* **322**, 1861-1865

Crawford J, Dale DC, Kuderer NM, Culakova E, Poniewierski MS, Wolff D, Lyman GH (2008). Risk and timing of neutropenic events in adult cancer patients receiving chemotherapy: the results of a prospective nationwide study of oncology practice. *Journal of the National Comprehensive Cancer Network,* **6**, 109-118

Cui X, Jing X, Yi Q, Xiang Z, Tian J, Tan B, Zhu J (2019). IL22 furthers malignant transformation of rat mesenchymal stem cells, possibly in association with IL22RA1/STAT3 signaling. *Oncology Reports,* **41**, 2148-2158

da Silva Meirelles L, Chagastelles PC, Nardi NB (2006). Mesenchymal stem cells reside in virtually all post-natal organs and tissues. *Journal of Cell Science,* **119**, 2204-2213

Derissen EJ, Beijnen JH, Schellens JH (2013). Concise drug review: azacitidine and decitabine. *Oncologist,* **18**, 619-624

Di Nicola M, Carlo-Stella C, Magni M, Milanesi M, Lononi PD, Matteucci P, Gristanti S, Gianni AM (2002). Human bone marrow stromal cells suppress T-lymphocyte prolifation induced by cellular or nonspecific mitogenic stimuli. *Blood,* **99**, 3838-3843

DiNardo CD, Pratz K, Pullarkat V, Jonas BA, Arellano M, Becker PS, Frankfurt O, Konopleva M, Wei AH, Kantarjian HM, Xu T, Hong WJ, Chyla B, Potluri J, Pollyea DA, Letai A (2019). Venetoclax combined with decitabine or azacitidine in treatment-naive, elderly patients with acute myeloid leukemia. *Blood,* **133**, 7-17

Ding L, Saunders TL, Enikolopov G, Morrison SJ (2012). Endothelial and perivascular cells maintain haematopoietic stem cells. *Nature,* **481**, 457-462

Domingues MJ, Cao H, Heazlewood SY, Cao B, Nilsson SK (2017). Niche Extracellular Matrix Components and Their Influence on HSC. *Journal of Cellular Biochemistry,* **118**, 1984-1993

Dominici M, Le Blanc K, Mueller I, Slaper-Cortenbach I, Marini F, Krause D, Deans R, Keating A, Prockop D, Horwitz E (2006). Minimal criteria for defining multipotent mesenchymal stromal cells. The International Society for Cellular Therapy position statement. *Cytotherapy,* **8**, 315-317

Duong JK, Veal GJ, Nath CE, Shaw PJ, Errington J, Ladenstein R, Boddy AV (2018). Population pharmacokinetics of carboplatin, etoposide and melphalan in children: a re-evaluation of paediatric dosing formulas for carboplatin in patients with normal or mild impairment of renal function. *British Journal of Clinical Pharmacology,* **85**, 136-146

Eladl E, Tremblay-LeMay R, Rastgoo N, Musani R, Chen W, Liu A, Chang H (2020). Role of CD47 in Hematological Malignancies. *Journal of Hematology & Oncology,* **13**, 96

Eriksson D, Stigbrand T (2010). Radiation-induced cell death mechanisms. *Tumour Biology,* **31**, 363-372

Fianchi L, Voso MT, Candoni A, Gaidano G, Criscuolo M, Specchia G, Pogliani EM, Monarca B, Maurillo L, Mecucci C, Breccia M, Aversa F, Musto P, Rondoni M, Fenu S, Buda G, Gobbi M, Santini V, Mancini S, Morra E, Pagano L, Leone G. (2013). *Therapy-related myeloid neoplasms.* Paper presented at the ASH Annual Meeting and Exposition.

Foucquier J, Guedj M (2015). Analysis of drug combinations: current methodological landscape. *Pharmacological Research Perspective,* **3**, e00149, 00141-00111

Franceschi S, Lise M, Trepo C, Berthillon P, Chuang SC, Nieters A, Travis RC, Vermeulen R, Overvad K, Tjonneland A, Olsen A, Bergmann MM, Boeing H, Kaaks R, Becker N, Trichopoulou A, Lagiou P, Bamia C, Palli D, Sieri S, Panico S, Tumino R, Sacerdote C, Bueno-de-Mesquita B, Peeters PH, Rodriguez L, Barroso LL, Dorronsoro M, Sanchez MJ, Navarro C, Barricarte A, Regner S, Borgquist S, Melin B, Hallmans G, Khaw KT, Wareham N, Rinaldi S, Hainaut P, Riboli E, Vineis P

(2011). Infection with hepatitis B and C viruses and risk of lymphoid malignancies in the European Prospective Investigation into Cancer and Nutrition (EPIC). *Cancer Epidemiology, Biomarkers & Prevention,* **20**, 208-214

Friedenstein AJ, Petrakova KV, Kurolesova AI, Frolova GP (1968). Heterotopic of bone marrow. Analysis of precursor cells for osteogenic and hematopoietic tissues. *Transplantation,* **6**, 230-247

Friedmann HS, Kerby T, Calvert H (2000). Temozolomide and Treatment of Malignant Glioma. *Clinical Cancer Research,* **6**, 2585-2597

Gattazzo F, Urciuolo A, Bonaldo P (2014). Extracellular matrix: a dynamic microenvironment for stem cell niche. *Biochimica et Biophysica Acta,* **1840**, 2506-2519

Geerman S, Brasser G, Bhushal S, Salerno F, Kragten NA, Hoogenboezem M, de Haan G, Wolkers MC, Pascutti MF, Nolte MA (2018). Memory CD8(+) T cells support the maintenance of hematopoietic stem cells in the bone marrow. *Haematologica,* **103**, e230-e233

Genovese G, Kahler AK, Handsaker RE, Lindberg J, Rose SA, Bakhoum SF, Chambert K, Mick E, Neale BM, Fromer M, Purcell SM, Svantesson O, Landen M, Hoglund M, Lehmann S, Gabriel SB, Moran JL, Lander ES, Sullivan PF, Sklar P, Gronberg H, Hultman CM, McCarroll SA (2014). Clonal hematopoiesis and blood-cancer risk inferred from blood DNA sequence. *New England Journal of Medicine,* **371**, 2477-2487

Gerson SL, Phillips W, Kastan M, Dumenco LL, Donovan C (1996). Human CD34+ Hematopoietic Progenitors Have Low, Cytokine-Unresponsice O6-Alkylguanine-DNA Alkyltransferase and Are Sensitive to O6-Benzylguanine Plus BCNU. *Blood,* **88**, 1649-1655

Geyh S, Oz S, Cadeddu RP, Frobel J, Bruckner B, Kundgen A, Fenk R, Bruns I, Zilkens C, Hermsen D, Gattermann N, Kobbe G, Germing U, Lyko F, Haas R, Schroeder T (2013). Insufficient stromal support in MDS results from molecular and functional deficits of mesenchymal stromal cells. *Leukemia,* **27**, 1841-1851

Geyh S, Rodriguez-Paredes M, Jager P, Khandanpour C, Cadeddu RP, Gutekunst J, Wilk CM, Fenk R, Zilkens C, Hermsen D, Germing U, Kobbe G, Lyko F, Haas R, Schroeder T (2016). Functional inhibition of mesenchymal stromal cells in acute myeloid leukemia. *Leukemia,* **30**, 683-691

Glennie S, Soeiro I, Dyson PJ, Lam EW, Dazzi F (2005). Bone marrow mesenchymal stem cells induce division arrest anergy of activated T cells. *Blood,* **105**, 2821-2827

Godley LA, Larson RA (2008). Therapy-Related Myeloid Leukemia. *Seminars in Oncology,* **35**, 418-429

Grafe I, Alexander S, Peterson JR, Snider TN, Levi B, Lee B, Mishina Y (2018). TGF-β Family Signaling in Mesenchymal Differentiation. *Cold Spring Harbor Perspectives in Biology,* **10**, a022202

Greaves M, Maley CC (2012). Clonal evolution in cancer. *Nature,* **481**, 306-313

Green DE, Rubin CT (2014). Consequences of irradiation on bone and marrow phenotypes, and its relation to disruption of hematopoietic precursors. *Bone,* **63**, 87-94

Griffiths EA, Roy V, Alwan L, Bachiashvili K, Baird J, Cool R, Dinner S, Geyer M, Glaspy J, Gojo I, Hicks A, Kallam A, Kidwai WZ, Kloth DD, Kraut EH, Landsburg D, Lyman GH, Mahajan A, Miller R, Nachar V, Patel S, Patel S, Perez LE, Poust A, Riaz F, Rosovsky R, Rugo HS, Simon S, Vasu S, Wadleigh M, Westbrook K, Westervelt P, Berardi RA, Pluchino L (2022). NCCN Guidelines(R) Insights: Hematopoietic Growth Factors, Version 1.2022. *Journal of the National Comprehensive Cancer Network,* **20**, 436-442

Gu YC, Kortesmaa J, Tryggvason K, Persson J, Ekblom P, Jacobsen SE, Ekblom M (2003). Laminin isoform-specific promotion of adhesion and migration of human bone marrow progenitor cells. *Blood,* **101**, 877-885

Guerra VA, DiNardo C, Konopleva M (2019). Venetoclax-based therapies for acute myeloid leukemia. *Best Practice & Research: Clinical Haematology,* **32**, 145-153

Hanahan D, Weinberg RA (2011). Hallmarks of cancer: the next generation. *Cell,* **144**, 646-674

Hartmann L, Hecker JS, Rothenberg-Thurley M, Riviere J, Jentzsch M, Ksienzyk B, Buck MC, van der Garde M, Fischer L, Winter S, Rauner M, Tsourdi E, Weidner H, Sockel K, Schneider M, Kubasch AS, Nolde M, Hausmann D, Lutzner J, Goralski S, Bassermann F, Spiekermann K, Hofbauer LC, Schwind S, Platzbecker U, Gotze KS, Metzeler KH (2022). Compartment-specific mutational landscape of clonal hematopoiesis. *Leukemia,* **36**, 2647-2655

Hecker JS, Hartmann L, Riviere J, Buck MC, van der Garde M, Rothenberg-Thurley M, Fischer L, Winter S, Ksienzyk B, Ziemann F, Solovey M, Rauner M, Tsourdi E, Sockel K, Schneider M, Kubasch AS, Nolde M, Hausmann D, Paulus AC, Lutzner J, Roth A, Bassermann F, Spiekermann K, Marr C, Hofbauer LC, Platzbecker U, Metzeler KH, Gotze KS (2021). CHIP and hips: clonal hematopoiesis is common in patients undergoing hip arthroplasty and is associated with autoimmune disease. *Blood,* **138**, 1727-1732

Hoffbrand VA, Moss PAH (2015). Hoffbrand's Essential Haematology. *(Editor:D. A. Warrel)*, John Wiley & Sons ISBN:1118408675, pages 1-320

Horwitz E, Andreef M, Frassoni F (2006). Mesenchymal stromal cells. *Current Opinion in Hematology,* **13**, 419-425

Horwitz EM, Keating A (2000). Nonhematopoietic mesenchymal stem cells: what are they? *Cytotherapy,* **2**, 387-388

Horwitz EM, Le Blanc K, Dominici M, Mueller I, Slaper-Cortenbach I, Marini FC, Deans RJ, Krause DS, Keating A, International Society for Cellular T (2005). Clarification of the nomenclature for MSC: The International Society for Cellular Therapy position statement. *Cytotherapy,* **7**, 393-395

Hu L, Yin C, Zhao F, Ali A, Ma J, Qian A (2018). Mesenchymal Stem Cells: Cell Fate Decision to Osteoblast or Adipocyte and Application in Osteoporosis Treatment. *International Journal of Molecular Sciences,* **19**, 360

Huan J, Hornick NI, Goloviznina NA, Kamimae-Lanning AN, David LL, Wilmarth PA, Mori T, Chevillet JR, Narla A, Roberts CT, Jr., Loriaux MM, Chang BH, Kurre P (2015). Coordinate regulation of residual bone marrow function by paracrine trafficking of AML exosomes. *Leukemia,* **29**, 2285-2295

Huang Y, Wu Q, Tam PKH (2022). Immunomodulatory Mechanisms of Mesenchymal Stem Cells and Their Potential Clinical Applications. *International Journal of Molecular Sciences,* **23**, 10023

Humphrey RW, Brockway-Lunardi LM, Bonk DT, Dohoney KM, Doroshow JH, Meech SJ, Ratain MJ, Topalian SL, Pardoll DM (2011). Opportunities and challenges in the development of experimental drug combinations for cancer. *Journal of the National Cancer Institute,* **103**, 1222-1226

In 't Anker PS, Scherjon SA, Kleijburg-van der Keur C, de Groot-Swings GM, Claas FH, Fibbe WE, Kanhai HH (2004). Isolation of mesenchymal stem cells of fetal or maternal origin from human placenta. *Stem Cells,* **22**, 1338-1345

Itkin T, Gur-Cohen S, Spencer JA, Schajnovitz A, Ramasamy SK, Kusumbe AP, Ledergor G, Jung Y, Milo I, Poulos MG, Kalinkovich A, Ludin A, Kollet O, Shakhar G, Butler JM, Rafii S, Adams RH, Scadden DT, Lin CP, Lapidot T (2016). Distinct bone marrow blood vessels differentially regulate haematopoiesis. *Nature,* **532**, 323-328

Jaffray DA, Gospodarowicz MK. (2015). Radiation Therapy for Cancer: The International Bank for Reconstruction and Development / The World Bank, Washington (DC).

Jäger P, Geyh S, Twarock S, Cadeddu RP, Rabes P, Koch A, Maus U, Hesper T, Zilkens C, Rautenberg C, Bormann F, Kohrer K, Petzsch P, Wieczorek D, Betz B, Surowy

H, Hildebrandt B, Germing U, Kobbe G, Haas R, Schroeder T (2021). Acute myeloid leukemia-induced functional inhibition of healthy CD34+ hematopoietic stem and progenitor cells. *Stem Cells,* **39**, 1270-1284

Jaiswal S, Fontanillas P, Flannick J, Manning A, Grauman PV, Mar BG, Lindsley RC, Mermel CH, Burtt N, Chavez A, Higgins JM, Moltchanov V, Kuo FC, Kluk MJ, Henderson B, Kinnunen L, Koistinen HA, Ladenvall C, Getz G, Correa A, Banahan BF, Gabriel S, Kathiresan S, Stringham HM, McCarthy MI, Boehnke M, Tuomilehto J, Haiman C, Groop L, Atzmon G, Wilson JG, Neuberg D, Altshuler D, Ebert BL (2014). Age-related clonal hematopoiesis associated with adverse outcomes. *New England Journal of Medicine,* **371**, 2488-2498

Jian H, Shen X, Liu I, Semenov M, He X, Wang X-F (2006). Smad3-dependent nuclear translocation of β-catenin is required for TGF-β1-induced proliferation of bone marrow-derived adult human mesenchymal stem cells. *Genes & Development,* **20**, 666-674

Jones P, May G, Healy L, Brown J, Hoyne G, Delassus S, Enver T (1998). Stromal expression of Jagged 1 promotes colony formation by fetal hematopoietic progenitor cells. *Blood,* **92**, 1505-1511

Jones RJ, Armstrong SA (2008). Cancer Stem Cells in Hematopoietic Malignancies. *Biology of Blood and Marrow Transplantation,* **14**, 12-16

Kaminskas E, Farrell AT, Wang Y-C, Sridhara R, Pazdur R (2005). FDA Drug Approval Summary: Azacitidine (5-azacytidine, VidazaTM) for Injectable Suspension. *Oncologist,* **10**, 176-182

Kapur R, Zhang L (2001). A Novel Mechanism of Cooperation between c-Kit and Erythropoietin Receptor. *Journal of Biological Chemistry,* **276**, 974-983

Karanu FN, Murdoch B, Gallacher L, Wu DM, Koremoto M, Sakano S, Bhatia M (2000). The notch ligand jagged-1 represents a novel growth factor of human hematopoietic stem cells. *Journal of Experimental Medicine,* **192**, 1365-1372

Kato Y, Nishimura S, Sakura N, Ueda K (2003). Pharmacokinetics of etoposide with intravenous drug administration in children and adolescents. *Pediatrics International,* **45**, 75-79

Keller-Juslen C, Kuhn M, Stahelin H, von Wartburg A (1971). Synthesis and antimitotic activity of glycosidic lignan derivatives related to podophyllotoxin. *Journal of Medicinal Chemistry,* **14**, 936-940

Kent D, Copley M, Benz C, Dykstra B, Bowie M, Eaves C (2008). Regulation of hematopoietic stem cells by the steel factor/KIT signaling pathway. *Clinical Cancer Research,* **14**, 1926-1930

Khoury JD, Solary E, Abla O, Akkari Y, Alaggio R, Apperley JF, Bejar R, Berti E, Busque L, Chan JKC, Chen W, Chen X, Chng WJ, Choi JK, Colmenero I, Coupland SE, Cross NCP, De Jong D, Elghetany MT, Takahashi E, Emile JF, Ferry J, Fogelstrand L, Fontenay M, Germing U, Gujral S, Haferlach T, Harrison C, Hodge JC, Hu S, Jansen JH, Kanagal-Shamanna R, Kantarjian HM, Kratz CP, Li XQ, Lim MS, Loeb K, Loghavi S, Marcogliese A, Meshinchi S, Michaels P, Naresh KN, Natkunam Y, Nejati R, Ott G, Padron E, Patel KP, Patkar N, Picarsic J, Platzbecker U, Roberts I, Schuh A, Sewell W, Siebert R, Tembhare P, Tyner J, Verstovsek S, Wang W, Wood B, Xiao W, Yeung C, Hochhaus A (2022). The 5th edition of the World Health Organization Classification of Haematolymphoid Tumours: Myeloid and Histiocytic/Dendritic Neoplasms. *Leukemia,* **36**, 1703-1719

Kim SJ, Park TS, Lee ST, Song J, Suh B, Kim SH, Jang SJ, Lee CH, Choi JR (2009). Therapy-Related Myelodysplastic Syndrome/Acute Myeloid Leukemia after Treatment with Temozolomide in a Patient with Glioblastoma Multiforme. *Annals of Clinical and Laboratory Science,* **39**, 392-398

Kimura Y, Ding B, Imai N, Nolan DJ, Butler JM, Rafii S (2011). c-Kit-mediated functional positioning of stem cells to their niches is essential for maintenance and regeneration of adult hematopoiesis. *PloS One,* **6**, e26918

Kitagawa M, Saito I, Kuwata T, Yoshida S, Yamaguchi S, Takahashi M, Tanizawa T, Kamiyama R, Hirokawa K (1997). Overexpression of tumor necrosis factor (TNF)-a and interferon (IFN)-y by bone marrow cells from patients with myelodysplastic syndromes. *Leukemia,* **11**, 2049-2054

Klein G (1995). The extracellular matrix of the hematopoietic environment. *Experientia,* **51**, 914-926

Kobayashi H, Butler JM, O'Donnell R, Kobayashi M, Ding BS, Bonner B, Chiu VK, Nolan DJ, Shido K, Benjamin L, Rafii S (2010). Angiocrine factors from Akt-activated endothelial cells balance self-renewal and differentiation of haematopoietic stem cells. *Nature Cell Biology,* **12**, 1046-1056

Kode A, Manavalan JS, Mosialou I, Bhagat G, Rathinam CV, Luo N, Khiabanian H, Lee A, Murty VV, Friedman R, Brum A, Park D, Galili N, Mukherjee S, Teruya-Feldstein J, Raza A, Rabadan R, Berman E, Kousteni S (2014). Leukaemogenesis induced by an activating beta-catenin mutation in osteoblasts. *Nature,* **506**, 240-244

Koenig KL, Borate U (2022). New investigational combinations for higher-risk MDS. *Hematology: The Education Program of the American Society of Hematology,* **2022**, 368-374

Kondo M, Weissman IL, Akashi K (1997). Identification of clonogenic common lymphoid progenitors in mouse bone marrow. *Cell,* **91**, 661-672

Korn C, Mendez-Ferrer S (2017). Myeloid malignancies and the microenvironment. *Blood,* **129**, 811-822

Kuendgen A, Nomdedeu M, Tuechler H, Garcia-Manero G, Komrokji RS, Sekeres MA, Della Porta MG, Cazzola M, DeZern AE, Roboz GJ, Steensma DP, Van de Loosdrecht AA, Schlenk RF, Grau J, Calvo X, Blum S, Pereira A, Valent P, Costa D, Giagounidis A, Xicoy B, Dohner H, Platzbecker U, Pedro C, Lubbert M, Oiartzabal I, Diez-Campelo M, Cedena MT, Machherndl-Spandl S, Lopez-Pavia M, Baldus CD, Martinez-de-Sola M, Stauder R, Merchan B, List A, Ganster C, Schroeder T, Voso MT, Pfeilstocker M, Sill H, Hildebrandt B, Esteve J, Nomdedeu B, Cobo F, Haas R, Sole F, Germing U, Greenberg PL, Haase D, Sanz G (2021). Therapy-related myelodysplastic syndromes deserve specific diagnostic sub-classification and risk-stratification-an approach to classification of patients with t-MDS. *Leukemia,* **35**, 835-849

Kunisaki Y, Bruns I, Scheiermann C, Ahmed J, Pinho S, Zhang D, Mizoguchi T, Wei Q, Lucas D, Ito K, Mar JC, Bergman A, Frenette PS (2013). Arteriolar niches maintain haematopoietic stem cell quiescence. *Nature,* **502**, 637-643

Larson RA (2009). Therapy-related myeloid neoplasms. *Haematologica,* **94**, 454-459

Le Blanc K, Davies LC (2015). Mesenchymal stromal cells and the innate immune response. *Immunology Letters,* **168**, 140-146

Leone G, Pagano L, Ben-Yehuda D, Voso MT (2007). Therapy-related leukemia and myelodysplasia: susceptibility and incidence. *Haematologica,* **92**, 1389-1398

Lerner UH (2012). Osteoblasts, Osteoclasts, and Osteocytes: Unveiling Their Intimate-Associated Responses to Applied Orthodontic Forces. *Seminars in Orthodontics,* **18**, 237-248

Libura J, Slater DJ, Felix CA, Richardson C (2005). Therapy-related acute myeloid leukemia-like MLL rearrangements are induced by etoposide in primary human CD34+ cells and remain stable after clonal expansion. *Blood,* **105**, 2124-2131

Lin AJ, Campian JL, Hui C, Rudra S, Rao YJ, Thotala D, Hallahan D, Huang J (2018). Impact of concurrent versus adjuvant chemotherapy on the severity and duration of

lymphopenia in glioma patients treated with radiation therapy. *Journal of Neuro-Oncology,* **136**, 403-411

Liu S, Ren J, Ten Dijke P (2021). Targeting TGFbeta signal transduction for cancer therapy. *Signal Transduction and Targeted Therapy,* **6**, 8

Lubeck DP, Danese M, Jennifer D, Miller K, Richhariya A, Garfin PM (2016). Systematic Literature Review of the Global Incidence and Prevalence of Myelodysplastic Syndrome and Acute Myeloid Leukemia. *Blood,* **128**, 5930-5930

Lutzkendorf J, Wieduwild E, Nerger K, Lambrecht N, Schmoll HJ, Muller-Tidow C, Muller LP (2017). Resistance for Genotoxic Damage in Mesenchymal Stromal Cells Is Increased by Hypoxia but Not Generally Dependent on p53-Regulated Cell Cycle Arrest. *PloS One,* **12**, e0169921

Luz-Crawford P, Djouad F, Toupet K, Bony C, Franquesa M, Hoogduijn MJ, Jorgensen C, Noel D (2016). Mesenchymal Stem Cell-Derived Interleukin 1 Receptor Antagonist Promotes Macrophage Polarization and Inhibits B Cell Differentiation. *Stem Cells,* **34**, 483-492

Manitta V, Zordan R, Cole-Sinclair M, Nandurkar H, Philip J (2011). The symptom burden of patients with hematological malignancy: a cross-sectional observational study. *Journal of Pain and Symptom Management,* **42**, 432-442

Marrari A, Hornick JL, Ramaiya NH, Manola A, Wagner AJ. (2011). *Expression of MGMT and response to treatment with temozolomide in patients with leiomyosarcoma*. Paper presented at the ASCO, Atlanta, Georgia, June 2-6, United States. https://hal.science/hal-00019908

McNerney ME, Godley LA, Le Beau MM (2017). Therapy-related myeloid neoplasms: when genetics and environment collide. *Nature Reviews: Cancer,* **17**, 513-527

Méndez-Ferrer S, Michurina TV, Ferraro F, Mazloom AR, MacArthur BD, Lira SA, Scadden DT, Ma'ayan A, Enikolopov GN, Frenette PS (2010). Mesenchymal and haematopoietic stem cells form a unique bone marrow niche. *Nature,* **466**, 829-834

Michelacci YM, Baccarin RYA, Rodrigues NNP (2023). Chondrocyte Homeostasis and Differentiation: Transcriptional Control and Signaling in Healthy and Osteoarthritic Conditions. *Life (Basel),* **13**, 1460

Moon J, Kitty I, Renata K, Qin S, Zhao F, Kim W (2023). DNA Damage and Its Role in Cancer Therapeutics. *International Journal of Molecular Sciences,* **24**, 4741

Muir H (1995). The chondrocyte, architect of cartilage. Biomechanics, structure, function and molecular biology of cartilage matrix macromolecules. *Bioessays,* **17**, 1039-1048

Muraglia A, Cancedda R, Quarto R (2000). Clonal mesenchymal progenitors from human bone marrow differentiate in vitro according to a hierachical model. *Journal of Cell Science,* **113**, 1161-1166

Nakamura Y, Arai F, Iwasaki H, Hosokawa K, Kobayashi I, Gomei Y, Matsumoto Y, Yoshihara H, Suda T (2010). Isolation and characterization of endosteal niche cell populations that regulate hematopoietic stem cells. *Blood,* **116**, 1422-1432

National Cancer Institute. (2024). Non-Hodgkin Lymphoma Treatment (PDQ®)–Health professional version. Retrieved 15.11.2024, 2024, from https://www.cancer.gov/types/lymphoma/patient/adult-nhl-treatment-pdq#_190

National Center for Biotechnology Information. (2024a). PubChem Compound Summary for CID 5394, Temozolomide. Retrieved 06.09.2024 https://pubchem.ncbi.nlm.nih.gov/compound/Temozolomide

National Center for Biotechnology Information. (2024b). PubChem Compound Summary for CID 9444, Azacitidine. Retrieved 06.09.2024 https://pubchem.ncbi.nlm.nih.gov/compound/Azacitidine.

National Center for Biotechnology Information. (2024c). PubChem Compound Summary for CID 36462, Etoposide. Retrieved 06.09.2024 https://pubchem.ncbi.nlm.nih.gov/compound/Etoposide.

National Center for Biotechnology Information. (2024d). PubChem Compound Summary for CID 49846579, Venetoclax. Retrieved 06.09.2024 https://pubchem.ncbi.nlm.nih.gov/compound/Venetoclax

Naveiras O, Nardi V, Wenzel PL, Hauschka PV, Fahey F, Daley GQ (2009). Bone-marrow adipocytes as negative regulators of the haematopoietic microenvironment. *Nature,* **460**, 259-263

Nicolay NH, Ruhle A, Perez RL, Trinh T, Sisombath S, Weber KJ, Schmezer P, Ho AD, Debus J, Saffrich R, Huber PE (2016). Mesenchymal stem cells exhibit resistance to topoisomerase inhibition. *Cancer Letters,* **374**, 75-84

Nifontova I, Svinareva D, Petrova T, Drize N (2008). Sensitivity of Mesenchymal Stem Cells and Their Progeny to Medicines Used for the Treatment of Hematoproliferative Diseases *Acta Haematologica,* **119**, 98-103

Nilsson SK, Johnston HM, Whitty GA, Williams B, Webb RJ, Denhardt DT, Bertoncello I, Bendall LJ, Simmons PJ, Haylock DN (2005). Osteopontin, a key component of the hematopoietic stem cell niche and regulator of primitive hematopoietic progenitor cells. *Blood,* **106**, 1232-1239

Nitiss JL (2009). DNA topoisomerase II and its growing repertoire of biological functions. *Nature Reviews Cancer,* **9**, 327-337

Noronha V, Berliner N, Ballen KK, Lacy J, Kracher J, Baehring J, Henson JW (2006). Treatment-related myelodysplasia/AML in a patient with a history of breast cancer and an oligodendroglioma treated with temozolomide: case study and review of the literature. *Neuro-Oncology,* **8**, 280-283

Nurgalieva Z, Liu CC, Du XL (2011). Chemotherapy use and risk of bone marrow suppression in a large population-based cohort of older women with breast and ovarian cancer. *Medical Oncology,* **28**, 716-725

Ogawa (1993). Differentiation and Proliferation of Hematopoietic Stem Cells. *Blood,* **81**, 2844-2853

Omatsu Y, Sugiyama T, Kohara H, Kondoh G, Fujii N, Kohno K, Nagasawa T (2010). The essential functions of adipo-osteogenic progenitors as the hematopoietic stem and progenitor cell niche. *Immunity,* **33**, 387-399

Owen M (1988). Marrow stromal stem cells. *Cell Science Supplements,* **10**, 63-76

Pasqualetti P, Casale R, Colantonio D, Collacciani A (1991). Occupational risk for hematological malignancies *American Journal of Hematology,* **38**, 147-149

Pedersen-Bjergaard J, Andersen MT, Andersen MK (2007). Genetic Pathways in the Pathogenesis of Therapy-Related Myelodysplasia and Acute Myeloid Leukemia. *Hematology: The Education Program of the American Society of Hematology*, 392-397

Pietras EM, Warr MR, Passegue E (2011). Cell cycle regulation in hematopoietic stem cells. *Journal of Cell Biology,* **195**, 709-720

Pievani A, Donsante S, Tomasoni C, Corsi A, Dazzi F, Biondi A, Riminucci M, Serafini M (2021). Acute myleoid leukemia shaphes the bone marrow stromal niche in vivo. *Haematologia,* **106**, 865-870

Plotkin MD, Goligorsky MS (2006). Mesenchymal cells from adult kidney support angiogenesis and differentiate into multiple interstitial cell types including erythropoietin-producing fibroblasts. *American Journal of Physiology: Renal Physiology,* **291**, 902-912

Pollyea DA, Amaya M, Strati P, Konopleva MY (2019). Venetoclax for AML: changing the treatment paradigm. *Blood Advances,* **3**, 4326-4335

Poulos MG, Guo P, Kofler NM, Pinho S, Gutkin MC, Tikhonova A, Aifantis I, Frenette PS, Kitajewski J, Rafii S, Butler JM (2013). Endothelial Jagged-1 is necessary for homeostatic and regenerative hematopoiesis. *Cell Reports,* **4**, 1022-1034

Poynter JN, Richardson M, Roesler M, Blair CK, Hirsch B, Nguyen P, Cioc A, Cerhan JR, Warlick E (2017). Chemical exposures and risk of acute myeloid leukemia and myelodysplastic syndromes in a population-based study. *International Journal of Cancer,* **140**, 23-33

Qi Z, Zhang Y, Liu L, Guo X, Qin J, Cui G (2012). Mesenchymal stem cells derived from different origins have unique sensitivities to different chemotherapeutic agents. *Cell Biology International,* **36**, 857-862

Raaijmakers MHGP, Mukherjee S, Guo S, Zhang S, Kobayashi T, Schoonmaker JA, Ebert BL, Al-Shahrour F, Hasserjian RP, Scadden EO, Aung Z, Matza M, Merkenschlager M, Lin C, Rommens JM, Scadden DT (2010). Bone progenitor dysfunction induces myelodysplasia and secondary leukaemia. *Nature,* **464**, 852-857

Rafei M, Hsieh J, Fortier S, Li M, Yuan S, Birman E, Forner K, Boivin MN, Doody K, Tremblay M, Annabi B, Galipeau J (2008). Mesenchymal stromal cell-derived CCL2 suppresses plasma cell immunoglobulin production via STAT3 inactivation and PAX5 induction. *Blood,* **112**, 4991-4998

Rafii S, Shapiro F, Pettengell R, Ferris B, Nachman RL, Moore MA, Asch AS (1995). Human bone marrow microvascular endothelial cells support long-term proliferation and differentiation of myeloid and megakaryocytic progenitors. *Blood,* **86**, 3353-3363

Reidel V, Kauschinger J, Hauch RT, Müller-Thomas C, Nadarajah N, Burgkart R, Schmidt B, Hempel D, Jacob A, Slotta-Huspenina J, Höckendorf U, Peschel C, Kern W, Haferlach T, Götze KS, Jilg S, Jost PJ (2018). Selective inhibition of BCL-2 is a promising target in patients with high-risk myelodysplastic syndromes and adverse mutational profile. *Oncotarget,* **9**, 17270-17281

Roberts KG (2018). Genetics and prognosis of ALL in children vs adults. *Hematology: The Education Program of the American Society of Hematology,* **1**, 137-145

Rodriguez-Abreu D, Bordoni A, Zucca E (2007). Epidemiology of hematological malignancies. *Annals of Oncology,* **18 Suppl 1**, i3-i8

Rosca AM, Burlacu A (2011). Effect of 5-azacytidine: evidence for alteration of the multipotent ability of mesenchymal stem cells. *Stem Cells and Development,* **20**, 1213-1221

Rühle A, Huber PE, Saffrich R, Lopez Perez R, Nicolay NH (2018). The current understanding of mesenchymal stem cells as potential attenuators of chemotherapy-induced toxicity. *International Journal of Cancer,* **143**, 2628-2639

Salik B, Smyth MJ, Nakamura K (2020). Targeting immune checkpoints in hematological malignancies. *Journal of Hematology & Oncology,* **13**, 111

San Miguel Amigo L, Franco Osorio R, Mercadal Vilchez S, Martinez-Frances A (2011). Azacitidine adverse effects in patients with myelodysplastic syndromes. *Advances in Therapy,* **28 Suppl 4**, 6-11

Scheffold A, Jebaraj BMC, Stilgenbauer S (2018). Venetoclax: Targeting BCL2 in Hematological Cancers. *Recent Results in Cancer Research,* **212**, 215-242

Schepers K, Pietras EM, Reynaud D, Flach J, Binnewies M, Garg T, Wagers AJ, Hsiao EC, Passegue E (2013). Myeloproliferative neoplasia remodels the endosteal bone marrow niche into a self-reinforcing leukemic niche. *Cell Stem Cell,* **13**, 285-299

Schofield R (1978). The relationship between the spleen colony-forming cell and the haemopoietic stem cell. *Blood Cells,* **4**, 7-25

Schroeder PE, Hofland KF, Jensen PB, Sehested M, Langer SW, Hasinoff BB (2003). Pharmacokinetics of etoposide in cancer patients treated with high-dose etoposide and with dexrazoxane (ICRF-187) as a rescue agent. *Cancer Chemotherapy and Pharmacology,* **53**, 91-93

Schürch CM, Caraccio C, Nolte MA (2021). Diversity localization and (patho)physiology of mature lymphocyte populations in the bone marrow. *Blood,* **137**, 3015-3026

Seita J, Weissman IL (2010). Hematopoietic stem cell: self-renewal versus differentiation. *Wiley Interdisciplinary Reviews: Systems Biology and Medicine,* **2**, 640-653

Sharpe AH (2017). Introduction to checkpoint inhibitors and cancer immunotherapy. *Immunological Reviews,* **276**, 5-8

Simmons DL, Satterthwaite AB, Tenen DG, Seed B (1992). Molecular cloning of a cDNA encoding CD34, a sialomucin of human hematopoietic stem cells. *Journal of Immunology,* **148**, 267-271

Sinkule JA (1984). Etoposide: A Semisynthetic Epipodophyllotoxin. *Pharmacotherapy,* **4**, 61-71

Slifka MK, Antia R, Whitmire JK, Ahmed R (1998). Humoral Immunity Due to Long-Lived Plasma Cells. *Immunity,* **8**, 363-372

Sorm F, Piskala A, Cihak A, Vesely J (1964). 5-Azacytidine, a new, highly effective cancerostatic *Experientia,* **20**, 202-203

Stik G, Crequit S, Petit L, Durant J, Charbord P, Jaffredo T, Durand C (2017). Extracellular vesicles of stromal origin target and support hematopoietic stem and progenitor cells. *Journal of Cell Biology,* **216**, 2217-2230

Stresemann C, Lyko F (2008). Modes of action of the DNA methyltransferase inhibitors azacytidine and decitabine. *International Journal of Cancer,* **123**, 8-13

Super HG, Strissel PL, Sobulo OM, Burian D, Reshmi SC, Roe B, Zeleznik-Le NJ, Diaz MO, Rowley JD (1997). Identification of complex genomic breakpoint junctions in the t(9;11) MLL-AF9 fusion gene in acute leukemia. *Genes Chromosomes Cancer,* **20**, 185-195

Swerdlow SH, Campo E, Pileri SA, Harris NL, Stein H, Siebert R, Advani R, Ghielmini M, Salles GA, Zelenetz AD, Jaffe ES (2016). The 2016 revision of the World Health Organization classification of lymphoid neoplasms. *Blood,* **127**, 2375-2390

Totiger TM, Ghoshal A, Zabroski J, Sondhi A, Bucha S, Jahn J, Feng Y, Taylor J (2023). Targeted Therapy Development in Acute Myeloid Leukemia. *Biomedicines,* **11**, 641

Travis LB (2006). The epidemiology of second primary cancers. *Cancer Epidemiology, Biomarkers & Prevention,* **15**, 2020-2026

Tsao T, Shi Y, Kornblau S, Lu H, Konoplev S, Antony A, Ruvolo V, Qiu YH, Zhang N, Coombes KR, Andreeff M, Kojima K, Konopleva M (2012). Concomitant inhibition of DNA methyltransferase and BCL-2 protein function synergistically induce mitochondrial apoptosis in acute myelogenous leukemia cells. *Annals of Hematology,* **91**, 1861-1870

U.S. Food and Drug Administration. (2004). Azacitidine for injection: Clinical review and approval history. Retrieved 18.11.2024, 2024, from https://www.accessdata.fda.gov

Vallet S, Pozzi S, Patel K, Vaghela N, Fulciniti MT, Veiby P, Hideshima T, Santo L, Cirstea D, Scadden DT, Anderson KC, Raje N (2011). A novel role for CCL3 (MIP-1alpha) in myeloma-induced bone disease via osteocalcin downregulation and inhibition of osteoblast function. *Leukemia,* **25**, 1174-1181

van Nieuwenhuijzen N, Spaan I, Raymakers R, Peperzak V (2018). From MGUS to Multiple Myeloma, a Paradigm for Clonal Evolution of Premalignant Cells. *Cancer Research,* **78**, 2449-2456

Visvader JE (2011). Cells of origin in cancer. *Nature,* **469**, 314-322

von der Heide EK, Neumann M, Vosberg S, James AR, Schroeder MP, Ortiz-Tanchez J, Isaakidis K, Schlee C, Luther M, Jöhrens K, Anagnostopoulos I, Mochmann LH, Nowak D, Hofmann WK, Greif PA, Baldus CD (2016). Molecular alterations in bone marrow mesenchymal stromal cells derived from acute myeloid leukemia patients. *Leukemia,* **31**, 1069-1078

Wagers AJ, Christensen JL, Weissman IL (2002). Cell fate determination from stem cells. *Gene Therapy,* **9**, 606-612

Wang Y, Probin V, Zhou D (2006). Cancer Therapy-Induced Residual Bone Marrow Injury: Mechanisms of Induction and Implication for Therapy. *Current Cancer Therapy Reviews,* **2**, 271-279

Warr MR, Pietras EM, Passegue E (2011). Mechanisms controlling hematopoietic stem cell functions during normal hematopoiesis and hematological malignancies. *Wiley Interdisciplinary Reviews: Systems Biology and Medicine,* **3**, 681-701

Warren CFA, Wong-Brown MW, Bowden NA (2019). BCL-2 family isoforms in apoptosis and cancer. *Cell Death & Disease,* **10**, 177

Wenk C, Garz A-K, Grath S, Huberle C, Witham D, Weickert M, Malinverni R, Niggemeyer J, Kyncl M, Hecker J, Pagel C, Mulholland CB, Müller-Thomas C, Leonhardt H, Bassermann F, Oostendorp RAJ, Metzeler KH, Buschbeck M, Götze KS (2018). Direct modulation of the bone marrow mesenchymal stromal cell compartment by azacitidine enhances healthy hematopoiesis. *Blood Advances,* **2**, 3447-3461

Winkler IG, Sims NA, Pettit AR, Barbier V, Nowlan B, Helwani F, Poulton IJ, van Rooijen N, Alexander KA, Raggatt LJ, Levesque JP (2010). Bone marrow macrophages maintain hematopoietic stem cell (HSC) niches and their depletion mobilizes HSCs. *Blood,* **116**, 4815-4828

Winter S, Gotze KS, Hecker JS, Metzeler KH, Guezguez B, Woods K, Medyouf H, Schaffer A, Schmitz M, Wehner R, Glauche I, Roeder I, Rauner M, Hofbauer LC, Platzbecker U (2024). Clonal hematopoiesis and its impact on the aging osteo-hematopoietic niche. *Leukemia,* **38**, 936-946

Wlodarski MW, Niemeyer CM (2017). Introduction: Genetic syndromes predisposing to myeloid neoplasia. *Seminars in Hematology,* **54**, 57-59

Wu J, Gu L, Wang H, Geacintov NE, Li GM (1999). Mismatch repair processing of carcinogen-DNA adducts triggers apoptosis. *Molecular and Cellular Biology,* **19**, 8292-8301

Wu Y, Aanei CM, Kesr S, Picot T, Guyotat D, Campos Catafal L (2017). Impaired Expression of Focal Adhesion Kinase in Mesenchymal Stromal Cells from Low-Risk Myelodysplastic Syndrome Patients. *Frontiers in Oncology,* **7**, 164

Wu Y, Chen L, Scott PG, Tredget EE (2007). Mesenchymal stem cells enhance wound healing through differentiation and angiogenesis. *Stem Cells,* **25**, 2648-2659

Xiao Y, McGuinness CS, Doherty-Boyd WS, Salmeron-Sanchez M, Donnelly H, Dalby MJ (2022). Current insights into the bone marrow niche: From biology in vivo to bioengineering ex vivo. *Biomaterials,* **286**, 121568

Xie Y, Yin T, Wiegraebe W, He XC, Miller D, Stark D, Perko K, Alexander R, Schwartz J, Grindley JC, Park J, Haug JS, Wunderlich JP, Li H, Zhang S, Johnson T, Feldman RA, Li L (2009). Detection of functional haematopoietic stem cell niche using real-time imaging. *Nature,* **457**, 97-101

Xu Q, Streuer A, Jann JC, Altrock E, Schmitt N, Flach J, Sens-Albert C, Rapp F, Wolf J, Nowak V, Weimer N, Oblander J, Palme I, Kuzina M, Jawhar A, Darwich A, Weis CA, Marx A, Wuchter P, Costina V, Jager E, Sperk E, Neumaier M, Fabarius A, Metzgeroth G, Nolte F, Steiner L, Levkin PA, Jawhar M, Hofmann WK, Riabov V, Nowak D (2023). Inhibition of lysyl oxidases synergizes with 5-azacytidine to restore erythropoiesis in myelodysplastic and myeloid malignancies. *Nature Communications,* **14**, 1497

Yan X, Ehnert S, Culmes M, Bachmann A, Seeliger C, Schyschka L, Wang Z, Rahmanian-Schwarz A, Stöckle U, De Sousa PA, Pelisek J, Nussler AK (2014). 5-Azacytidine Improves the Osteogenic Differentiation Potential of Aged Human Adipose-Derived Mesenchymal Stem Cells by DNA Demethylation. *PloS One,* **9**, e90846

Yang GC, Xu YH, Chen HX, Wang XJ (2015). Acute Lymphoblastic Leukemia Cells Inhibit the Differentiation of Bone Mesenchymal Stem Cells into Osteoblasts In Vitro by Activating Notch Signaling. *Stem Cells International,* **2015**, 162410

Zanetti C, Krause DS (2020). "Caught in the net": the extracellular matrix of the bone marrow in normal hematopoiesis and leukemia. *Experimental Hematology,* **89**, 13-25

Zhang J, Niu C, Ye L, Huang H, He X, Tong WG, Ross J, Haug J, Johnson T, Feng JQ, Harris S, Wiedemann LM, Mishina Y, Li L (2003). Identification of the haematopoietic stem cell niche and control of the niche size. *Nature,* **425**, 836-841

Zhang J, Supakorndej T, Krambs JR, Rao M, Abou-Ezzi G, Ye RY, Li S, Trinkaus K, Link DC (2019). Bone marrow dendritic cells regulate hematopoietic stem/progenitor cell trafficking. *Journal of Clinical Investigation,* **129**, 2920-2931

Zhang N, Wu J, Wang Q, Liang Y, Li X, Chen G, Ma L, Liu X, Zhou F (2023). Global burden of hematologic malignancies and evolution patterns over the past 30 years. *Blood Cancer Journal,* **13**, 82

Zhou BO, Yu H, Yue R, Zhao Z, Rios JJ, Naveiras O, Morrison SJ (2017). Bone marrow adipocytes promote the regeneration of stem cells and haematopoiesis by secreting SCF. *Nature Cell Biology,* **19**, 891-903

Zhou P, Xia C, Wang T, Dong Y, Weng Q, Liu X, Geng Y, Wang J, Du J (2021). Senescent bone marrow microenvironment promotes Nras-mutant leukemia. *Journal of Molecular Cell Biology,* **13**, 72-74

Zuk PA, Zhu M, Ashjian P, De Ugarte DA, Huang JI, Mizuno H, Alfonso ZC, Fraser JK, Benhaim P, Hedrick MH (2002). Human adipose tissue is a source of multipotent stem cells. *Molecular Biology of the Cell,* **13**, 4279-4295

5. Appendix

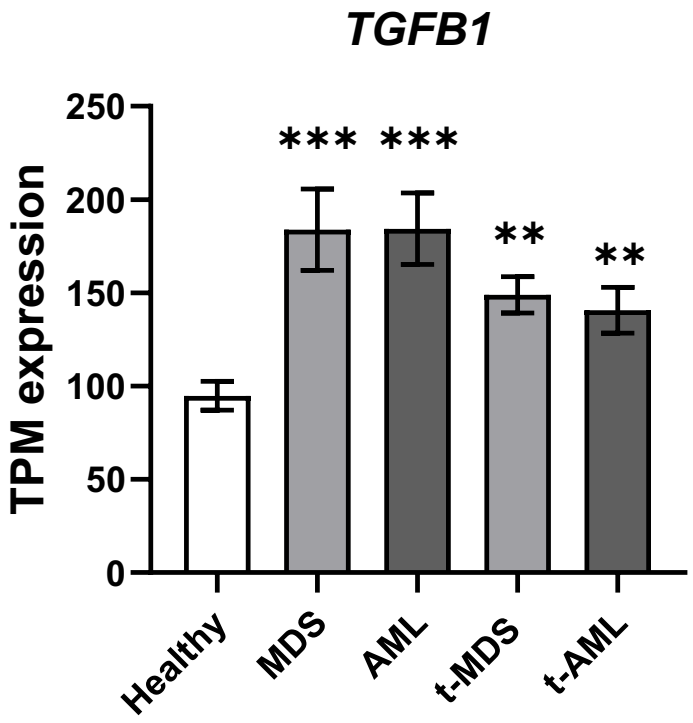

Appendix Figure 1. Increased *TGFB1* expression in MDS, AML, t-MDS, and t-AML versus healthy controls. Transcripts per million (TPM) of TGFB1 were determined from RNA sequencing data and compared for patient-derived MSC and healthy controls for at least four independent samples. Student's unpaired t-test **p <0.01, ***p <0.001.

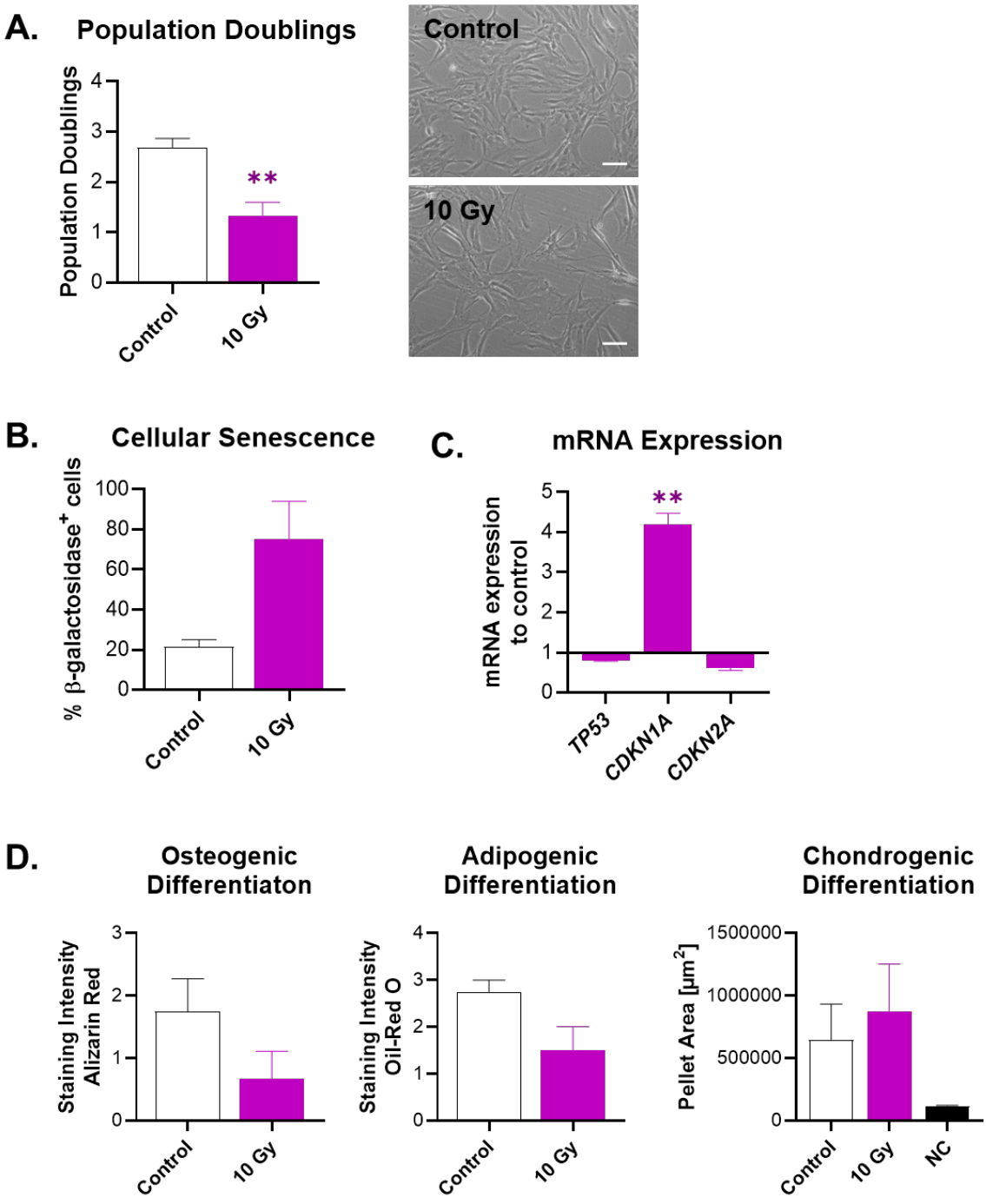

Appendix Figure 2. Exposure of healthy MSC to 10 Gy IR. Healthy MSC were exposed to 10 Gy, medium was exchanged after 24 hours and cells were harvested after another 24 hours. Population doublings were calculated and representative images are shown with scale bars indicating 100 μm (A.). Harvested cells were used for cellular senescence assay (B.), qPCR analysis (C.), and differentiation assessment (D.). A control was always handled in parallel without IR exposure. Independent experiments were repeated 2-4 times, significance was indicated at least with n=3 using Student's paired t-test **p <0.01. NC= negative control.

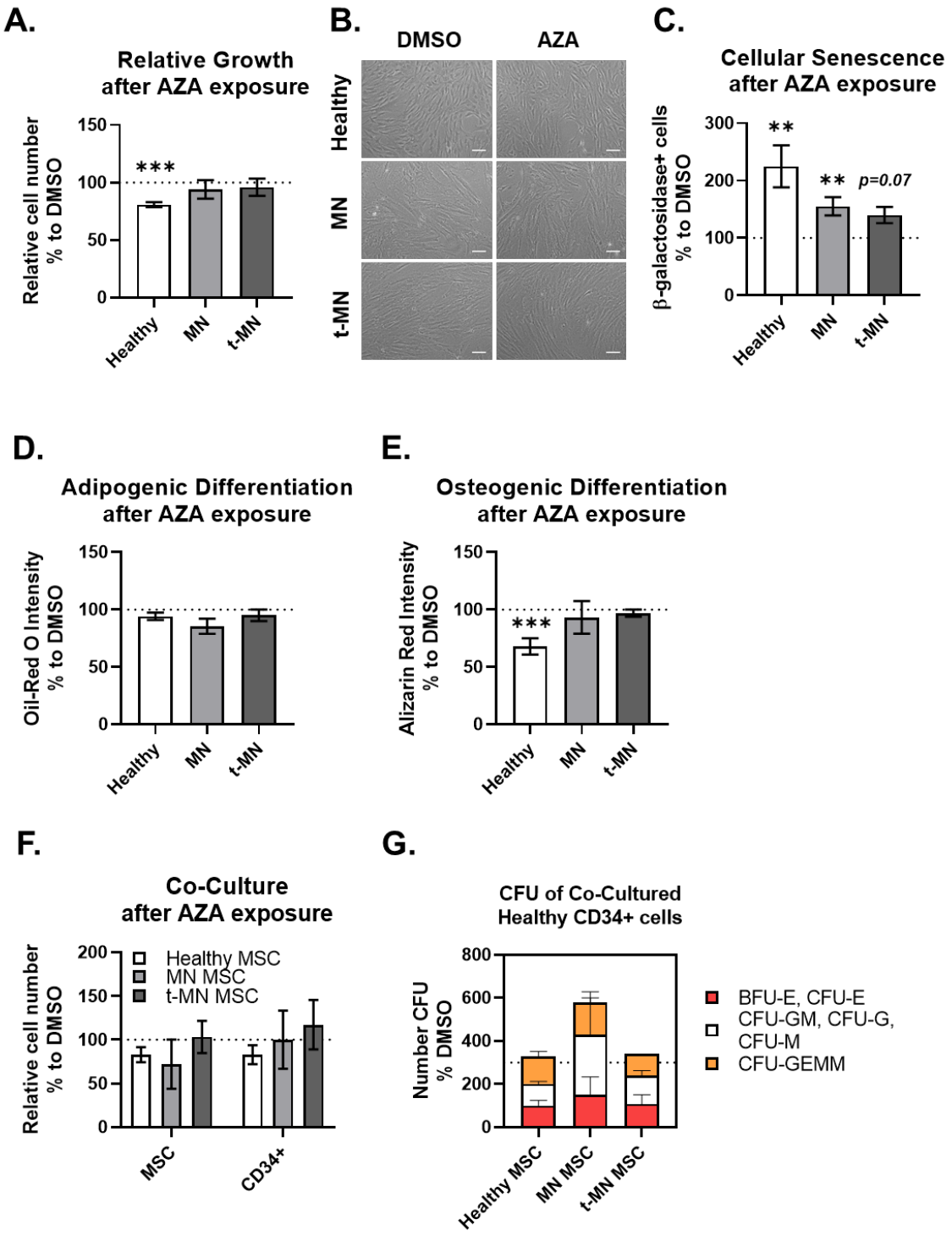

Appendix Figure 3. Comparative analysis of AZA response on healthy and patient-derived MSC. MSC were exposed to 2.5 μM AZA for seven days and subsequently analyzed for their growth (A.), morphology (B.), cellular senescence (C.), differentiation capacity (D., E.), and hematopoietic support capacity (F., G.). Patient-derived MSC were less responsive towards AZA compared to healthy samples; however, MN MSC exhibited increased hematopoietic support capacity as shown by Colony Forming Units (CFU) assay. Experiments were conducted with at least three independent samples (except F. and G. for MN MSC), and statistical analysis was performed using Student's

paired t-test comparing AZA vs. DMSO treatment, **p <0.01, ***p <0.001). Scale bars indicate 100 μm.

Primary Cancer Diagnosis	Therapy	t-MN Diagnosis	Morphology P3 (*P4) 5X objective	Adipogenesis 10X objective	Osteogenesis 5X objective	Chondro-genesis 2.5X objective
B-ALL	8# GMALL B-ALL	t-MDS	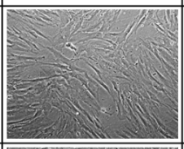	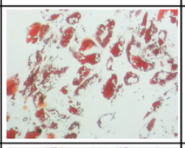	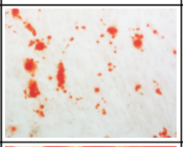	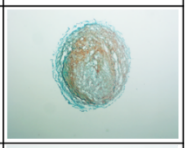
Testis	4# PEI	t-MDS	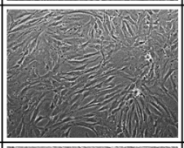	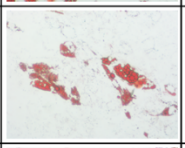	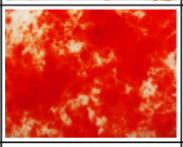	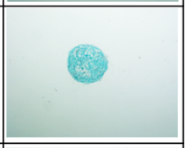
BCL	6# R-CHOP	t-AML	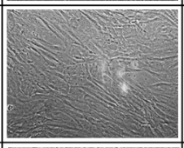	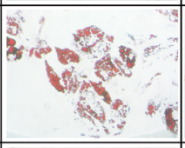	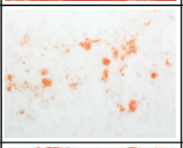	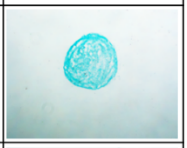
Hodgkin lymphoma	7# BEACOPPesc	t-AML	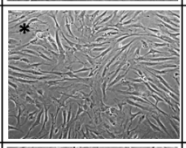	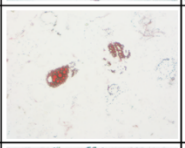	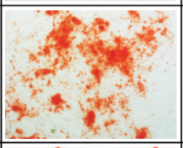	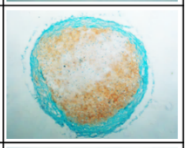
NHL	8# GMALL B-ALL +HD-BEAM	t-AML	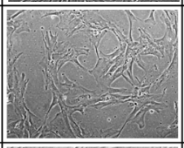	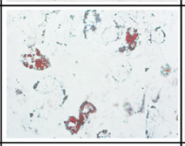	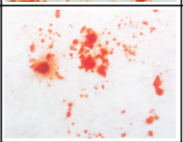	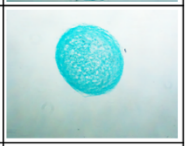
CLL	6# FC	t-AML	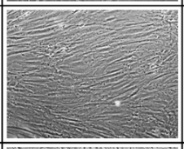	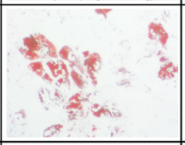	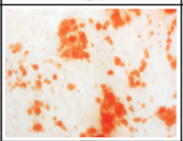	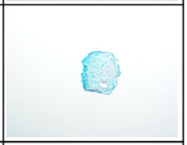
Papillary thyroid	RJT 3.7GBq	t-AML	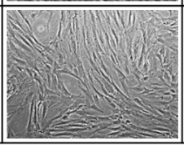	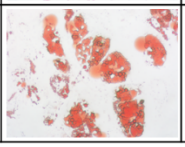	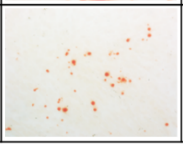	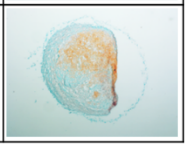

Appendix Figure 4. Phenotypical characterization and differentiation capacity of seven t-MN patients. Depicted are representative images of MSC morphology and histochemical stainings (Adipogenesis: Oil Red O, Osteogenesis: Alizarin Red, Chondrogenesis: Safranin-O/Fast Green) for individual patients. Patient selection for this figure was based on the complete availability of collected data. *Abbreviations: B-ALL, B-lymphoblastic acute lymphocytic leukemia; BCL, B-cell lymphoma; NHL, non-hodgkin lymphoma; CLL, chronic lymphocytic leukemia; #, number of therapeutic cycles; GMALL, German Multicenter Study Group for Adult Acute Lymphoblastic Leukemia (treatment protocol); PEI, cisplatin, etoposide, ifosfamide; R-CHOP, rituximab, cyclophosphamide, hydrocydaunorubicin, oncovin, prednisone; BEACOPPesc, bleomycin, etoposide, Adriamycin, cyclophosphamide, oncovin, procarbazin, prednisone, escalated; HD-BEAM, high dose carmustine, etoposide, cytarabine, melphalan; FC, fludarabine, cyclophosphamide; RJT 3.7GBq, radioactive iodine therapy with 3.7 gigabecquerels.*

Acknowledgments/Danksagung

Diese Doktorarbeit zu verfassen war eine unglaubliche Reise für mich. Ein Abenteuer, welches ich nicht hätte alleine bewältigen können. Dank der Unterstützung, die ich durch so viele inspirierende Menschen erfahren durfte, kann ich immer mit einem Lächeln auf diesen Lebensabschnitt zurückblicken.

Mein besonderer Dank an dieser Stelle gilt Dr. Stefanie Geyh: meiner Mentorin, meinem Vorbild und meiner standhaftesten Unterstützerin. Danke, dass du während meiner Promotionszeit und darüber hinaus stets an meiner Seite warst - mit einem offenen Ohr, ermutigenden Worten und unermüdlicher Begeisterung für unsere gemeinsame Arbeit. Als Laborbetreuerin hast du mich mit deiner Erfahrung und deinem Wissen geprägt und maßgeblich dazu beigetragen, dass ich heute eine starke und unabhängige Wissenschaftlerin bin. Darüber hinaus hast du meine persönliche Entwicklung entscheidend gefördert und mir zu mehr Selbstbewusstsein verholfen. Vielen Dank für deine enorme Unterstützung und dein stetiges Engagement für mich und das gesamte Team.

Auch danke ich Prof. Dr. med. Thomas Schroeder für das mir entgegengebrachte Vertrauen dieses spannende Projekt zu erforschen und für die Aufnahme in ein tolles Team, das die Aspekte der Grundlagenforschung und translationellen Forschung in herausragender Zusammenarbeit vereint.

Prof. Dr. Sebastian Wesselborg danke ich herzlichst für die immer konstruktive Unterstützung und Ihre wertvolle Zeit und Bereiterklärung diese Arbeit als mein Zweitgutachter zu unterstützen. Danke, für die Möglichkeit in Ihrem Labor zusammen mit Ihrem herausragenden Team (Dr. Laura Schmitt, Karina S. Krings und Ilka Lechtenberg) gearbeitet haben zu dürfen.

Des Weiteren danke ich Prof. Dr. Gerhard Fritz, für Ihre unermüdliche Unterstützung und Ihren Einsatz für das GRK, mein Projekt, und für mich als Wissenschaftlerin. Ihre Förderung und Forderung der letzten Jahre, hat dazu beigetragen mich für die Wissenschaft der Toxikologie zu begeistern und eine wissenschaftliche Karriere weiterzuverfolgen.

Genauso danke ich Dr. Sebastian Honnen, meinen ersten Mentor in meiner wissenschaftlichen Karriere, der mich bereits während meiner Bachelorarbeit inspiriert hat. Sebastian, du hast mich mein Potenzial in der Wissenschaft erkennen lassen und motiviert diesen Weg weiter zu verfolgen. Danke!

Genauso dankbar bin ich für den riesigen emotionalen Support durch meine Kolleg:innen, die mir in herausfordernden Zeiten Kraft gaben, und in erfolgreichen Zeiten Freude teilten. Besonders hervorheben möchte ich an dieser Stelle Anne Koch, mein *Cell Culture Buddy* Luci Bogun und Laura Tillmann. Ihr habt unser Labor zu einem Ort gemacht, an den ich jeden Tag mit Freude erscheinen konnte. Die Kollegialität und gegenseitige Unterstützung in diesem Team ist unvergleichlich. Hervorheben möchte ich außerdem meine wöchentliche Doppelkopfrunde: Christian Kroll, Melanie Pahl, Kevin Schlüppmann und Marlene Piribauer. Die Interaktion mit euch als Freunden und Wissenschaftlern mit ähnlichen Herausforderungen hat mich stets vorangetrieben.

Zu guter Letzt, danke ich meiner Familie und meinen Freunden von Herzen. Danke fürs Zuhören, Ermutigen und euer Anfeuern durch jedwede Herausforderungen und Triumphe. Besonders hervorheben möchte ich meine Eltern für die unaufhörliche Unterstützung auf diesem Weg. Danke auch an meine Schwester Leo und an Marvin, dass ihr diesen Weg mit mir zusammen bestritten habt und immer mit Rat und Tat zur Seite standet. Danke David, dass du mich über die vier Jahre hinweg so unglaublich unterstützt und aufgebaut hast. Ich hätte es nicht ohne euch machen wollen.